Florida Department of Health
Onsite Sewage Program

# Lysimeter Research Management and Support

Report of Activities under Contracts LPB85 and LPD01

January 1998

# Florida Department of Health
## Onsite Sewage Program

# Lysimeter Research Management and Support
Report of Activities under Contracts LPB85 and LPD01

January 1998

Prepared by:
Paul Sherblom, Ph.D.
Department of Environmental and Occupational Health
College of Public Health
University of South Florida
13201 Bruce B. Downs Blvd.
Tampa, Florida 33612

Other contributors:
Marylynn V. Yates, Ph.D.
Department of Soil and Environmental Sciences,
University of California, Riverside

Richard Mines, Jr., P.E., Ph.D.
Ms. Rene Montplaiser
Department of Environmental Engineering,
College of Engineering, USF

Ms. April Turner
Mr. Brian Pisaneschi
Department of Environmental and Occupational Health,
College of Public Health, USF

# Table of Contents


| Section | Page |
|---|---|
| List of Tables | ii |
| List of Figures | ii |
| Executive Summary | iii |
| Introduction | |
| Objectives | 1 |
| Scope of work | 2 |
| Data collection and Analytical methods | |
| Sampling Methods | 3 |
| Analytical Methods | 4 |
| Results and Discussion | |
| Operation and Maintenance | 5 |
| Measurements of Effluent Quality, Soil and water quality impacts | 6 |
| Temperature | |
| Infiltration Rate | |
| Oxidation-reduction potential | |
| Soil moisture | |
| Fecal coliforms and fecal streptococci | |
| Biological oxygen demand ($BOD_5$) | |
| Total organic carbon (TOC) | |
| Oil and grease measurement | |
| Methylene blue active substances | |
| Total kjeldahl nitrogen (TKN) and ammonia, nitrate | |
| Solids | |
| Chloride, sulfate and phosphate ions | |
| Virus Transport Model | 23 |
| Conclusions and Recommendations | 23 |
| References | 25 |
| Appendix: Predicting Virus Transport in Lysimeters | 26 |

List of Tables Page

Table 1. Soil Temperature (°C) and Infiltration (inch/minute) Results. . . . . 7

Table 2. Oxidation/Reduction Potential (mV) and Soil moisture (mbar) data. . . . . 9

Table 3. STE Bacterial results (Log # colonies per 100 ml). . . . . 10

Table 4. Lysimeter Station 1996-1997 BOD (mg/L) results[1]. . . . . 11

Table 5. Lysimeter Station 1996-1997 TOC (mg/L) results. . . . . 13

Table 6. "Oil and Grease" results as Hexane Extractable Material (mg/L). . . . . 15

Table 7. Methylene Blue Active Substances (MBAS in mg/L) results. . . . . 15

Table 8. Total Kjeldahl Nitrogen and Ammonia results (mg/L). . . . . 17

Table 9. Nitrate Ion Concentrations (mg/L) . . . . . 18

Table 10. Total Dissolved, Total Suspended and Volatile Suspended Solids (mg/L). 19

Table 11. Chloride Ion Concentrations (mg/L). . . . . 21

Table 12. Sulfate Ion Concentrations (mg/L). . . . . 21

Table 13. Phosphate Ion Concentrations (mg/L). . . . . 22

List of Figures Page

Figure 1. 1997 TOC concentrations and rainfall at Lysimeter station. . . . . 14

Figure 2. 1997 Nitrate and Phosphate ion concentrations and rainfall. . . . . 24

## Introduction

The research lysimeter facility located on the campus of the University of South Florida was constructed as part of the Florida Department of Health's Onsite Sewage Disposal System (OSDS) Research Project. Construction of the research facility was completed in 1992 and preliminary testing performed (Ayers 1993). Subsequent to these preliminary studies the facility continued dosing the infiltration beds, but effluent and soil quality remained unmonitored. The current project was initiated in 1995 to alleviate the maintenance problems which had arisen at the facility and to provide monitoring support for a virus transport study conducted by the Department of Health's Tampa Branch Laboratory. Thus scheduling of samples collected for this project depended on the sample collection schedule of the virus study. This project was originally planned to begin in the fall of 1995, however, due to delays in contracting and renovation of the facility, as well as personnel hiring and training at the Tampa Branch Laboratory, the field work began in late June of 1996. Prior to initiating sampling for this project, all sampling gear and ports were cleansed at that time with a three percent solution of hydrogen peroxide to reduce endogenous bacterial populations. Subsequently, soil water samples were drawn for several days in an attempt to ensure that the system was in functioning order and to reduce the amount of fine grain sand which would be present in samples collected later. The initial sampling of the facility for a subset of parameters was conducted on July 2, 1996, with later sampling dates providing more complete analyses. Sampling for the parameters discussed here usually occurred during the week prior to the infiltration cells being dosed in the virus study.

## Objectives

This project had three objectives. The first was repair and maintenance of the structure and equipment of the research lysimeter facility to allow its use for the Department of Health's virus transport study. The second objective was to acquire effluent and soil water quality measurements to supplement and support the virus

transport study. An ancillary benefit of these data is the ability to evaluate the continued performance of the infiltration beds in their removal of wastewater constituents after several years of continuous performance. The third objective was to support the development of an unsaturated zone virus transport model and comparison of this model with data generated in these studies.

## Scope of work

Operation and Maintenance of the Lysimeter Station Facility. The research facility is intended to provide an infiltration setting which is similar to that of a typical installed onsite wastewater disposal system, i.e. a drainfield under a lawn environment. Thus, this aspect of the work ensures that the lawn and structure remain in or near their desired conditions and provides for monitoring the function of the pumps, dose pots, flow lines and artificial water tables which constitute the dosing and experimental system. This portion of the project will only be further discussed concerning those events which could potentially affect system performance or the data collected.

Measurements of Effluent Quality, Soil and water quality impacts. Evaluation of the performance of the infiltration beds in terms of contaminant removal requires data on the effluent quality entering the beds and the ground water quality below the infiltration cells. Ancillary data required in evaluating the soil impacts include rainfall and temperature, soil moisture tension, soil redox potential and cell infiltration rates. Water quality was determined by measuring the total organic carbon, the five day biological oxygen demand, the presence of nitrogen species (TKN, $NH_3$-N and $NO_3$-N), phosphate, sulfate, chloride, Surfactants (measured as methylene blue active substances), oil and grease (measured as hexane extractable material), Fecal coliforms and Fecal streptococci, and solids concentrations (total dissolved, suspended and volatile) in both the effluent and ground water collected from a two foot depth.

Model Development and Performance. To assist in understanding the results of this and the virus transport studies, an unsaturated transport zone model for virus was developed.

The model was tested using data collected by the Tampa Branch Laboratory. The model was developed and validated by Dr. Marylynn Yates of the University of California at Riverside through a subcontract from this contract. Her report, describing the model and results of the validation, is included in this report.

Timeframe covered by this report. The initial contract (LPB85) supporting this project was for the period of October 15, 1995 to 1996. Since this project depended on the scheduling of the virus transport studies, sampling was not initiated until July of 1996. In October the contract was extended six months. Thus contract LPB85 ended in March 1997 and the Department of Health issued a stop work order for this project. Since the virus transport study continued beyond the end of March 1997, a new contract (LPD01) was issued to complete the work. This contract covered the project period from June 16, 1997 to August 29, 1997 to allow a final sampling event (end of June/early July) and compilation of the resulting data. The virus study was extended into the fall of 1997 which resulted in contract LPD01 being extended until December to continue providing maintenance and repair services at the lysimeter facility. This report provides all data generated during both contracts LPB85 and LPD01 and reviews major maintenance and repair activities undertaken for those contracts.

## Data Collection / Analytical Methods

### Sampling Methods

Samples of soil water were collected from the two foot zone under each of the experimental cells. Reference samples of the septic tank effluent (STE) were collected at each sampling date, water representative of that dosing the water control cells (City of Tampa potable supply) has also been collected at most time points. Soil water is collected by applying gentle vacuum (-5 to -7 psi) to sample bottles attached to the drain of the lysimeter pan. This method allows the collection of 1 liter samples in time periods of between twenty (20) and one hundred and twenty minutes (120) depending on soil moisture content available. There were occasions where sufficient water volumes to

conduct all analyses, could not be acquired from cell 3 (Effluent, high flow). These occasions are designated in the data tables as being not available (NA). STE and Tap water control samples were collected while the soil water samples were being drawn. Sample bottles were precleaned by normal washing (soap and water), rinsed with tap water, then deionized water and then autoclaved for sterilization. Bottles were transported to the facility sealed and attached to the sampling pans as aseptically as feasible. After filling, the bottles were resealed and stored in a cooler (blue or wet ice) for transport to the laboratory. Subsamples for $BOD_5$ and bacteriological analysis were taken prior to storing the remaining samples in a refrigerator, or separate samples were collected in the field. Separate samples were also collected in precleaned jars for measurement of the dissolved ions and total organic carbon. TKN and $NH_3$-N measurements were also made on samples collected separately from those collected for the remaining parameters.

Analytical Methods

All methods utilized for these samples (except for oil and grease) are taken from Standard Methods for the Examination of Water and Wastewater 19th edition. An ion chromatographic method (Method 4110 B) was used for the analysis of nitrate, phosphate, sulfate and chloride. Total Kjeldahl nitrogen and ammonia nitrogen were determined using method 4500-$N_{org}$ C. Methylene blue active substances (MBAS) were determined using method 5540 C. Solids were measured using methods 2540 C (total Dissolved), 2540 D (total Suspended) and 2540 E (Volatile Suspended). Fecal coliforms and Fecal streptococci were determined using methods 9222 D and 9230 C respectively. Oil and grease were analyzed using the proposed EPA Method 1664 which is a replacement method for the Freon based method used in Standard Methods. Briefly, for determination of n-hexane extractable material (HEM), samples are acidified to pH 2 and serially extracted three times with n-hexane in a separatory funnel. The extract is filtered through sodium sulfate to remove residual water, and the solvent is evaporated by heating with a steam or water bath (for this work the solvent was concentrated using rotary evaporation

under gentle vacuum). The HEM that remains in a small, known volume, is weighed and the concentration calculated in mg/L.

Soil moisture, temperature and ORP measurements were made in situ. Soil moisture measurements were made using a hand held electronic tensiometer. Temperature and ORP were directly read from probes installed in the soil at the lysimeter facility. The ORP measurements were collected with the use of a Corning model 140 pH/mV meter.

## Results and Discussion

Operation and Maintenance of the Lysimeter Station Facility.

Facility maintenance has been an ongoing challenge. In addition to the routine cleaning, pest control (rat removal during the winter of 1995, ongoing spider control) and lawn maintenance, several events may have impacted the studies being done. When the project was initiated in 1995, the lysimeter station had been functioning but unmaintained since the 1992 study. The facility had become severely overgrown by large weeds and small bushes. The removal of these plants and return of the surface to one which resembles a suburban lawn was achieved, but the possibility exists that root channels from these plants could have affected the performance of the drainfield of specific cells. The lawn has been maintained at a reasonable grass height at all times while under contract, during periods of contract interruption the grass heights have been somewhat deeper.

In March of 1997 it became evident that there was a problem with the septic tank effluent supply for the facility. It was determined that some debris clogging the supply line between the supply pump and the holding tank at the facility had impeded the flow of effluent to the holding tank and caused the supply pump to burn out. The supply pump was replaced and the line cleaned out. This problem caused an interruption of about one month in the supply of septic tank effluent to the infiltration cells.

There have been three interruptions to the water supply of the artificial water tables. These have been in late July 1997 when a lighting surge tripped the circuit breaker, in late

October 1997 when unknown persons closed a valve on the supply line between the well and the artificial water tables, resulting excessive back pressure on the well which shut the pump off (the valve handle has since been removed to prevent a recurrence), and in late November when a lightning strike or other cause apparently shorted out the pump resulting in a cessation of flow. This last incident was initially diagnosed as a faulty switch in the control box, but the pump was implicated by further testing. Since the support contract ended in early December, replacement of the pump was not achieved under these contracts.

Near the start of this project the Lysimeter facility was equipped with an onsite weather monitoring system. This system has the capacity of storing several months of data between retrievals. An electrical spike from a lightning storm in late September 1996 resulted in the loss of several months of stored data (i.e. the summer months of 1996). The system was downloaded on a monthly schedule after this event, but software problems have resulted in smaller interruptions in the data record during the winter and spring of 1996 and 1997 (specific downloads of roughly a month duration each have been lost). These problems were eliminated by placing a computer in the facility which allows data to be downloaded on a more frequent basis (directly to the weather database).

Measurements of Effluent Quality, Soil and water quality impacts.

Temperatures recorded at the Lysimeter facility during sampling visits from October 1996 to April 1997 are shown in Table 1. Corresponding indoor and outdoor temperatures recorded by the weather station for the nearest dates are also listed. While outside air temperatures ranged from 5 to 35 °C, soil temperatures were always between 20 and 25 °C. Infiltration rates for the experimental cells were measured on three occasions during this work, and are also shown in Table 1. Infiltration rates were measured using the falling head test. Since exact calculation requires a knowledge of the porosity of the gravel of the infiltration bed and we had only an estimate of the gravel bed porosity (35%), both the uncorrected and porosity corrected infiltration rates are shown in Table 1. The first infiltration test was performed without pre-saturating the soil, which for

Table 1. Lysimeter Station 1996-1997 Soil Temperature (°C) and Infiltration (inch/minute) Results.

| **Temperature (°C)** | Cell Number | | | | | Inside | | Outside | |
|---|---|---|---|---|---|---|---|---|---|
| | 1 | 4 | 6 | | 10 | High | Low | High | Low |
| Depth (ft) | 1 | 1 | 0.5 | 1 | 0.5 | | | | |
| Oct. 3, 96 | 24.9 | 24.8 | -- | 25 | 25 | 26.8 | 25.6 | 31.0 | 22.5 |
| Nov. 2, 96 | 25 | 24.1 | 24.6 | 24.2 | 25 | 26.2 | 24.2 | 32.0 | 17.0 |
| Dec. 6, 96 | 21 | 19.9 | -- | 21.5 | 21.5 | 23.4[1] | 21.9[1] | 24.5[1] | 12.8[1] |
| Jan 31, 97 | 21 | 20 | 22 | 22 | 22 | 20.8 | 17.4 | 23.2 | 12.7 / 5[2] |
| Feb 28, 97 | 24 | 23.5 | 23.5 | 23.5 | 23.5 | 24.3[1] | 22.2[1] | 28.2[1] | 15.5[1] |
| Mar 25, 97 | -- | 24 | 24 | 24 | 24 | 26[3] | | 35[3] | |
| April 15, 97 | -- | 24 | 23.5 | 23.5 | 23.5 | 24.9 | 22.7 | 30.0 | 14.8 |

| Average InfiltrationRate (in./min.) | | Cell Number | | | | | | | |
|---|---|---|---|---|---|---|---|---|---|
| | | 2 | 5 | 8 | 4 | 3 | 6 | 9 | 7 |
| Jun 28,96[4] | uncorrected | 1.17 | 1.94 | 2.63 | 1.16 | 2.31 | 2.07 | 2.83 | 0.96 |
| | corrected | 0.41 | 0.68 | 0.92 | 0.41 | 0.81 | 0.72 | 0.99 | 0.34 |
| Nov. 17,96[5] | uncorrected | 0.60 | 0.59 | 0.67 | 1.17 | 0.83 | 0.75 | 0.61 | 0.79 |
| | corrected | 0.21 | 0.21 | 0.23 | 0.41 | 0.29 | 0.26 | 0.21 | 0.28 |
| July 26,97[5] | uncorrected | 0.41 | 0.44 | 0.43 | 0.73 | 0.31 | 0.48 | 0.45 | 0.41 |
| | corrected | 0.14 | 0.15 | 0.15 | 0.26 | 0.11 | 0.17 | 0.16 | 0.14 |

1. Data for sampling date unavailable, data from December 2, 1996 and February 23, 1997 used in table. These are the closest dates for which complete twenty four hour data available.
2. The low temperatures of the night prior and subsequent to sampling differed a great deal, thus they are listed respectively.
3. Data for this date are missing, these are the inside and outside temperatures recorded during sampling.
4. Test conducted with unsaturated soil.
5. Test conducted after soil saturation.

most cells resulted in significantly faster infiltration rates. Exceptions to this were the two water control cells (4 and 7). These cells show essentially the same infiltration rates during the June 28th and November 17th tests. The differences between the November 17th (1996) and July 26th (1997) test results may indicate less clogging of the infiltrative surface at the later date, or it may reflect better saturation of the soil during the summer wet season.

The oxidation-reduction potential of the soil measured is shown in Table 2. Cells which had ORP probes in the 1992 study (Ayers 1993) provided essentially the same ranges of data as were seen in the previous work. There were no consistent trends in ORP values between treatments, or between depths. In general, the system appears to be functioning in an aerobic condition. There are items of interest in this data set, the first is that the probe in cell 5, at the depth of two feet, provided generally higher ORP measurements than was observed in the 1992 study. Since the probes in this cell at 0.5 and 1 foot show the same ranges of ORP as was seen in 1992, it is unclear what the increase in ORP values for the two foot depth indicates. It could imply that there is air movement from the interior of the station into the collection pan at two feet which could allow greater aeration of the soil at that depth, or the sand around the probe may have undergone some wash out between 1992 and 1996 which could also result in greater aeration of the soil around the probe (or the probe itself). The second interesting point is the consistently negative values recorded at the 0.1 foot depth in cell 7 (high flow water control cell). This data is in stark contrast to that recorded for the 0.1 foot depth in cell 4 (low flow water control cell), and most likely indicates a peculiarity of the probe rather than the actual redox potential of the soil at the surface of cell 7.

Soil moisture measurements made during this project are also shown in table 2. This data is presented as soil suction, i.e. the pressure available to remove soil moisture away from the cells. Comparison with the data provided in the earlier report would require conversion not only from soil suction to soil moisture content, but also correction for the angle of each soil moisture probe installed at the facility. The previous investigators were

Table 2. Lysimeter Station 1996-1997 Oxidation/Reduction Potential (mV) and Soil moisture (mbar) measurements.

**ORP reading (mV)**

| | Cell Number | | | | | | | | | | | | | | | | | | | |
|---|---|---|---|---|---|---|---|---|---|---|---|---|---|---|---|---|---|---|---|---|
| | 3 | | | | 4 | | 5 | | | | 6 | | | 7 | | 8 | | | | 10 |
| Depth (ft) | 0.1 | 0.5 | 1 | 2 | 0.1 | 0.5 | 0.1 | 0.5 | 1 | 2 | 0.1 | 0.5 | 1 | 0.1 | 0.5 | 0.1 | 0.5 | 1 | | 0.5 |
| July 2, 96 | 334 | 730 | 362 | 913 | -- | -- | 413 | 352 | 317 | 828 | -- | -- | -- | -85 | 130 | -- | -- | -- | | -- |
| Sept 4, 96 | 408 | 384 | 282 | 906 | 429 | 355 | 404 | 344 | 308 | 537 | 422 | 430 | 354 | -112 | 532 | 403 | 405 | 317 | | 440 |
| Oct 3, 96 | 422 | 363 | 399 | 921 | -- | -- | 409 | 302 | 328 | 622 | -- | -- | -- | -- | -- | 208[1] | 442 | -- | | -- |
| Nov 2, 96 | 406 | 390 | 407 | 937 | 463 | 401 | 411 | 362 | 642 | 713 | 428 | 445 | 382 | -115 | 115 | 339 | 411 | 322 | | 452 |
| Dec 6, 96 | 437 | 412 | 341 | 935 | 254 | 302 | 424 | 312 | 329 | 587 | 418 | 408 | 431 | -48 | 119 | 360 | 481 | 303 | | 428 |
| Jan 31, 97 | 426 | 417 | 411 | 952 | 393 | 333 | 398 | 361 | 316 | 492 | 415 | 444 | 410 | -43 | 111 | 384 | 399 | 359 | | 459 |
| Feb 28, 97 | 393 | 428 | 413 | 954 | 456 | 257 | 420 | 363 | 375 | 511 | 388 | 454 | 408 | -42 | 103 | 414 | 422 | 366 | | 446 |
| Mar 25, 97 | 410 | 402 | 406 | 960 | 443 | 352 | 407 | 360 | 357 | 888 | 412 | 427 | 400 | -26 | 201 | 425 | 413 | 361 | | 428 |
| Apr 15, 97 | 410 | 387 | 407 | 981 | 500 | 361 | 414 | 370 | 362 | 626 | 348 | 433 | 404 | -24 | 215 | 428 | 423 | 364 | | 439 |

**Soil Moisture (mbar)[2]**

| | Cell Number | | | | | | | | | | | | | | | | | | | | | | | |
|---|---|---|---|---|---|---|---|---|---|---|---|---|---|---|---|---|---|---|---|---|---|---|---|---|
| | 2 | | | 3 | | 4 | | | 5 | | | 6 | | | 7 | | | 8 | | | 9 | | | 10 |
| Depth (ft) | 0.5 | 1 | 2 | 0.5 | 2 | 0.5 | 1 | 2 | 0.5 | 1 | 2 | 0.5 | 1 | 2 | 0.5 | 1 | 2 | 0.5 | 1 | 2 | 0.5 | 1 | 2 | 0.5 |
| July 2, 96 | -45 | -68 | -26 | -44 | -29 | -72 | -52 | -43 | -34 | -41 | -27 | -39 | -61 | -44 | -8 | -55 | -43 | -35 | -64 | -45 | -49 | -52 | -31 | -83 |
| Oct 3, 96 | -59 | -51 | -24 | -52 | -- | -64 | -54 | -32 | -41 | -65 | -14 | -- | -49 | -38 | -59 | -49 | -26 | -68 | -56 | -35 | -65 | -49 | -32 | -- |
| Nov 2, 96 | -58 | -53 | -20 | -46 | -20 | -9 | -53 | -30 | -12 | -27 | -34 | 65 | -21 | -20 | -57 | -57 | -31 | -40 | -55 | -34 | -55 | -46 | -23 | -- |
| Dec 6, 96 | -73 | -60 | -68 | -60 | -33 | -68 | -47 | | -- | -36 | -- | -53 | -64 | -48 | -63 | -43 | | -17 | -70 | -41 | -73 | -62 | -39 | -- |
| Jan 31, 97 | -80 | -66 | -34 | -42 | 77 | -38 | -63 | -20 | -- | -50 | 13 | -45 | -59 | -45 | -- | -62 | -40 | -67 | -66 | -40 | -80 | -62 | -39 | -- |
| Feb 28, 97 | -75 | -73 | -47 | -- | -29 | -66 | -69 | -49 | -- | -67 | -- | -- | -61 | -48 | -- | -55 | -37 | -17 | -63 | -35 | -69 | -51 | -30 | -- |
| Mar 25, 97[3] | -75 | -43 | -19 | -38 | 53 | -52 | -56 | -38 | -- | -- | -- | -- | -- | -- | -- | -- | -- | -- | -- | -- | -- | -- | -- | -- |
| Apr 15, 97[3] | -- | -- | -- | -25 | 62 | -58 | -62 | -40 | -- | -32 | -24 | -- | -- | -- | -- | -- | -- | -- | -- | -- | -- | -- | -- | -- |

1. may represent electrode problem (failure) rather than real value.
2. Uncorrected for probe angle.
3. Incomplete data due to water getting into needle of electronic tensimeter.

unable to provide these correction factors and thus the data is presented as collected (in soil suction). The fact that most measurements are negative indicates that neither the continued cell dosing nor the presence of the artificial water table has completely saturated these soils.

Measurement of fecal coliforms and fecal streptococci was consistently negative for all soil water samples collected. Data for the concentrations in the septic tank effluent is shown in Table 3, and are consistent with the concentrations observed in the earlier study (Ayres 1993). These data show that the septic tank effluent being applied to the drainfield have fairly consistent numbers of fecal organisms and these values are in the range one would expect for residential domestic wastewater. The fact that these organisms were consistently absent from the soil water samples indicates that the drain fields are still providing effective removal of these types of bacteria during transit of the two foot unsaturated zone.

Table 3. Lysimeter Station 1996-1997 STE Bacterial results (Log # colonies per 100 ml).

| | July 31, 96 | Sept 4, 96 | Oct 2, 96 | Oct 31, 96 | Dec 19, 96 | Mar. 13, 97 |
|---|---|---|---|---|---|---|
| Fecal Coliform | 4.90 | 5.15 | 3.95 | 5.04 | 5.15 | 5.04 |
| Fecal Strep. | 4.85 | 5.28 | 3.26 | 3.95 | 5.75 | 3.95 |

The applied wastewater and soil water samples were monitored for total organic carbon (TOC) and their biological oxygen demand ($BOD_5$). These parameters should also indicate the removal efficiency of the system after prolonged use. In a general sense TOC and $BOD_5$ measurements are separate measures of the same thing. They are used as indicators of the potential amount of bacterial growth which could be sustained by the carbon introduced in the waste stream. The $BOD_5$ data produced during this project are shown in Table 4. The wastewater being applied had $BOD_5$ values ranging from 30 to 80 mg/L, which is generally lower than the wastewater concentrations observed in the 1992 study. The soil water samples $BOD_5$ ranged from negligible to a high of 25, but were

predominantly very low. Thus, the $BOD_5$ data would suggest that there is little breakthrough of wastewater constituents occurring in the unsaturated soils being studied.

The TOC data are presented in Table 5, most TOC concentrations observed in this study were similar to those found in the previous work (Ayers 1993). The STE data mostly ranged from just under 30 to 74 mg/L, with three of the fifteen values exceeding 100 mg/L. These high values, and similar unusually high values for some soil water samples may in fact be real, but may also result from contamination of the samples by bacterial growth on the tubing of the sampling ports, this is particularly likely to explain the high value (121 mg/L) obtained for the July 10, 1997 sample collected from the no dose control cell (cell 10). Other than these few exceptionally high values, the data tend to be higher during the warmer months and lower during the cooler. This may reflect enhanced bacterial activity in the infiltration bed during the warmer months which could lead to greater release of dissolved organics. The soil water TOC data for the sampling events in 1997 are plotted with the available rainfall data from January to July in Figure 1. This figure illustrates that there is no significant difference in TOC concentrations between high and low effluent dose cells, nor is there an apparent correlation with rain events. The low TOC values for samples collected during the interruption of effluent flow during March does suggest that the soil water TOC concentration is impacted by the effluent discharge.

Two other measures of the organic content of wastewater and potentially impacted ground water results from the measurement of oil and grease and of anionic surfactants as methylene blue active substances. Results for the oil and grease analyses are shown in Table 6. The wastewater oil and grease content ranged from a low of 4 mg/L to a high of 30 mg/L which is a slightly lower range of values than were observed in the 1992 study (Ayers 1993). The soil water samples were consistently low, with no significant differences between high and low treatment cells, the tap water and no dose control cells or the potable (tap) water blank. The methylene blue active substance (MBAS) data are shown in Table 7. The septic tank effluent usually showed unexpectedly low levels of the

Table 6. Lysimeter Station 1996-1997 "Oil and Grease" results as Hexane Extractable Material (mg/L).

| Sample Date | STE | Tap | Cell 10 | Low Flow (0.75 gal/ft²/day) Cell 2 | Cell 5 | Cell 8 | Cell 4 | High Flow (1.50 gal/ft²/day) Cell 3 | Cell 6 | Cell 9 | Cell 7 |
|---|---|---|---|---|---|---|---|---|---|---|---|
| July 31,96 | 3.87 | | | 0.74 | 0.68 | 0.26 | 0.79 | 0.25 | 0.54 | 0.83 | lost [2] |
| Sept 4,96 | 29.99 | 0.51 | 0.40[1] | 0.33 | 0.38 | 0.75 | 0.59 | 0.39 | 0.27 | 0.38 | 0.66 |
| Oct 2, 96 | 16.78 | 0.65 | 0.52[1] | 1.11 | 0.30 | 1.03 | 2.94 | 0.71 | 0.93 | 0.34 | 0.5 |
| Oct 31,96 | 7.63 | 0.51 | 0.40[1] | 1.11 | 2.82[3] | 0.43 | 1.30[3] | - -[3] | 0.64 | 1.57 | 0.4 |
| Dec19,96 | 16.73 | 0.78 | 0.61[1] | 0.97 | 0.77 | 0.91 | 0.86 | 0.90 | 0.75 | 0.80 | 0.76 |
| 2/10/1997 | 18.29 | 1.54 | 1.67[1] | 2.01 | 1.33 | 2.77 | 2.20 | 3.22 | 2.08 | 1.65 | 2.5 |
| July 7,97 | - -[4] | 0.03 | 0.28 | 0.53 | 0.09 | 0.12 | 0.72 | NA | 0.17 | 0.07 | 0.19 |

1. These numbers are for the analysis of distilled water, only the last value is for a sample collected from cell 10.
2. The extract was lost during processing.
3. Some of the extract from cell 4 was spilled and thus the true value may have been higher, the extracts from cells 5 and 3 were accidently combined during processing and the combined value is reported under cell 5.
4. This extract gave extremely variable results during gravimetric analysis, and was deemed unreliable.



Table 7. Lysimeter Station 1996-1997 Methylene Blue Active Substances (MBAS in mg/L) results.

| Date | STE | Tap | Blank[1] | Low Flow (0.75 gal/ft²/day) Cell 2 | Cell 5 | Cell 8 | Cell 4 | High Flow (1.50 gal/ft²/day) Cell 3 | Cell 6 | Cell 9 | Cell 7 |
|---|---|---|---|---|---|---|---|---|---|---|---|
| July 3, 96 | 1.36 | - | | 0 | 0 | 0 | 0.02 | 0.02 | 0 | 0.03 | 0 |
| July 31, 96 | 1.45 | 0.02 | | 0.04 | 0.02 | 0.02 | 0.01 | 0.05 | 0.07 | 0.03 | 0.45 |
| Sept 4, 96 | 2.93 | 0.05 | | 0.01 | 0.01 | 0.01 | 0.02 | 0.01 | 0 | 0.01 | 0.04 |
| Oct 2, 96 | 3.15 | 0.06 | 0.03 | 0.05 | 0.02 | 0.03 | 0.04 | 0.03 | 0.04 | 0.08 | 0.03 |
| Oct 31, 96 | 1.71 | 0.03 | 0.05 | 0.02 | 0.02 | 0.01 | 0.01 | 0.04 | 0.02 | 0.05 | 0.03 |
| Dec 5, 96 | 2.75 | - | 0.03 | 0.06 | 0.02 | 0.1 | 0.07 | 0.05 | 0.06 | 0.03 | 0.06 |
| Jan 22, 97 | 1.42 | 0.06 | 0.07 | 0.16 | 0.06 | 0.26 | 0.18 | 0.12 | 0.15 | 0.08 | 0.14 |
| Jan 31, 97 | 1.84 | 0.22 | 0.08 | 0.23 | 0.21 | 0.37 | 0.04 | 0.08 | 0.09 | 0.18 | 0.19 |
| Jul 21, 97 | 14.00 | 0.03 | 0.02 | 0.12 | 0.12 | 0.07 | 0.03 | NA | 0.06 | 0.18 | 0.10 |

1. All of these blanks were distilled water except the July 97 sample which was collected from no dose control cell number 10.

surfactants, while the soil water samples provided only background levels. There were no differences in MBAS concentrations in samples collected from low or high flow experimental cells or between cells receiving wastewater and those receiving potable water or no dose. This data again indicates that the system is still efficiently removing these contaminants from the waste stream.

The total kjeldahl nitrogen (TKN) and ammonia results are provided in Table 8. The effluent had TKN values between 8 and 77 mg/L and ammonia concentrations ranged from 12 to 144 mg/L. Duplicate analyses (second column) showed some variability in these analyses, but the variability appeared to be greater between sample dates than that observed within sample dates. All control and soil water samples provided very low concentrations of TKN (essentially zero) and ammonia (highest around 5 mg/L). This is in contrast to the nitrate-nitrogen data for these samples, shown in Table 9. For nitrate, the effluent, the potable supply, the water and no dose control cells all showed very low concentrations (except the effluent of Jan. 31, 1997 which may be in error), while the soil water samples were usually elevated. Two anomalies are evident in the soil water nitrate data. The first is that cell 2, a low dose effluent cell, usually had very low nitrate concentrations, similar to those of the water dose control cells. At the moment, we can offer no explanation for this. The other observation concerns samples collected on the March 1997 sampling date, which was during the flow interruption of the septic tank effluent, all soil water samples have essentially background nitrate concentrations. This will be discussed further below, but is taken as a confirmation that nitrate loadings to ground water are alleviated with the cessation of wastewater flow.

The solids analyses proved to be most challenging during this project. The available solids data are listed in Table 10. The total dissolved solids (TDS) of the effluent samples ranged from 443 to 610 mg/L, which overlapped those of the potable water supply (306 to 466 mg/L), while the soil water samples were generally higher. There were no consistent differences between the low and high flow cells, or the effluent treated cells from the water control cells. This indicates that the major contribution to dissolved solids

Table 8. Lysimeter Station 1996-1997 Total Kjeldahl Nitrogen and Ammonia results (mg/L).

| Sample Date and measurement | STE | Dup. | Tap | Low Flow (0.75 gal/ft²/day) Cell 2 | Cell 5 | Cell 8 | Cell 4 | High Flow (1.50 gal/ft²/day) Cell 3 | Cell 6 | Cell 9 | Cell 7 | DI Blank |
|---|---|---|---|---|---|---|---|---|---|---|---|---|
| Jun. 28, 96 [NH3-N] | 42.4 | - | - | 0.30 | 0.10 | 0.10 | 0.20 | 0.30 | 0.10 | - | 0.1 | -- |
| Sept. 20, 96 [NH3-N] | 29.4 | - | - | 3.23 | 1.50 | 1.37 | 3.8 | 3.34 | 1.70 | - | 1.26 | -- |
| Oct. 9, 96 [NH3-N] | 50.1 | - | 0 | 0.62 | 0.38 | 0.19 | 0.96 | 0.32 | 0.29 | 0.2 | 0.23 | 0.36 |
| Oct. 31, 96 [NH3-N] | 12.2 | - | 0.06 | 0.06 | 0.02 | 0.02 | 0.05 | 0.04 | 0.03 | 0.02 | 0.02 | 0.02 |
| Nov. 2, 96 [TKN] | 8.38 | - | 0.14 | 0.23 | 0.09 | 0.09 | - | 0.16 | - | 0.09 | 0.08 | 0.08 |
| Dec. 17, 96 [NH3-N] | 49.2 | - | - | - | 0.18 | 0.24 | 0.55 | 0.28 | 0.18 | 0.21 | 0.13 | -- |
| Dec. 17, 96 [TKN] | 27 | - | - | - | 0.33 | 57.9 | 0.16 | 0.73 | 0.27 | 101 | - | -- |
| Jan 31, 97 [NH3-N] | 78.7 | 77.1 | - | 2.62 | 0.42 | 1.59 | 3.14 | 2.17 | 0.87 | 0.57 | 0.57 | -- |
| Jan 31, 97 [TKN] | 55.1 | 35.7 | - | 3.64 | 0.47 | 3.04 | 1.32 | 1.13 | 2.10 | 0.74 | 0.82 | -- |
| Feb 28, 97 [NH3-N] | 143.5 | 136.2 | 0 | 2.45 | 4.25 | 5.11 | 4.91 | 3.60 | 0.86 | 1.75 | 1.09 | -- |
| Feb 28, 97 [TKN] | 76.6 | 97.7 | 0 | 0.31 | 0.45 | 0.29 | 0.39 | 0.20 | 0.15 | 0.93 | 0.40 | -- |
| Mar 25, 97 [NH3-N] | 52.1 | 51.8 | 0.11 | 0.36 | 0.35 | 0.44 | 0.09 | 0.50 | 0.33 | 0.35 | 0.01 | -- |
| Mar 25, 97 [TKN] | 43.5 | 43.3 | 0.02 | 0.18 | 0.21 | 0.27 | 0.23 | 0.72 | 0.20 | 0.27 | 0.22 | -- |
| April 15, 97 [NH3-N] | 52.1 | 51.8 | 0.11 | 0.24 | 0.23 | 0.28 | 0.06 | 0.32 | 0.21 | 0.23 | 0.01 | -- |
| April 15, 97 [TKN] | 48.3 | 53.9 | 0.01 | 0.19 | 0.25 | 0.18 | 0.29 | 0.41 | 0.12 | 0.23 | 0.21 | -- |
| July 10, 97 [NH3-N] | 92.2 | - | 1.4 1.2 | 2.54 | 0.53 | 1.36 | 0.32 | NA | 1.12 | 0.48 | 0.34 | -- |

Table 9. Lysimeter Station 1996-1997 Nitrate Ion Concentrations (mg/L).

| Sample Date | STE | Tap | No Dose C10 | Low Flow (0.75 gal/ft²/day) Cell 2 | Cell 5 | Cell 8 | Water Cell 4 | High Flow (1.50 gal/ft²/day) Cell 3[1] | Cell 6 | Cell 9 | Water Cell 7 |
|---|---|---|---|---|---|---|---|---|---|---|---|
| Jan 31, 97 | 18.8 | 0.15 | - - | 0.49 | 8.19 | 29.62 | 0.24 | 12.64 | 24.13 | 28.17 | 0.54 |
| Feb 28, 97 | 0.13 | 0.09 | - - | 0.38 | 30.22 | 29.61 | 0.21 | 32.33 | 31.83 | 32.68 | 0.34 |
| Mar 25, 97[2] | 0.00 | 0.21 | 0.43 | 0.00 | 0.84 | 2.85 | 0.00 | N/A | 0.21 | 0.49 | 0.00 |
| Apr 15, 97 | 0.00 | 0.00 | 0.21 | BLQ | 22.06 | 29.25 | BLQ | 26.66 | 30.89 | 32.50 | 1.53 |
| May 5, 97 | BLQ | 0.51 | 0.31 | BLQ | 5.62 | 24.80 | BLQ | 4.22 | 17.38 | 20.09 | BLQ |
| July 10, 97 | 0.30 | BLQ | 0.31 | 17.63 | 17.50 | 10.02 | 0.25 | 4.22 | 23.86 | 25.09 | 0.63 |
| July 10, 97 | | 0.50 | | | | | | | | | |

1. December 5th 1996 sample from cell 3 was analyzed in January and gave a concentration of 29.15 mg/L.
2. STE pump to holding tank was not functioning prior to this sampling event.

Table 10. Lysimeter Station 1996-1997 Total Dissolved, Total Suspended and Volatile Suspended Solids (mg/L).

| Sample Date | STE | Tap | Low Flow (0.75 gal/ft²/day) Cell 2 | Cell 5 | Cell 8 | Cell 4 | High Flow (1.50 gal/ft²/day) Cell 3 | Cell 6 | Cell 9 | Cell 7 | DI Blank |
|---|---|---|---|---|---|---|---|---|---|---|---|
| TDS mg/L | | | | | | | | | | | |
| Sept. 4, 96 | 443 | 306 | 905 | 499 | 416 | 478 | 355 | 554 | 502 | 328 | -- |
| Oct. 31,96 | 450 | -[1] | 1406 | 1148 | 430 | 1240 | 995[2] | 1192 | 615 | 667 | -- |
| Dec. 5, 96 | 476 | 466 | 1245 | 925 | 669 | 1166 | 814 | 1006 | 754 | 367 | 20 |
| Jan 31, 97 | 535 | 454 | 1381 | 1486 | 830 | 1438 | 1642 | 1338 | 1305 | 1110 | 11 |
| Mar 14, 97 | 610 | 306 | 1260 | 1038 | 715 | 485 | NA | 928 | 1006 | 279 | 3 |
| TSS mg/L | | | | | | | | | | | |
| Sept. 4, 96 | *[1] | * | * | * | * | * | 16.1 | * | * | * | * |
| Oct. 31,96 | 3.5 | - | 3.4 | * | 15 | 49 | 179[2] | * | 21.6 | * | * |
| Dec. 5, 96 | 15.0 | * | * | * | * | * | 17.5 | * | 4.4 | * | * |
| Jan 29, 97 | 16.5 | 0.8 | 3.8 | 7.2 | 3.8 | 75.8 | 9.0 | 21.3 | * | * | 1.5 |
| Mar 14, 97 | 72.4 | * | 9.2 | 7.5 | 27.5 | 4.4 | NA | 3.50 | 2.4 | 1 | 1.3 |
| VSS[3] mg/L | | | | | | | | | | | |
| Oct. 31,96 | * | * | * | * | * | 28.8 | 58.5[2] | * | * | * | * |
| Jan 29, 97 | 4.2 | * | * | 1.4 | * | 60.7 | 1.8 | 19.3 | * | * | * |
| Mar 14, 97 | 17.7 | lost | * | * | 7.2 | * | NA | * | * | * | * |

1. Dash indicates sample not collected or insufficient volume, star indicates mass residual was within the measurement error and can be presumed to be equal to zero.
2. This sample was significantly impacted by the presence of fine grain sand in the soil water collected from the pan and even the filtrate had a sandy coloration.
3. Samples from September 4 and December 5 analyzed for volatile suspended solids provided no samples with a mass significantly different from zero.

in the soil water samples is likely to be from the soil rather than the effluent. The suspended solids and the volatile suspended solids were usually so low in the soil water samples as to preclude achieving an accurate measurement. The data which are available show extreme variability in the concentrations measured, with no consistency between cell treatment and the measured concentrations. The suspended solids data were greatly impacted by the presence of fine sand in the pan samples. The sand accumulated in the pan samplers between sampling events and likely reflects washout from the overlying soil. Thus the suspended solids data may more accurately reflect washout events than contributions from the applied wastewater.

The chloride ion concentrations for samples analyzed during this project are shown in Table 11. The effluent concentrations ranged from roughly 78 to 225 mg/L, while the potable water supply ranged from 35 to 61 mg/L. The soil water samples generally fell between these ranges. The no dose and water control cells generally provided the lowest concentrations, but were erratic. There was no significant difference between the high and low effluent flow samples. These data most likely reflect the degree of dilution provided by other soil water within a cell rather than reflecting actual impacts of the amount of effluent applied to a given cell. That ambient soil water can contribute to the chloride signature is evident from the no dose control cell having concentrations ranging from less than one to almost thirty mg/L. The sulfate ion data shown in Table 12 are similar in nature to the chloride ion data. The effluent ranged from 36 to 99 mg/L, but the potable supply had a similar range (12 to 94 mg/L). The soil water sulfate ion concentrations again showed no differentiation between cells treated with either low or high effluent flow rates, untreated or those treated with potable water. These results, like the chloride ion results, indicate that the effluent provides little impact on the sulfate ion concentration of the ground water at this site.

Phosphate ion concentrations for these samples are shown in Table 13. The potable supply, the no dose control cell and the water treatment cells all gave consistently zero or very low concentrations of phosphate ion. Effluent concentrations ranged from roughly

Table 11. Lysimeter Station 1996-1997 Chloride Ion Concentrations (mg/L).

| Sample | | | No Dose | Low Flow (0.75 gal/ft²/day) | | | | High Flow (1.50 gal/ft²/day) | | | |
|---|---|---|---|---|---|---|---|---|---|---|---|
| Date | STE | Tap | C10 | Cell 2 | Cell 5 | Cell 8 | Water Cell 4 | Cell 3[1] | Cell 6 | Cell 9 | Water Cell 7 |
| Jan 31, 97 | 86.06 | 56.28 | - - | 23.97 | 51.94 | 108.9 | 23.54 | 201.0 | 82.54 | 100.3 | 54.65 |
| Feb 28, 97 | 225.2 | 54.15 | - - | 21.29 | 88.20 | 86.01 | 45.14 | 88.97 | 85.44 | 87.42 | 54.50 |
| Mar 25, 97[2] | 91.80 | 41.70 | 6.11 | 17.08 | 16.46 | 25.72 | 34.13 | N/A | 15.73 | 15.09 | 26.46 |
| Apr 15, 97 | 78.34 | 60.75 | 29.91 | 40.31 | 86.05 | 81.27 | 50.06 | 74.97 | 71.76 | 73.93 | 55.54 |
| May 5, 97 | 94.73 | 54.26 | 20.99 | 37.77 | 41.03 | 69.52 | 35.54 | 43.68 | 62.72 | 70.15 | 83.89 |
| July 10, 97 | 78.48 | 38.94 | 0.65 | 36.34 | 52.51 | 49.71 | 5.66 | 8.14 | 69.49 | 50.03 | 50.73 |
| July 10, 97 | | 35.17 | | | | | | | | | |

1. December 5th 1996 sample from cell 3 was analyzed in January and gave a concentration of 77.69 mg/L.
2. STE pump to holding tank was not functioning prior to this sampling event.



Table 12. Lysimeter Station 1996-1997 Sulfate Ion Concentrations (mg/L).

| Sample | | | No Dose | Low Flow (0.75 gal/ft²/day) | | | | High Flow (1.50 gal/ft²/day) | | | |
|---|---|---|---|---|---|---|---|---|---|---|---|
| Date | STE | Tap | C10 | Cell 2 | Cell 5 | Cell 8 | Water Cell 4 | Cell 3[1] | Cell 6 | Cell 9 | Water Cell 7 |
| Jan 31, 97 | 46 | 88 | - - | 165 | 100 | 79 | 165 | 117 | 130 | 88 | 121 |
| Feb 28, 97 | 84 | 93 | - - | 50 | 97 | 91 | 137 | 96 | 94 | 94 | 93 |
| Mar 25, 97[2] | 99 | 12 | 41 | 14 | 43 | 67 | 29 | N/A | 28 | 78 | 15 |
| Apr 15, 97 | 44 | 51 | 28 | 402 | 172 | 236 | 219 | 129 | 196 | 135 | 172 |
| May 5, 97 | 45 | 51 | 280 | 485 | 117 | 144 | 125 | 153 | 137 | 207 | 416 |
| July 10, 97 | 36 | 45 | 27 | 33 | 15 | 20 | 9 | 9 | 20 | 16 | 17 |
| July 10, 97 | | 39 | | | | | | | | | |

1. December 5th 1996 sample from cell 3 was analyzed in January and gave a concentration of 112 mg/L.
2. STE pump to holding tank was not functioning prior to this sampling event.

Table 13. Lysimeter Station 1996-1997 Phosphate Ion Concentrations (mg/L).

| Sample Date | STE | Tap | No Dose C10 | Low Flow (0.75 gal/ft²/day) Cell 2 | Cell 5 | Cell 8 | Water Cell 4 | High Flow (1.50 gal/ft²/day) Cell 3[1] | Cell 6 | Cell 9 | Water Cell 7 |
|---|---|---|---|---|---|---|---|---|---|---|---|
| Jan 31,97 | 3.4 | 0 | - - | 0.18 | 1.03 | 0.68 | 0 | 1.34 | 1.06 | 2.45 | 0 |
| Feb 28, 97 | 4.00 | 0 | - - | 0.39 | 2.24 | 1.50 | 0 | 2.51 | 2.35 | 3.23 | 0 |
| Mar 25, 97[2] | 1.55 | 0.53 | 0 | BLQ | 0.92 | 1.51 | 0 | 0 | 1.22 | 1.39 | 0.42 |
| Apr 15, 97 | 4.13 | BLQ | 0 | 0.21 | 0.83 | 0.71 | 0 | 1.69 | 1.18 | 1.73 | 0 |
| May 5, 97 | 3.89 | 0 | 0 | 0.42 | 1.09 | 2.52 | 0 | 1.42 | 2.17 | 2.07 | 0 |
| July 10, 97 | 4.77 | 0 | 0 | 0.84 | 1.40 | 3.36 | 1.24 | 3.28 | 1.79 | 2.57 | 1.38 |
| July 10, 97 | | 0 | | | | | | | | | |

1. December 5th 1996 sample from cell 3 was analyzed in January and gave a concentration of 1.42 mg/L.
2. STE pump to holding tank was not functioning prior to this sampling event.

1.6 to 4.8 mg/L phosphate ion. Treatment cell 2 (low effluent flow) had consistently low phosphate ion concentrations (0.2 to 0.8 mg/L), just as it had usually had low nitrate concentrations. Otherwise, soil water phosphate concentrations for the effluent treated cells ranged from roughly 0.8 to 3.2 mg/L, with the high effluent loading cells having generally higher phosphate concentrations. This is further illustrated in Figure 2, which shows the 1997 sampling date phosphate and nitrate concentrations from the high and low dose cells as well as the available rainfall data. Another important point observed in this figure is that while the soil water nitrate ion concentrations go to background during the effluent interruption in March, the phosphate ion concentrations are only slightly impacted. This implies that the phosphate ion is reversibly adsorbed to the soil particles and that a decommissioned infiltration bed will continue to be a source of phosphate contamination of groundwater after effluent flow has stopped.

### Virus Transport Model

The report for the subcontract to develop an unsaturated virus transport model and compare it with data generated by the Tampa Branch Laboratory study is included as an Appendix. The model demonstrated that virus transport to groundwater (i.e. the two foot sampling depth) is dependant on soil type, temperature and hydralic loading (either anthropogenic or rain).

## Conclusions and Recommendations

The water quality parameters monitored in this project are traditionally utilized to evaluate the impact of wastewater discharge on a receiving water. In this research the receiving water in question is the groundwater underlying the infiltration beds of an onsite wastewater disposal facility. In this context, the current study can be considered an evaluation of the potential breakthrough (failure) of the treatment zone by contaminants present in domestic wastewater into the underlying groundwater. The results of this investigation indicate that the infiltration beds of a well designed and constructed onsite wastewater treatment and disposal system effectively remove most

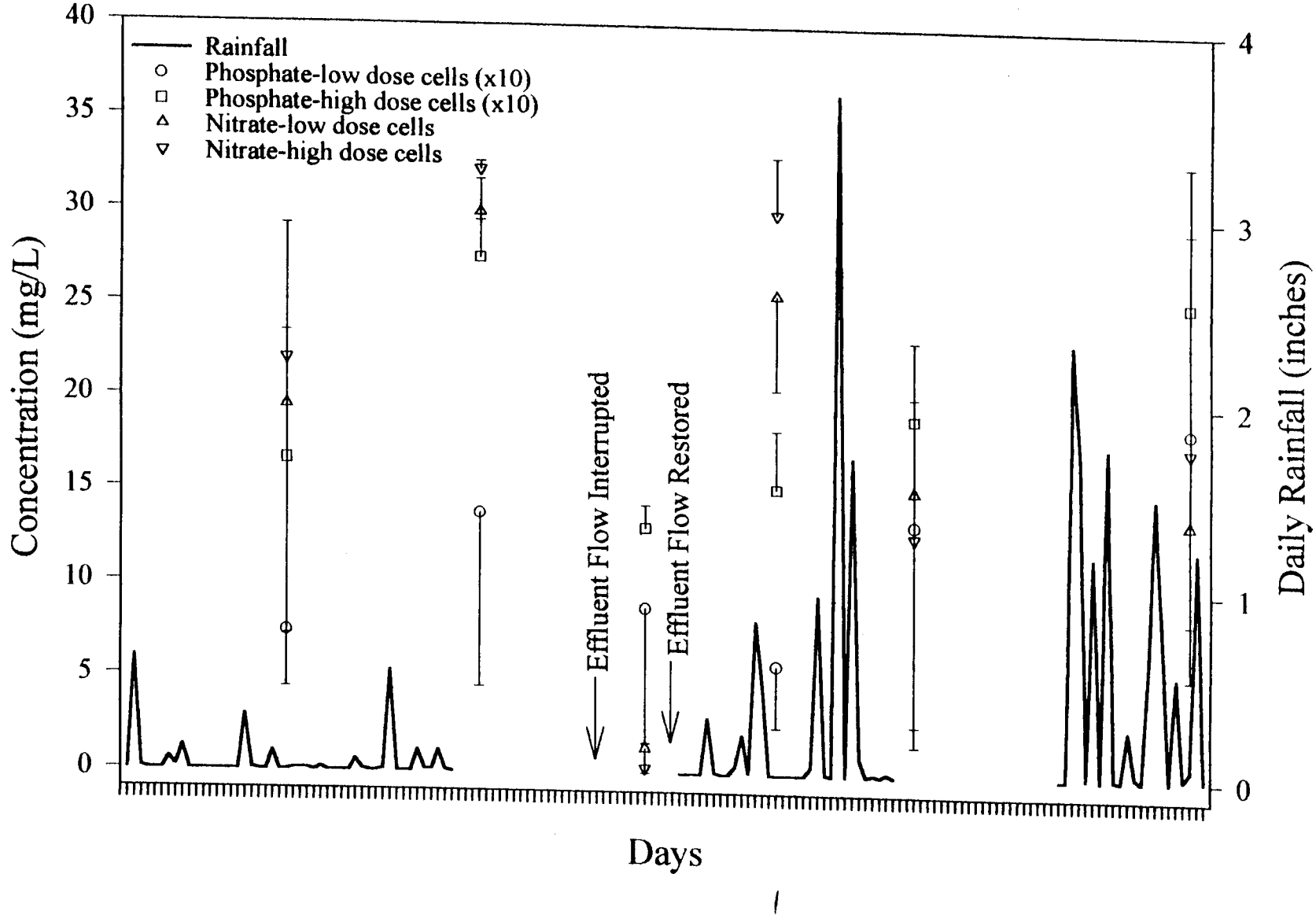
Rainfall
Phosphate-low dose cells (x10)
Phosphate-high dose cells (x10)
Nitrate-low dose cells
Nitrate-high dose cells
Concentration (mg/L)
Daily Rainfall (inches)
Effluent Flow Interrupted
Effluent Flow Restored
Days
0
5
10
15
20
25
30
35
40
0
1
2
3
4

contaminants of concern in a normal domestic wastewater. The data do indicate that the infiltration beds may be a source of nitrate and phosphate contamination of the underlying groundwater system. The virus transport model indicates that under certain environmental conditions (low temperature, high water flows) these systems may also allow viable virus to enter the underlying groundwater.

The results of these studies suggest that in addition to the ongoing virus transport studies which should clarify the potential of virus transport to groundwater, it may be advisable to consider further investigation conditions which provide greater saturated flow in the treatment zone. This could be done as an evaluation of the impact of external hydraulic loading (simulated rainfall), or the experimental system could be modified to provide less unsaturated soil. The former of these could be readily achieved once the groundwater well at the research site is returned to operation, the latter would require the facilty to be extensively modified. Another avenue of further research would entail the replacement of the existing infiltration beds with other types of soils to compare their treatment efficiencies to the fine grain sand native to this site.

## References

Ayers Associates 1993. Onsite sewage disposal system (OSDS) research in Florida. The capability of fine sandy soil for septic tank effluent treatment: A field investigation at an *in-situ* lysimeter facility in Florida. Report to the Florida State Department of Health and Rehabilitative Services. Contract LP-596.

# Appendix:

## Predicting Virus Transport in Lysimeters

by:

Marylynn V. Yates

TABLE OF CONTENTS


| | PAGE |
|---|---|
| INTRODUCTION | 4 |
| LYSIMETER FACILITY SITE DESCRIPTION | 4 |
| HYDRUS-2D | 6 |
| ***Description of Model*** | 6 |
| ***Finite Element Mesh*** | 8 |
| ***Boundary Conditions*** | 8 |
| *Water Flow Boundary Conditions* | 8 |
| *Solute Transport Boundary Conditions* | 10 |
| *Initial Conditions* | 10 |
| ***Implementation of HYDRUS-2D*** | 10 |
| ***System Configuration*** | 11 |
| ***Finite Element Grid Configurations*** | 13 |
| ***Calibration*** | 17 |
| PREDICTING TRANSPORT IN TWO-FOOT CELLS | 28 |
| ***Bromide Transport, Fine Sand, High Dose*** | 28 |
| ***Virus Transport, Fine Sand, High Dose*** | 30 |
| ***Effect of Inactivation Rate on Virus Transport*** | 38 |
| ***Effect of Soil Type on Virus Transport*** | 40 |
| *Sandy Loam Soil* | 40 |
| *Loam Soil* | 45 |
| ***Effect of Rainfall on Virus Transport*** | 51 |
| EFFECT OF COLLECTION PAN ON TRANSPORT | 54 |
| PREDICTING TRANSPORT IN FOUR-FOOT CELLS | 59 |
| DISCUSSION | 66 |
| REFERENCES | 71 |
| APPENDIX 1: MODEL TESTING | |
| APPENDIX 2: ATMOSPHERIC INPUT DATA | |
| APPENDIX 3: SIMULATION DETAILS | |

## LIST OF FIGURES


| FIGURE | PAGE |
|---|---|
| 1 Cross Section of Lysimeter Facility at the University of South Florida | 5 |
| 2 Grid 3 Configuration | 12 |
| 3a-c Nodal Configurations | 14-16 |
| 4a Soil-Moisture Release Curve for Fine Sand | 18 |
| 4b Hydraulic Conductivity Curve for Fine Sand | 18 |
| 5 Test Bromide Breakthrough Curve for Fine Sand, Low Dose, 2 Foot Cell | 20 |
| 6 Bromide Breakthrough Curve for Fine Sand, Low Dose, 2 Foot Cell | 21 |
| 7a-f Bromide Color Contours During Transport | 22-27 |
| 8 Bromide Breakthrough Curve for Fine Sand, High Dose, 2 Foot Cell | 29 |
| 9a Virus Breakthrough Curve for Fine Sand, High Dose, 2 Foot Cell, $\mu$= 0.33 | 32 |
| 9b Virus Breakthrough Curves for Fine Sand, High Dose, 2 Foot Cell, $\mu$ = 0.33 | 33 |
| 10a-d Virus Color Contours During Transport | 34-37 |
| 11 Effect of Inactivation Rate on Virus Transport, Fine Sand, High Dose, 2 Foot Cell | 39 |
| 12 Grid 1 Configuration | 41 |
| 13 Bromide Breakthrough Curves, Grids 3 and 1, Low Dose, 2 Foot Cell | 42 |
| 14a Soil-Moisture Release Curve for Sandy Loam | 43 |
| 14b Hydraulic Conductivity Curve for Sandy Loam | 43 |
| 15 Virus Breakthrough Curve for Sandy Loam, Low Dose, 2 Foot Cell, $\mu$ = 0 | 44 |
| 16 Virus Breakthrough Curve for Sandy Loam, Low Dose, 2 Foot Cell, $\mu$ = 0.25 | 46 |
| 17a Soil-Moisture Release Curve for Loam | 47 |
| 17b Hydraulic Conductivity Curve for Loam | 47 |
| 18 Virus Breakthrough Curve for Loam, Low Dose, 2 Foot Cell, $\mu$ = 0 | 49 |
| 19 Virus Breakthrough Curve for Loam, Low Dose, 2 Foot Cell, $\mu$ = 0.25 | 50 |
| 20 Virus Breakthrough Curves for Different Soils, R = 1, $\mu$ = 0 | 52 |
| 21 Virus Breakthrough Curves for Different Soils, $\mu$ = 0 | 53 |
| 22a Effect of Rainfall on Virus Transport, R=1, $\mu$ = 0 | 55 |
| 22b Effect of Rainfall on Virus Transport, R=1, $\mu$ = 0.33 | 56 |
| 23 Grid 4 Configuration | 57 |
| 24 Bromide Breakthrough Curve, Low Dose, 2 Foot Water Table | 58 |

LIST OF FIGURES


| FIGURE | | PAGE |
|---|---|---|
| 25 | Bromide Breakthrough Curve, High Dose, 2 Foot Water Table | 60 |
| 26 | Virus Breakthrough Curve, Low Dose, 2 Foot Water Table, $\mu = 0$ | 61 |
| 27 | Virus Breakthrough Curve, High Dose, 2 Foot Water Table, $\mu = 0$ | 62 |
| 28 | Grid 4 Configuration, Four-Foot Water Table | 63 |
| 29 | Bromide Breakthrough Curve, Low Dose, 4 Foot Water Table | 64 |
| 30 | Bromide Breakthrough Curve, High Dose, 4 Foot Water Table | 65 |
| 31 | Virus Breakthrough Curve, High Dose, 4 Foot, Grids 3 and 4, $\mu = 0$ | 67 |
| 32 | Virus Breakthrough Curve, High Dose, 4 Foot, Grids 3 and 4, $\mu = 0.33$ | 68 |
| 33 | Virus Breakthrough Curve, High Dose, 4 Foot, $\mu = 0.33$, intermediate depths | 69 |

## INTRODUCTION

The purpose of this project was to model the fate and transport of viruses in septic tank effluent through a leach field. Data from a bromide tracer study conducted in February 1996 at the USF Lysimeter site were used to calibrate the model. The calibrated model was used to predict the behavior of viruses during a tracer study conducted in April 1997. The calibrated model was then used to predict virus behavior under a variety of theoretical scenarios, including different soils and different environmental conditions (e.g., rainfall and temperature). Predictions of virus transport in the four-foot infiltration cells were also made.

## LYSIMETER FACILITY SITE DESCRIPTION

The lysimeter facility was constructed to emulate an actual septic tank system and leach field. The site consists of 20 infiltration cells, which are separated from one another to prevent wastewater movement between cells, allowing individual cell operation. The cells were constructed by installing stainless steel pans at either 2 ft or 4 ft depths in the native soil in a manner to limit disturbance of the soil. Two water tables are maintained artificially at the site; one at two ft and the other at four ft depth. Thus, one-half of the cells have a 2-ft unsaturated zone, and the other half have a 4-ft unsaturated zone for contaminant removal.

Each of the cells has an infiltration surface measuring 2 ft by 6 ft. Nine inches of gravel was placed on the top of the infiltration surface to aid in distribution of the wastewater to the soil surface. Wastewater is applied to the cells by means of a 1-inch diameter perforated pipe that runs the length of the cell, that was placed on top of the gravel. Three inches of gravel was placed over the pipe, which was then covered with a 12-inch layer of the native soil. Leachate can be collected from the cells by means of suction cups which were installed at 6", 12", and 2 ft (12", 2', and 4' in the 4-ft cells). A cross-sectional view of the lysimeter facility is shown in Figure 1.

The cells are dosed with wastewater from a nearby facility's septic tank through individual dose pots that feed the perforated pipe in each cell. One-half of the cells are dosed at a rate of 0.75 gpd/ft$^2$; the other half are dosed with 1.5 gpd/ft$^2$. The wastewater is applied to the cells in 6 equal doses throughout the day at 6 a.m., 7 a.m., 12 p.m., 6 p.m., 7 p.m., and 8 p.m.

Figure 1. Cross-Section of Lysimeter Facility at the University of South Florida

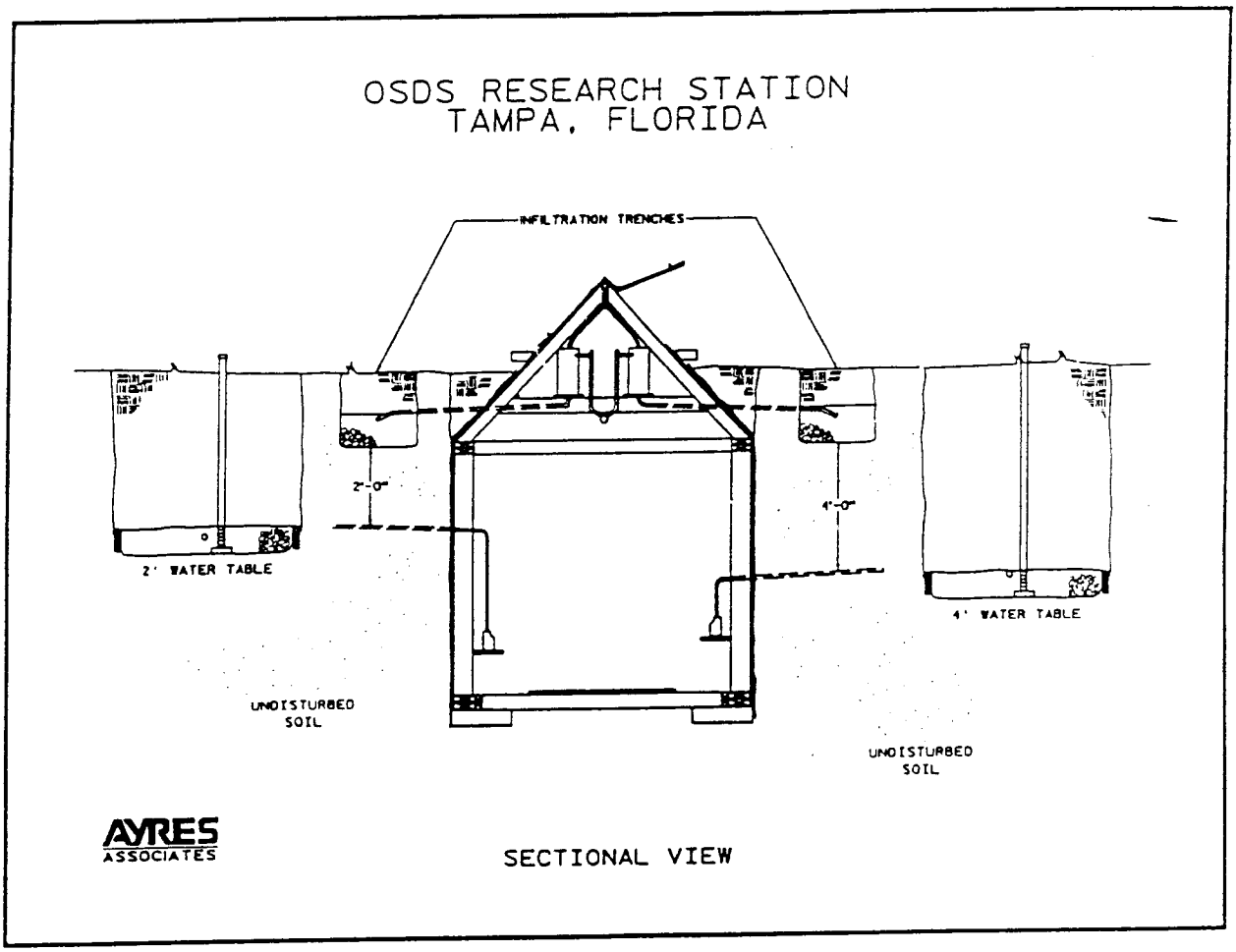

## HYDRUS-2D

### *Description of Model*

HYDRUS-2D couples a Windows®-based graphical user interface, mesh generator and graphical output routines to the SWMS-2D simulation algorithm. SWMS-2D (Simunek and van Genuchten, 1994) is a comprehensive two-dimensional finite element model which can be used to simulate the fate and transport of solutes in soil. The model uses the Galerkin finite element procedure to solve the two-dimensional nonlinear partial differential equations for simultaneous transport of water and solutes in a variably saturated porous medium. A first-order solute decay reaction during transient water flow can be considered for solutes in liquid and/or solid phases. For a nonvolatile organic chemical or colloidal particles which are transported as solutes, the governing transport equation can be written as (Simunek and van Genuchten, 1994):

*Water Flow*

$$\frac{\partial \theta}{\partial t} = \frac{\partial}{\partial x_i}\left[ K_{ij}(h)\ \frac{\partial h}{\partial x_j} + K_{iz}(h) \right] - S \qquad (1)$$

$$K(h) = K_s \frac{\left[1 - \beta^{n-1}(1+\beta^n)^{\frac{1-n}{n}}\right]^2}{\left[1+\beta^n\right]^{\frac{n-1}{2n}}}; \qquad \beta = \alpha |h| \qquad (2)$$

$$\theta(h) = \theta_r + \frac{\theta_s - \theta_r}{\left[1+\beta^n\right]^{\frac{n-1}{n}}} \qquad (3)$$

where $\theta$, is the volumetric water content, $h$ is the hydraulic head, $K(h)$ is the unsaturated hydraulic conductivity, $K_s$ is the saturated hydraulic conductivity and S is a source or sink term. The $\theta_r$ is the residual water content and $\theta_s$ is the saturated water content. The parameters $\alpha$ and $n$ are used to fit the moisture release and unsaturated hydraulic conductivity functions to measured data. For a two-dimensional system, $i$ and $j$ take on the values 1 and 2.

*Solute Transport*

$$\frac{\partial \theta C_l}{\partial t} + \frac{\partial \rho_b C_s}{\partial t} = \frac{\partial}{\partial x_i}\left(\theta D_{ij}^{w} \frac{\partial C_l}{\partial x_i}\right) - \frac{\partial q_i C_l}{\partial x_j} - \theta \mu_l C_l - \rho_b \mu_s C_s - S_r C_r \qquad (4)$$

where $C_L$ and $C_S$ are solute concentrations for the liquid and solid phases, respectively; $q$ is the volumetric flux density; $\mu_w$ and $\mu_s$ are first-order rate constants for solutes in the liquid and solid phases, respectively; $\rho$ is the soil bulk density, $S_r$ is the sink term in the water flow, $C_r$ is the concentration of the sink term, $D_{ij}^{w}$ is the dispersion coefficient tensor for the liquid phase, and $D_{ij}^{g}$ is the diffusion coefficient tensor for the gas phase; $t$ is time, $x$ is distance, and indices $i$ and $j$ represent the horizontal and vertical directions.

The individual components of $\theta D_{ij}$ in the soil matrix for two-dimensional transport are:

$$\theta D_{xx} = D_L \frac{q_x^2}{|q|} + D_T \frac{q_z^2}{|q|} + \theta D_w \tau_w$$

$$\theta D_{zz} = D_L \frac{q_z^2}{|q|} + D_T \frac{q_x^2}{|q|} + \theta D_w \tau_w \qquad (5)$$

$$\theta D_{xz} = (D_L - D_T) \frac{q_x q_z}{|q|}$$

where $D_L$ and $D_T$ are the longitudinal and transverse dispersivities; $q_x$ and $q_z$ are the components of the Darcian fluid flux density; $D_w$ is the molecular diffusion coefficient in free water and $\tau_w$ is the tortuosity factor for the liquid phases. While $\tau_w$ was calculated from the widely used Millington-Quirk equation (Millington and Quirk, 1960):

$$\tau_w = \frac{\theta^{10/3}}{\phi^2} \qquad (6)$$

where $\phi$ was soil porosity.

***Finite Element Mesh***

An external program MESHGEN was used to discretize the two-dimensional flow region into an unstructured triangular mesh. This algorithm is run from the HYDRUS-2D menu system and can be used for any flow region consistent with certain rules concerning connectedness of the bounding lines. The first step is to produce the boundaries of the flow region. Next, is the discretization of boundary curves. The boundary nodes are automatically (default) placed equal distance around the boundary. The module has features to increase the number of boundary nodes, or change the nodal density in certain regions (i.e., where high gradients are expected).

The second step is mesh generation which consists of five steps: 1) Basic Triangulation, 2) Refinement, 3) Remeshing, 4) Smoothing, 5) Convexity check. An iterative procedure is used to repeat steps 2 to until no new points are needed.

Although this procedure can be accomplished manually, the program has an option to automatically generate the mesh. Smoothness of the finite element mesh is controlled by the user using a smoothing factor which influences the permitted changes in size between two adjacent triangles.

***Boundary Conditions***

Once the mesh is generated, the conditions at the boundary of the flow domain must be specified. A variety of boundary conditions can be simulated using HYDRUS-2D. The boundaries are specified using the module BOUNDARY. This module is used to enter specific initial and boundary conditions for both water flow and solute transport, as well as the distribution of soil materials, root water uptake, anisotropy coefficients, among other parameters.

*Water Flow Boundary Conditions*

*No-flux boundary conditions* are specified for impermeable boundaries where the component of the flux perpendicular to the boundary is zero. Examples of no-flux boundaries include impermeable layers, walls or other structures in the flow domain which form boundaries that are impervious to flow or transport.

*Constant pressure-head boundary condition.* Along this boundary, the value for the pressure head remains constant throughout the simulation. Examples of constant

pressure head boundary condition are: constant groundwater or perched ground-water level, infiltration into a constant-head ring infiltrometer, and ponding in a furrow (if constant).

*Constant flux boundary conditions* are specified along boundaries where the rate of water during a particular time period perpendicular to the boundary remains constant. Examples of constant flux boundary conditions include: sprinkler irrigation, precipitation and infiltration into soil from a slotted pipe.

*A Seepage face boundary condition* occurs where water leaves the saturated part of a flow domain through seepage face. The seepage face forms only when the matric potential is greater than or equal to zero (i.e., no soil suction). The length of the seepage face is not known a priori and changes with prevailing conditions. The algorithm was written so that the pressure head is always uniformly equal to zero along the saturated part of a seepage face, and that the outflow flux is equal to zero on the unsaturated part of a seepage face boundary. Examples of seepage faces include seeps from hillslopes and water accumulating at a pan placed in soil and intercepting water infiltrating from a source.

*A free drainage boundary condition* can be used to allow water to leave a flow domain under conditions non-forced drainage conditions (i.e., no externally imposed head or flux). Free drainage simulates gravity drainage and assumes a unit vertical hydraulic gradient. This situation is often observed in field studies of water flow and drainage/redistribution in the unsaturated soil. The conditions is a reasonable boundary condition at the bottom of a flow domain for situations where the water table is located far below the study zone.

*Variable pressure head and variable flux boundary conditions* These conditions extend the constant head and constant flux boundary conditions described above. They are used to simulate variable groundwater level, pulsing of water input into the system, etc.

*An atmospheric boundary condition* is used to incorporate the effects of precipitation, evapotranspiration, root-water uptake along with variable head and variable flux

boundary conditions. The potential fluid flux across the soil surface is determined by the variable rSoilPrec, but the actual surface flux is calculated internally by the program. Two limiting values for the surface pressure head must be provided. The first is hCritS and specifies the maximum allowed pressure head at the soil surface. The second is hCritA which specifies the minimum allowed surface pressure head. The program automatically switches between Dirichlet and Neumann boundary conditions if one of these two limiting points is reached.

*Solute Transport Boundary Conditions*

*No-flux boundary conditions* are specified for impermeable boundaries where the component of the solute flux perpendicular to the boundary is zero. Impermeable walls or planes of symmetry are examples of no-flow boundary conditions.

*Dirichlet, (or first-type)* boundary conditions are used when the concentration along a boundary is known.

*Cauchy, (or third-type)* boundary conditions are used when the solute flux along a boundary is known.

*Initial Conditions*

The initial hydraulic head and, therefore, the water content of the soil was determined specifying an equilibrium distribution of the pressure head with depth starting with the lowest point in the flow domain. Generally, the value of the head at the lowest point of the flow domain was set such that the water content was at saturation.

***Implementation of HYDRUS-2D***

Before performing any simulations, the model was tested for numerical accuracy by comparing it to analytical solutions for simplified cases. A more detailed description of the testing is provided in Appendix 1. Variably-saturated water flow was simulated using the Richards' equation (i.e., Eq. 1) with the unsaturated soil hydraulic functions described by a set of closed-form equations of van Genuchten (1980). Five parameters,

$\theta_r$, $\theta_s$, $\alpha$, $n$, $K_s$, are required by the model. Of these, $\theta_r$ and $\theta_s$ represent residual and saturated volumetric soil water content; $\alpha$ and $n$ are characteristic hydraulic parameters of the soil. Because a mean $K_s$ value was found to be about 5.0 cm/day, the remaining four parameters were taken to be those of the silt loam G.E. 3 of van Genuchten (1980), leading to the following values: $\theta_r$ = 0.131, $\theta_s$ = 0.396, $\alpha$ = 0.00423 (1/cm), and n = 2.06.

The boundary conditions used in the simulation are determined by the type of water application methods involved. The wetted area was assumed to be at water saturation (h -> 0). The remaining part of the soil surface was again subjected to evaporation.

Because of symmetry, a zero flux boundary condition was used for the sides of the simulation domains. A unit flux boundary condition was used for the bottom boundary. An initial soil water pressure head of -150 cm was used. The simulation involved only one application event, which was initiated on day 5, whereas the simulation itself was run for 15 days to allow sufficient time for redistribution.

***System Configuration***

The mathematical representation of the lysimeter system was configured to match the actual conditions at the research facility, as closely as possible. The general configuration for a cell with a two-ft unsaturated zone is shown in Figure 2. Wastewater enters the system through the perforated pipe which is located in a zone of gravel that measures 12 inches deep by two feet wide by 6 feet long. Above the gravel zone is 12 inches of the native soil that is open to atmospheric influences such as evapotranspiration and rainfall. Below the gravel zone is 2 (or 4) feet of native soil and is the test zone. Below this zone a stainless steel pan was installed to capture infiltrating water. Mathematically, this can be represented by a seepage face boundary condition. To the left of the pan, and at the same depth, is a constructed perched water table. The water from this flows towards the pan since this side of the reservoir is 0.1 foot lower than the others. Between the perched water table and the seepage face boundary is a free drainage zone, comprised of the native soil, which is approximately 6 inches wide. Water from the pan leaves the system through the free drainage zone, flows out through the seepage face (when soil conditions are appropriate), or into a

# Figure 2. Grid 3

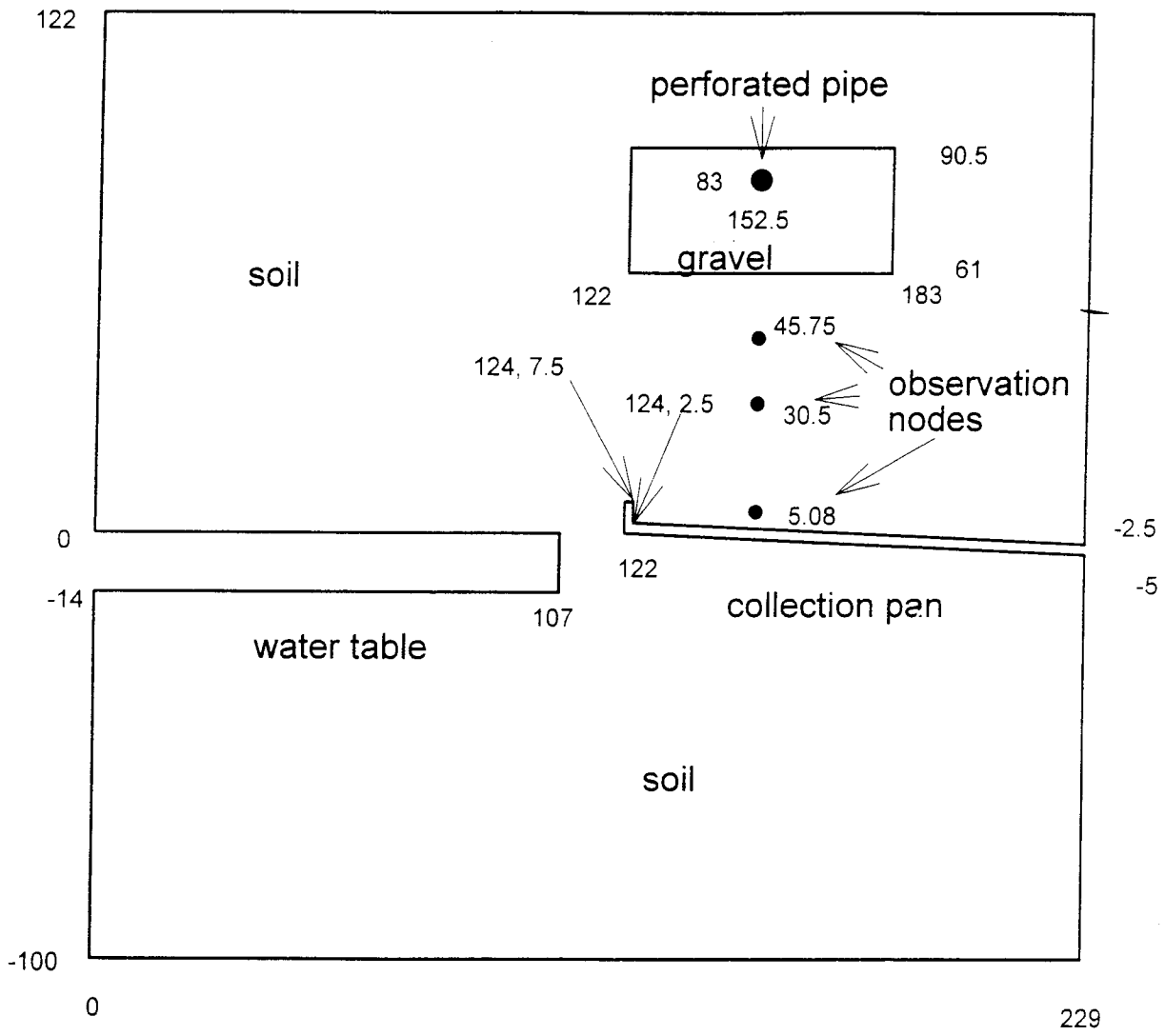

collection device during sampling. During the simulations, water was never observed to flow out of the pan into an collection device except when there was a very heavy rainfall event. This numerical observation corresponds to the observations made by the individuals who collect samples at the site: a vacuum must be applied to the soil in order to obtain a sample for analysis unless there is a very heavy rainfall. Therefore, all concentration readings were obtained from an observation node placed 2 inches above the collection pan and centered under the inflow pipe. Also, two or three other observation nodes where installed at a position half the distance between the pipe and pan, at one quarter the distance, and for the four foot test zones, at 1 eighth the distance.

***Finite Element Grid Configurations***

Several different grids were tested to determine which one gave the best results. Considerations in selecting an appropriate grid included computational time required to perform a simulation, convergence, and numerical error. For most simulations, the default settings for the grid generator provided a grid configuration that produced an accurate simulation of transport for a 20-30 day simulation period using 6 to 12 hours of computer time. When simulating virus transport including the effects of adsorption (i.e., R=10; $t_{max}$=110 days), the simulation times were greater than 18 hours.

Shown in Figures 3a-c are the finite element grid patterns for the three cases studied. Grid 3 (Figure 3a) most closely represents the physical system and was used wherever possible. For some conditions, the finite element solution would not converge and an alternate grid structure was found to produce very similar solutions and not suffer from convergence problems. This is shown in Figure 3b as Grid 1. The third grid system represents a natural condition where the ground water table is located at 2 or 4 feet and flow from the inlet pipe is not influenced by the collection pan or perched water table. This is shown in Figure 3c and is termed Grid 4. A fourth grid system (Grid 2), where the gravel was assumed to be absent and the flow of water was uniformly distributed at the soil-test-zone surface, was found to produce unrealistic results and will not be discussed further.

**Figure 3a. Finite Element Grid 1**

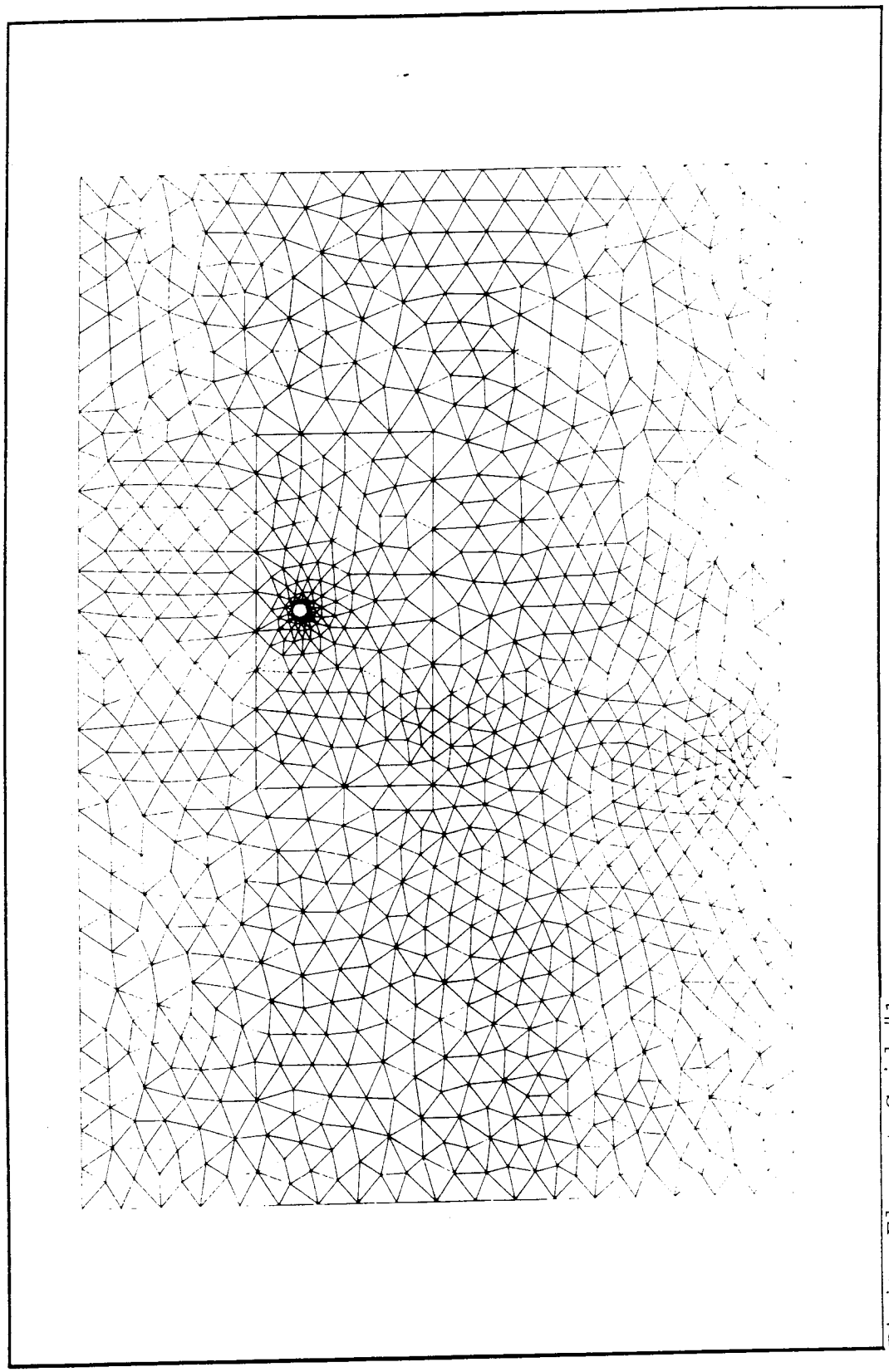

**Figure 3b. Finite Element Grid 3**

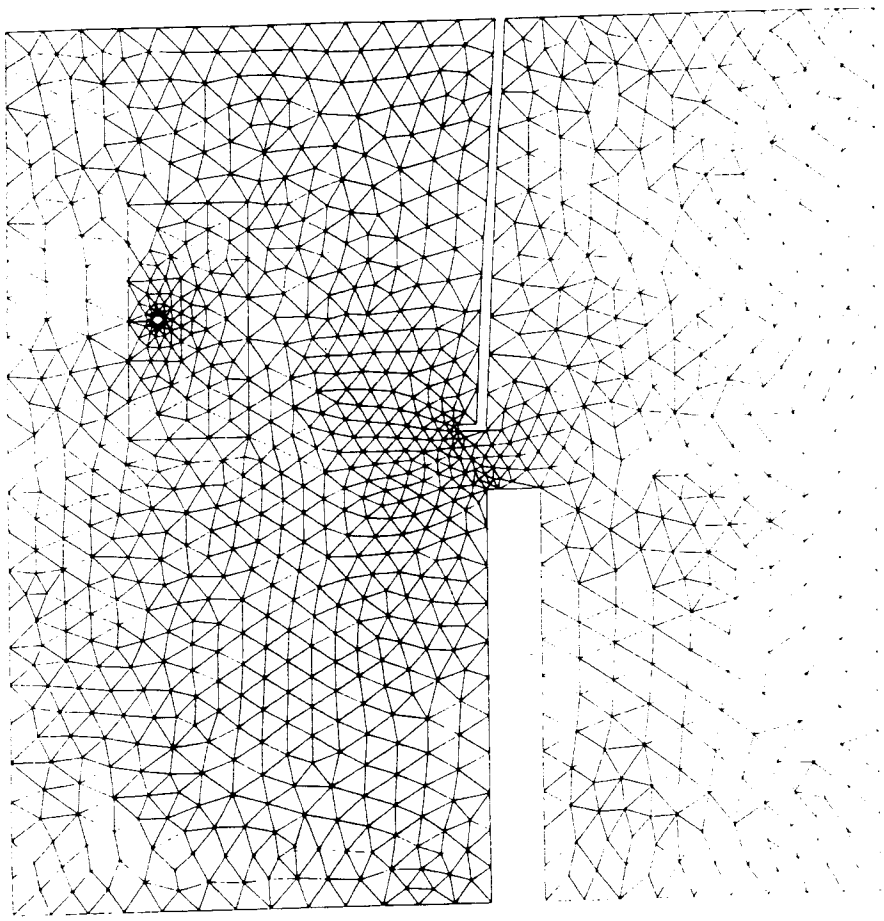

Finite Element Grid #3

**Figure 3c. Finite Element Grid 4**

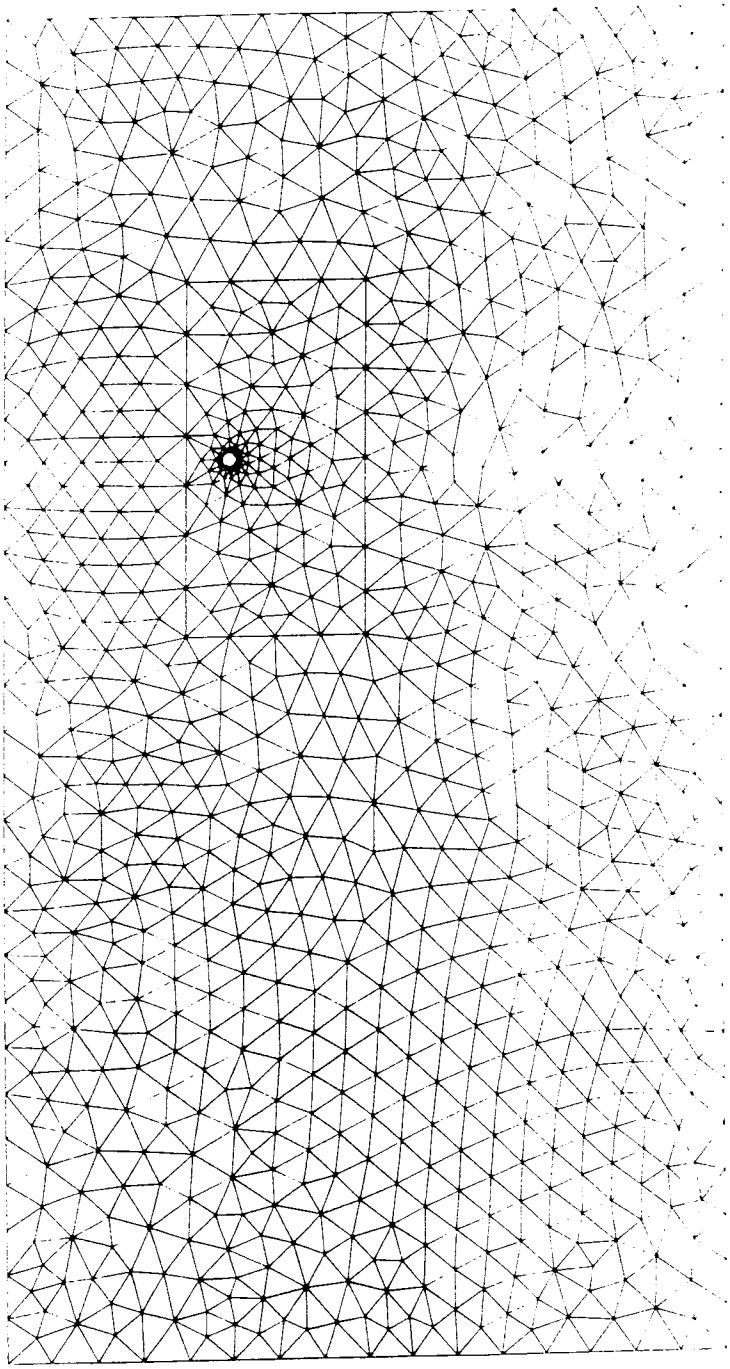

Finite Element Grid #4

### *Calibration*

The model was calibrated using data obtained from the February 1996 tracer experiment performed on the 2-ft cell receiving the low dose of wastewater. To conduct the simulation, the three-dimensional physical system must be rendered into an equivalent two-dimensional system. This was accomplished by distributing all water and chemical inputs over either the entire 12' length of the lysimeter, or some smaller length, as described below. Ten grams of bromide were added to each cell in a total volume of 500 ml water at 4:30 p.m. over a 10-minute period. The wastewater was added to the cell 6 times per day at the times and volumes used during the actual tracer study. The atmospheric inputs were obtained from the weather station on site (Appendix 2). The evapotranspiration was assumed to be 0.5 cm/d (Jury et al., 1983) during daylight hours (600 to 1800) and zero, otherwise.

The soil properties required as model input are shown in Table 1. In addition, the soil-water release curve and the hydraulic conductivity curve for the fine sand are shown in Figure 4. Most of the properties were measured by Ayres, Associates. However, values for some of the parameters were unknown and had to be taken from the library of default values contained in HYDRUS-2D. None of the properties of the gravel were known; these had to be assumed using best professional judgment. The values used for the hydraulic properties of the gravel are shown in Table 1.

Table 1. Hydraulic properties of fine sand and gravel used in simulations

| Property | Fine Sand | Gravel |
|---|---|---|
| soil bulk density, $\rho_b$ | 1.5 | 1.5 |
| residual moisture content, $\theta_r$ | 0.02 | 0.02 |
| saturated moisture content, $\theta_s$ | 0.414 | 0.414 |
| vanGenuchten parameters: | | |
| $\alpha$ | 0.0183 | 0.0183 |
| n | 3.88 | 3.88 |
| saturated hydraulic conductivity, $K_s$ | 549 | 1500 |

# Figure 4. Properties of Fine Sand

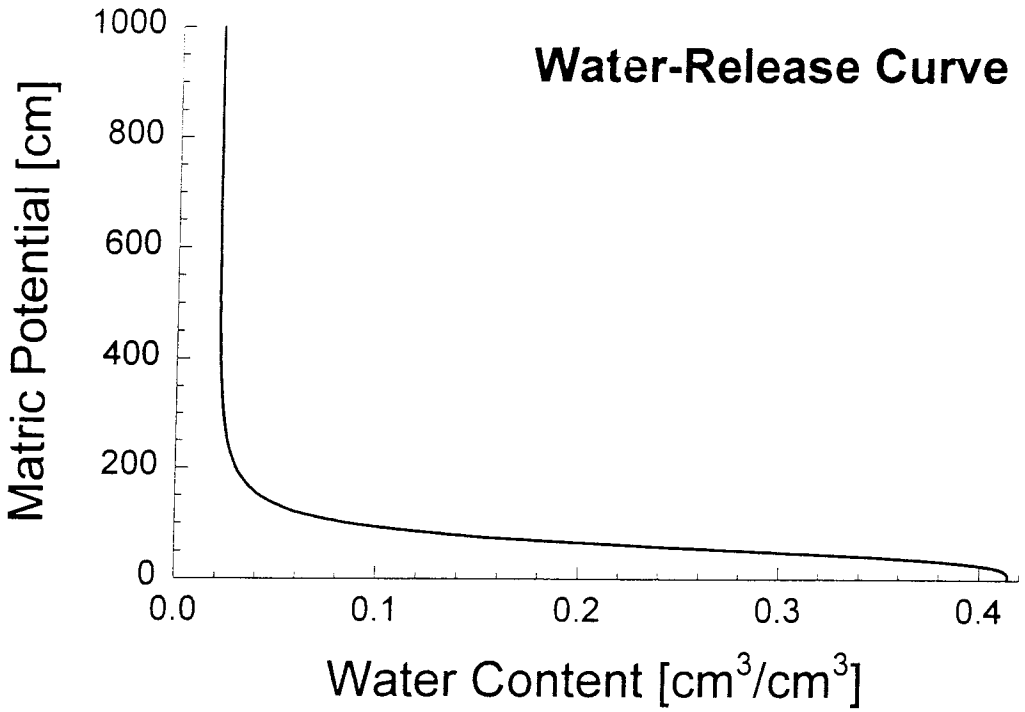


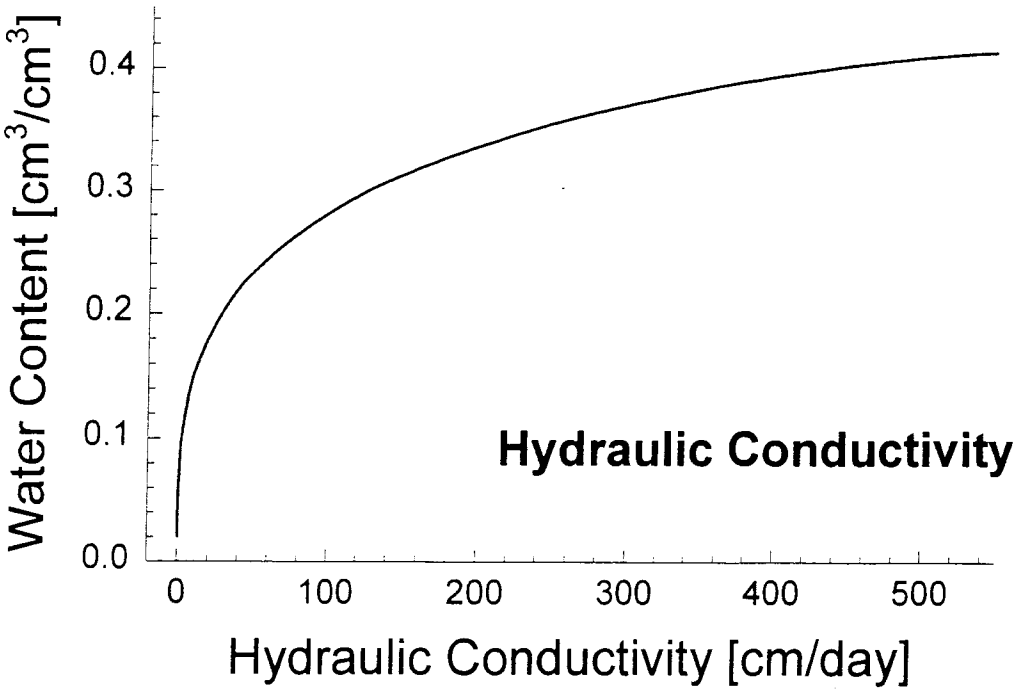

The tracer experiment in 1996 was performed by adding to bromide to the dose pot, which feeds the perforated pipe in the infiltration cell. In the initial simulations, it was assumed that the tracer was added to the cells along the entire length of the pipe (6 ft) and spread out laterally with the infiltrating water a radial distance of .067 inches away from the pipe. This results in an infiltration volume of 500 mL. The results of these simulations gave peak concentrations of bromide that were extremely low compared to the measured values - on the order of 10-20 mg/L (see Figure 5).

In order to resolve this large discrepancy between the measured values and the predicted concentrations, the possibility that the tracer was not being applied through the entire length of the pipe was considered. Since for some experiments, the water was input through a 4" diameter PVC pipe, yielding an infiltrative surface area of 12.6 $in^2$ (81 $cm^2$), to determine the consequence of this method for introducing the viruses, the length of pipe to which the tracer was applied to the lysimeter was reduced from 6 ft (183 cm) to 0.3 ft (10.2 cm). This resulted in a breakthrough curve that was very similar to the measured values. It is suspected that even when the viruses were added to the infiltration pipe, that only a small section was hydraulically active. Much of the variability in the measured values may be due to slight differences in how each lysimeter was construction. Factors such as the how level the pipe was installed, any bowing of the pipe, clogging of the slots, etc. could have affected the uniformity of the application. Shown in Figure 6 are the breakthrough curves for the 4 infiltration cells that received the low dose of wastewater. Because there was considerable variability in the measured values between the 4 cells, two curves are shown: one for the low range (- 1 standard deviation from the mean) and the other for the high range (+1 standard deviation from the mean). The predicted breakthrough curve simulates the measured curves very well: the predicted peak value occurred at approximately 4 days after introduction of the tracer, just as the measured values did, and the predicted peak concentration was approximately 350 mg/L, which is within the measured range of 150 to 600 mg/L.

The distribution of the bromide as it was transported through the infiltration cell at several times (0.08 d, 0.1 d, 2 d, 5 d, and 7 d) is shown in Figures 7a-f. Figure 7a shows the water flow pattern in the infiltration cell, indicating that a large amount of water passes through the free drainage zone between the collection pan and the

# Figure 5. Test Bromide Breakthrough Curve

## 2 ft, fine sand, low dose

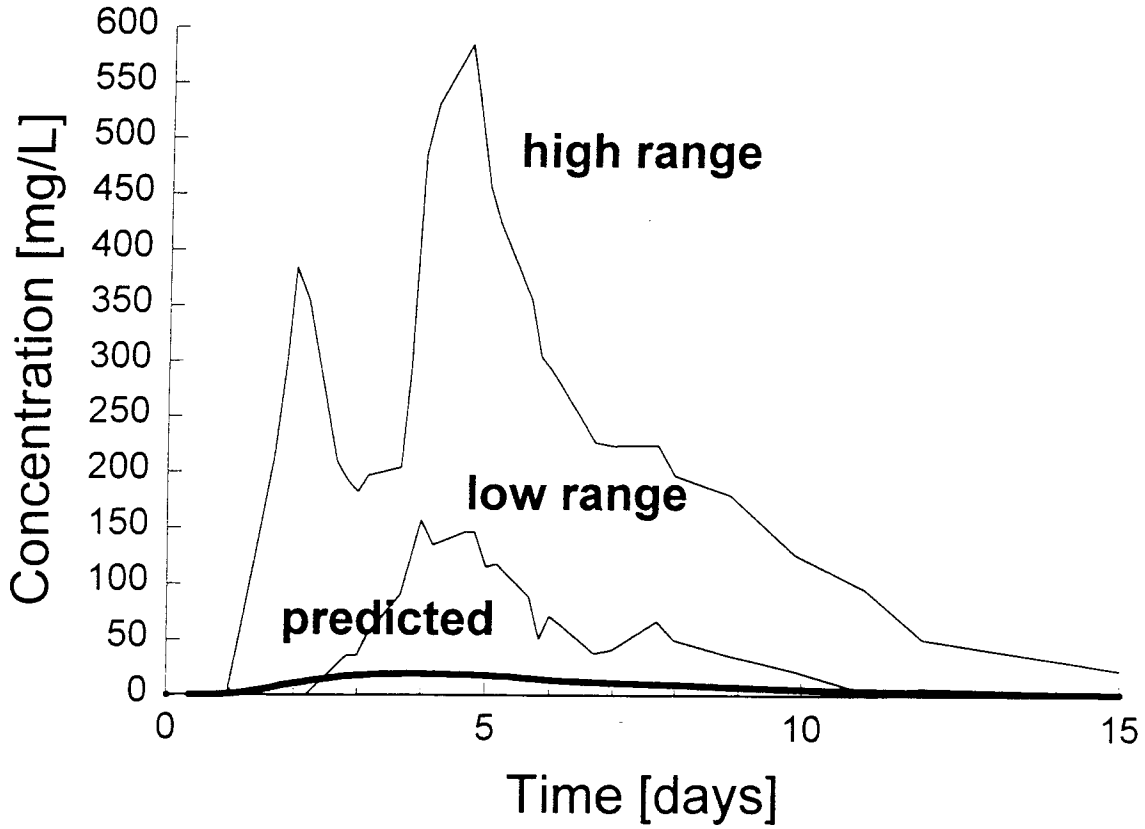

# Figure 6. Bromide Breakthrough Curve

## 2 ft, fine sand, low dose

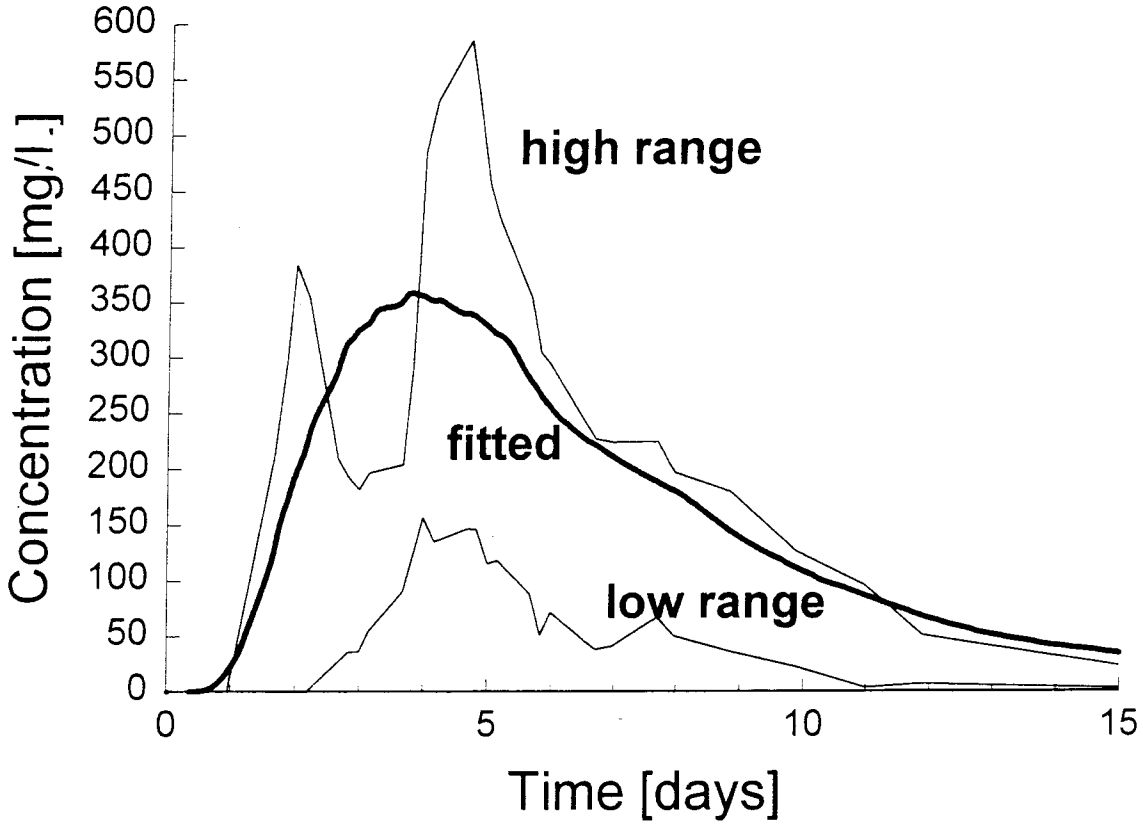

perched water table. Examination of Figures 7d-7f shows the effect of this water movement on the transport of the bromide. It can be seen that some of the bromide mass is lost as the water is diverted around the collection pan through the adjacent soil.

Appendix 3 contains more complete information about the results of each of the simulations described in this report. The curves include:

- the bromide or virus concentration at the observation points (6", 12", and 2' (in the case of the 4-ft cells))
- the bromide or virus concentration at the sampling point
- the cumulative solute flux into the lysimeter (gives the total mass in the 2-D system)
- the solute flux at the free drainage boundary (when present)
- the solute flux at the perched water table (when present)
- the solute flux at the seepage face (i.e., the pan, when present)
- the hydraulic head at the sampling point
- the water content at the sampling point

as a function of simulation time.

## PREDICTING TRANSPORT IN TWO-FOOT CELLS

### *Bromide Transport, Fine Sand, High Dose*

The calibrated model that resulted from the simulations in the cells receiving the low dose (0.75 gpd/ft$^2$) of wastewater was then used to predict bromide transport in the infiltration cells that receive wastewater at the high dose (1.5 gpd/ft$^2$). The predicted breakthrough curve is compared to the measured high- and low-range curves in Figure 8. The predicted peak occurred at approximately the same time as the measured peak for the high range, although it was slightly later than that for the low range curve. The most significant difference is in the predicted peak concentration, which was approximately 250 mg/L, compared to 325 mg/L for the low range and 800 mg/L for the high range. Overall, it was felt that the model performed well in simulating the measured data.

# Figure 8. Bromide Breakthrough Curve

## 2 ft, fine sand, high dose

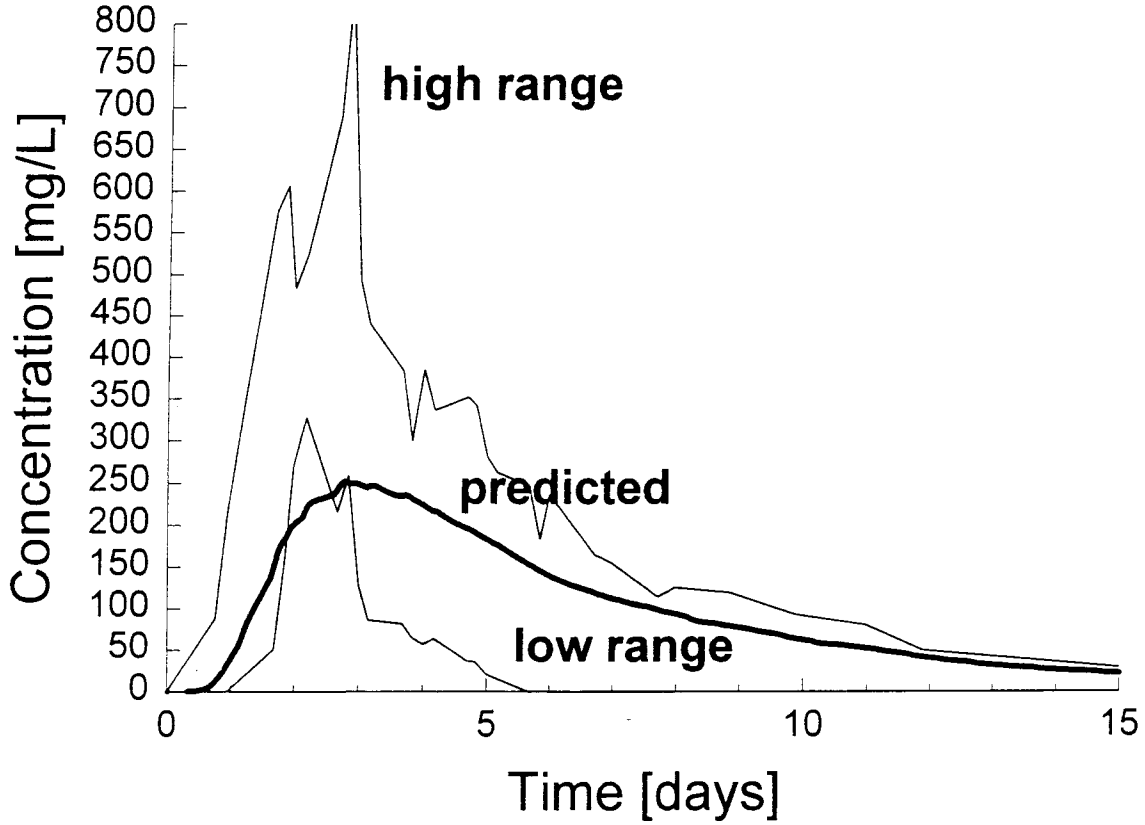

### *Virus Transport, Fine Sand, High Dose*

The model was used to predict the transport of viruses in the high dose cells with the two-ft water table. The system configuration used for this series of simulations was the same as that used for the bromide simulations, shown in Figure 2. Viruses were added to the cell via the observation port, which has an area of 0.3 $ft^2$. A total of 5.8 x $10^{13}$ pfu of viruses were added to the cell in a volume of 500 ml. The soil hydraulic properties used were the same as those used in the bromide simulation, which are shown in Table 1. The atmospheric inputs (i.e., rainfall) were obtained from the weather station at the test facility (see Appendix 2). Evapotranspiration was assumed to be 0.5 cm per day.

Unlike bromide, which is a non-reactive (conservative) tracer, viruses can be affected by processes such as adsorption to the soil particles and inactivation as they are transported through the soil. The soil at the lysimeter facility is a fine sand, containing 97.4 to 98.2% sand particles, 0.1 to 0.5% silt, and 1.5 to 3.1% clay. Grain size analyses revealed that the particles were fine to very fine grained. Information in the published literature would suggest that very little to no adsorption of the viruses to a soil with these textural characteristics would be expected (Goyal and Gerba, 1979). The reactive fraction of the soil is the clay fraction, as clay particles contain charged sites to which contaminants can adsorb. Sand particles, in general, do not have charged sites, so contaminant adsorption is minimal. Therefore, for the purposes of these simulations, it was assumed that the soil adsorption coefficient was 0.

In the model, soil adsorption is expressed as a retardation factor, R. The retardation factor describes the transport of a contaminant relative to the transport of water. Thus, a non-reactive tracer such as bromide is expected to move as rapidly as the water and therefore has an R value of 1. A contaminant that adsorbs to soil would be transported more slowly than the water because some of the contaminant is adsorbed to the soil at any given time, therefore it would have an R value greater than one. For example, a compound that moves twice as slowly as the water would have an R value of 2. The retardation factor is calculated using the soil adsorption coefficient, $K_d$, by means of the following equation:

$$R = 1 + (\rho_b K_d/\theta)$$

where $\rho_b$ is the bulk density of the soil and $\theta$ is the moisture content of the soil. For a non-sorbing contaminant, which has a $K_d$ of 0, it can be seen that the R is 1. Therefore, in these simulations, since it was assumed that the viruses did not adsorb to the soil, a value of 1 was used for the retardation factor.

Another factor that can have an effect on the system is the inactivation of viruses as they are being transported through the soil. It is well documented that the temperature of the environment has a significant effect on the rate of virus inactivation in soils and water. For these simulations, the rate of virus inactivation was calculated based on a published relationship established between temperature and the rate of virus inactivation in ground water. (Yates and Yates, 1988). During the April 1997 tracer experiment, which is the experiment that was being simulated, the soil temperature averaged 23.9 C (75 F). The equation used to calculate the inactivation rate is:

$$\text{Inactivation rate } (\log_{10} \text{day}^{-1}) = -0.181 + 0.0214 \times T\ (C).$$

The calculated inactivation rate used for this simulation was 0.33 $\log_{10}$ $day^{-1}$.

Using these values and the soil hydraulic properties discussed above, the virus breakthrough curve shown in Figure 9a was predicted. For comparison, the measured virus concentrations in the leachate from the infiltration cell are also shown. The model predictions compared very well to the measured values, especially considering the fact that the model was not calibrated using these data, it was calibrated using bromide data from a low-dose cell. The predicted peak concentration was $2.29 \times 10^8$ pfu/mL, compared with a measured peak value of $3.08 \times 10^8$ pfu/mL. The predicted peak value occurred at approximately the same time (1.8 days) as the measured peak value (2.67 days).

The breakthrough curves predicted for three depths in the soil, 6", 12, and 24", directly below the perforated pipe are shown in Figure 9b. The concentrations of viruses throughout the lysimeter system as they were transported downward through the soil are shown for several times after tracer introduction are shown in Figures 10a-d. Again, a portion of the viruses were transported out of the system through the free drainage surface located between the collection pan and the perched water table. While it is difficult to discern this phenomenon from the figures (10a-d), examination of the solute

# Figure 9a. Virus Breakthrough Curve

## 2 ft, fine sand, high dose, R=1

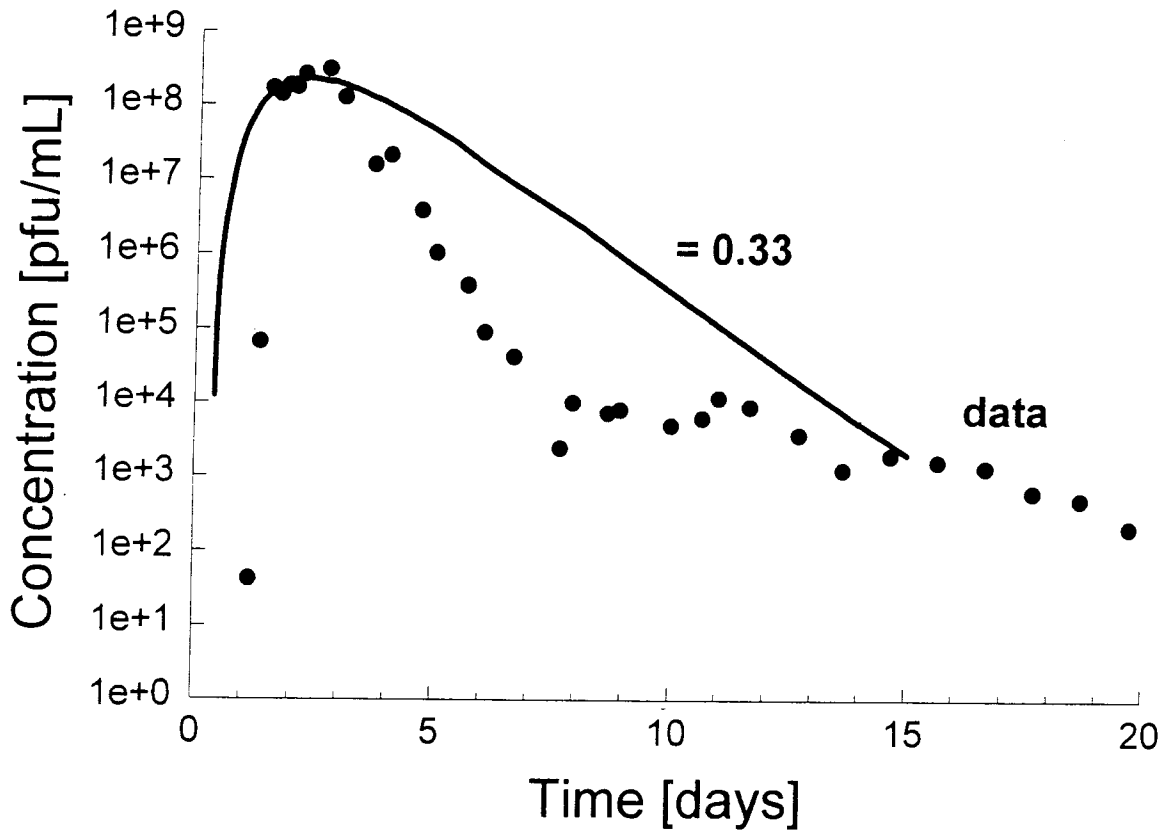

# Figure 9b. Virus Breakthrough Curves

## 2 ft, fine sand, high dose, R=1, μ=0.33

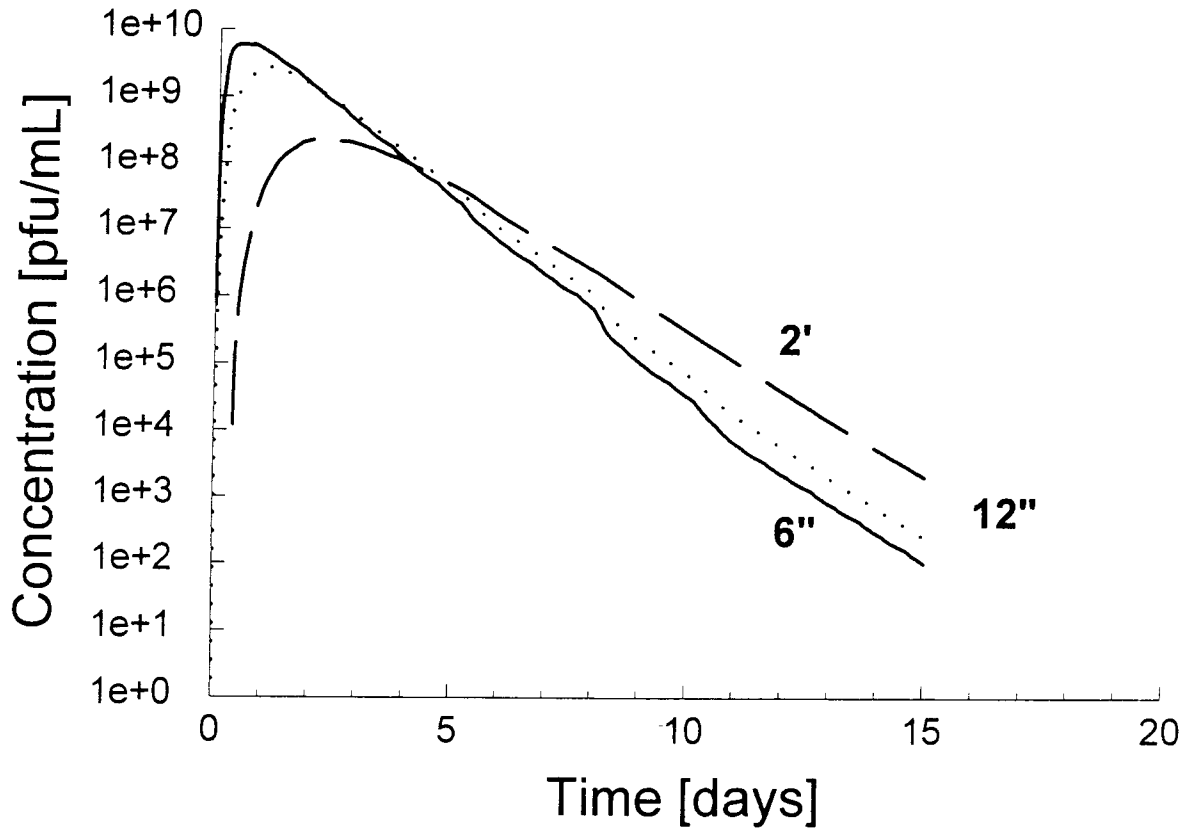

flux at the free drainage surface for this simulation (Grid 3a, Va33fsh) can be clearly seen in the figure in Appendix 3.

### *Effect of Inactivation Rate on Virus Transport*

As discussed previously, the inactivation rate of viruses has been found to be affected by the temperature of the environment, among other factors. In order to examine the virus behavior at other times of the year when the temperature would be different from that in April (75 F), several simulations were run. In these simulations, the inactivation rates were varied from 0 $\log_{10}$ $day^{-1}$ to 1 $\log_{10}$ $day^{-1}$. The temperatures and their associated inactivation rates are shown in Table 2. The breakthrough curves from these simulations are shown in Figure 11, along with the measured values for comparison. Examination of this figure reveals that, while the simulation using 0.33 $\log_{10}$ $day^{-1}$ fits the measured data most closely overall, other simulations describe the behavior of the viruses in the system better at certain times. For example, the simulation in which the inactivation rate was assumed to be 1 $\log_{10}$ $day^{-1}$ mimics the slope of the breakthrough curve very well for the first 6 days of the study. However, the peak value is simulated best using an inactivation rate of 0.1 $\log_{10}$ $day^{-1}$. These curves illustrate the behavior that might be expected at different times of the year as the temperature changes.

Table 2. Virus Inactivation Rates at Temperatures used in Simulations

| Temperature | | |
|---|---|---|
| F | C | Inactivation Rate ($\log_{10}$ $day^{-1}$) |
| 47.2 | 8.5 | 0 |
| 55.6 | 13.1 | 0.1 |
| 75 | 23.9 | 0.33 |
| 89.3 | 31.8 | 0.5 |
| 131.3 | 55.2 | 1.0 |

# Figure 11. Effect of Inactivation Rate on Virus Breakthrough Curve

## 2 ft, fine sand, high dose, R=1

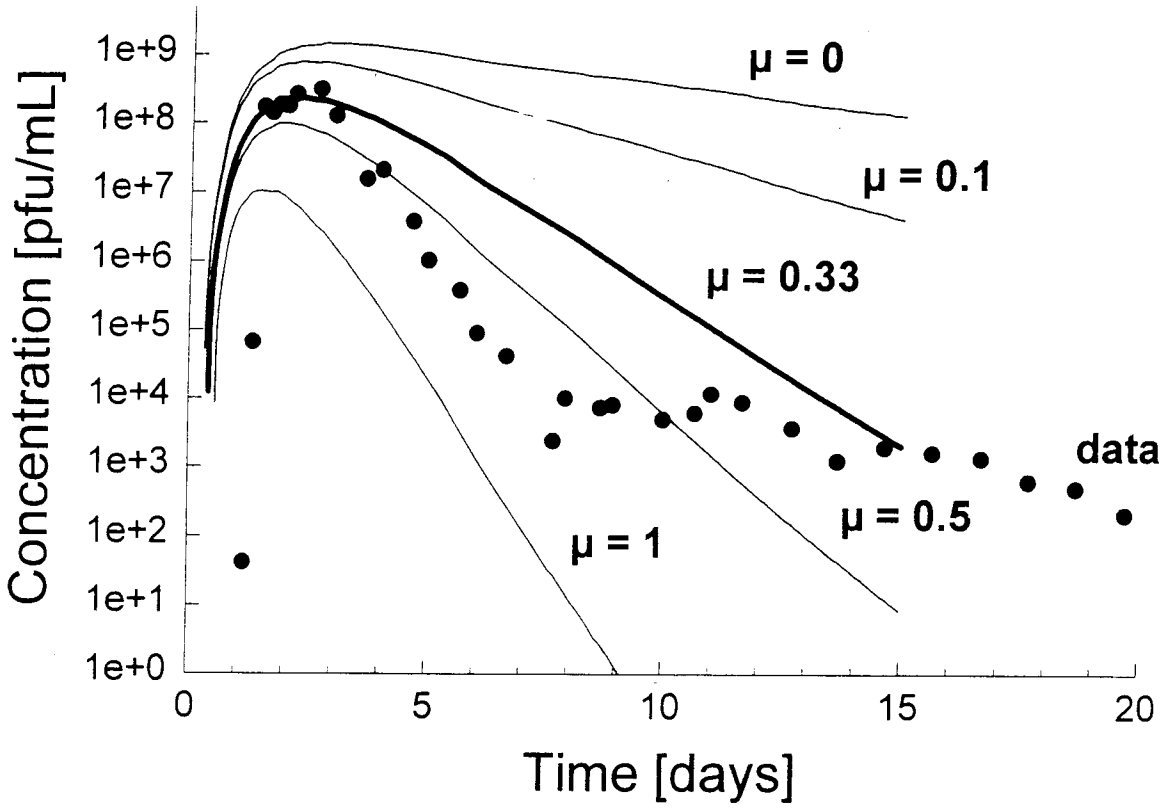

### *Effect of Soil Type on Virus Transport*

It is recognized that the fine sandy soil at the lysimeter site is only one type of soil in which a septic tank and leach field system would be operated. Therefore, the transport of viruses through two other soil types, a sandy loam and a loam, was investigated. In order to perform these simulations, new grids had to be constructed because the system configuration used to run the simulations in the fine sand produced numerically unstable results. A new configuration was constructed that was similar to the previous one (Grid 3, Figure 2) except that the soil underneath the collection pan was removed (Grid 1, Figure 12). In order to ascertain that the results produced using this configuration were comparable to those for the previous configuration, simulations were run using bromide. Bromide transport through the fine sandy soil configured without the soil underlying the collection pan was simulated. The resulting breakthrough curve was compared to that of the original configuration; the two breakthrough curves are shown in Figure 13. The behavior was considered to be acceptably similar, so the revised configuration was used for the simulations run on the loamy and sandy loam soils. All simulations were run for the two ft water table cells with the wastewater being applied at the low dose.

*Sandy Loam Soil*

The hydraulic properties of the sandy loam soil used for these simulations are shown in Table 3. Graphs of the water release curve and the hydraulic conductivity are shown in Figures 14a and b. Two sets of simulations were run for the virus transport in the sandy loam soil. In all simulations, the viruses were added to the infiltration cells in the same manner as in the field tracer study. In addition, the atmospheric inputs were the same as those used in the simulations in the fine sand (i.e., those shown in Appendix 1). In the first pair of simulations, the virus inactivation rate was assumed to be zero, which represents a worst-case scenario. In one simulation, the soil adsorption coefficient was assumed to be zero (i.e., R=1), also representing a worst-case scenario. It is unlikely that there would be no virus adsorption to a sandy loam soil, however, so another simulation was run in which the retardation factor was assumed to be 10 (i.e., the viruses are transported through the soil ten times more slowly than the water). The breakthrough curves produced by these simulations are shown in Figure 15. The main

# Figure 12. Grid 1

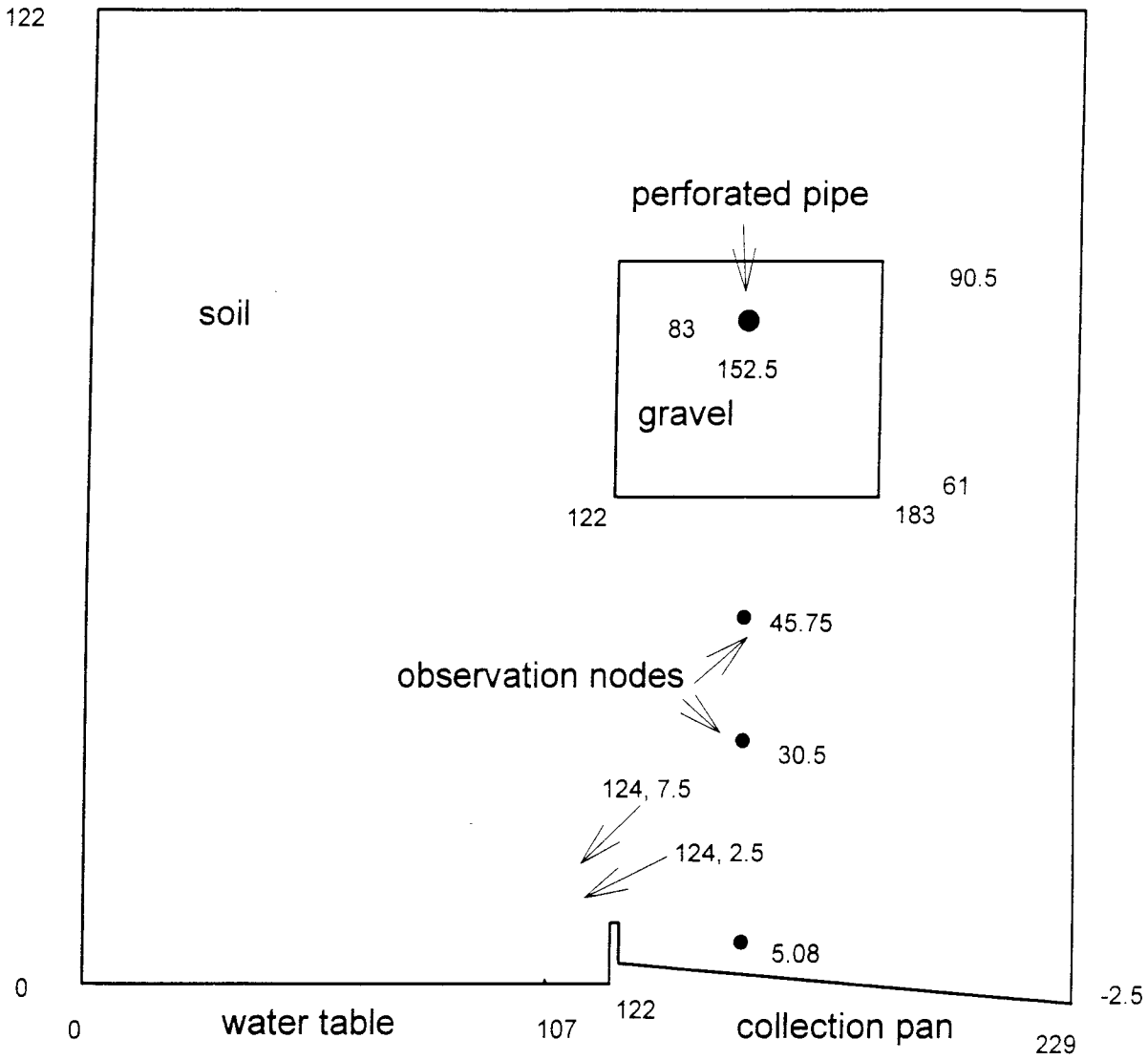

# Figure 13. Effect of System Configuration on Bromide Breakthrough Curve

## 2 ft, fine sand, low dose

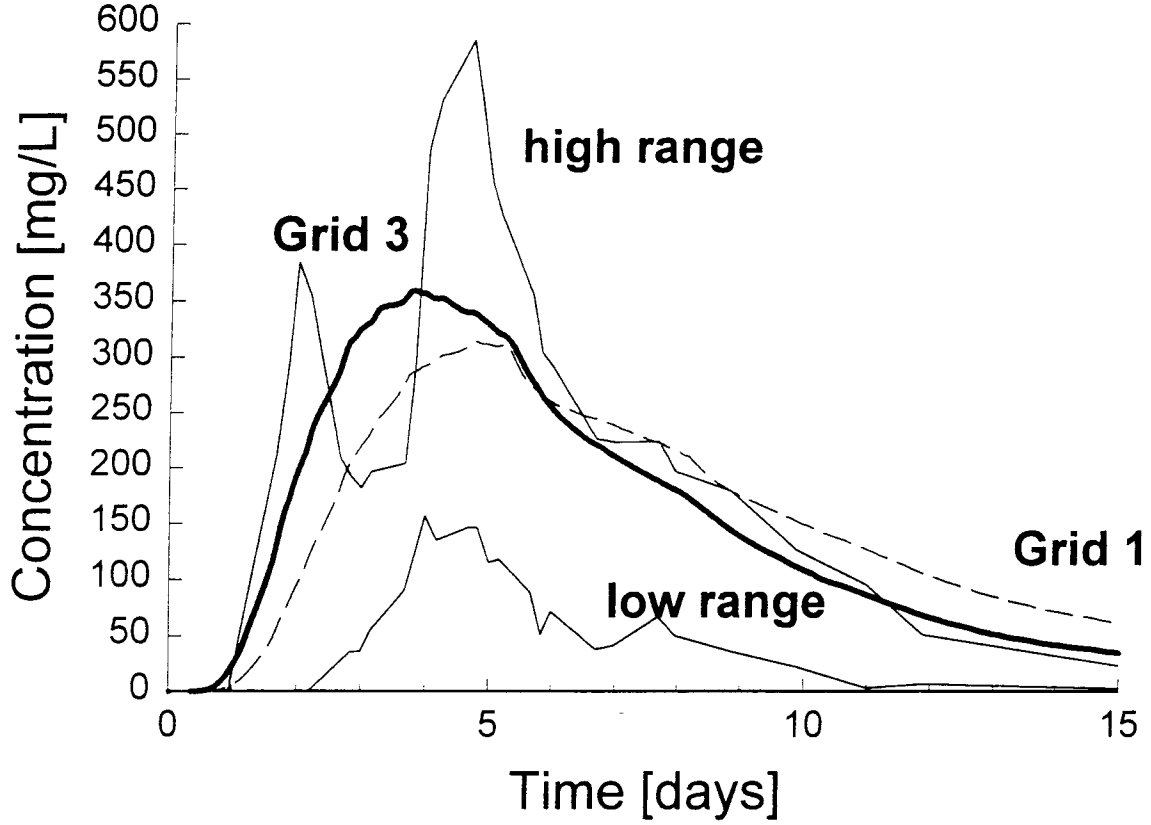

# Figure 14. Properties of Sandy Loam

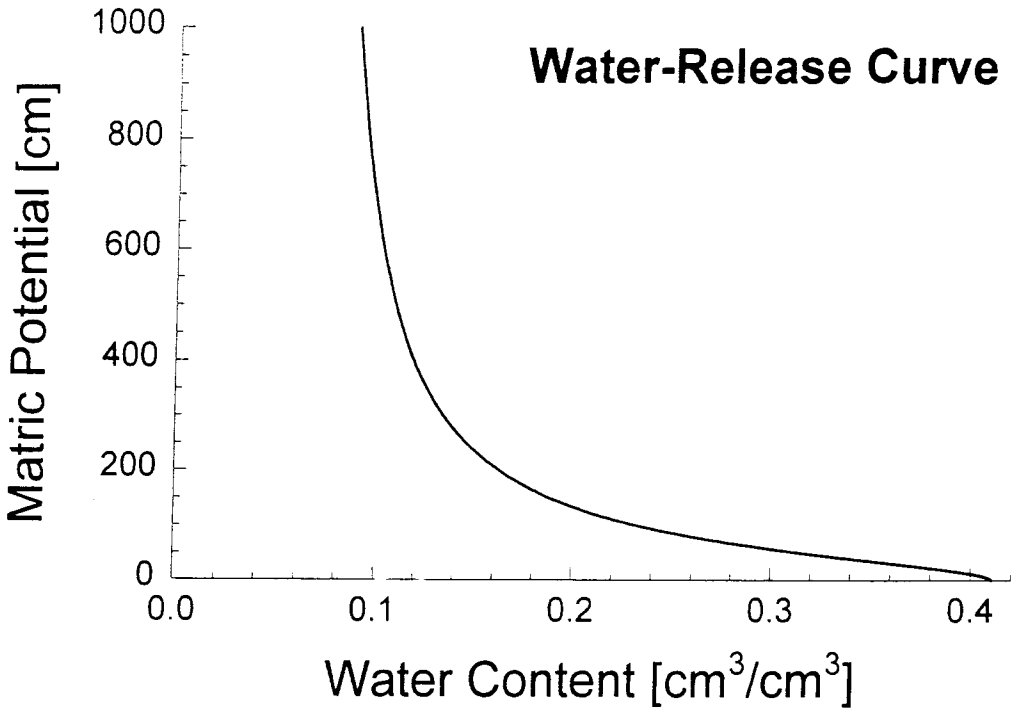


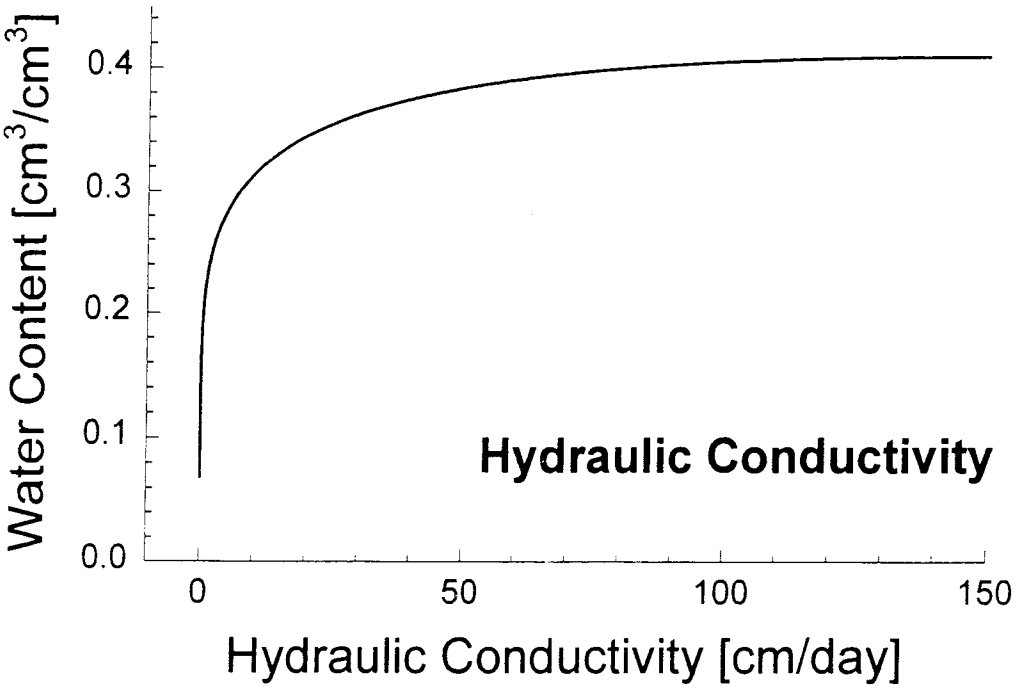

# Figure 15. Virus Breakthrough Curves

## 2 ft, sandy loam, low dose

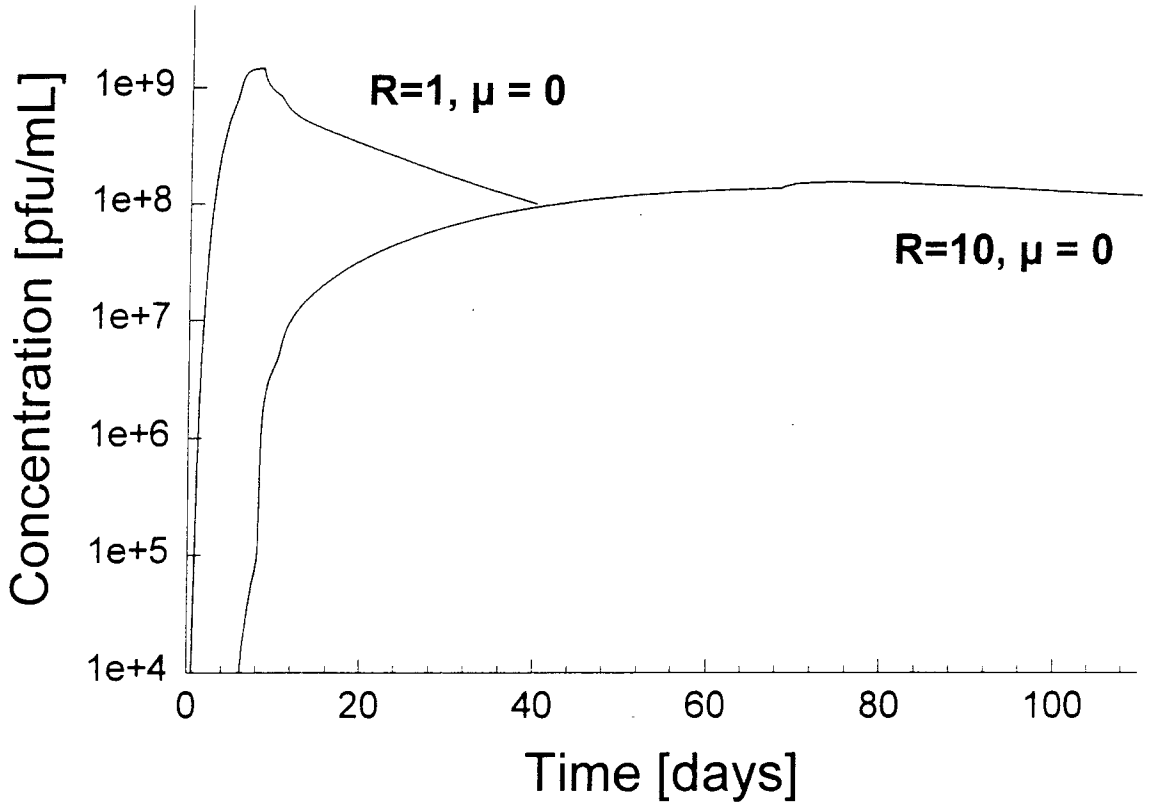

difference between the two curves is the predicted virus concentration that will appear in the collection device. When the virus transport is not retarded, the peak predicted virus concentration is approximately $10^9$ pfu/mL. In the second case, when the virus transport is slowed considerably, the virus concentration is predicted to be approximately $10^8$ pfu/mL. Because neither of these cases allowed virus inactivation, the concentrations in the leachate were predicted to remain high for several months.

Table 3. Hydraulic properties of sandy loam and gravel used in simulations

| Property | Sandy Loam | Gravel |
|---|---|---|
| soil bulk density, $\rho_b$ | 1.564 | 1.5 |
| residual moisture content, $\theta_r$ | 0.065 | 0.02 |
| saturated moisture content, $\theta_s$ | 0.41 | 0.414 |
| vanGenuchten parameters: | | |
| $\alpha$ | 0.0183 | 0.0183 |
| n | 1.89 | 3.88 |
| saturated hydraulic conductivity, $K_s$ | 150 | 1500 |

In the second pair of simulations, the virus inactivation rate was assumed to be 0.25 $\log_{10}$ $day^{-1}$, which corresponds to a temperature of 20 C (68F). In one case, the retardation factor was assumed to be 1, in the other a value of 10 was used. The two breakthrough curves produced using these values (Figure 16) are strikingly different. In the case in which virus movement is not retarded, the virus concentration peaks after approximately 5 days, then sharply falls to undetectable levels by day 35. However, in the case when the virus transport is slowed relative to that of the water, the virus concentration reaches a peak value of approximately $10^7$ pfu/mL on day 25 and slowly declines to 5 x $10^5$ pfu/mL by day 100.

*Loam Soil*

The hydraulic properties of the loam soil are shown in Table 4. Graphs of the water release curve and the hydraulic conductivity are shown in Figures 17a and b. Two sets of simulations were run for the virus transport in the loam soil. In all simulations, the viruses were added to the infiltration cells in the same manner as in the field tracer

# Figure 16. Virus Breakthrough Curves

## 2 ft, sandy loam, low dose

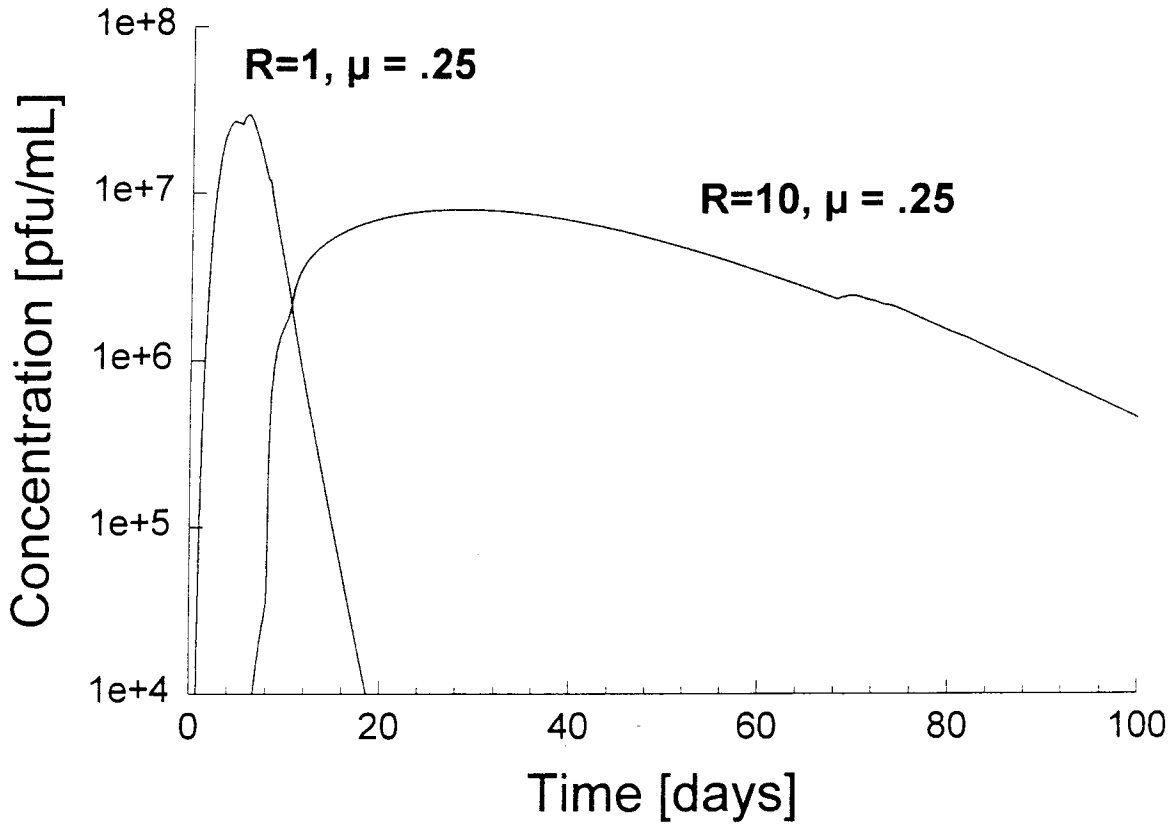

# Figure 17. Properties of Loam Soil

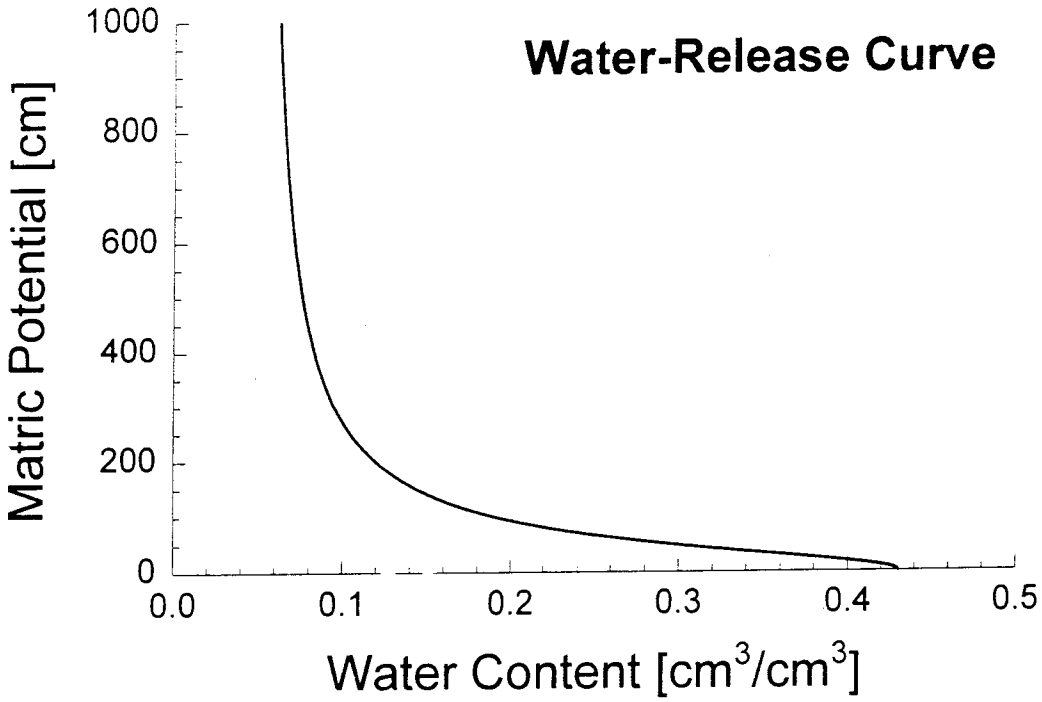


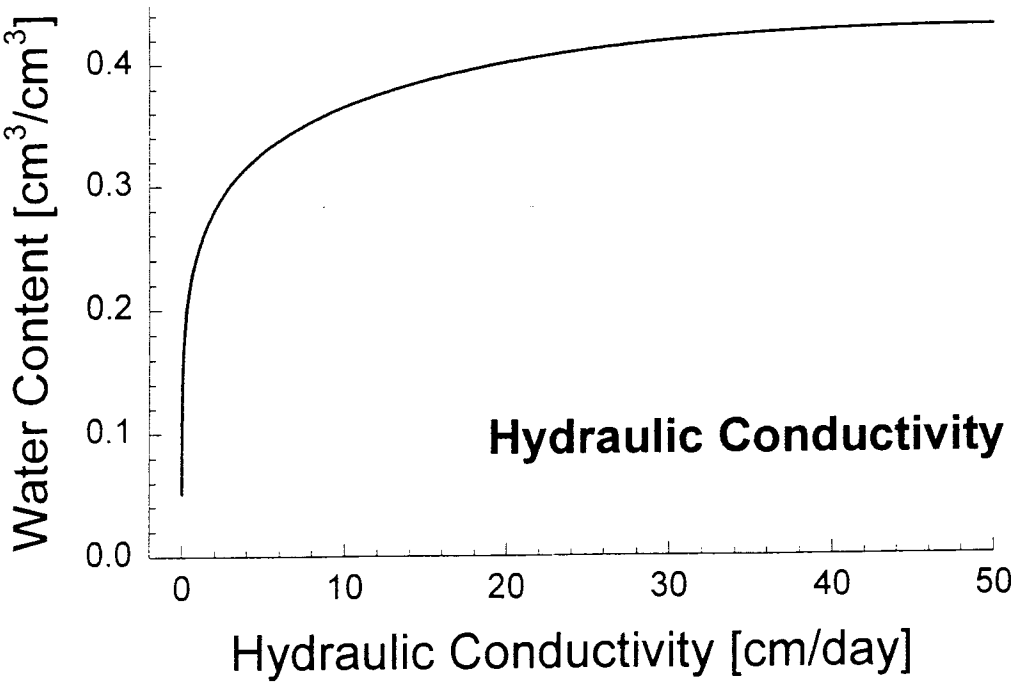

study. In addition, the atmospheric inputs were the same as those used in the simulations in the fine sand (i.e., those shown in Appendix 2). In the first pair of simulations, the virus inactivation rate was assumed to be zero. In one simulation, the soil adsorption coefficient was assumed to be zero (i.e., R=1). It is unlikely that there would be no virus adsorption to a loamy soil, however, so another simulation was run in which the retardation factor was assumed to be 10 (i.e., the viruses are transported through the soil ten times more slowly than the water). The breakthrough curves produced by these simulations are shown in Figure 18. The main difference between the two curves is the predicted virus concentration that will appear in the collection device. When the virus transport is not retarded, the predicted virus concentration is approximately $10^8$ pfu/mL. In the second case, when the virus transport is slowed considerably, the virus concentration is predicted to be approximately $10^7$ pfu/mL. Because neither of these cases allowed virus inactivation, the concentrations in the leachate would remain high for several months.

Table 4. Hydraulic properties of loam and gravel used in simulations

| Property | Loam | Gravel |
|---|---|---|
| soil bulk density, $\rho_b$ | 1.51 | 1.5 |
| residual moisture content, $\theta_r$ | 0.05 | 0.02 |
| saturated moisture content, $\theta_s$ | 0.43 | 0.414 |
| vanGenuchten parameters: | | |
| $\alpha$ | 0.023 | 0.0183 |
| n | 2.1 | 3.88 |
| saturated hydraulic conductivity, $K_s$ | 50 | 1500 |

In the second pair of simulations, the virus inactivation rate was assumed to be 0.25 $\log_{10}$ $day^{-1}$, which corresponds to a temperature of 20 C (68F). In one case, the retardation factor was assumed to be 1, in the other a value of 10 was used. The two breakthrough curves produced using these values (Figure 19) are very different. In the case in which virus movement is not retarded, the virus concentration peaks after approximately 5 days, then sharply falls to undetectable levels by day 35. However, in the case when the virus transport is slowed relative to that of the water, the virus

# Figure 18. Virus Breakthrough Curves

## 2 ft, loam, low dose

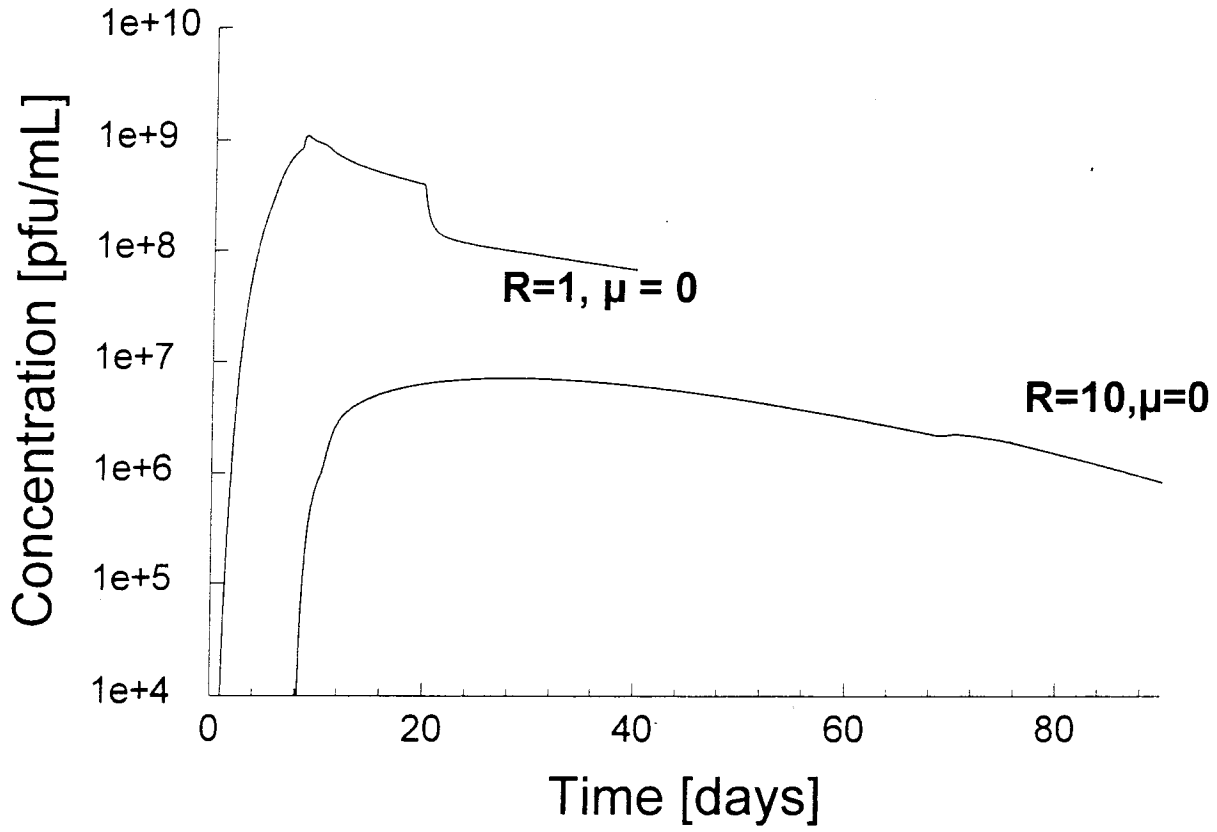

# Figure 19. Virus Breakthrough Curves

## 2 ft, loam, low dose

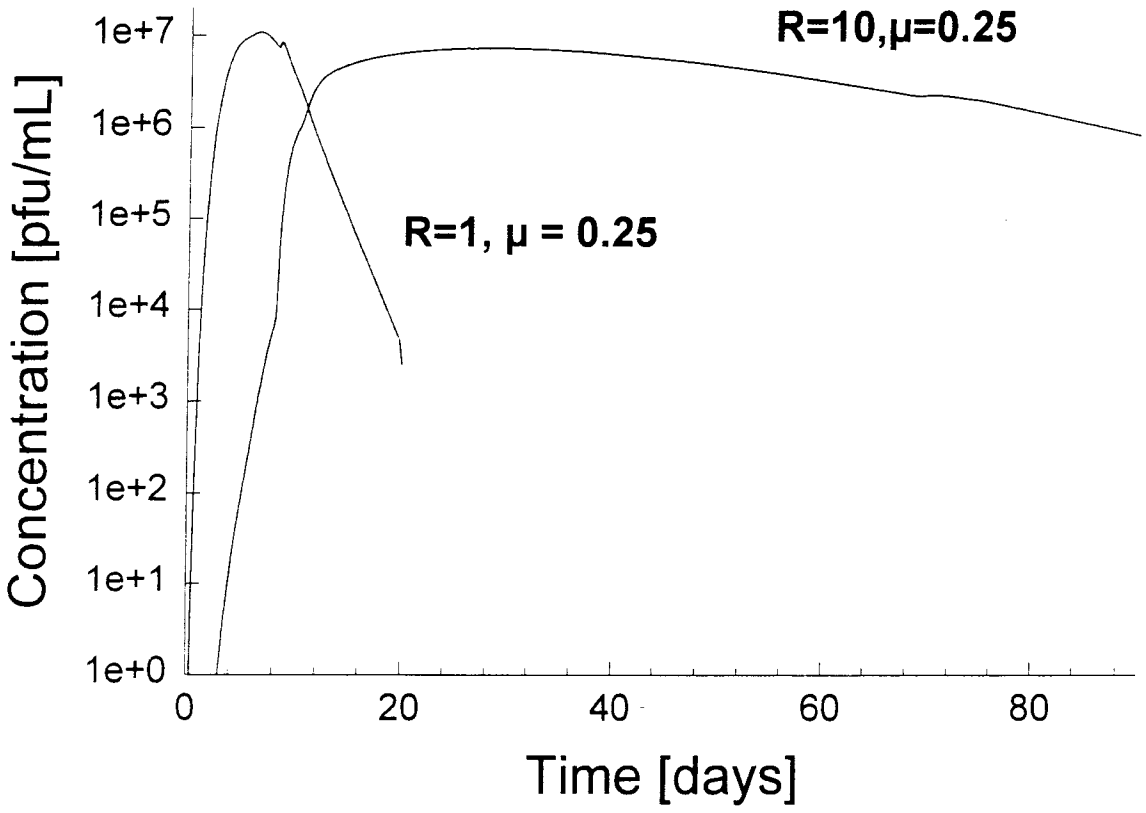

concentration reaches a peak value of approximately 7.5 x $10^6$ pfu/mL on day 20 and slowly declines to 7.5 x $10^5$ pfu/mL by day 90.

The predicted virus behavior in the 3 soils in a low dose cell assuming an adsorption coefficient of zero and an inactivation rate of zero is shown in Figure 20. As one would predict, the time to reach the peak virus concentration is the least in the sand, followed by the sandy loam and finally the loam. As no adsorption has been allowed in these simulations, the differences are not due to retardation of virus movement, rather to a lower rate of water movement in the finer textured soils (i.e., the hydraulic conductivity of the loam and sandy loam are 50 and 150 cm/day compared to 549 cm/day for the fine sand). The predicted peak concentrations also decrease from the sand to the sandy loam to the loam; however, the differences in the peak concentrations are very small: from 3 x $10^9$ to 1 x $10^9$ pfu/mL.

In the field, it is unlikely that there would be no virus adsorption to the loam and sandy loam soils; therefore the predicted breakthrough curves with an R=10 are shown on the same figure (Figure 21) with the curve for the fine sand (R=1). It is apparent on examination of these curves that the behavior of the viruses in these three soils would be very different. The adsorption of the viruses to the loam and sandy loam soils delays their predicted peak concentrations for several weeks, compared to less than 5 days for the sandy soil. In addition, the virus concentration is not predicted to exceed 1 x $10^8$ pfu/mL in the sandy loam and 5 x $10^7$ pfu/mL in the loam soil compared to 3 x $10^9$ pfu/mL in the fine sand. The virus concentrations are predicted to remain at approximately these levels for at least 100 days after application.

***Effect of Rainfall on Virus Transport***

Although there was some rainfall during the tracer experiments, and thus rainfall was incorporated into the simulations, on occasion large rainfall events may occur. It is these events that are likely to have the most impact on virus (and other contaminant) transport, as the added water will transport the contaminants through the soil more rapidly. A series of simulations was performed using the fine sand, high dose, 2 foot infiltration cell (Grid 3) in which a 6-inch rainfall over a 6-hour period was superimposed on the atmospheric inputs to the model. The rainfall occurred between 12:00 p.m. and 6:00 p.m. on the day after the viruses were applied at 4:30 p.m. The soil adsorption coefficient was assumed to be zero, and the virus inactivation rate was assumed to be

# Figure 20. Virus Breakthrough Curves in Different Soils

## 2 ft, low dose, R=1, μ=0

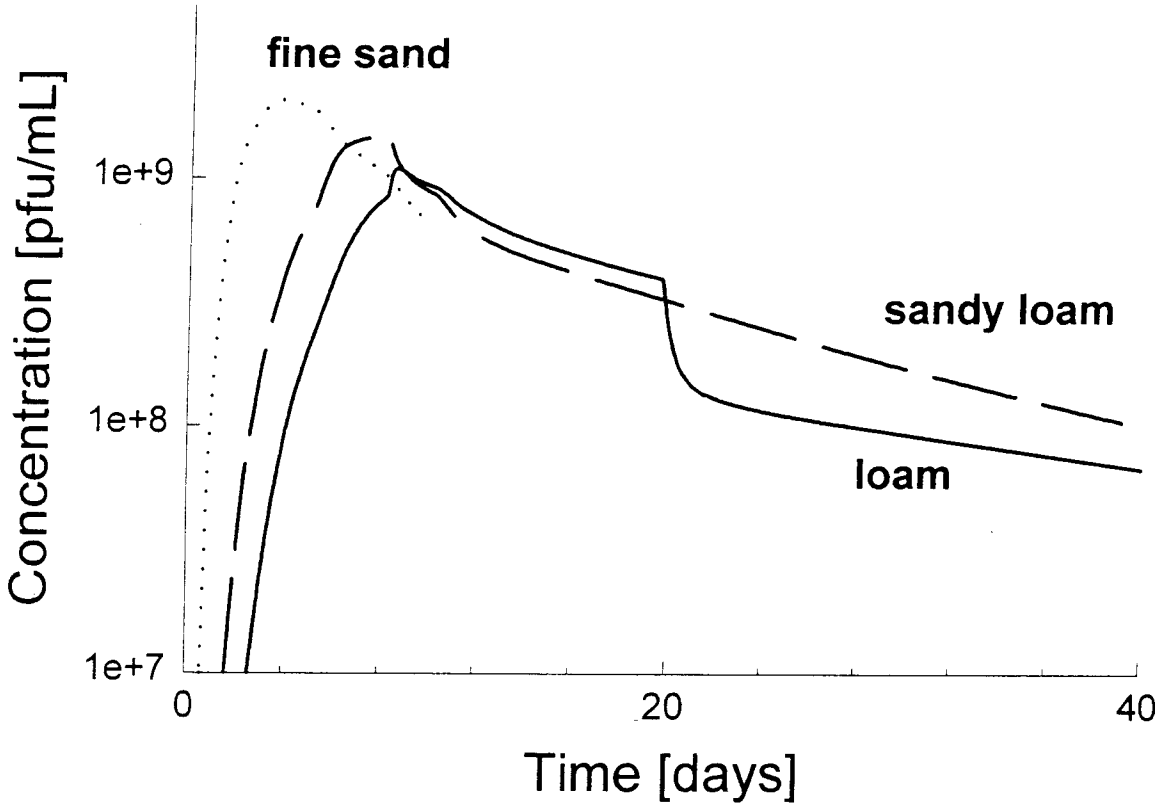

# Figure 21. Virus Breakthrough Curves in Different Soils

## 2 ft, low dose, μ=0

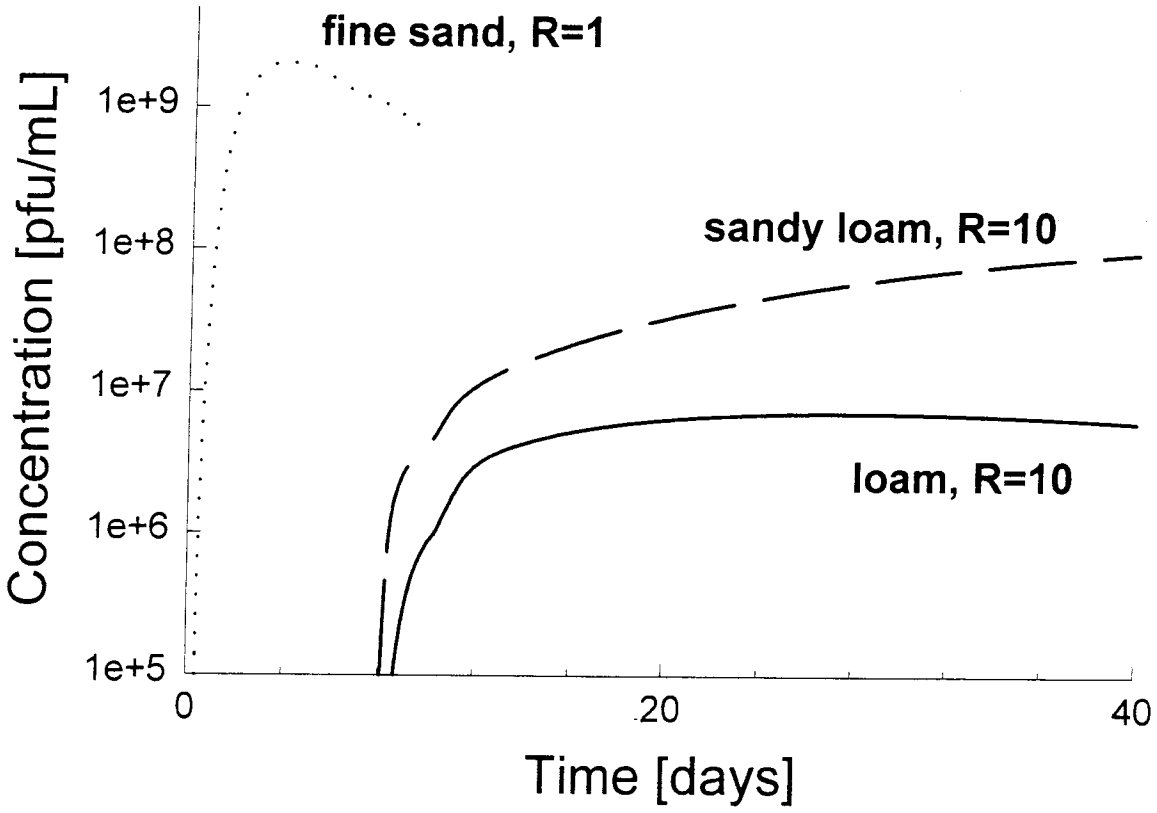

either zero or 0.33 $\log_{10}$ $day^{-1}$. Figure 22a shows the predicted breakthrough curves for the case where the inactivation rate was assumed to be zero. The rainfall causes the viruses to be transported through the cell very rapidly, reaching a peak concentration of greater than $10^{10}$ pfu/mL in 1.5 days. When virus inactivation is assumed to occur, a similar trend is seen (Figure 22b) - the virus concentration peaks at a level approximately ten times higher than is seen without the rainfall, approximately 1.5 days earlier in time.

## EFFECT OF COLLECTION PAN ON TRANSPORT

All of the simulations described to this point have conformed to the configuration of the system at the lysimeter facility, i.e., the grids contain a collection pan at 3 ft below the soil surface and an artificially-maintained water table (Figures 2 and 12). Obviously, this configuration would not exist at a normal septic tank leach field. The effluent would be applied to the soil via perforated pipes and allowed to infiltrate through the unsaturated soil to the underlying ground water. Therefore, a series of simulations was performed to examine the predicted contaminant behavior in a system that was configured to match natural conditions more closely. To perform these simulations, a new grid (Grid 4) was constructed that contained a water table at 2 feet below the infiltration surface (Figure 23) (i.e., a 2-ft unsaturated zone). The tracers (viruses and bromide) were applied using the same method as was used at the lysimeter facility, as was the wastewater dosing.

Simulations were run for the two-foot cells using both the high and low dosing rates. The results for bromide with the low wastewater dose are shown in Figure 24. The water table configuration (Grid 4) results in a breakthrough curve that is skewed toward a later time than was predicted for the pan configuration (Grid 3): the peak occurs at 8 days rather than 3. In addition, the predicted peak concentration was lower (280 mg/l) compared to the pan configuration (360 mg/l). These differences may be attributed to the fact that the water flow streamlines are more widely distributed across the soil in the water table configuration (Grid 4). Thus, the center of contaminant mass is delayed and the contaminant is diluted by the soil water as it travels to the saturated zone. In the case of the collection pan configuration (Grid 3), the wastewater and

# Figure 22a. Effect of Rain on Virus Transport

## 2 ft, fine sand, high dose

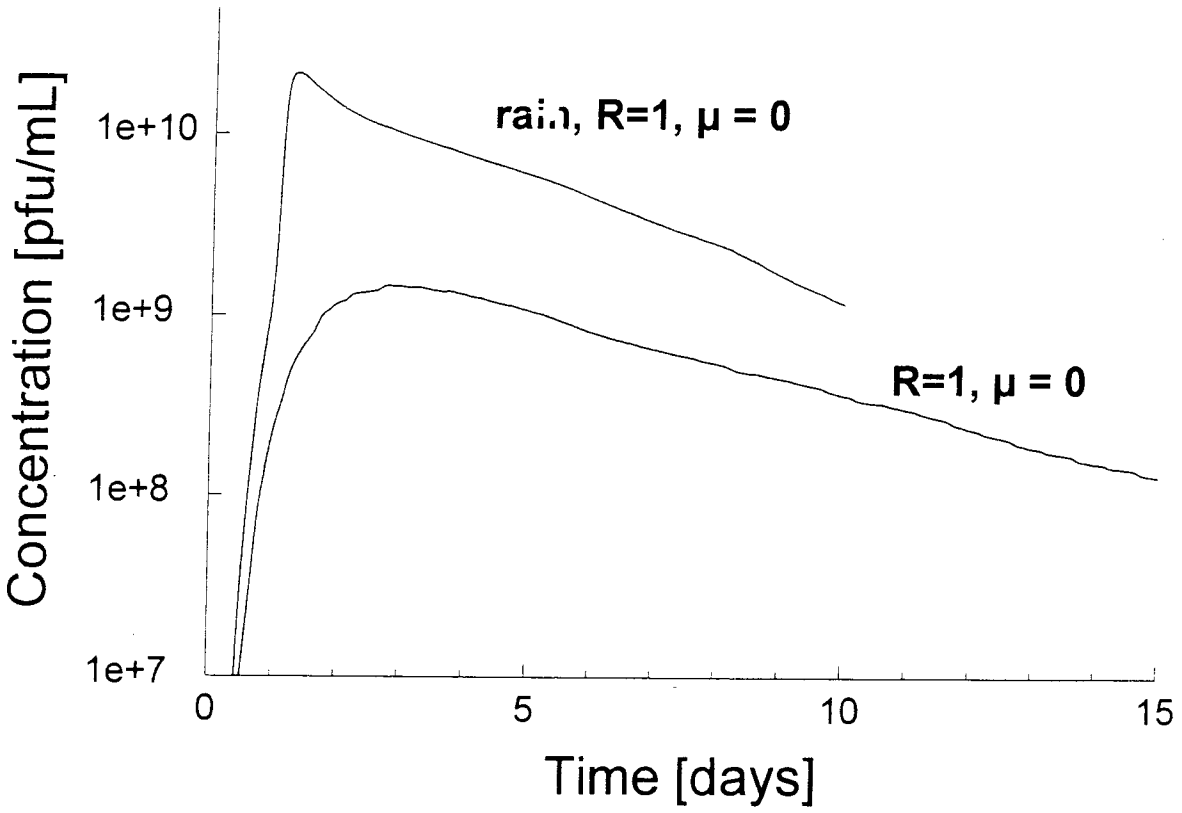

# Figure 22b. Effect of Rain on Virus Transport

## 2 ft, fine sand, high dose

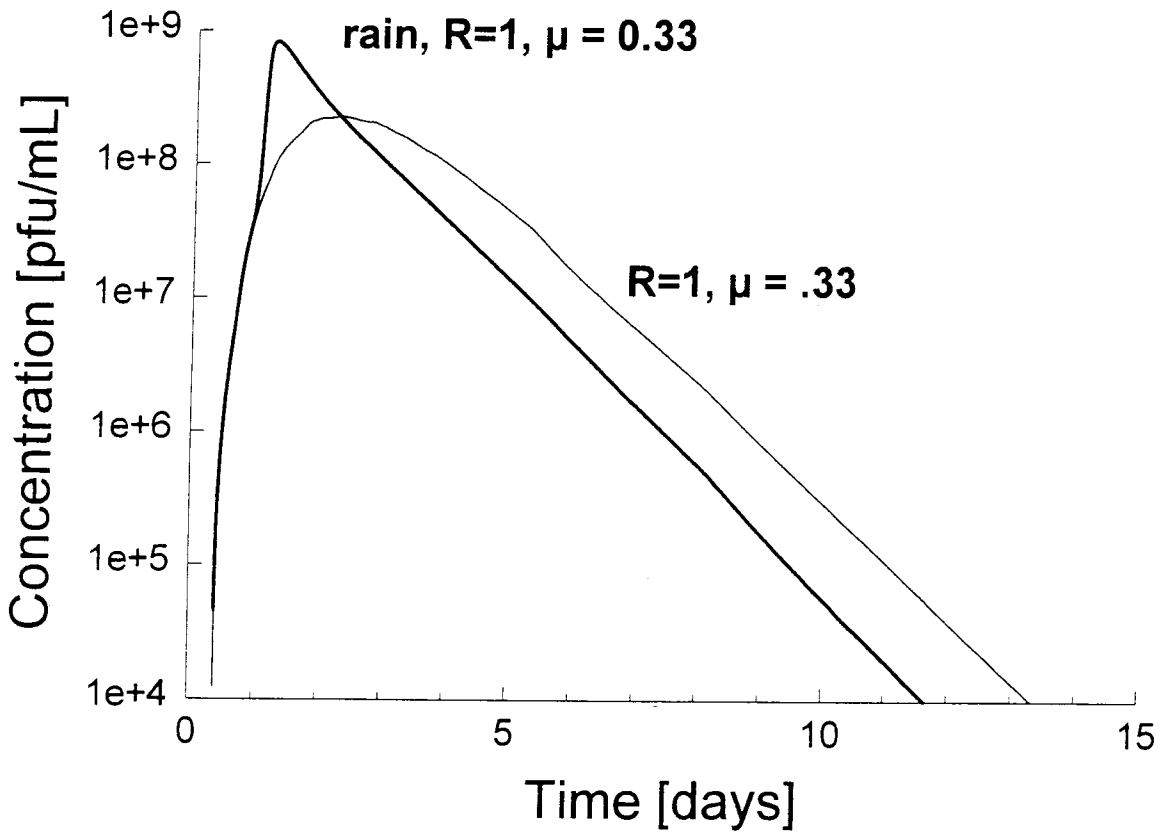

# Figure 23. Grid 4

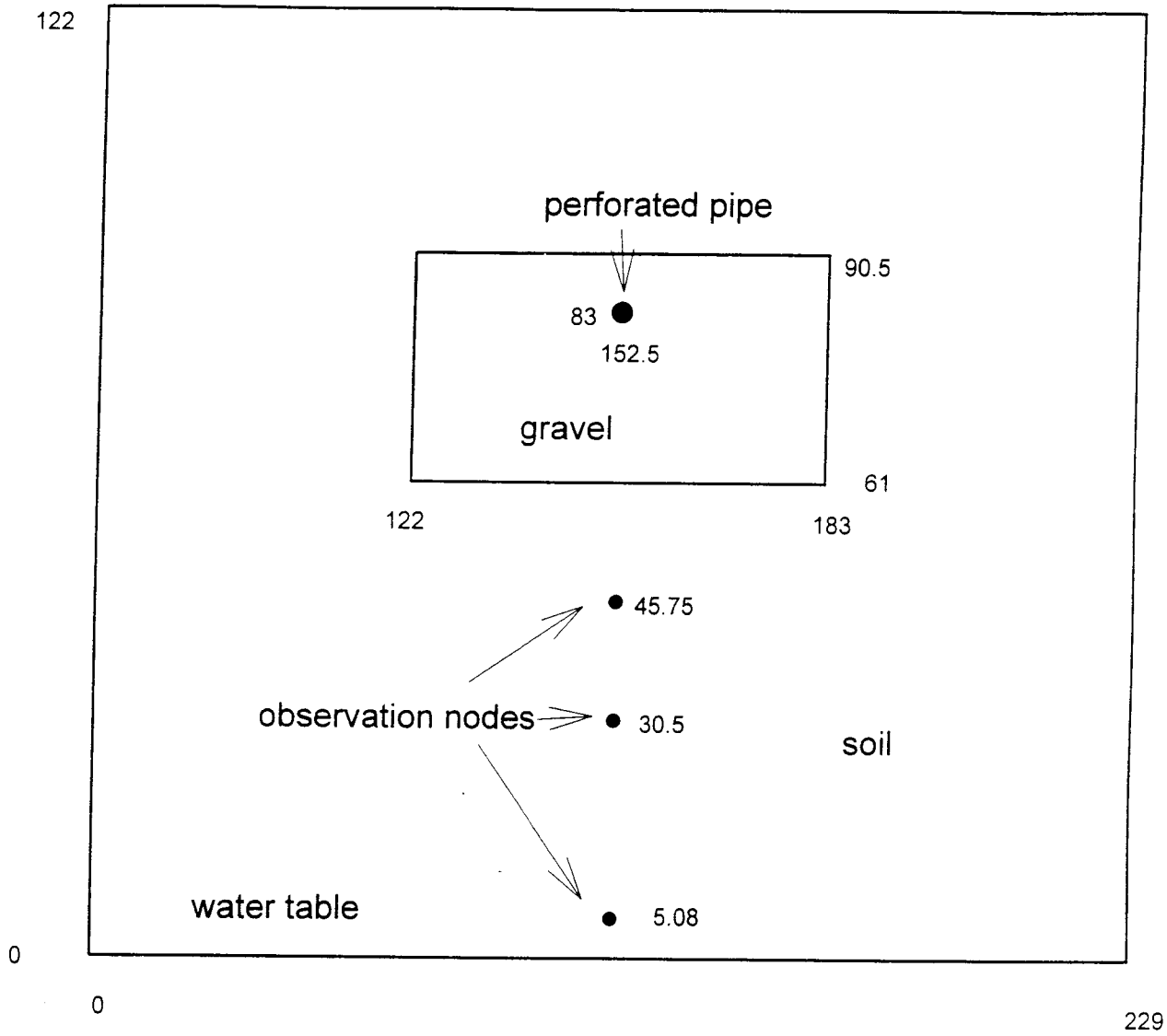

# Figure 24. Bromide Breakthrough Curve

**fine sand, low dose, 2 foot**

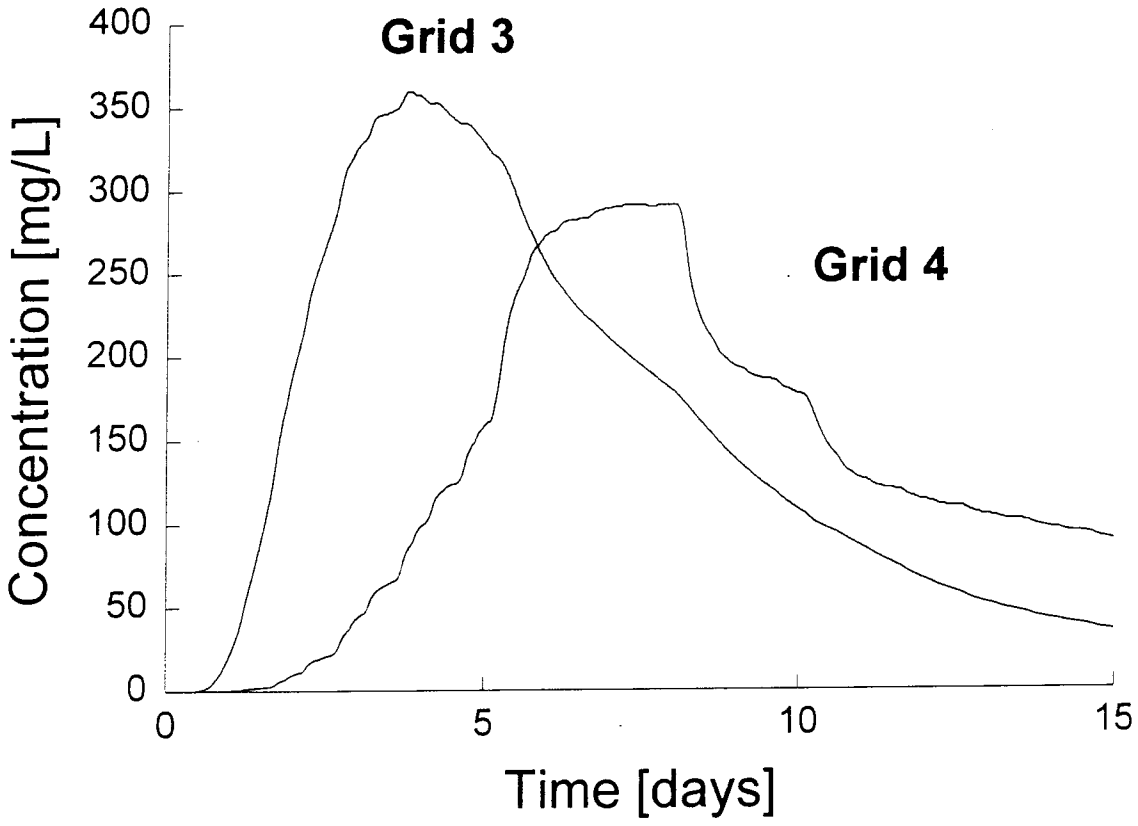

contaminants travel through the soil in a more concentrated pulse, which is pulled toward the artificially maintained water table (see Figures 7 and 10).

The differences between the breakthrough curves for the water table and pan configurations for the high dose situation are shown in Figure 25. The breakthrough curve for the water table configuration is again skewed toward a later time, with the peak predicted to occur at 6 days rather than the 2.5 days predicted for the pan configuration. In this case, the predicted concentration is higher than for the pan configuration, with a predicted peak concentration of approximately 300 mg/L rather than 250 mg/L.

The predicted breakthrough curves for viruses, assuming and inactivation rate of zero and a soil adsorption coefficient of zero, for the low and high wastewater does are shown in Figures 26 and 27. These curves are identical to those predicted for the bromide because there was no adsorption or inactivation (i.e., the viruses behaved like non-reactive tracers). The differences in the virus concentrations predicted using the different grid configurations appear to be relatively small; this is an artifact of the use of a logarithmic scale to report virus concentrations.

## PREDICTING TRANSPORT IN FOUR-FOOT CELLS

To this point, the discussion has focused on the behavior of the tracers in the 2-foot infiltration cells. This is due to the fact that almost all of the data from the tracer studies have been obtained from these cells. No virus tracer studies have been performed in the four-foot cells. However, there were data obtained from the 4-foot cells during the February 1996 bromide tracer study. This study was performed in the same manner as those described previously, and the wastewater application doses were the same as for the 2-foot cells. The model that was calibrated using the 2-foot cells receiving the low dose of wastewater, grid 3 (modified for a 4-foot cell), was used to simulate bromide movement in the four-foot cell (Figure 28). All simulations were performed using the fine sand with the hydraulic properties shown in Table 1.

The predicted breakthrough curve for the low dose cell is shown in Figure 29, along with the high range and low range of the measured values. The model predictions fall within the measured range for the first 8 days after application; however the model predicts higher than measured concentrations for several days, until day 15 when the predicted values approach the measured values. Figure 30 shows the results for the

# Figure 25. Bromide Breakthrough Curve

## fine sand, high dose, 2 foot

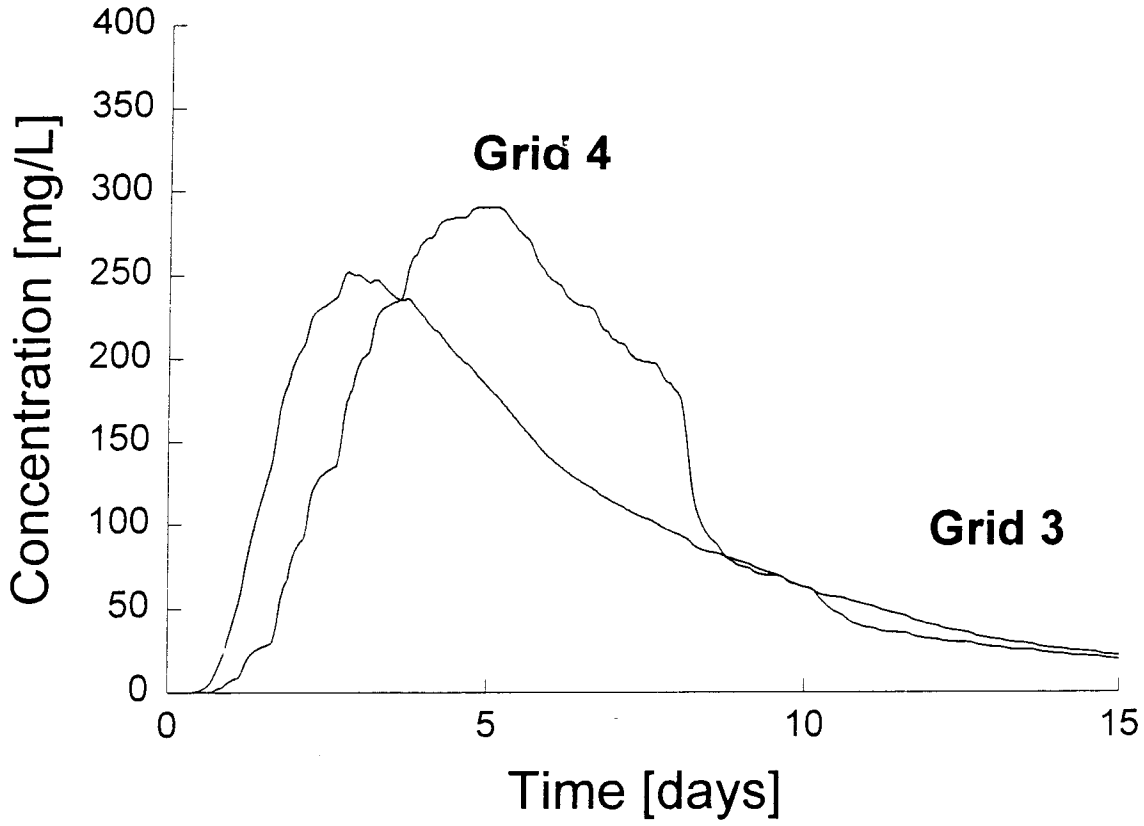

# Figure 26. Virus Breakthrough Curves

## 2 foot, low dose, R=1, μ=0

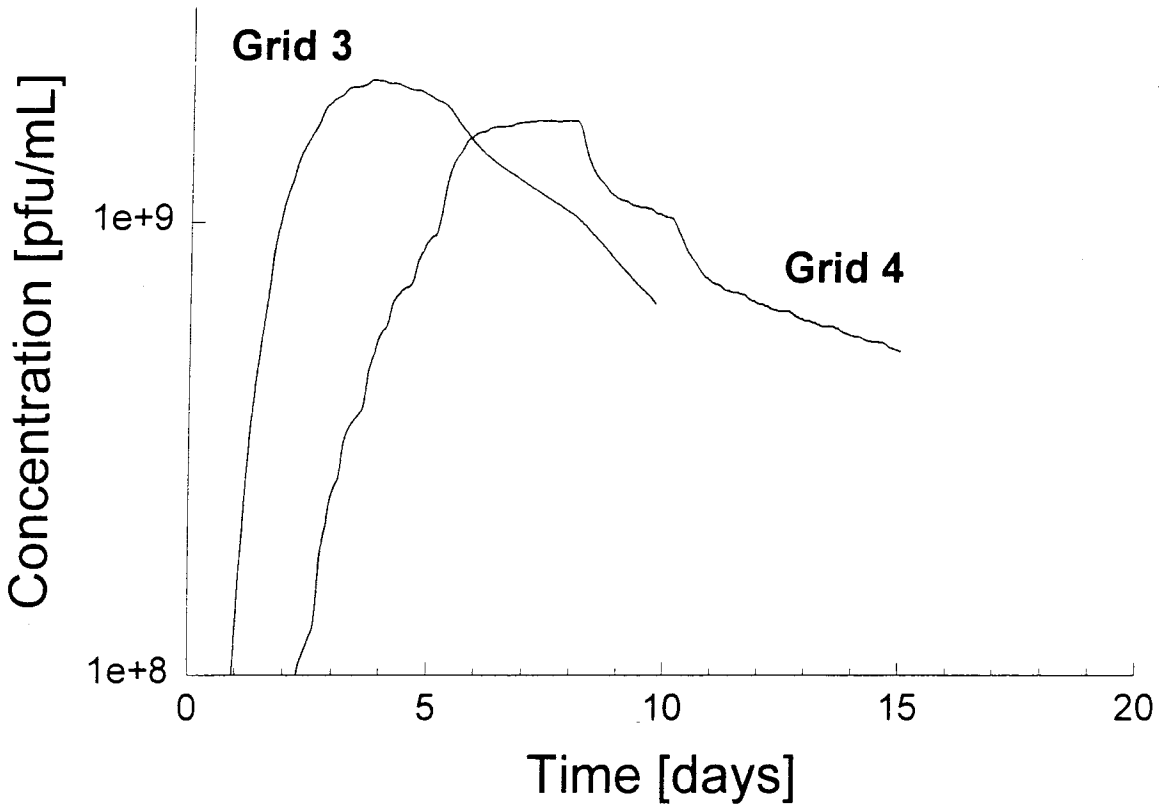

# Figure 27. Virus Breakthrough Curves

## 2 foot, high dose, R=1, μ=0

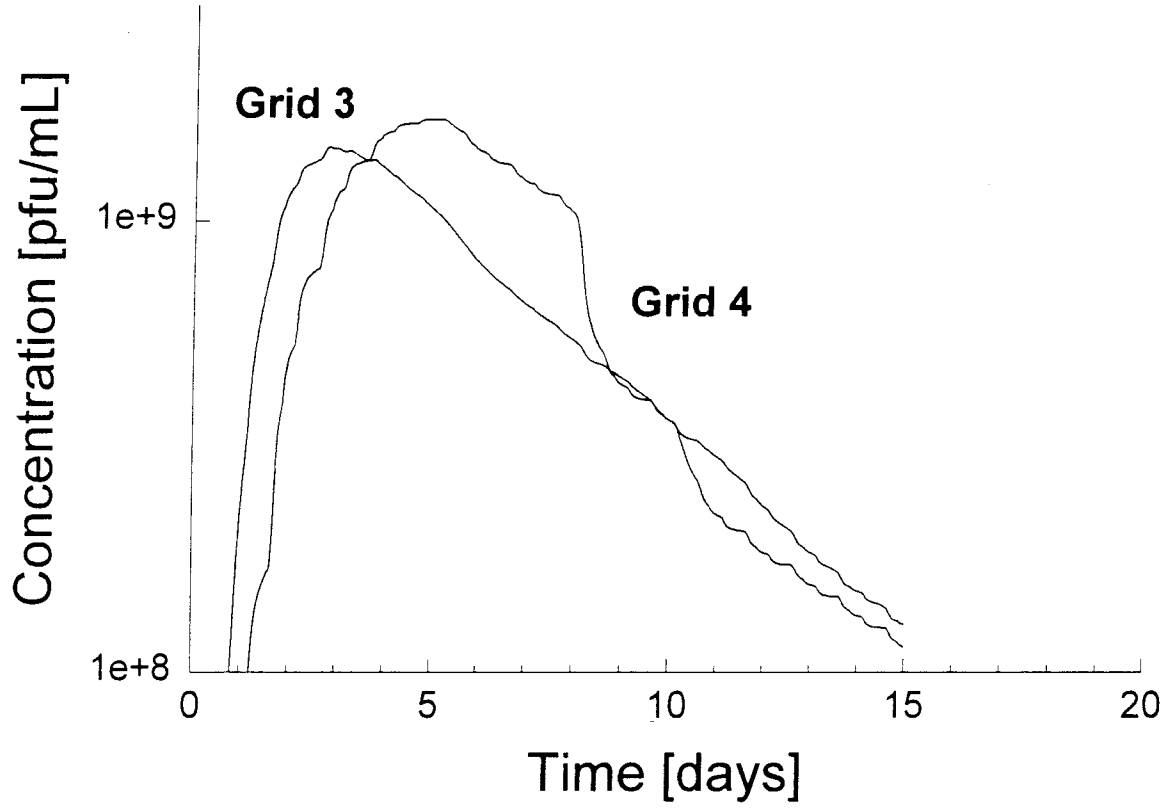

# Figure 28. Grid 3, Four-Foot Cell

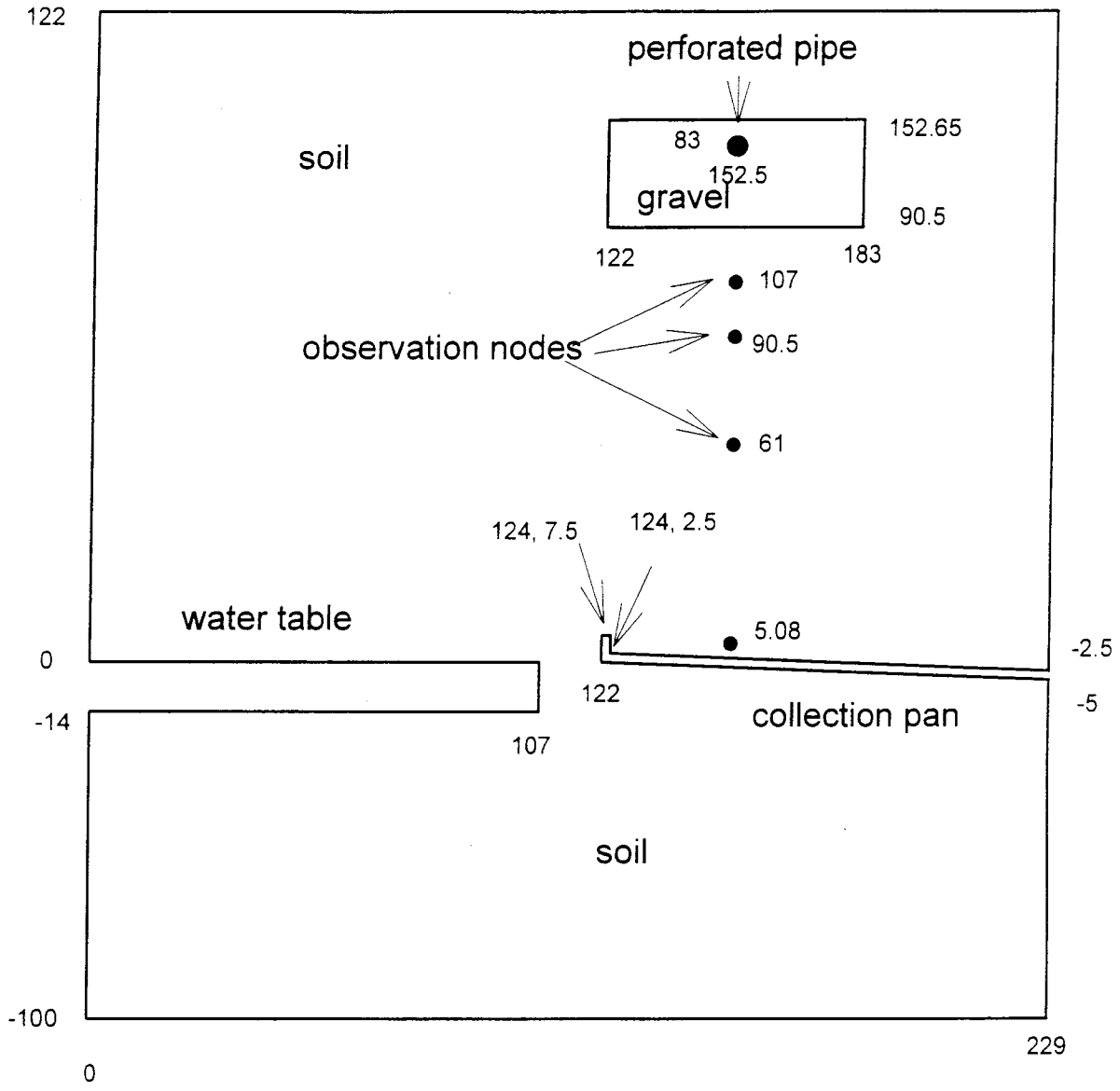

# Figure 29. Bromide Breakthrough Curves

**fine sand, low dose 4 ft**

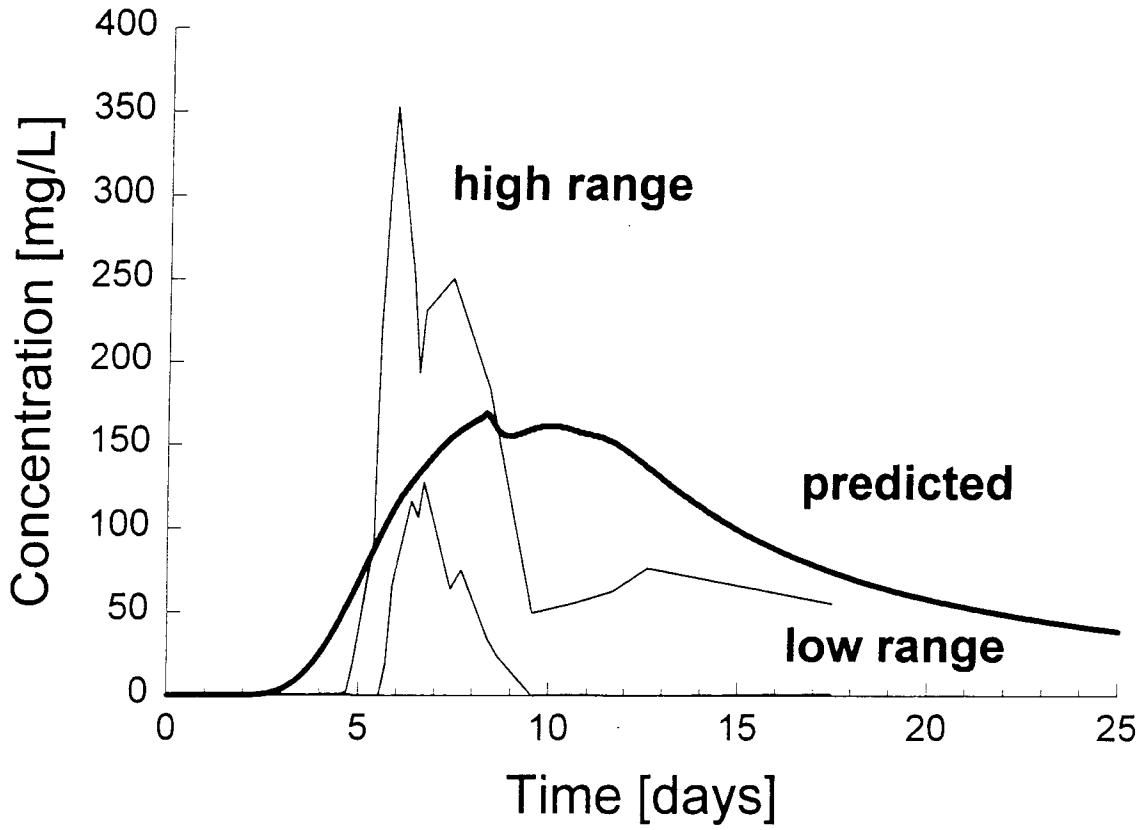

# Figure 30. Bromide Breakthrough Curves

## fine sand, high dose, 4 ft cell

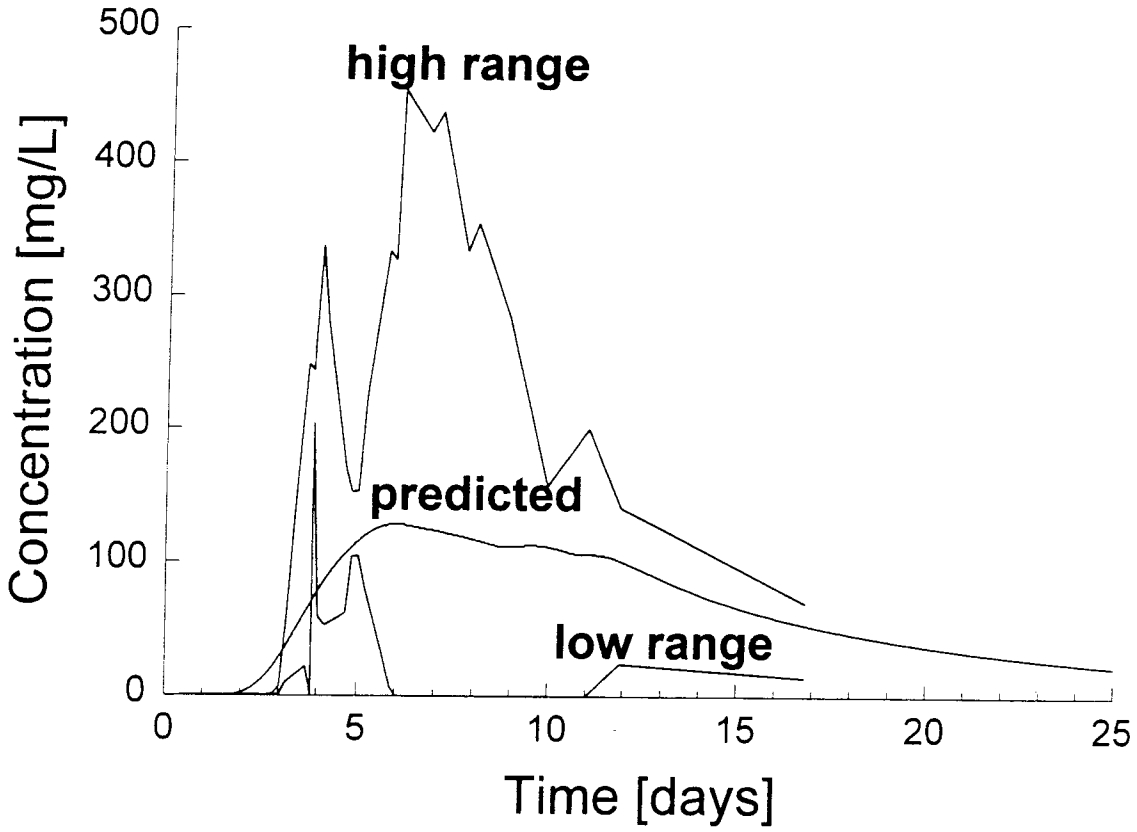

high dose cell. In this case, the predicted value was well within the range of the measured values for the entire 15-day time period.

The model predictions made using the pan configuration (grid 3) for the 4-foot cells were compared to those made using a water table configuration (grid 4). The results for the high dose case, assuming a non-reactive tracer, are shown in Figure 31. In this case, the virus peak occurs several days earlier in the water table simulations (day 2) compared to day 6 for the pan configuration. The predicted peak concentration is slightly higher for the water table case as well.

Another simulation was performed to examine the effects of the collection pan on the model results. In this case, the virus inactivation rate was assumed to be 0.33 $\log_{10}$ $day^{-1}$ and the soil adsorption coefficient was assumed to be zero. Figure 32 shows the results of the simulation in which the predicted concentration at the water table is approximately 0.5 $\log_{10}$ lower than that predicted using the pan configuration. The predicted virus concentrations in the soil at 6", 12", 2', and 4' below the perforated pipe are shown in Figure 33.

## DISCUSSION

The virus breakthrough curve that was predicted using a model calibrated with bromide data matched the measured virus concentrations at the lysimeter facility extremely well. This was especially noteworthy because the model was not calibrated using the virus data, nor was it calibrated for the high effluent dose rate. Because of this, it was felt to be appropriate to utilize the model to predict what type of virus behavior might be expected under other situations. The dramatic effect of the virus inactivation rate on predicted breakthrough curves was shown (Figure 11). At times of the year when the temperatures are high (over 80 F), viruses are inactivated very rapidly, and the concentrations would reach undetectable levels in the water very quickly, in a matter of several days. In contrast, when temperatures are very low (50 F), the viruses in the system may remain infective for several weeks to months.

Virus transport through two other soil types was examined to illustrate how the predictions for the fine sand would change at other sites. The presence of clay particles in soils will allow adsorption of some viruses, resulting in slowed transport to the underlying water. Examples using sandy loam and loam soils illustrated that virus transport to the saturated zone could be delayed by a few weeks (e.g., Figure 21). In

# Figure 31. Virus Breakthrough Curves

## 4 foot, high dose, R=1, μ=0

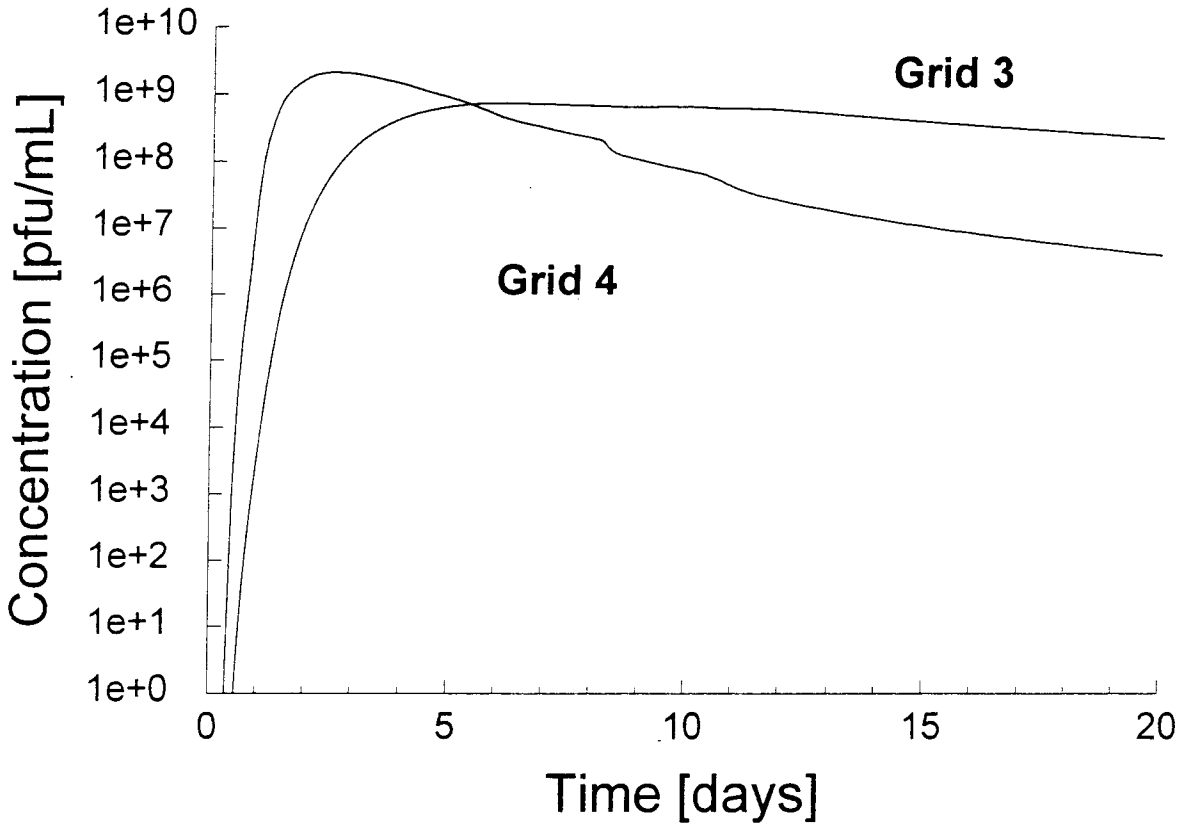

# Figure 32. Virus Breakthrough Curves

## 4 foot, high dose, R=1, μ=0.33

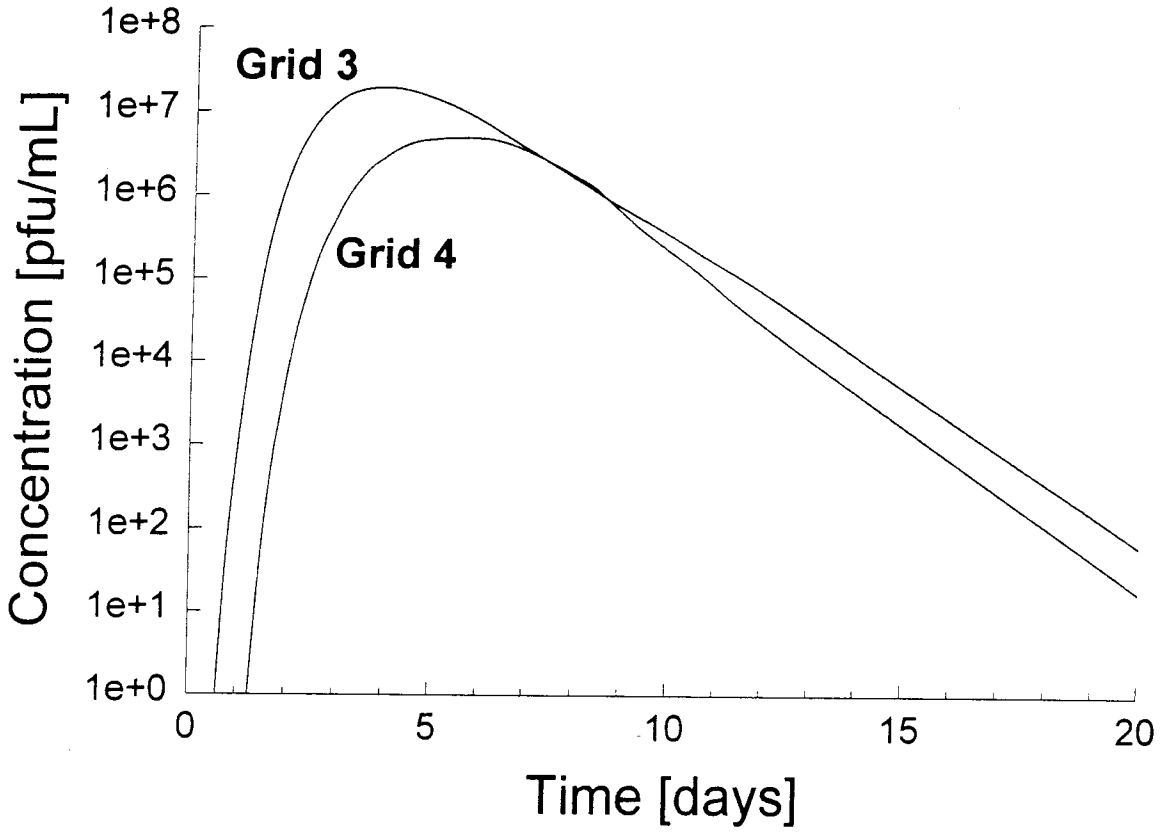

# Figure 33. Virus Breakthrough Curves

## 4 foot, high dose, water table, R=1, μ=0.33

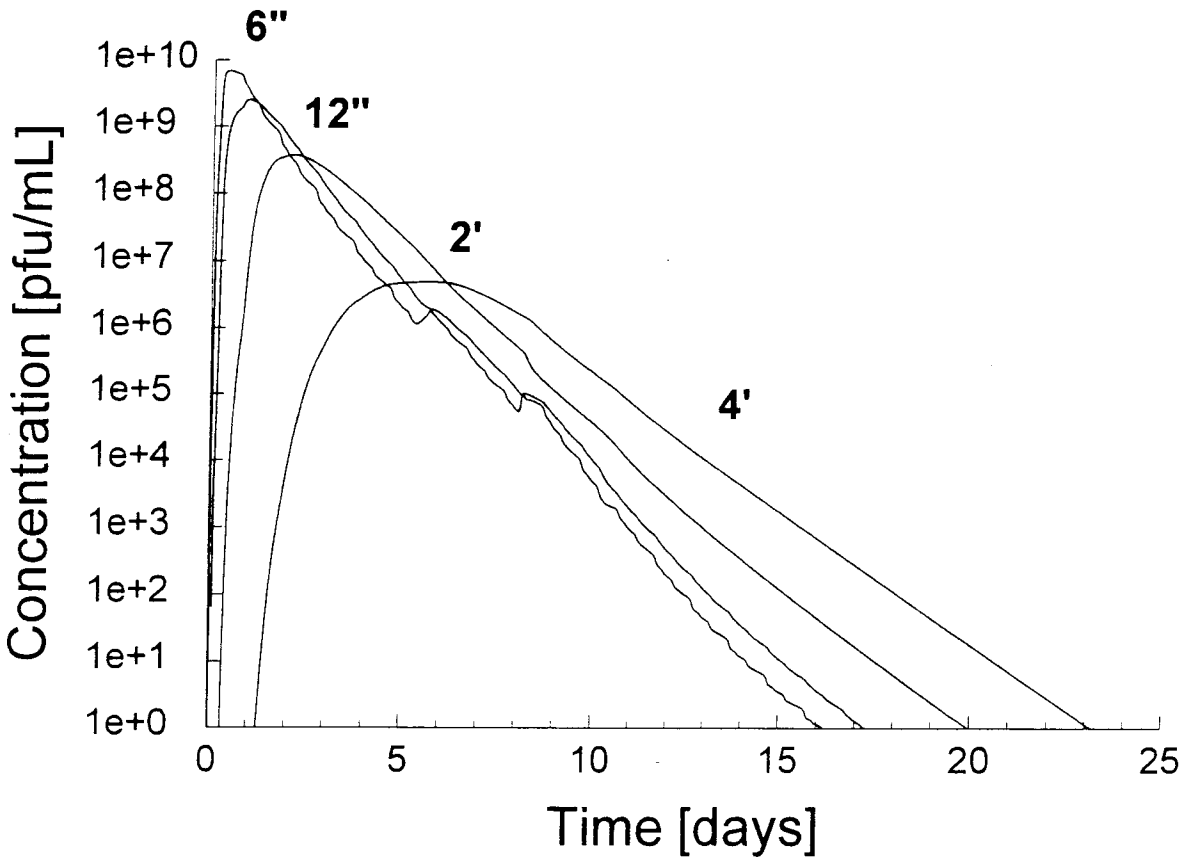

enhance our knowledge of the factors that affect our predictive capabilities.

## REFERENCES

Goyal, S.M. and C.P. Gerba. 1979. Comparative adsorption of human enteroviruses, simian rotavirus, and selected bacteriophages to soils. Appl. Environ. Microbiol. 38:241-246.

Simunek, J., and M. Th. van Genuchten. 1994. The SWMS_2D code for simulating water flow and solute transport in two-dimensional variably saturated media version 1.2. U.S. Salinity Laboratory, Report No. 132. Agricultural Research Service, U.S. Department of Agriculture, Riverside, California.

Yates, M.V. and S.R. Yates. 1988. Modeling microbial fate in the subsurface environment. CRC Crit. Rev. Environ. Contr. 17:307-344.

Table 1. Values Used for Testing HYDRUS-2d with a Constant Concentration Boundary Condition

| | | |
|---|---|---|
| Residual water content, $\theta_r$ | 0.001 | |
| Saturated water content, $\theta_s$ | 0.462 | |
| Moisture release parameter, $\alpha$ | 0.89 | m |
| Moisture release parameter, $n$ | 2.345 | |
| Saturated hydraulic conductivity, $K_s$ | $1.0(10)^{-10}$ | m/d |
| Bulk density, $\rho_b$ | 1.43 | $gm/cm^3$ |
| Longitudinal and Transverse dispersivity | 0.10 | m |
| Diffusion coefficient | 0.2 | $m^2/d$ |
| Degradation coefficient | 0.088 | $d^{-1}$ |

An additional test includes a pulse initial condition and a volatilization surface boundary condition. This case involves the use of CHAIN-2D which will be incorporated into the next version of HYDRUS-2D. This provides a good test of numerical accuracy when a highly localized initial distribution of chemical occurs, since the solute transport and water flow routines for CHAIN-2D are the same as those used in the present version of HYDRUS-2D. (Figures 2-3).

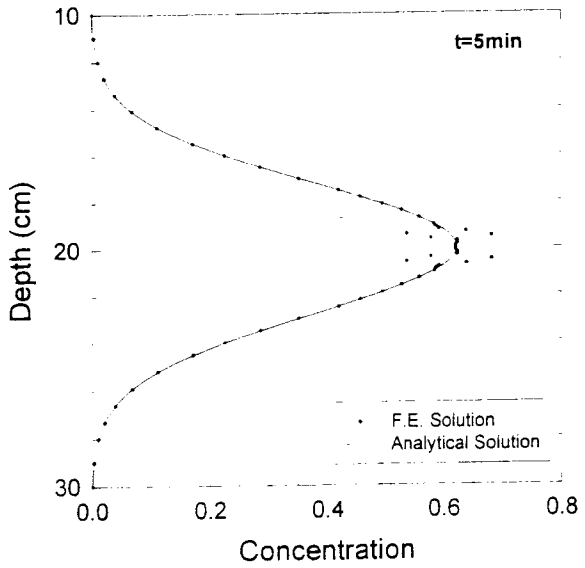


Figure 2. Test of numerical accuracy. Comparison of analytical solution (line) with CHAIN-2D (symbols) for an initially concentrated source and a volatilization boundary condition 5 min after injection.

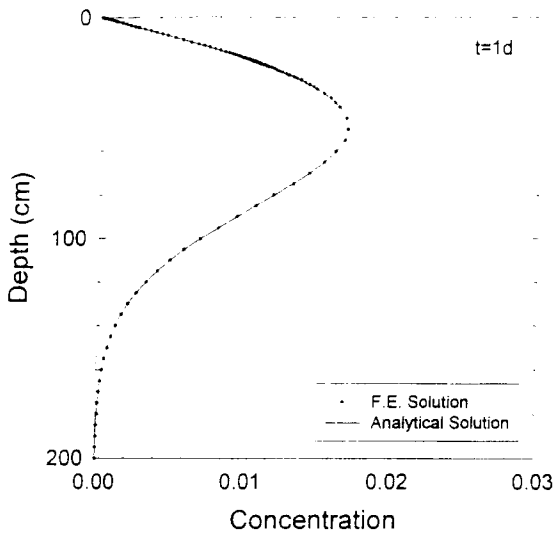


Figure 3. Test of numerical accuracy. Comparison of analytical solution (line) with CHAIN-2D (symbols) for an inititially concentrated source and a volatilization boundary condition 24 hours after injection.

| Date | Time | Temperature | Rain |
|---|---|---|---|
| 4/16/97 | 0 - 2400 | 73.2489796 | 0 |
| 4/17/97 | 0 - 2400 | 72.044898 | 0 |
| 4/18/97 | 0 - 2400 | 72.9530612 | 0 |
| 4/19/97 | 0 - 2400 | 74.1081633 | 0 |
| 4/20/97 | 0 - 430 | 75.83 | 0 |
| 4/20/97 | 500 | 75 | 0.04 |
| 4/20/97 | 530 | 74.9 | 0.01 |
| 4/20/97 | 600 - 2400 | 75.5054054 | 0 |
| 4/21/97 | 0 - 1700 | 76.9742857 | 0 |
| 4/21/97 | 1730 | 76.8 | 0.08 |
| 4/21/97 | 1800 | 76.3 | 0.41 |
| 4/21/97 | 1830 | 75.8 | 0.45 |
| 4/21/97 | 1900 | 75.5 | 0.02 |
| 4/21/97 | 1930 - 2400 | 75.11 | 0 |
| 4/22/97 | 0 - 900 | 73.7842105 | 0 |
| 4/22/97 | 930 | 72.5 | 0.01 |
| 4/22/97 | 1000 - 2400 | 73.7793103 | 0 |
| 4/23/97 | 0 - 2400 | 74.744898 | 0 |
| 4/24/97 | 0 - 1100 | 76.4 | 0 |
| 4/24/97 | 1130 | 75.3 | 0.01 |
| 4/24/97 | 1200 | 75.3 | 0.02 |
| 4/24/97 | 1230 | 75.3 | 0.06 |
| 4/24/97 | 1300 | 75.3 | 0.05 |
| 4/24/97 | 1330 | 75.3 | 0.2 |
| 4/24/97 | 1400 | 75.2 | 0.14 |
| 4/24/97 | 1430 | 75.1 | 0.48 |
| 4/24/97 | 1500 | 74.8 | 0.35 |
| 4/24/97 | 1530 | 74.6 | 0.26 |
| 4/24/97 | 1600 | 74.5 | 0.2 |
| 4/24/97 | 1630 | 74.3 | 0.28 |
| 4/24/97 | 1700 | 74.2 | 0.26 |
| 4/24/97 | 1730 | 74.1 | 0.24 |
| 4/24/97 | 1800 | 74 | 0.22 |
| 4/24/97 | 1830 | 73.9 | 0.18 |
| 4/24/97 | 1900 | 73.8 | 0.16 |
| 4/24/97 | 1930 | 73.7 | 0.14 |
| 4/24/97 | 2000 | 73.7 | 0.12 |
| 4/24/97 | 2030 | 73.8 | 0.1 |
| 4/24/97 | 2100 | 74 | 0.07 |
| 4/24/97 | 2130 | 74.3 | 0.04 |
| 4/24/97 | 2200 | 74.7 | 0.02 |
| 4/24/97 | 2230 | 75.5 | 0.02 |
| 4/24/97 | 2300 | 75.8 | 0.01 |
| 4/24/97 | 2330 | 75.8 | 0.01 |
| 4/24/97 | 2400 | 75.9 | 0 |
| 4/25/97 | 0 - 2400 | 75.9306122 | 0 |
| 4/26/97 | 0 - 1400 | 77.237931 | 0 |
| 4/26/97 | 1430 | 76.4 | 0.02 |

| Date | Time | Temperature | Rain |
|---|---|---|---|
| 4/26/97 | 1500 | 76.3 | 0.04 |
| 4/26/97 | 1530 | 76.2 | 0.05 |
| 4/26/97 | 1600 | 76.2 | 0.08 |
| 4/26/97 | 1630 | 76.1 | 0.1 |
| 4/26/97 | 1700 | 76.1 | 0.1 |
| 4/26/97 | 1730 | 76 | 0.11 |
| 4/26/97 | 1800 | 76 | 0.26 |
| 4/26/97 | 1830 | 75.9 | 0.24 |
| 4/26/97 | 1900 | 75.9 | 0.19 |
| 4/26/97 | 1930 | 75.9 | 0.14 |
| 4/26/97 | 2000 | 75.9 | 0.11 |
| 4/26/97 | 2030 | 75.8 | 0.09 |
| 4/26/97 | 2100 | 75.8 | 0.05 |
| 4/26/97 | 2130 | 75.8 | 0.04 |
| 4/26/97 | 2200 | 75.8 | 0.03 |
| 4/26/97 | 2230 | 75.8 | 0.02 |
| 4/26/97 | 2300 | 75.8 | 0.01 |
| 4/26/97 | 2330 | 75.9 | 0.01 |
| 4/26/97 | 2400 | 75.9 | 0.01 |
| 4/27/97 | 0 | 75.9 | 0.01 |
| 4/27/97 | 30 | 75.9 | 0.01 |
| 4/27/97 | 100 | 75.9 | 0.01 |
| 4/27/97 | 130 | 75.9 | 0 |
| 4/27/97 | 200 | 75.8 | 0.01 |
| 4/27/97 | 230 | 75.7 | 0.01 |
| 4/27/97 | 300 | 75.6 | 0 |
| 4/27/97 | 330 | 75.4 | 0.01 |
| 4/27/97 | 400 - 430 | 75.2 | 0 |
| 4/27/97 | 500 | 75 | 0.01 |
| 4/27/97 | 500 - 630 | 74.87 | 0 |
| 4/27/97 | 700 | 74.7 | 0.01 |
| 4/27/97 | 730 - 1000 | 74.35 | 0 |
| 4/27/97 | 1030 | 74 | 0.01 |
| 4/27/97 | 1100 - 1500 | 73.7888889 | 0 |
| 4/27/97 | 1530 | 74 | 0.01 |
| 4/27/97 | 1600 - 2400 | 75.8588235 | 0 |
| 4/28/97 | 0 - 2400 | 74.8734694 | 0 |
| 4/29/97 | 0 - 1330 | 74.4392857 | 0 |
| 4/29/97 | 1400 | 72.6 | 0.01 |
| 4/29/97 | 1430 - 2400 | 76.12 | 0 |
| 4/30/97 | 0 - 2400 | 76.6714286 | 0 |
| 5/1/97 | 0 - 2330 | 78.9041667 | 0 |
| 5/1/97 | 2400 | 81.6 | 0.02 |
| 5/2/97 | 0 | 81.6 | 0.02 |
| 5/2/97 | 30 - 1430 | 76.3103448 | 0 |
| 6/21/97 | 1230 - 2400 | 86.1666667 | 0 |
| 6/22/97 | 0 - 2400 | 84.0632653 | 0 |
| 6/23/97 | 0 - 1700 | 83.4428571 | 0 |

| Date | Time | Temperature | Rain |
|---|---|---|---|
| 6/23/97 | 1730 | 86.7 | 1.51 |
| 6/23/97 | 1800 | 85.8 | 0.67 |
| 6/23/97 | 1830 | 85.2 | 0.02 |
| 6/23/97 | 1900 | 84.7 | 0.01 |
| 6/23/97 | 1930 | 84.4 | 0.02 |
| 6/23/97 | 2000 | 84.1 | 0.02 |
| 6/23/97 | 2030 | 83.7 | 0.03 |
| 6/23/97 | 2100 | 83.4 | 0.02 |
| 6/23/97 | 2130 | 83.2 | 0.01 |
| 6/23/97 | 2200 | 83 | 0.01 |
| 6/23/97 | 2230 | 82.9 | 0.01 |
| 6/23/97 | 2300 - 2400 | 82.5 | 0 |
| 6/24/97 | 0 - 200 | 81.98 | 0 |
| 6/24/97 | 230 | 81.6 | 0.01 |
| 6/24/97 | 0 - 1500 | 81.776 | 0 |
| 6/24/97 | 1530 | 84.9 | 0.06 |
| 6/24/97 | 1600 | 84.8 | 0 |
| 6/24/97 | 1630 | 85 | 0.39 |
| 6/24/97 | 1700 | 84.9 | 0.71 |
| 6/24/97 | 1730 | 84.4 | 0.02 |
| 6/24/97 | 1800 | 84 | 0.44 |
| 6/24/97 | 1830 | 83.6 | 0.04 |
| 6/24/97 | 1530 - 2000 | 83.0333333 | 0 |
| 6/24/97 | 2030 | 82.6 | 0.03 |
| 6/24/97 | 2100 - 2300 | 81.98 | 0 |
| 6/24/97 | 2330 | 81.5 | 0.01 |
| 6/24/97 | 2400 | 81.4 | 0 |
| 6/25/97 | 0 - 2230 | 82.223913 | 0 |
| 6/25/97 | 2300 | 82.5 | 0.01 |
| 6/25/97 | 2330 - 2400 | 82.1 | 0 |
| 6/26/97 | 0 - 1100 | 81.1869565 | 0 |
| 6/26/97 | 1130 | 81.9 | 0.01 |
| 6/26/97 | 1200 - 1900 | 83.9866667 | 0 |
| 6/26/97 | 1930 | 84.6 | 0.32 |
| 6/26/97 | 2000 | 83.8 | 0.82 |
| 6/26/97 | 2030 | 83.1 | 0.03 |
| 6/26/97 | 2100 - 2230 | 82.225 | 0 |
| 6/26/97 | 2300 | 81.8 | 0.01 |
| 6/26/97 | 2330 - 2400 | 81.4 | 0 |
| 6/27/97 | 0 - 2400 | 82.2857143 | 0 |
| 6/28/97 | 0 - 1430 | 82.05 | 0 |
| 6/28/97 | 1500 | 84.7 | 0.13 |
| 6/28/97 | 1530 | 84.3 | 1.46 |
| 6/28/97 | 1600 | 83.6 | 0.09 |
| 6/28/97 | 1630 | 83.2 | 0.01 |
| 6/28/97 | 1700 | 82.9 | 0.03 |
| 6/28/97 | 1730 | 82.6 | 0.03 |
| 6/28/97 | 1800 | 82.4 | 0.02 |

| Date | Time | Temperature | Rain |
|---|---|---|---|
| 6/28/97 | 1830 - 2400 | 81.8166667 | 0 |
| 6/29/97 | 0 - 1130 | 80.4708333 | 0 |
| 6/29/97 | 1200 | 81.6 | 0.01 |
| 6/29/97 | 1230 - 2400 | 83.6333333 | 0 |
| 6/30/97 | 0 - 2400 | 82.8632653 | 0 |
| 7/1/97 | 0 - 1000 | 81.752381 | 0 |
| 7/1/97 | 1100 - 1330 | 82.4333333 | 0 |
| 7/1/97 | 1400 | 83.4 | 0.16 |
| 7/1/97 | 1430 - 2400 | 83.945 | 0 |
| 7/2/97 | 0 - 830 | 82.05 | 0 |
| 7/2/97 | 900 | 81.8 | 0.02 |
| 7/2/97 | 930 | 81.8 | 0 |
| 7/2/97 | 1000 | 81.8 | 0.01 |
| 7/2/97 | 1030 - 2400 | 84.5678571 | 0 |
| 7/3/97 | 0 - 2400 | 84.7632653 | 0 |
| 7/4/97 | 0 - 1900 | 84.8974359 | 0 |
| 7/4/97 | 1930 | 87 | 0.42 |
| 7/4/97 | 2000 | 86.4 | 0.1 |
| 7/4/97 | 2030 | 85.8 | 0.01 |
| 7/4/97 | 2100 | 85.2 | 0.02 |
| 7/4/97 | 2130 | 84.7 | 0.07 |
| 7/4/97 | 2200 | 84.5 | 0.02 |
| 7/4/97 | 2230 - 2400 | 83.825 | 0 |
| 7/5/97 | 0 - 300 | 83.0714286 | 0 |
| 7/5/97 | 330 | 82.5 | 0.01 |
| 7/5/97 | 400 - 1430 | 82.5818182 | 0 |
| 7/5/97 | 1500 | 84.4 | 0.33 |
| 7/5/97 | 1530 | 83.9 | 0.83 |
| 7/5/97 | 1600 | 83.4 | 0.04 |
| 7/5/97 | 1630 - 1800 | 82.875 | 0 |
| 7/5/97 | 1830 | 82.5 | 0.01 |
| 7/5/97 | 1900 | 82.4 | 0.04 |
| 7/5/97 | 1930 | 82.1 | 0.02 |
| 7/5/97 | 2000 | 81.9 | 0.05 |
| 7/5/97 | 2030 | 81.8 | 0.04 |
| 7/5/97 | 2100 | 81.7 | 0.05 |
| 7/5/97 | 2130 | 81.6 | 0.07 |
| 7/5/97 | 2200 | 81.4 | 0.02 |
| 7/5/97 | 2230 | 81.2 | 0.01 |
| 7/5/97 | 2300 - 2400 | 81.0666667 | 0 |
| 7/6/97 | 0 - 1100 | 80.6043478 | 0 |
| 7/6/97 | 1130 | 81.5 | 0.31 |
| 7/6/97 | 1200 | 81.4 | 0.26 |
| 7/6/97 | 1230 | 81.3 | 0.07 |
| 7/6/97 | 1300 | 81 | 0.03 |
| 7/6/97 | 1330 | 80.9 | 0.03 |
| 7/6/97 | 1400 - 2400 | 82.4047619 | 0 |
| 7/7/97 | 0 - 2400 | 82.8897959 | 0 |

| Date | Time | Temperature | Rain |
|---|---|---|---|
| 7/8/97 | 0 - 1500 | 82.5 | 0 |
| 7/8/97 | 1530 | 84.7 | 0.39 |
| 7/8/97 | 1600 | 84.3 | 0.08 |
| 7/8/97 | 1630 | 83.8 | 0.09 |
| 7/8/97 | 1700 - 2400 | 82.88 | 0 |
| 7/9/97 | 0 - 830 | 81.0222222 | 0 |
| 7/9/97 | 900 | 80.7 | 0.01 |
| 7/9/97 | 930 - 1500 | 83.425 | 0 |
| 7/9/97 | 1530 | 83.8 | 0.01 |
| 7/9/97 | 1600 - 2400 | 83.3823529 | 0 |
| 7/10/97 | 0 - 1800 | 81.1243243 | 0 |
| 7/10/97 | 1830 | 86.7 | 0.07 |
| 7/10/97 | 1900 - 2400 | 84.6090909 | 0 |
| 7/11/97 | 0 - 1200 | 82.196 | 0 |
| 7/11/97 | 1230 | 83.6 | 0.01 |
| 7/11/97 | 1300 - 1500 | 84.74 | 0 |
| 7/11/97 | 1530 | 85.7 | 0.96 |
| 7/11/97 | 1600 | 85 | 0.23 |
| 7/11/97 | 1630 | 84.2 | 0.01 |
| 7/11/97 | 1700 - 1830 | 83.325 | 0 |
| 7/11/97 | 1900 | 82.8 | 0.01 |
| 7/11/97 | 1930 | 82.7 | 0.01 |
| 7/11/97 | 2000 - 2400 | 81.9555556 | 0 |
| 7/12/97 | 0 - 400 | 81.0333333 | 0 |
| 7/12/97 | 430 | 80.6 | 0.01 |
| 7/12/97 | 500 - 2400 | 81.9974359 | 0 |
| 7/13/97 | 0 - 2400 | 82.9367347 | 0 |
| 7/14/97 | 0 - 1730 | 83.2222222 | 0 |
| 7/14/97 | 1800 | 85.1 | 0.08 |
| 7/14/97 | 1830 - 1930 | 84.2666667 | 0 |
| 7/14/97 | 2000 | 83.6 | 0.01 |
| 7/14/97 | 2030 - 2400 | 82.575 | 0 |
| 7/15/97 | 0 - 1130 | 81.0458333 | 0 |
| 7/15/97 | 1200 | 82.4 | 0.01 |
| 7/15/97 | 1230 - 2400 | 84.3791667 | 0 |
| 7/16/97 | 0 - 1600 | 82.5787879 | 0 |
| 7/16/97 | 1630 | 86.2 | 0.01 |
| 7/16/97 | 1700 | 85.8 | 0.01 |
| 7/16/97 | 1730 | 85.5 | 0.01 |
| 7/16/97 | 1800 - 2400 | 83.6692308 | 0 |
| 7/17/97 | 0 - 800 | 81.5058824 | 0 |
| 7/17/97 | 830 | 81 | 0.23 |
| 7/17/97 | 900 - 1600 | 83.2733333 | 0 |
| 7/17/97 | 1630 | 84.4 | 0.06 |
| 7/17/97 | 1700 - 2400 | 83.28 | 0 |
| 7/18/97 | 0 - 200 | 82.7253333 | 0 |
| 7/18/97 | 230 | 81.8 | 0.01 |
| 7/18/97 | 300 - 1600 | 82.1407407 | 0 |

| Date | Time | Temperature | Rain |
|---|---|---|---|
| 7/18/97 | 1630 | 85 | 0.01 |
| 7/18/97 | 1700 | 84.7 | 0.03 |
| 7/18/97 | 1730 - 2400 | 83.6357143 | 0 |
| 7/19/97 | 0 - 1130 | 81.5708333 | 0 |
| 7/19/97 | 1200 | 82.2 | 0.08 |
| 7/19/97 | 1230 | 82 | 0.01 |
| 7/19/97 | 1300 | 81.9 | 0.03 |
| 7/19/97 | 1330 | 81.9 | 0.01 |
| 7/19/97 | 1400 - 1730 | 82.5875 | 0 |
| 7/19/97 | 1800 | 83.1 | 0.13 |
| 7/19/97 | 1830 | 82.8 | 0.04 |
| 7/19/97 | 1900 | 82.5 | 0.01 |
| 7/19/97 | 1930 | 82.3 | 0.04 |
| 7/19/97 | 2000 | 82.1 | 0.03 |
| 7/19/97 | 2030 | 82 | 0.01 |
| 7/19/97 | 2100 - 2400 | 81.4571429 | 0 |
| 7/20/97 | 0 - 630 | 80.7071429 | 0 |
| 7/20/97 | 700 | 80.2 | 0.01 |
| 7/20/97 | 730 - 1330 | 81.2 | 0 |
| 7/20/97 | 1400 | 83.5 | 0.07 |
| 7/20/97 | 1430 | 83.5 | 0.36 |
| 7/20/97 | 1500 | 83.3 | 0.01 |
| 7/20/97 | 1530 - 1630 | 83.25 | 0 |
| 7/20/97 | 1700 | 82.7 | 0.04 |
| 7/20/97 | 1730 | 82.5 | 0.02 |
| 7/20/97 | 1800 - 2400 | 81.9733333 | 0 |
| 7/21/97 | 0 - 230 | 81.1666667 | 0 |
| 7/21/97 | 300 | 80.9 | 0.01 |
| 7/21/97 | 330 - 1630 | 82.0444444 | 0 |
| 7/21/97 | 1700 | 84.5 | 0.17 |
| 7/21/97 | 1730 | 84.3 | 0.02 |
| 7/21/97 | 1800 - 2400 | 83.2692308 | 0 |
| 7/22/97 | 0 - 1730 | 82.7388889 | 0 |
| 7/22/97 | 1800 | 86.2 | 0.95 |
| 7/22/97 | 1830 | 85.6 | 0.15 |
| 7/22/97 | 1900 | 85.2 | 0 |
| 7/22/97 | 1930 | 84.8 | 0.01 |
| 7/22/97 | 2000 | 84.5 | 0.01 |
| 7/22/97 | 2030 - 2400 | 83.3375 | 0 |
| 7/23/97 | 0 - 2400 | 83.3755102 | 0 |
| 7/24/97 | 0 - 530 | 83.0166667 | 0 |
| 7/24/97 | 600 | 82.1 | 0.01 |
| 7/24/97 | 630 - 1930 | 84.1851852 | 0 |
| 7/24/97 | 2000 | 85.6 | 0.08 |
| 7/24/97 | 2030 | 85.3 | 0.01 |
| 7/24/97 | 2100 - 2400 | 84.0142857 | 0 |
| 7/25/97 | 0 - 430 | 82.56 | 0 |
| 7/25/97 | 500 | 81.9 | 0.01 |

| Date | Time | Temperature | Rain |
|---|---|---|---|
| 7/25/97 | 530 - 2400 | 84.2026316 | 0 |
| 7/26/97 | 0 - 1200 | 83.036 | 0 |
| 7/26/97 | 1230 | 83.5 | 0.04 |
| 7/26/97 | 1300 | 83.4 | 0.35 |
| 7/26/97 | 1330 | 83.2 | 0 |
| 7/26/97 | 1400 | 83 | 0.02 |
| 7/26/97 | 1430 - 1700 | 83.4333333 | 0 |
| 7/26/97 | 1730 | 83.9 | 0.01 |
| 7/26/97 | 1800 - 2400 | 83.8846154 | 0 |
| 7/27/97 | 0 - 1500 | 82.3903226 | 0 |
| 7/27/97 | 1530 | 85.5 | 0.3 |
| 7/27/97 | 1600 | 85.2 | 0.02 |
| 7/27/97 | 1630 - 2400 | 83.325 | 0 |
| 7/28/97 | 0 - 830 | 81.0166667 | 0 |

# Observation Nodes: Concentrations

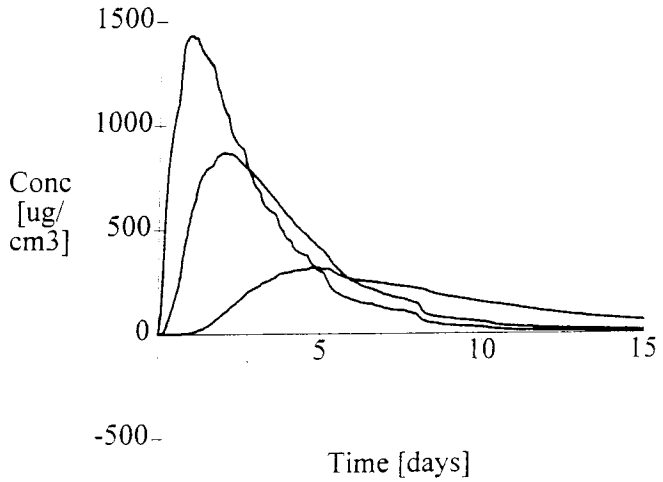


# Observation Nodes: Concentrations

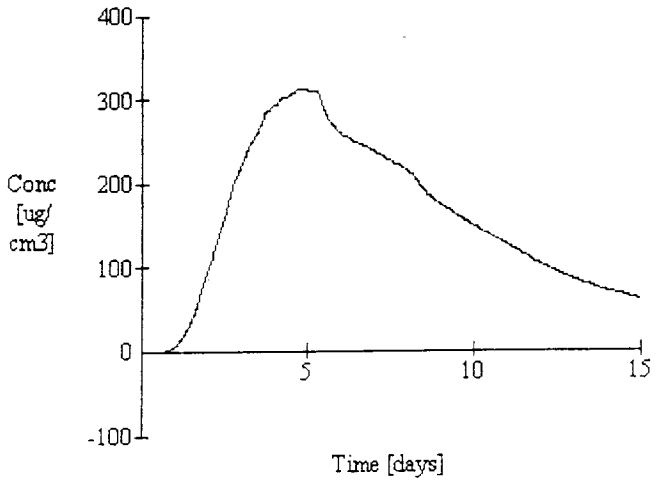

# Cumulative Variable Boundary Solute Flux

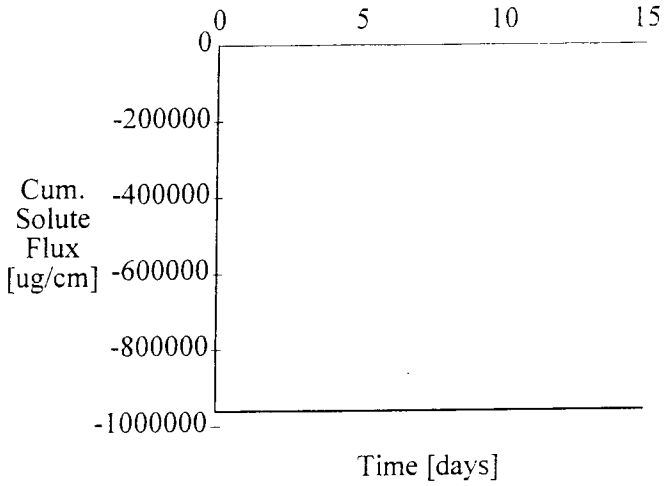


# Free or Deep Drainage Boundary Solute Flux

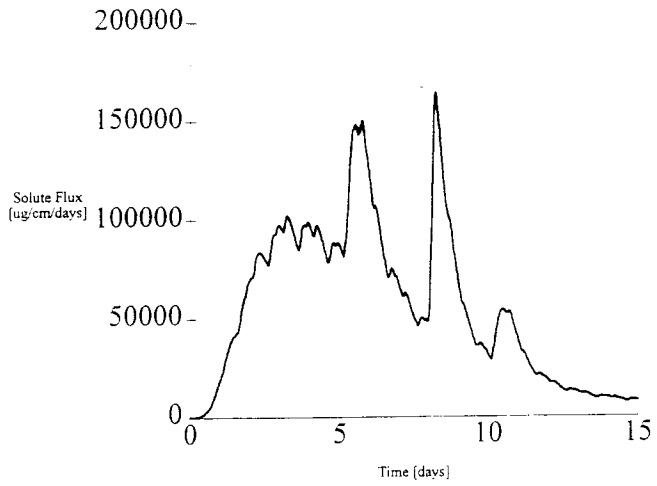

# Constant Boundary Solute Flux

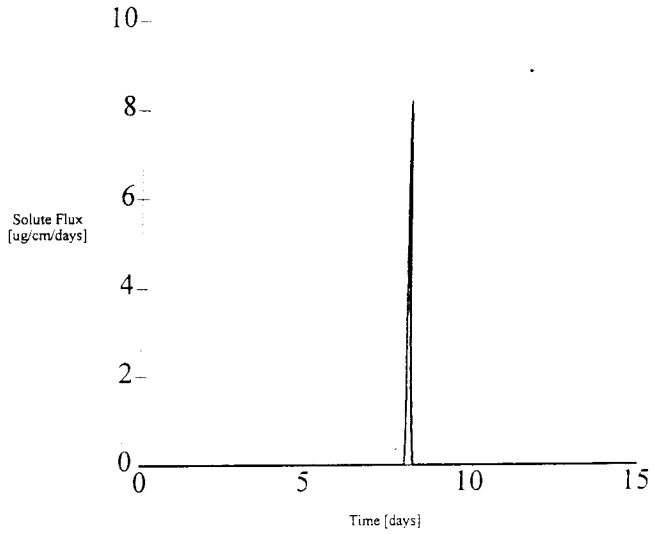


# Seepage Face Solute Flux

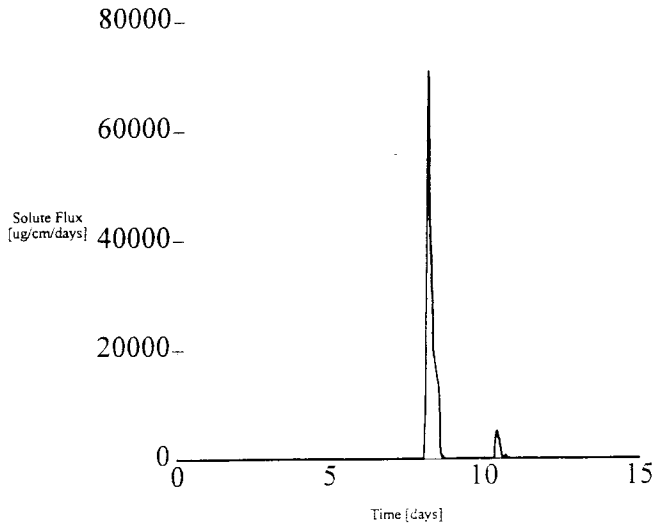

# Observation Nodes: Concentrations

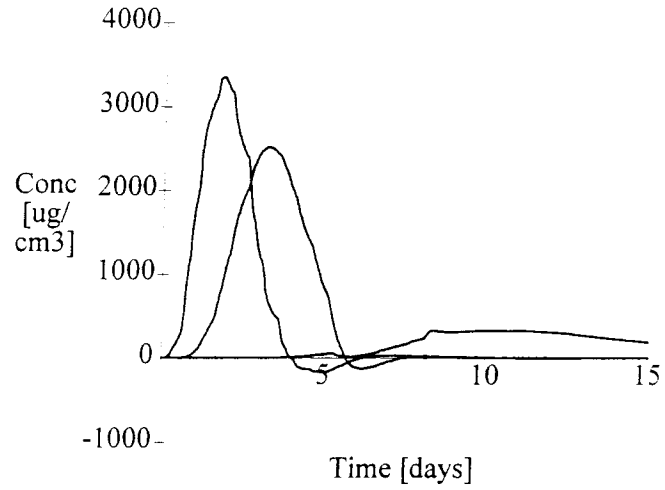


# Observation Nodes: Concentrations

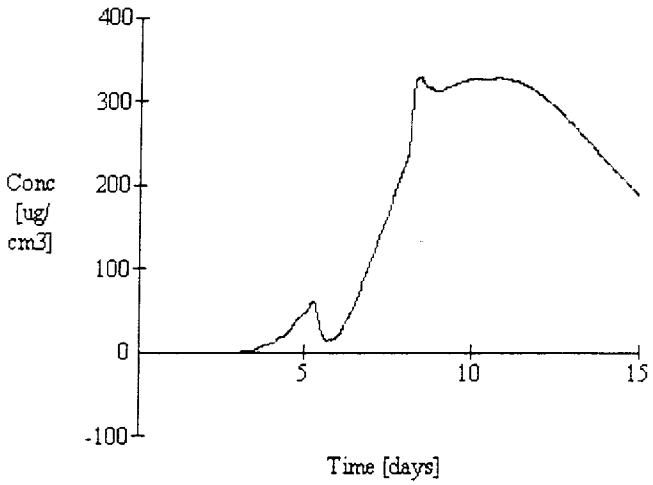

# Cumulative Variable Boundary Solute Flux

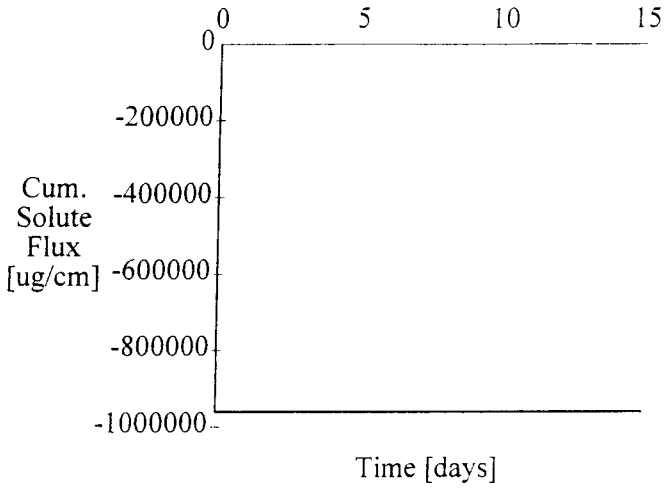


# Free or Deep Drainage Boundary Solute Flux

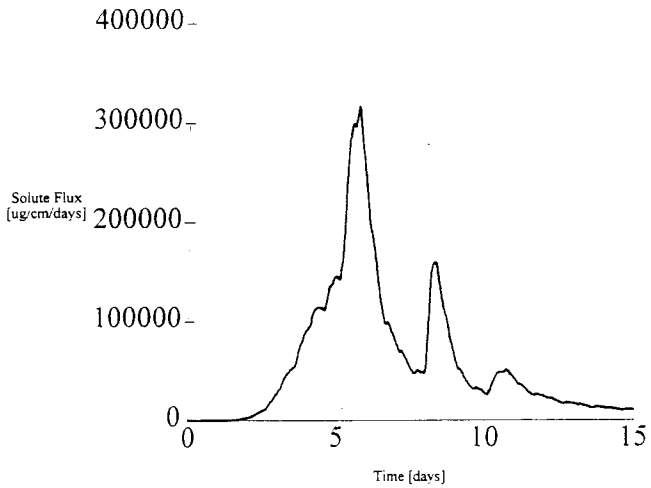

# Constant Boundary Solute Flux

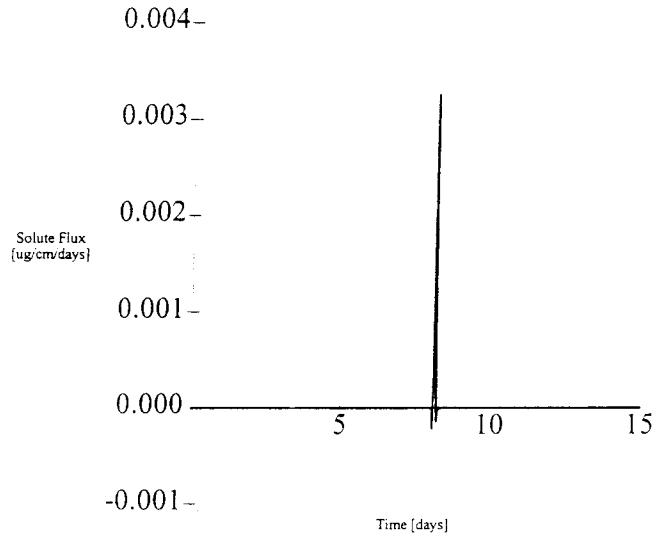


# Seepage Face Solute Flux

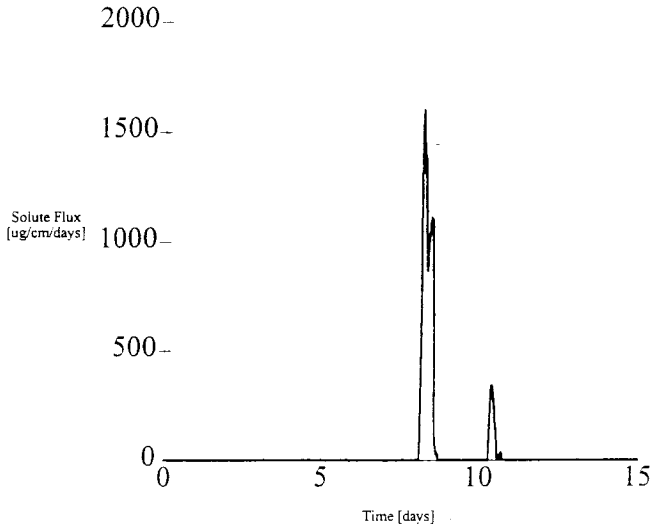

# Observation Nodes: Concentrations

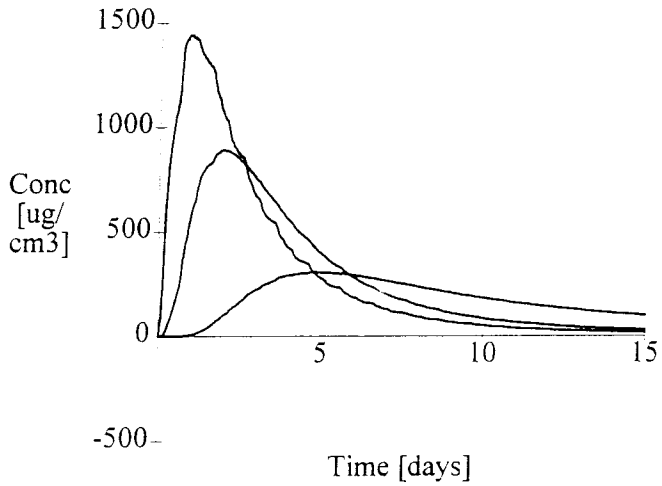


# Observation Nodes: Concentrations

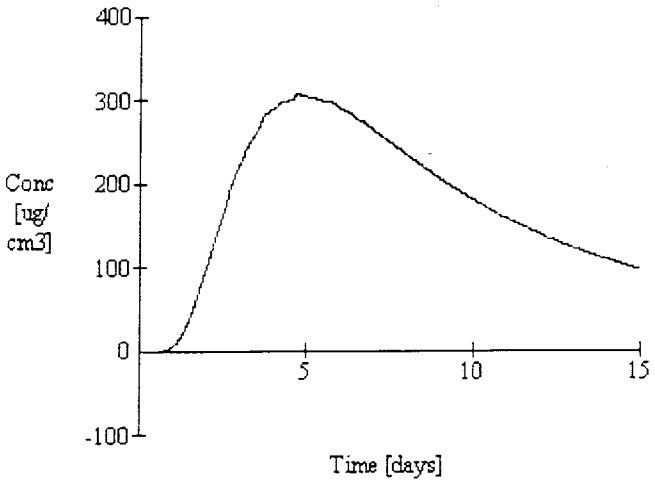

# Cumulative Variable Boundary Solute Flux

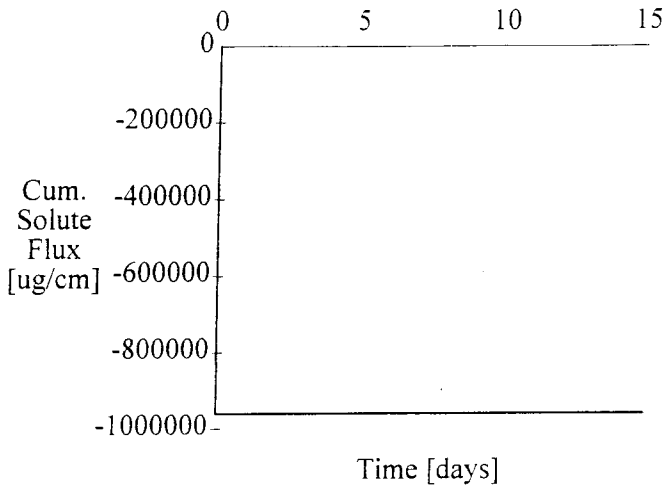


# Free or Deep Drainage Boundary Solute Flux

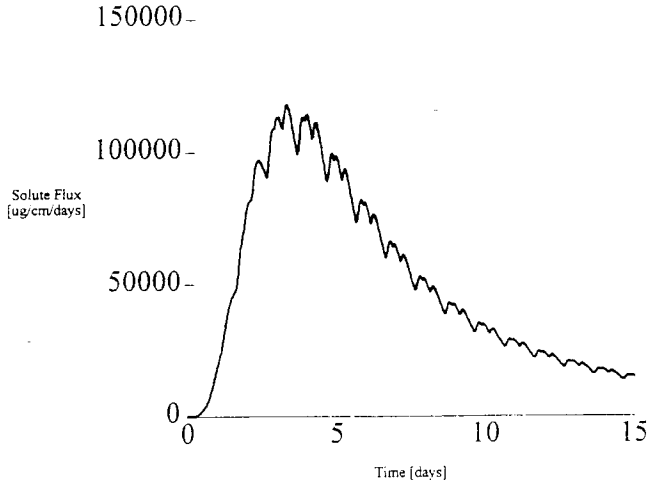

# Constant Boundary Solute Flux

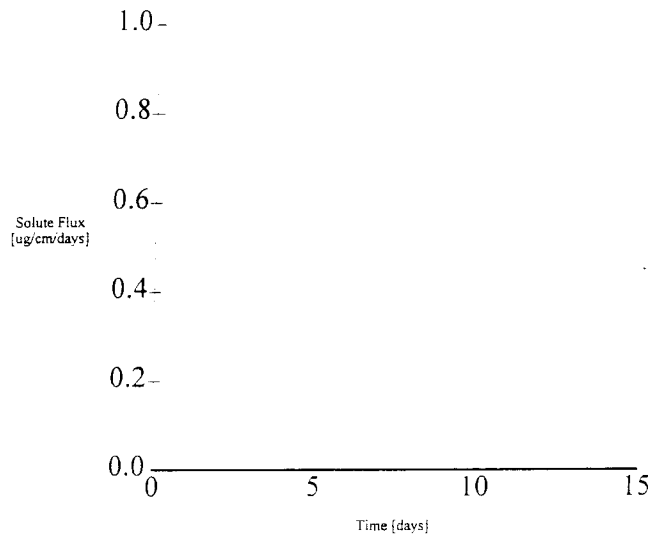


# Seepage Face Solute Flux

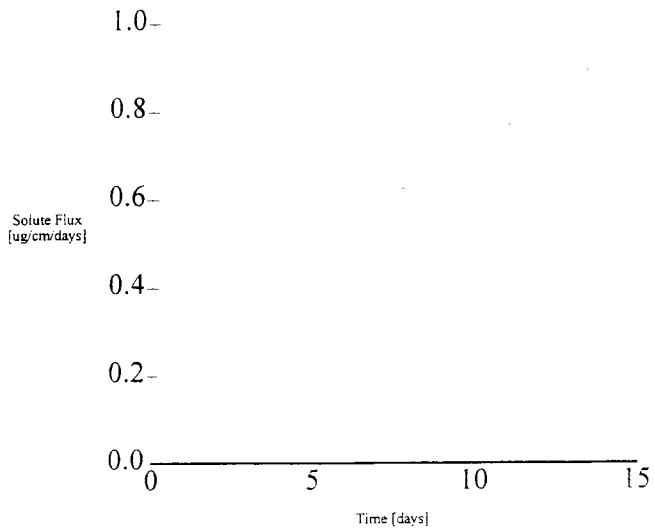

# Observation Nodes: Concentrations

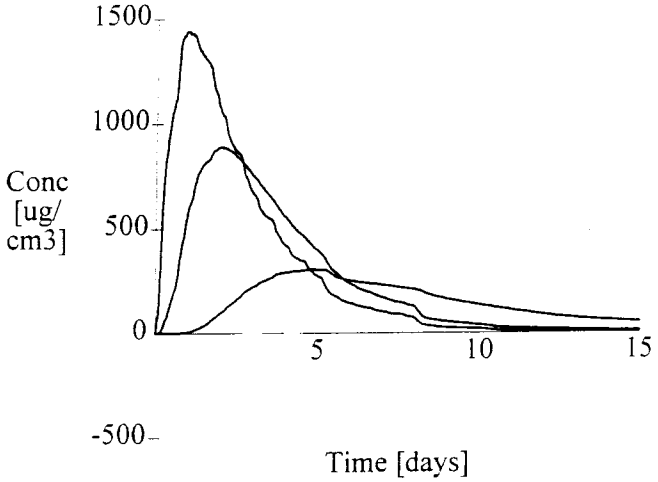


# Observation Nodes: Concentrations

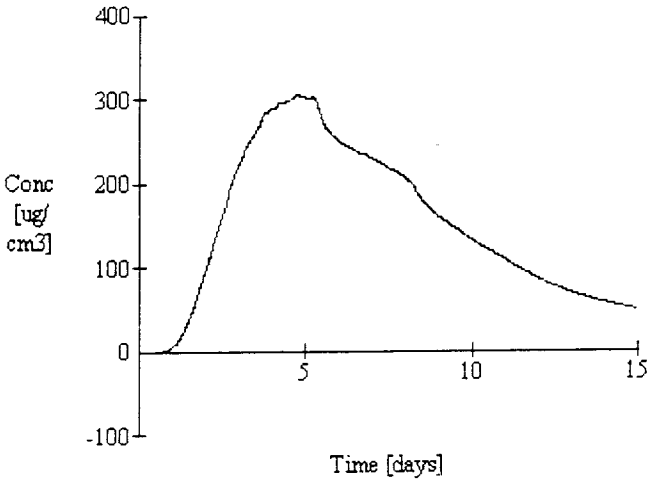

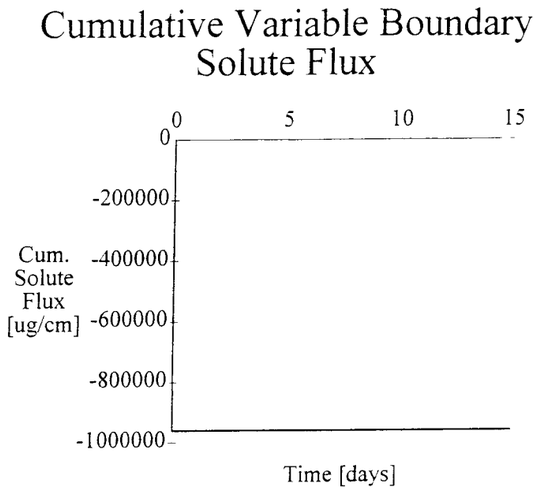
Cumulative Variable Boundary
Solute Flux
0
5
10
15
0
-200000
-400000
-600000
-800000
-1000000
Cum.
Solute
Flux
[ug/cm]
Time [days]

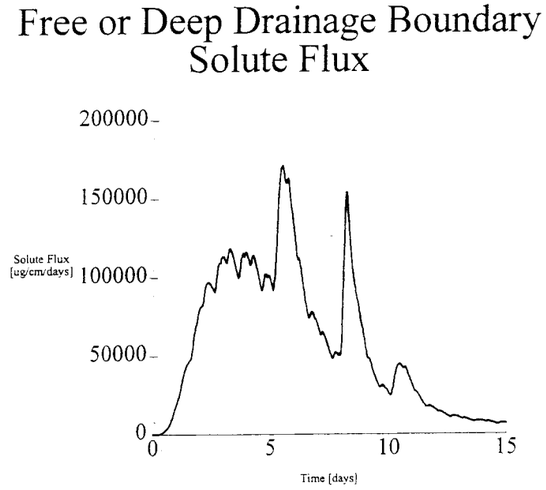
Free or Deep Drainage Boundary
Solute Flux
200000
150000
100000
50000
0
Solute Flux
[ug/cm/days]
0
5
10
15
Time [days]

# Constant Boundary Solute Flux

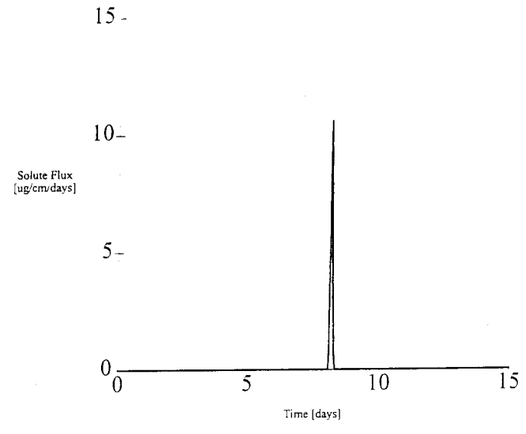


# Seepage Face Solute Flux

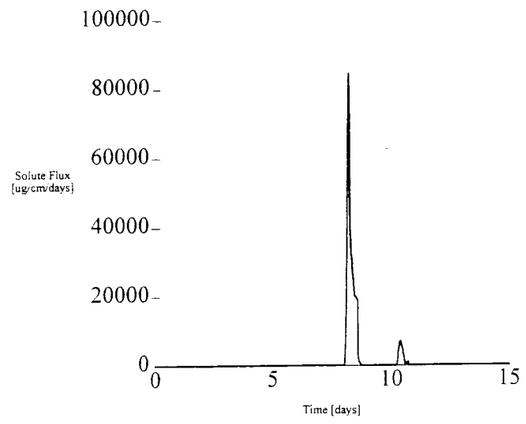

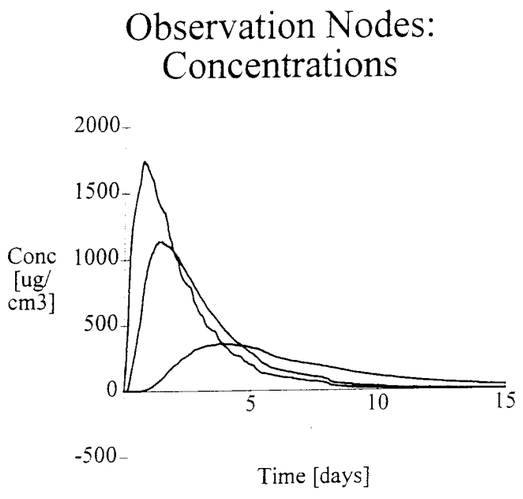
Observation Nodes:
Concentrations
2000
1500
1000
500
0
-500
Conc
[ug/
cm3]
5
10
15
Time [days]

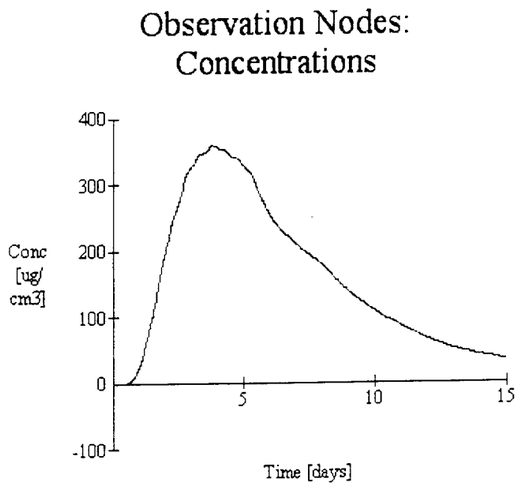
Observation Nodes:
Concentrations
400
300
200
100
0
-100
Conc
[ug/
cm3]
5
10
15
Time [days]

# Constant Boundary Solute Flux

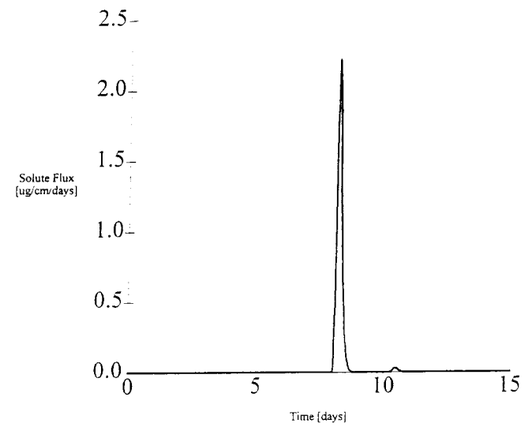


# Seepage Face Solute Flux

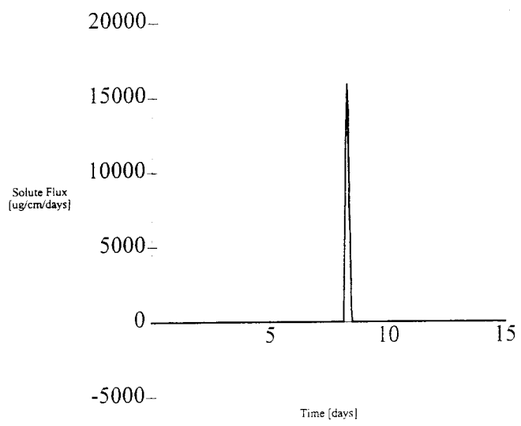

## Cumulative Variable Boundary Solute Flux

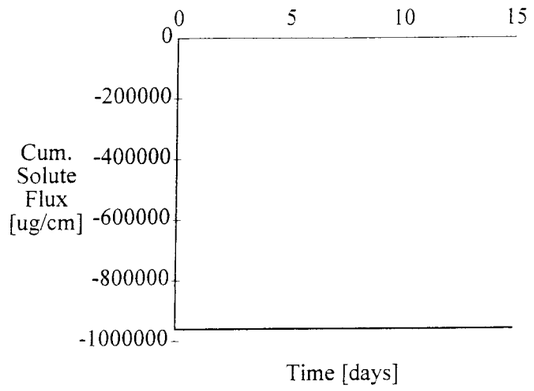


## Free or Deep Drainage Boundary Solute Flux

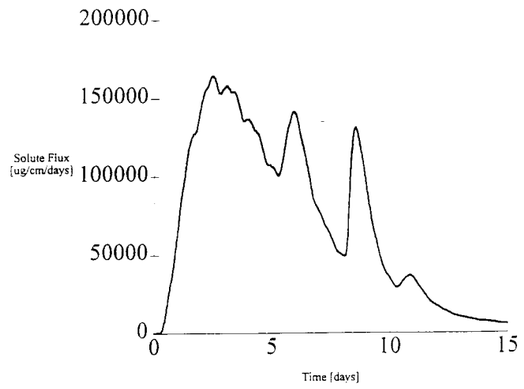

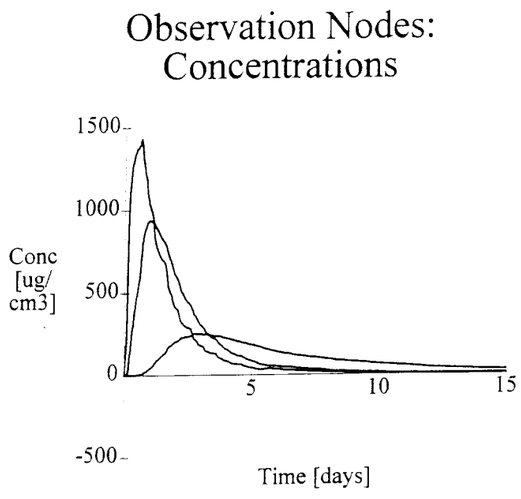
Observation Nodes:
Concentrations
1500
1000
500
0
-500
Conc
[ug/
cm3]
5
10
15
Time [days]

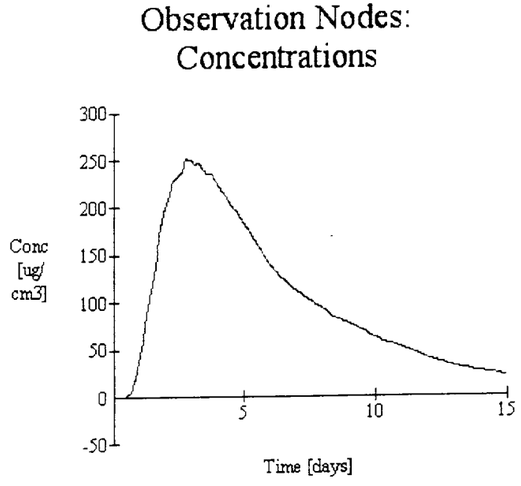
Observation Nodes:
Concentrations
300
250
200
150
100
50
0
-50
Conc
[ug/
cm3]
5
10
15
Time [days]

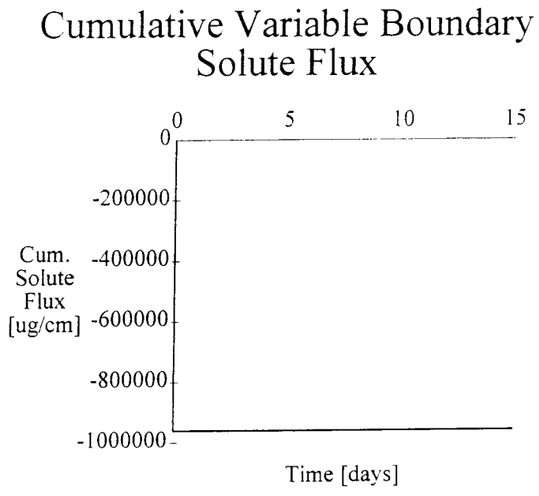
Cumulative Variable Boundary
Solute Flux
0
5
10
15
0
-200000
-400000
-600000
-800000
-1000000
Cum.
Solute
Flux
[ug/cm]
Time [days]

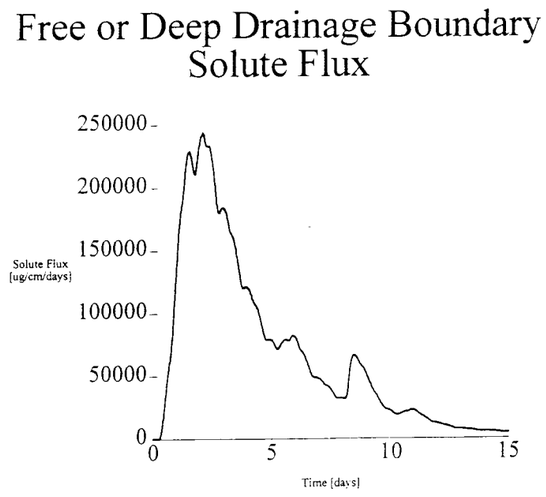
Free or Deep Drainage Boundary
Solute Flux
250000
200000
150000
100000
50000
0
Solute Flux
[ug/cm/days]
0
5
10
15
Time [days]

# Constant Boundary Solute Flux

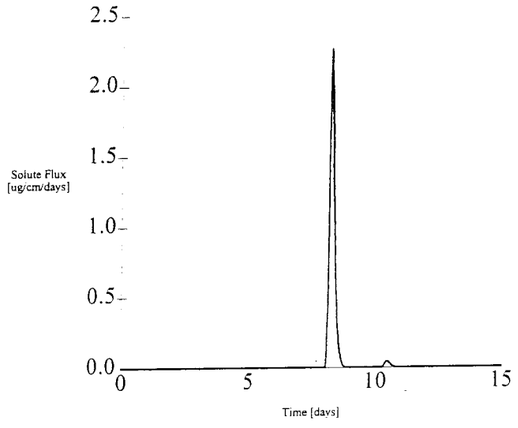


# Seepage Face Solute Flux

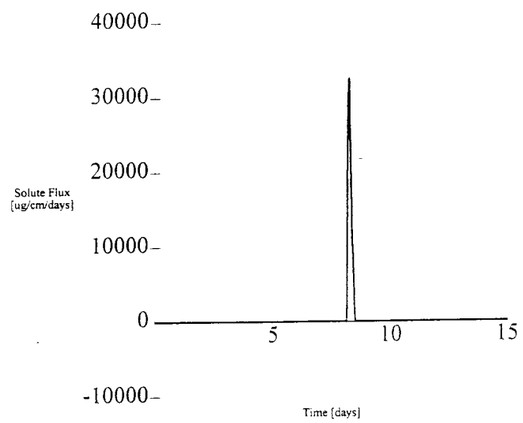

Observation Nodes:
Concentrations

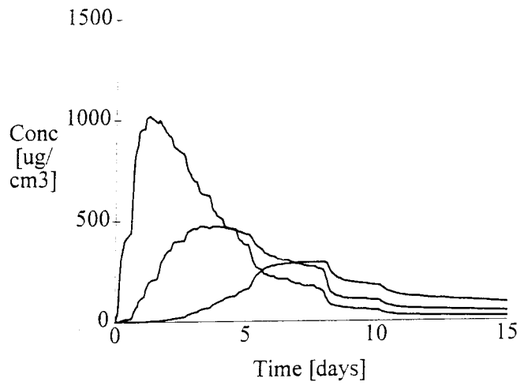


Observation Nodes:
Concentrations

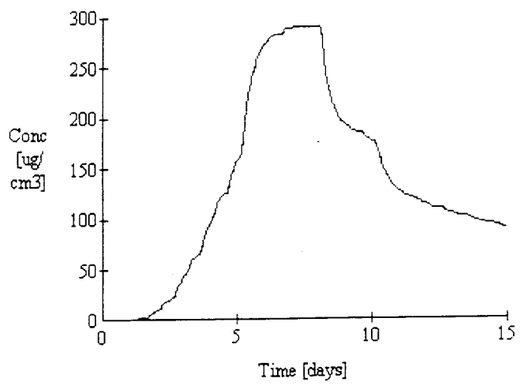

## Cumulative Variable Boundary Solute Flux

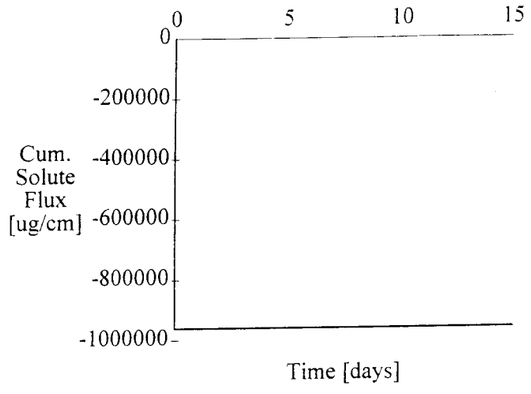


## Constant Boundary Solute Flux

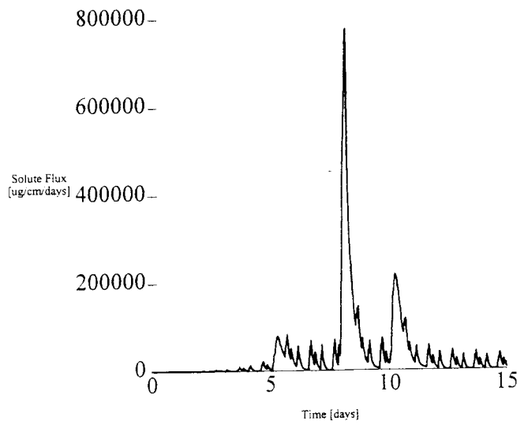

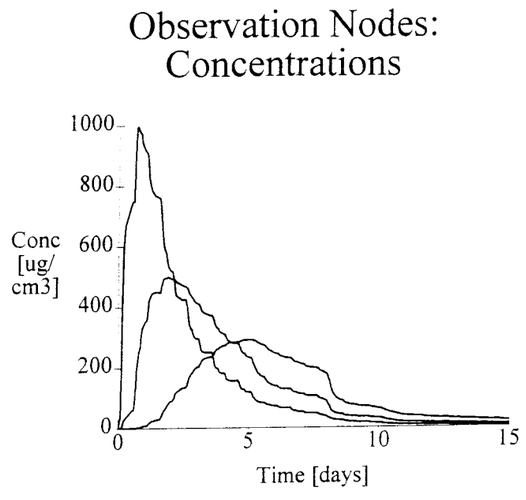
Observation Nodes:
Concentrations
1000
800
600
400
200
0
Conc
[ug/
cm3]
0
5
10
15
Time [days]

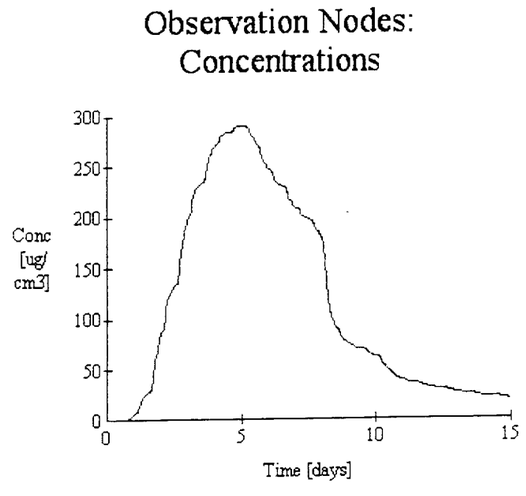
Observation Nodes:
Concentrations
300
250
200
150
100
50
0
Conc
[ug/
cm3]
0
5
10
15
Time [days]

## Cumulative Variable Boundary Solute Flux

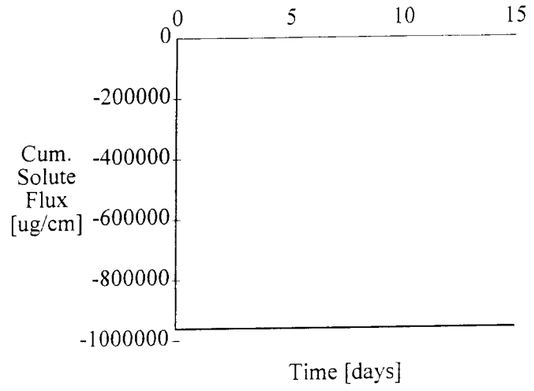


## Constant Boundary Solute Flux

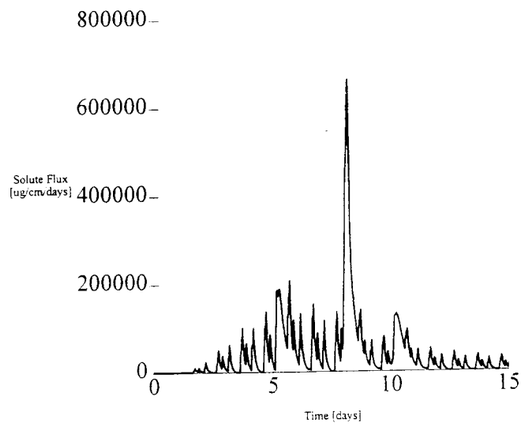

## Observation Nodes: Concentrations

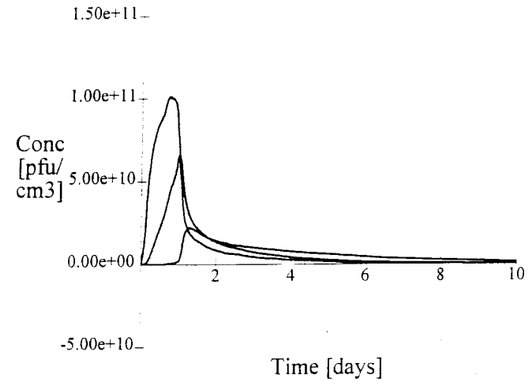


## Observation Nodes: Concentrations

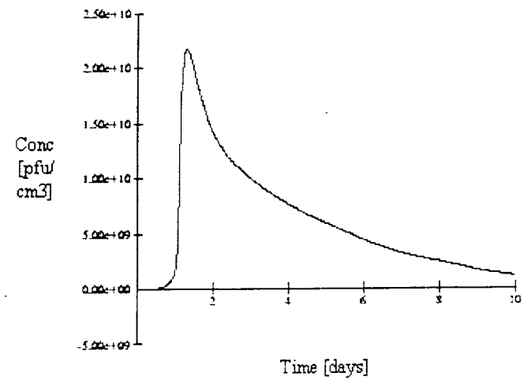

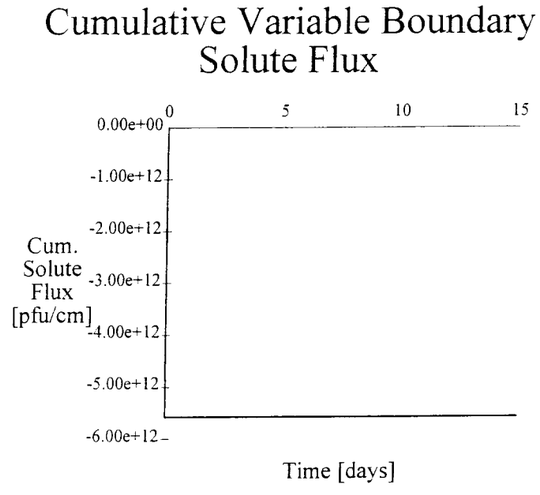
Cumulative Variable Boundary
Solute Flux
0
5
10
15
0.00e+00
-1.00e+12
-2.00e+12
-3.00e+12
-4.00e+12
-5.00e+12
-6.00e+12
Cum.
Solute
Flux
[pfu/cm]
Time [days]

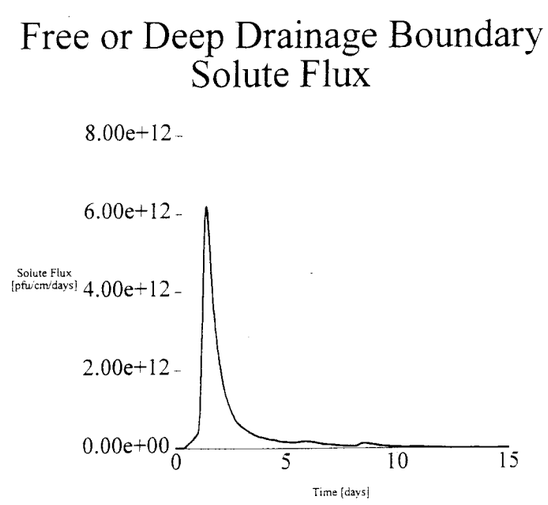
Free or Deep Drainage Boundary
Solute Flux
8.00e+12
6.00e+12
4.00e+12
2.00e+12
0.00e+00
Solute Flux
[pfu/cm/days]
0
5
10
15
Time [days]

Observation Nodes: Concentrations

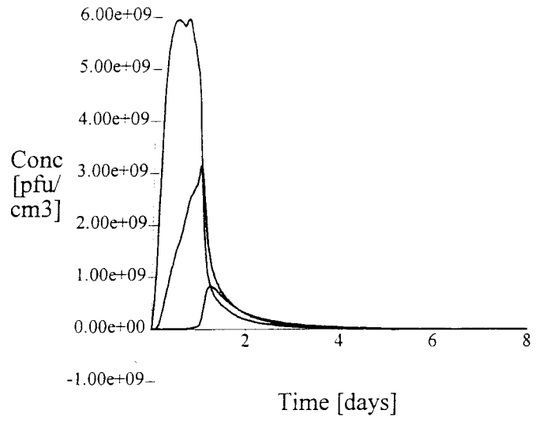


Observation Nodes: Concentrations

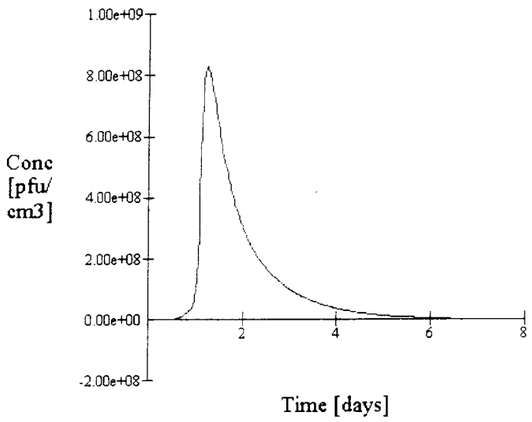

## Cumulative Variable Boundary Solute Flux

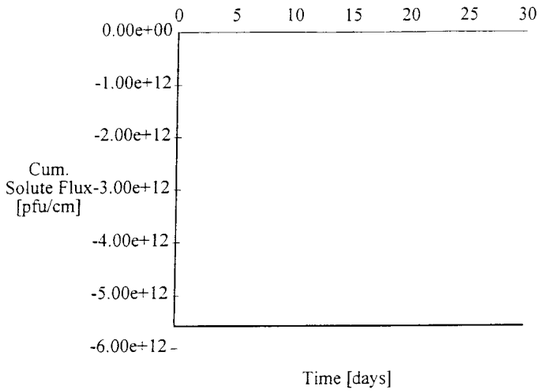


## Free or Deep Drainage Boundary Solute Flux

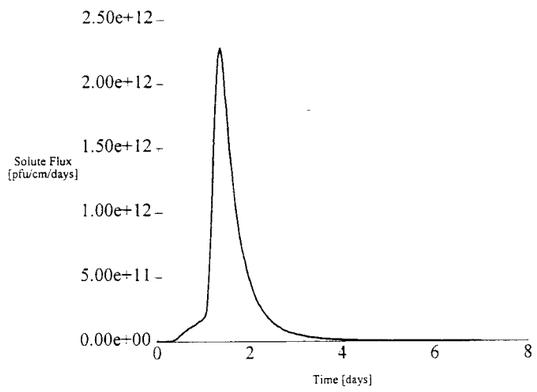

# Constant Boundary Solute Flux

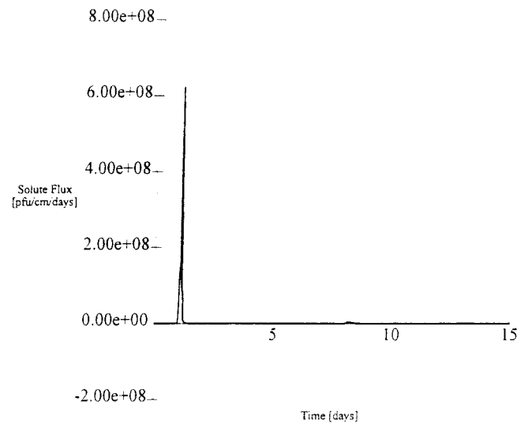


# Seepage Face Solute Flux

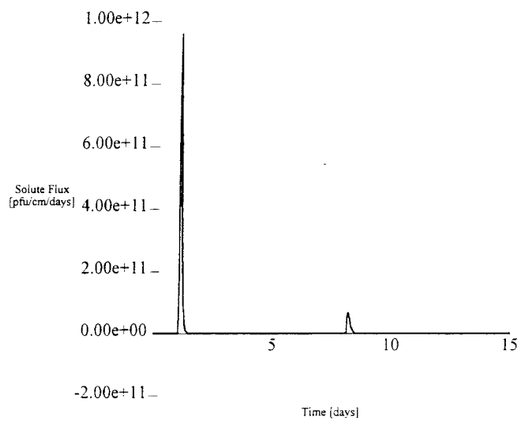

# Constant Boundary Solute Flux

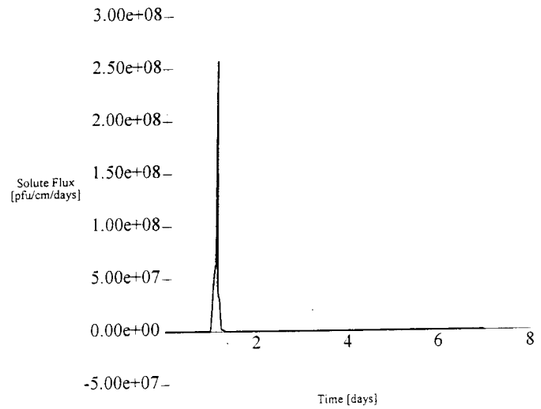


# Seepage Face Solute Flux

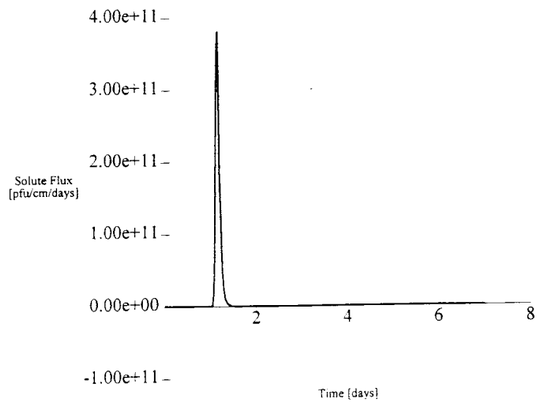

Observation Nodes: Pressure Heads

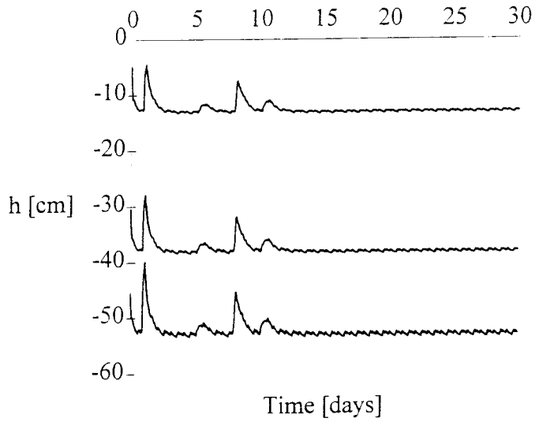


Observation Nodes: Water Contents

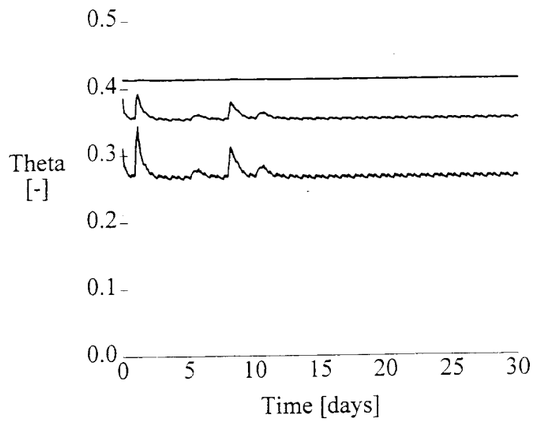

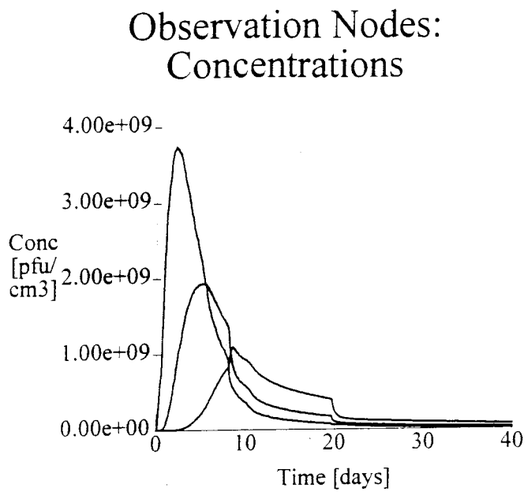
Observation Nodes:
Concentrations
4.00e+09
3.00e+09
2.00e+09
1.00e+09
0.00e+00
Conc
[pfu/
cm3]
0
10
20
30
40
Time [days]

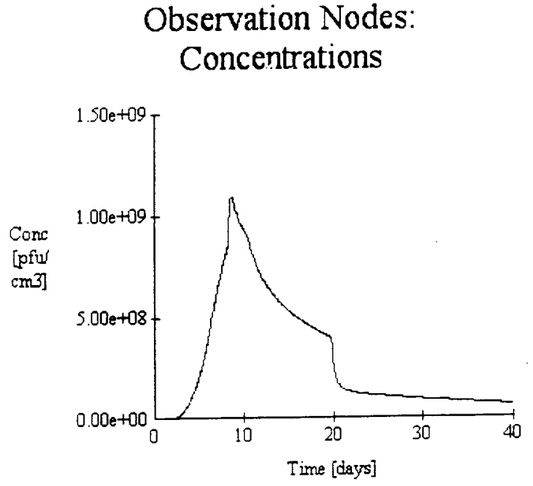
Observation Nodes:
Concentrations
1.50e+09
1.00e+09
5.00e+08
0.00e+00
Conc
[pfu/
cm3]
0
10
20
30
40
Time [days]

## Cumulative Variable Boundary Solute Flux

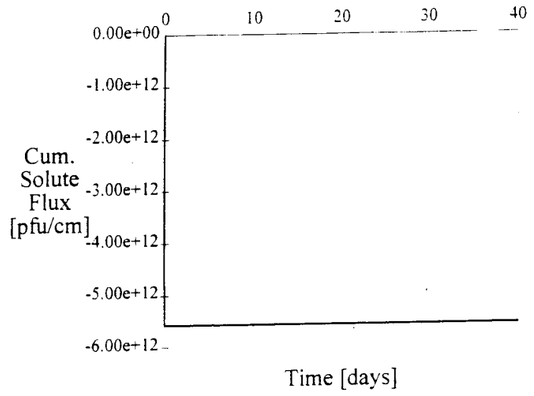


## Free or Deep Drainage Boundary Solute Flux

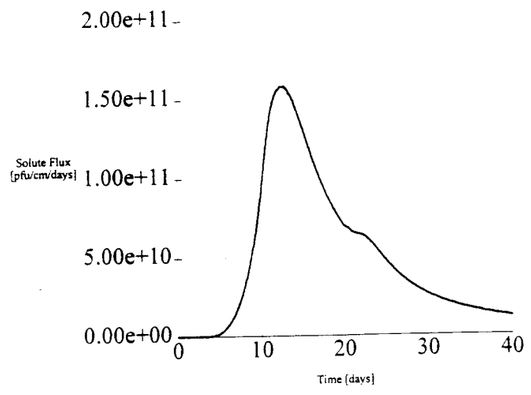

# Constant Boundary Solute Flux

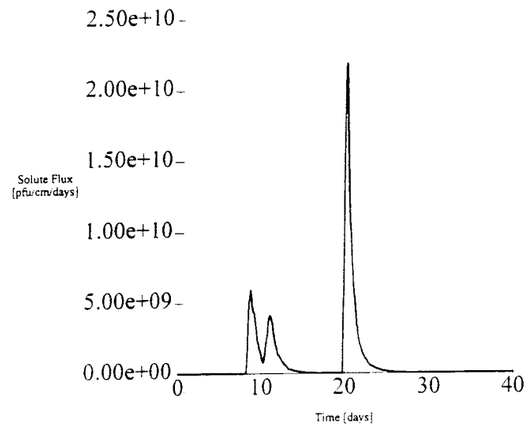


# Seepage Face Solute Flux

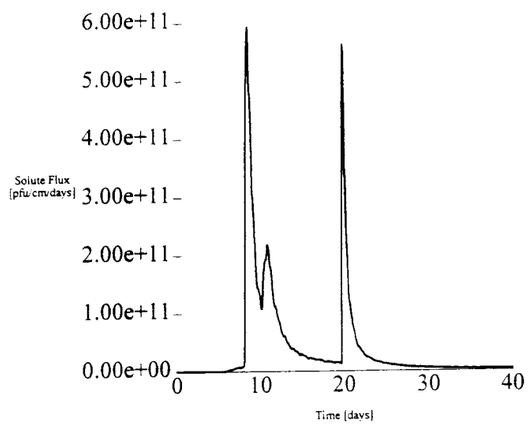

Observation Nodes: Pressure Heads

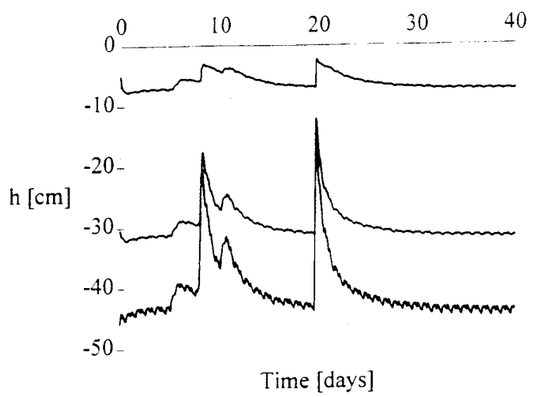


Observation Nodes: Water Contents

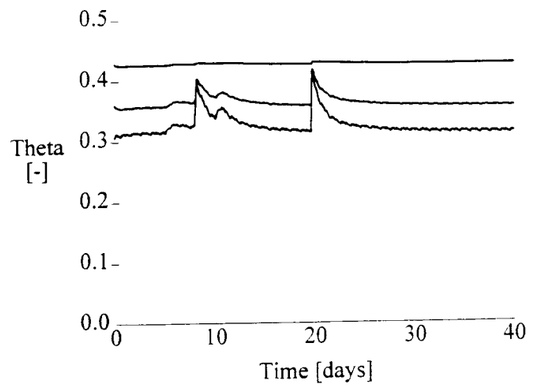

## Observation Nodes: Concentrations

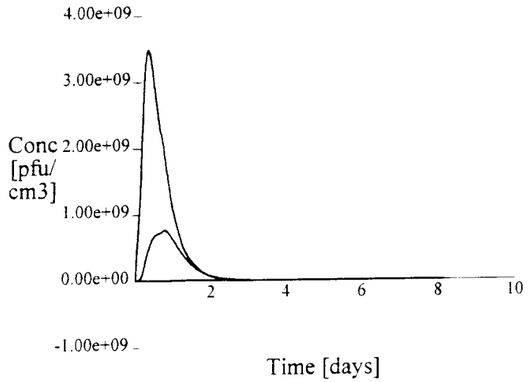


## Observation Nodes: Concentrations

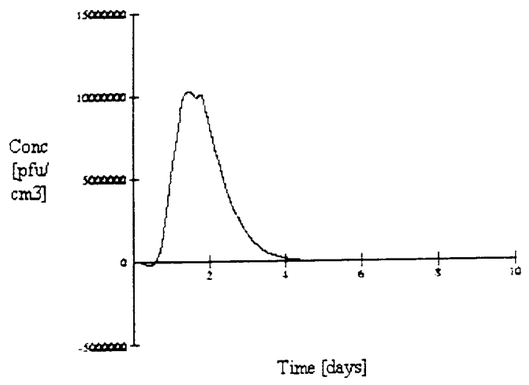

Observation Nodes: Concentrations

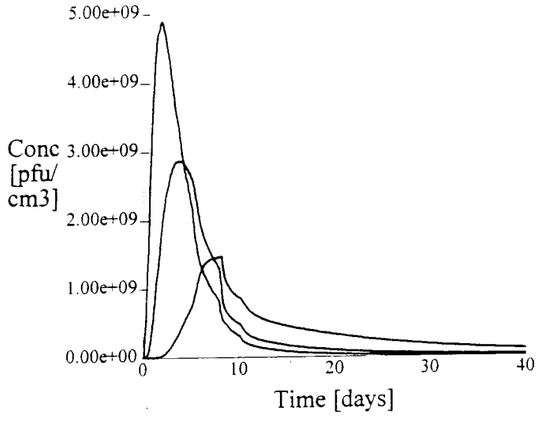


Observation Nodes: Concentrations

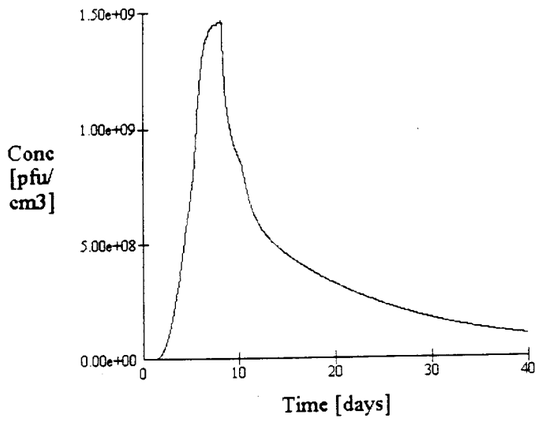

## Cumulative Variable Boundary Solute Flux

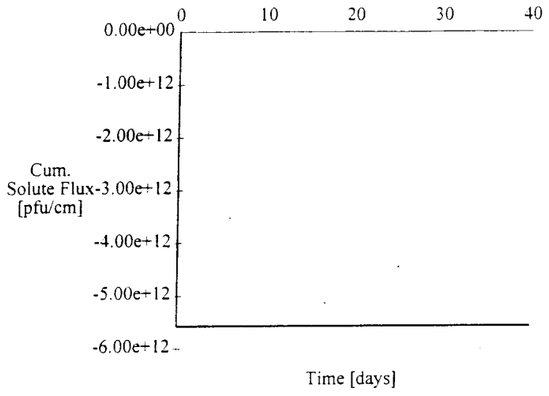


## Free or Deep Drainage Boundary Solute Flux

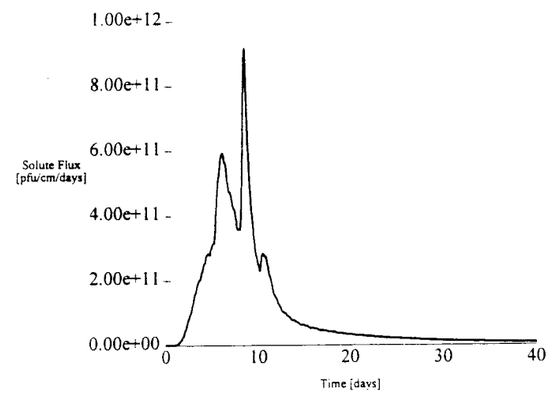

# Constant Boundary Solute Flux

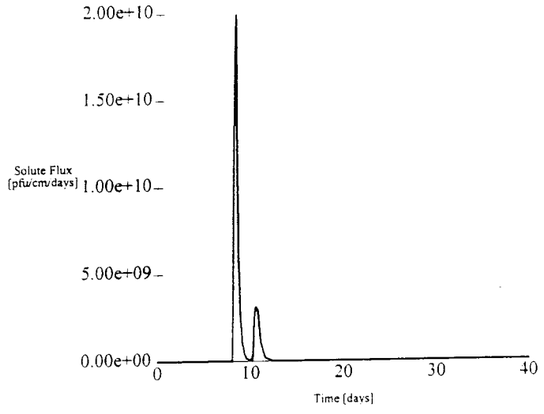


# Seepage Face Solute Flux

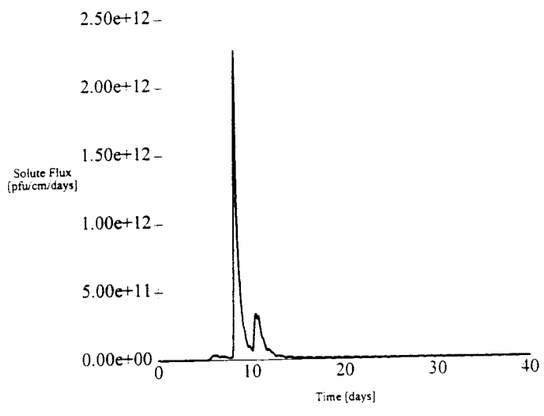

Observation Nodes: Pressure Heads

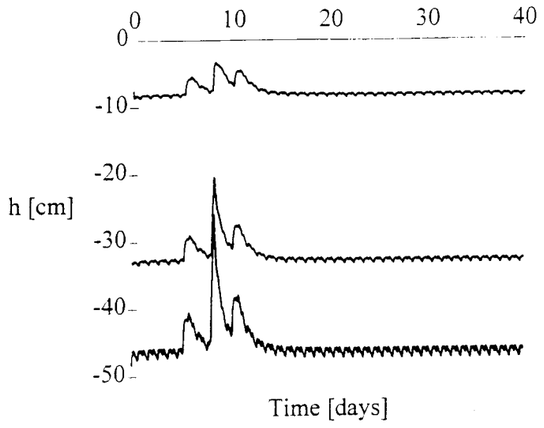


Observation Nodes: Water Contents

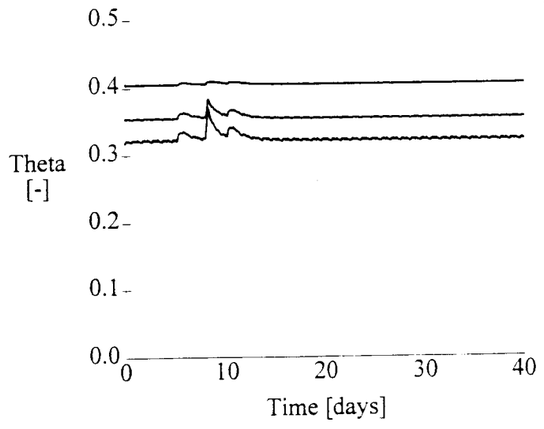

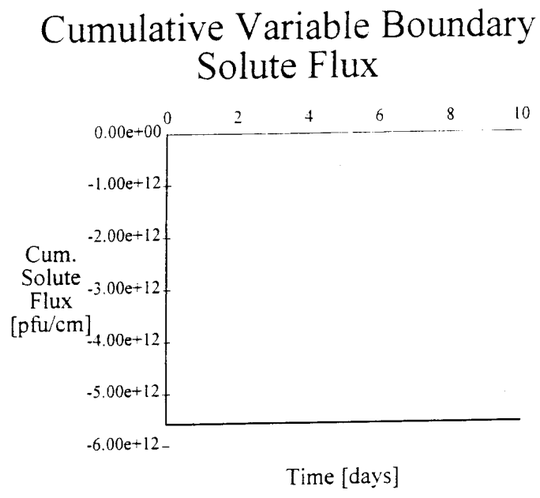
Cumulative Variable Boundary
Solute Flux
0
2
4
6
8
10
0.00e+00
-1.00e+12
-2.00e+12
-3.00e+12
-4.00e+12
-5.00e+12
-6.00e+12
Cum.
Solute
Flux
[pfu/cm]
Time [days]

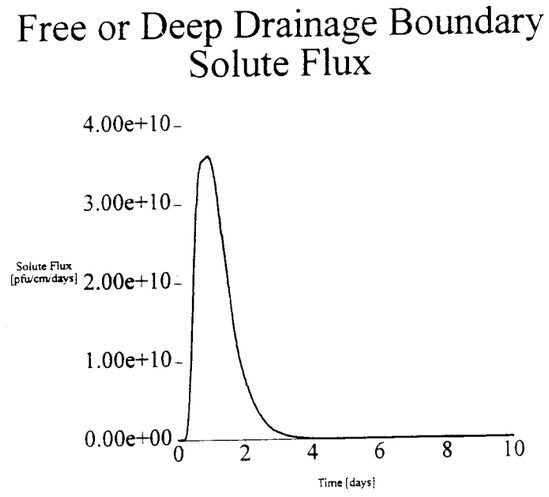
Free or Deep Drainage Boundary
Solute Flux
4.00e+10
3.00e+10
2.00e+10
1.00e+10
0.00e+00
Solute Flux
[pfu/cm/days]
0
2
4
6
8
10
Time [days]

# Constant Boundary Solute Flux

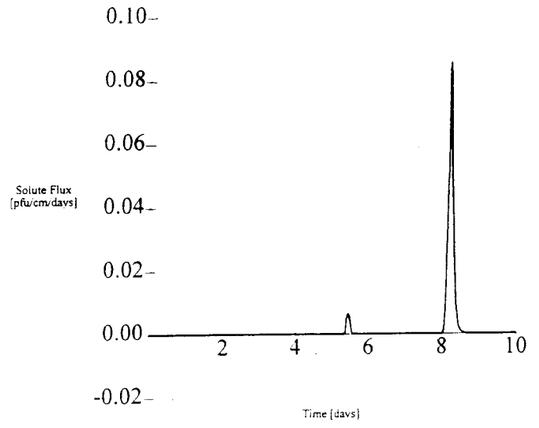


# Seepage Face Solute Flux

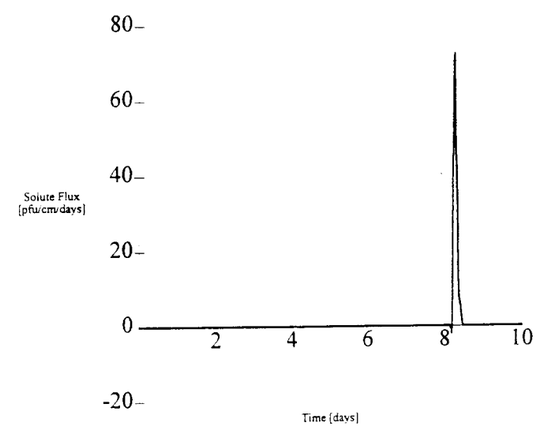

## Observation Nodes: Pressure Heads

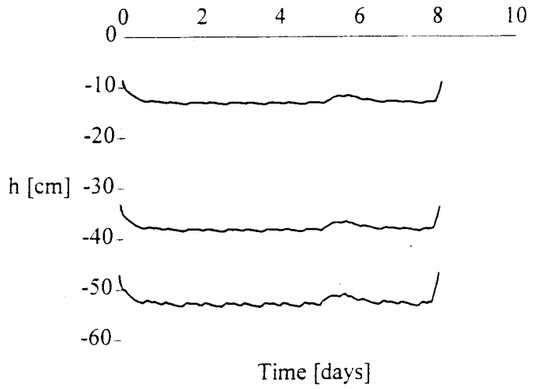


## Observation Nodes: Water Contents

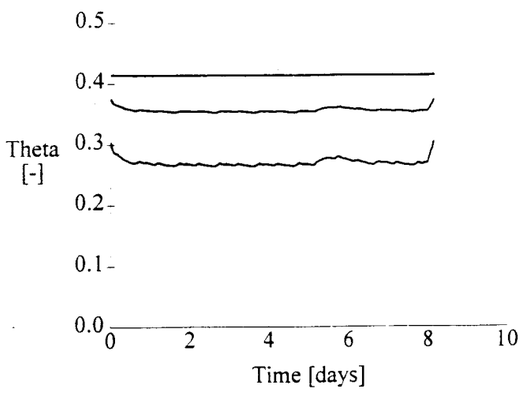

# Constant Boundary Solute Flux

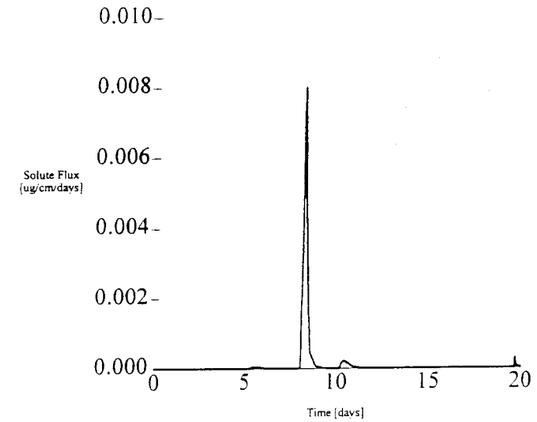


# Seepage Face Solute Flux

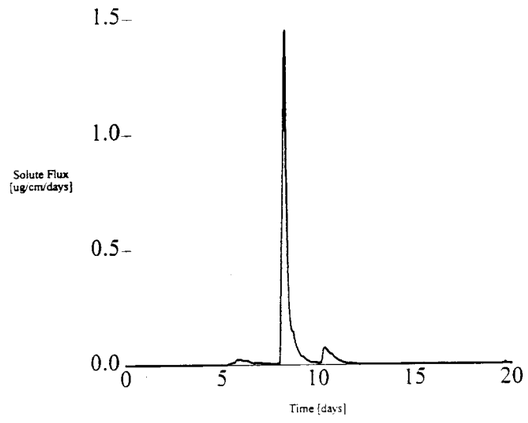

Observation Nodes:
Concentrations

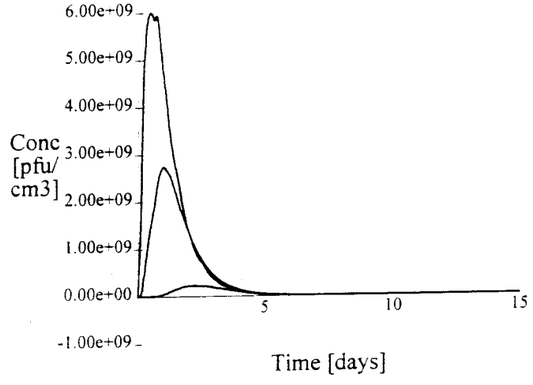


Observation Nodes:
Concentrations

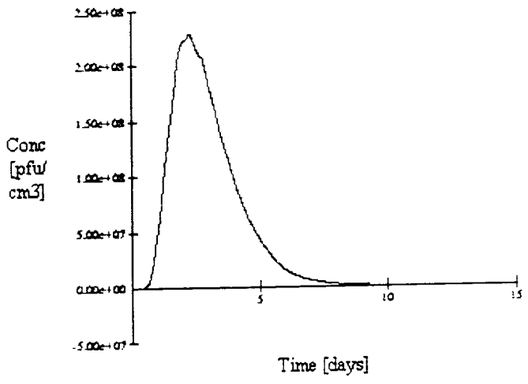

## Cumulative Variable Boundary Solute Flux

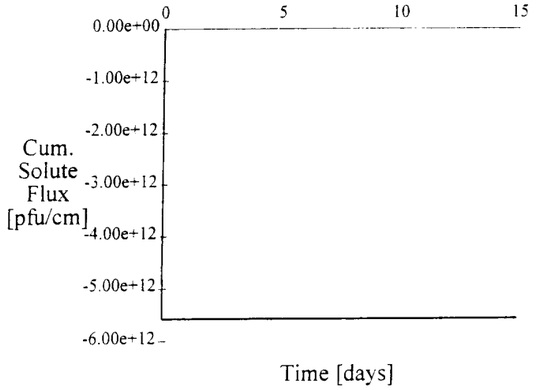


## Free or Deep Drainage Boundary Solute Flux

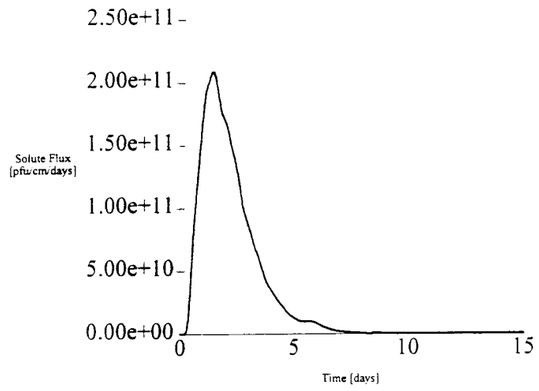

# Constant Boundary Solute Flux

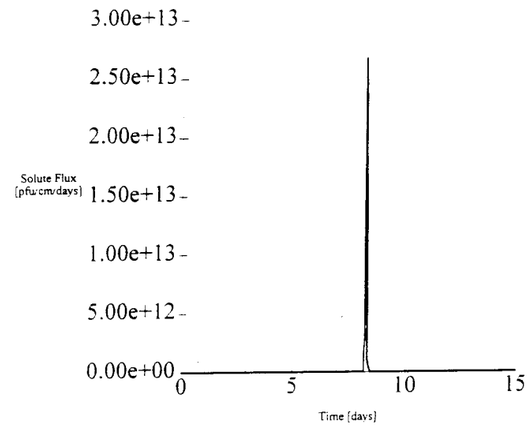


# Seepage Face Solute Flux

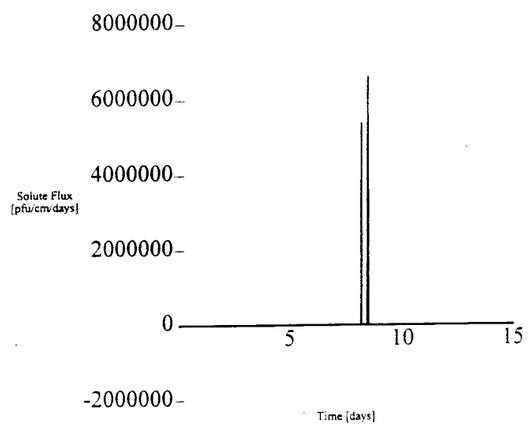

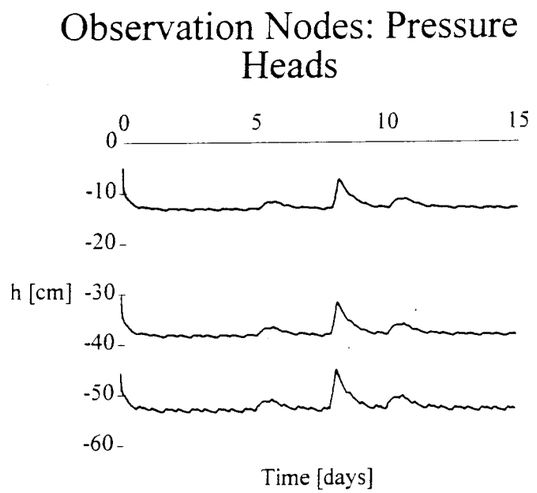
Observation Nodes: Pressure Heads
0
5
10
15
0
-10
-20
-30
-40
-50
-60
h [cm]
Time [days]

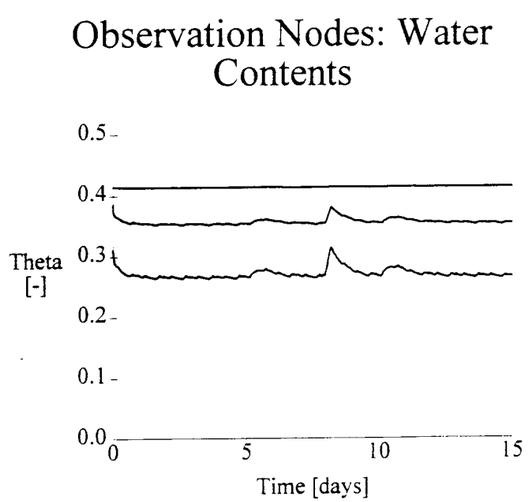
Observation Nodes: Water Contents
0.5
0.4
0.3
0.2
0.1
0.0
Theta [-]
0
5
10
15
Time [days]

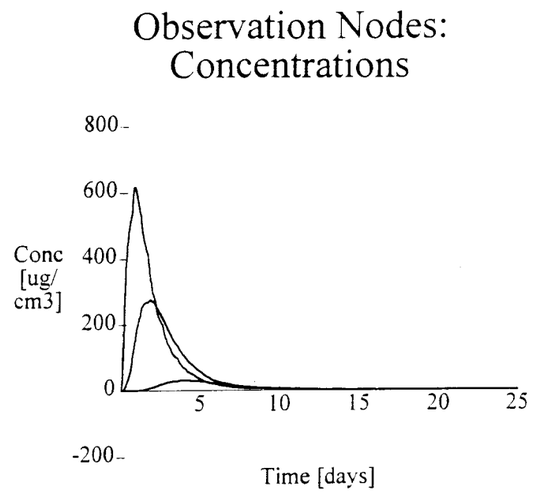
Observation Nodes:
Concentrations
800
600
400
200
0
-200
Conc
[ug/
cm3]
5
10
15
20
25
Time [days]

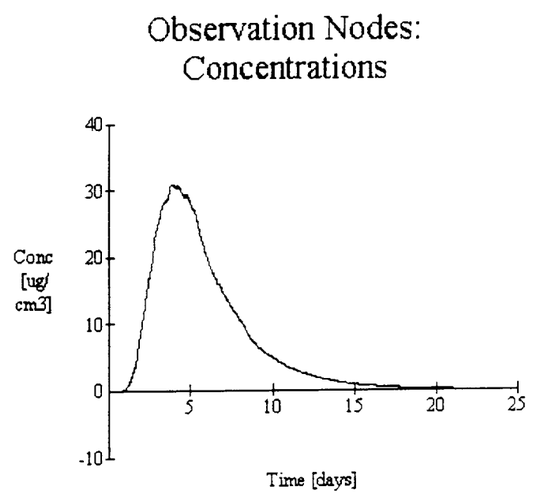
Observation Nodes:
Concentrations
40
30
20
10
0
-10
Conc
[ug/
cm3]
5
10
15
20
25
Time [days]

## Cumulative Variable Boundary Solute Flux

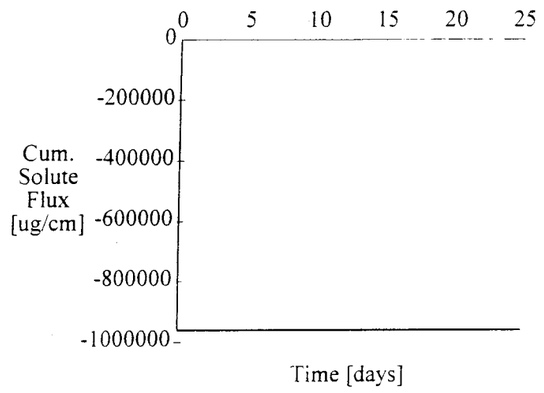


## Free or Deep Drainage Boundary Solute Flux

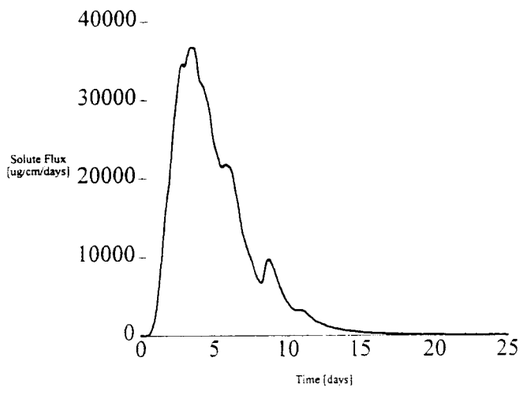

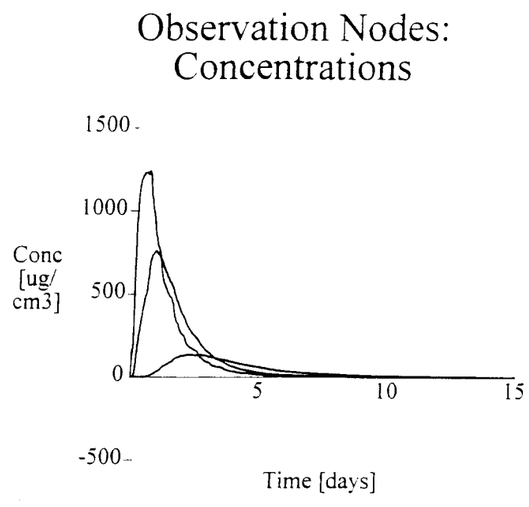
Observation Nodes:
Concentrations
1500
1000
500
0
-500
Conc
[ug/
cm3]
5
10
15
Time [days]

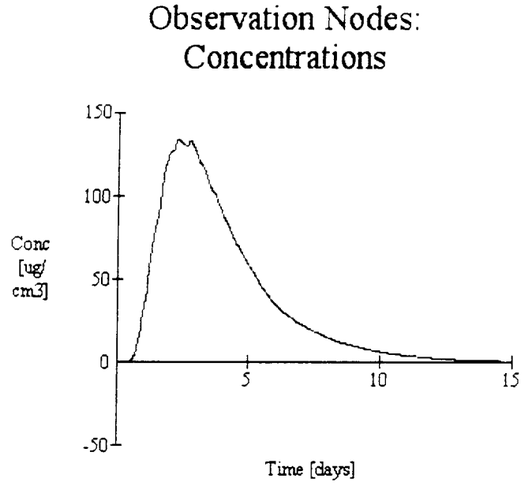
Observation Nodes:
Concentrations
150
100
50
0
-50
Conc
[ug/
cm3]
5
10
15
Time [days]

Cumulative Variable Boundary
Solute Flux

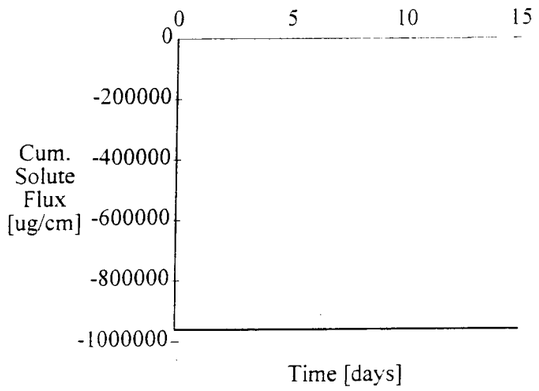


Free or Deep Drainage Boundary
Solute Flux

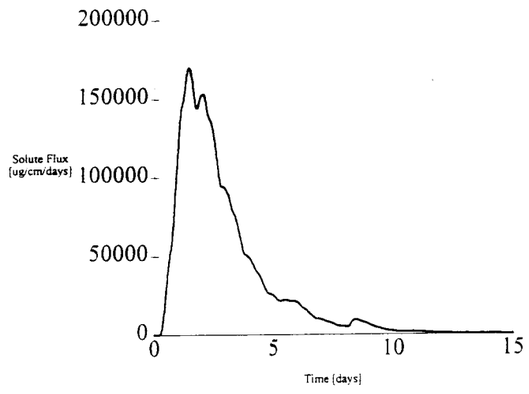

## Constant Boundary Solute Flux

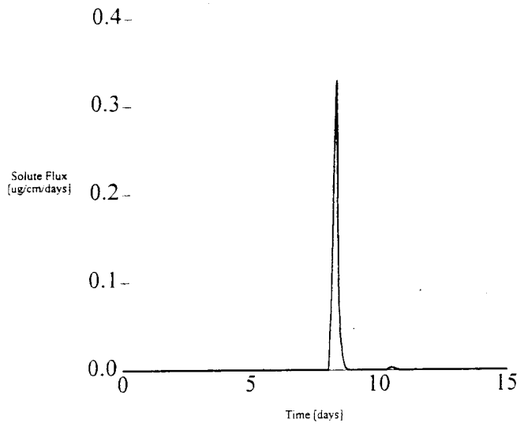


## Seepage Face Solute Flux

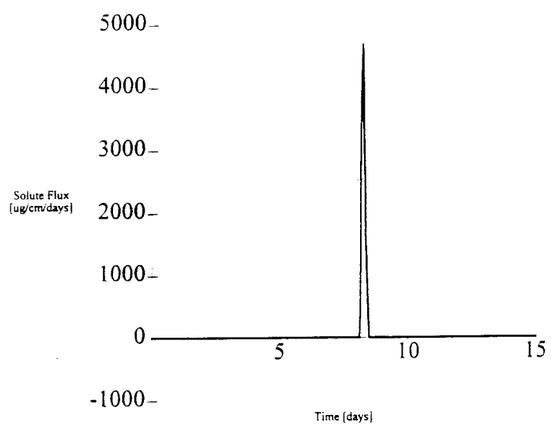

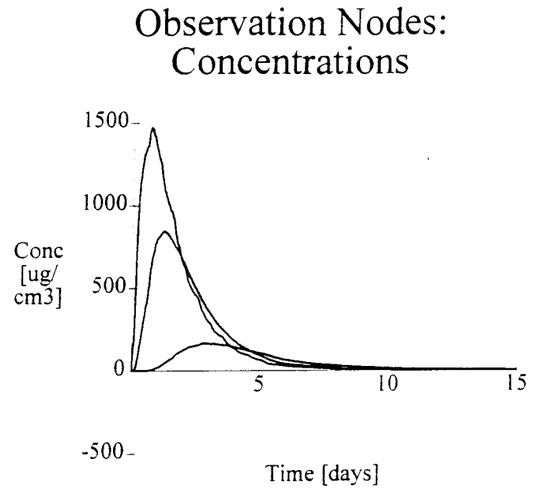
Observation Nodes:
Concentrations
1500
1000
500
0
-500
Conc
[ug/
cm3]
5
10
15
Time [days]

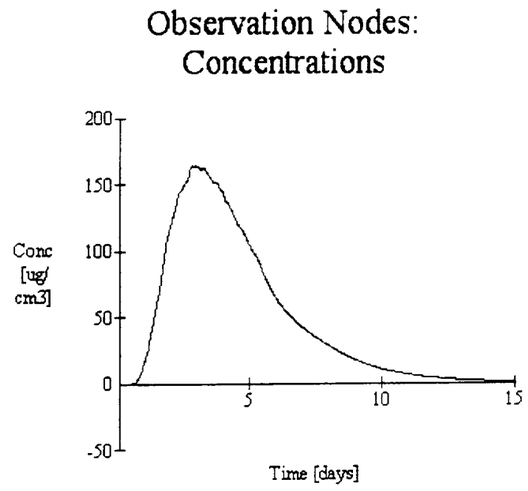
Observation Nodes:
Concentrations
200
150
100
50
0
-50
Conc
[ug/
cm3]
5
10
15
Time [days]

## Cumulative Variable Boundary Solute Flux

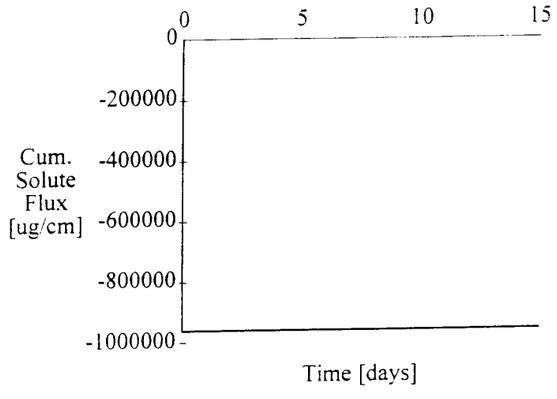


## Free or Deep Drainage Boundary Solute Flux

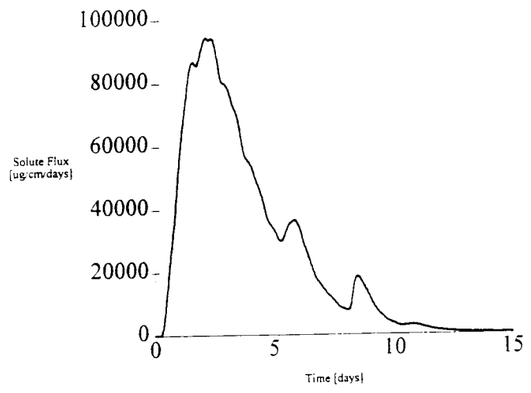

# Constant Boundary Solute Flux

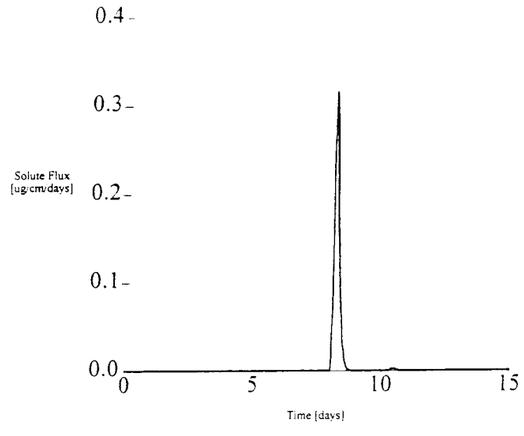


# Seepage Face Solute Flux

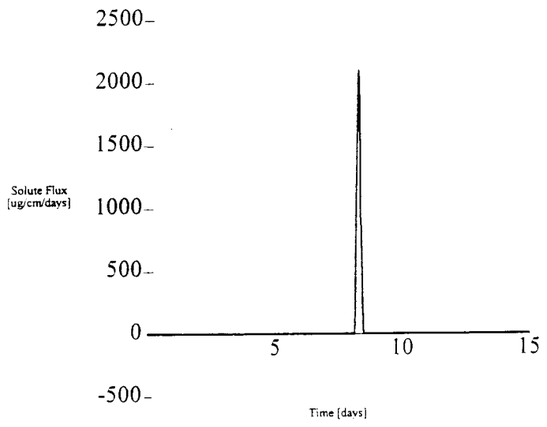

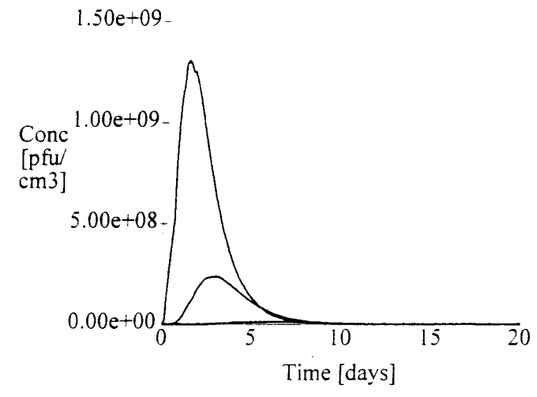
Observation Nodes:
Concentrations
1.50e+09
1.00e+09
5.00e+08
0.00e+00
Conc
[pfu/
cm3]
0
5
10
15
20
Time [days]

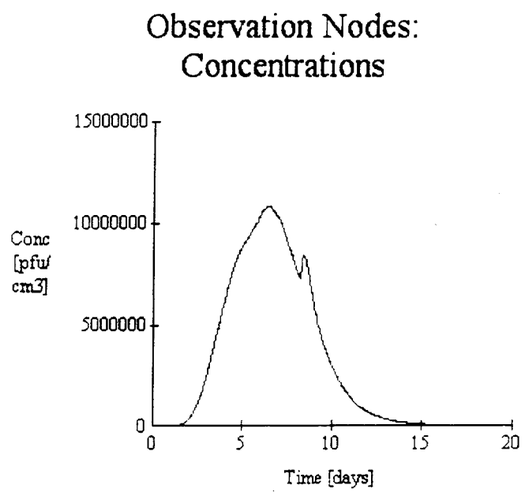
Observation Nodes:
Concentrations
15000000
10000000
5000000
0
Conc
[pfu/
cm3]
0
5
10
15
20
Time [days]

Loam

## Cumulative Variable Boundary Solute Flux

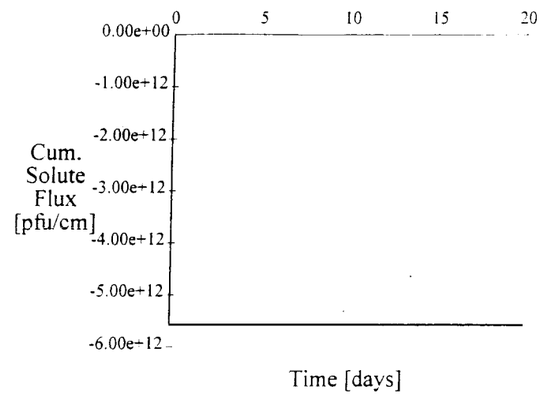


## Free or Deep Drainage Boundary Solute Flux

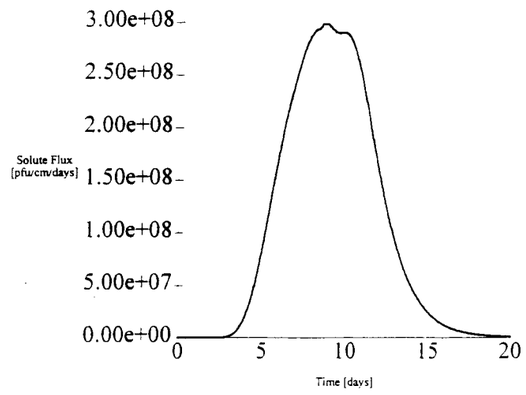

# Constant Boundary Solute Flux

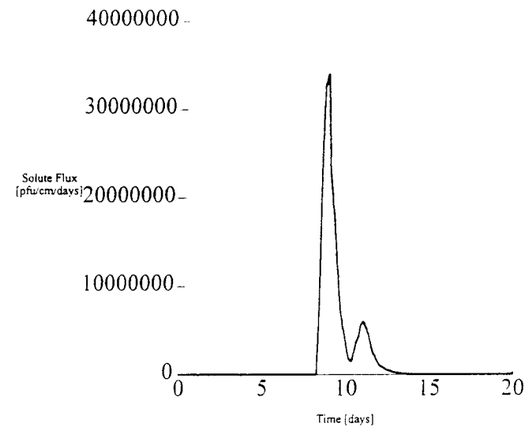


# Seepage Face Solute Flux

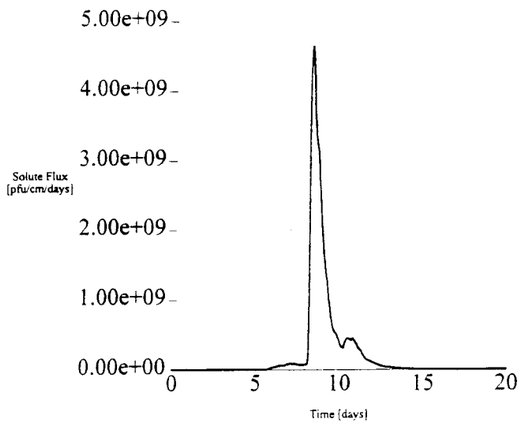

# Cumulative First-Order Reactions

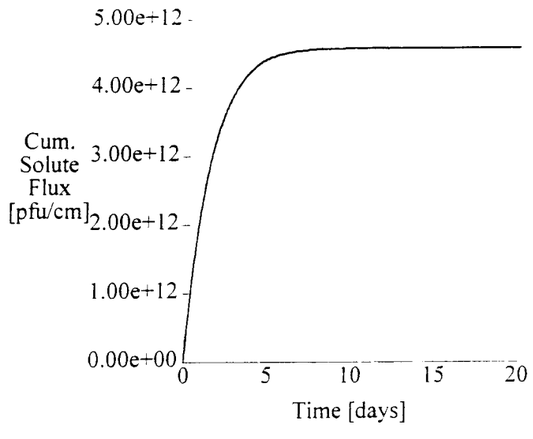

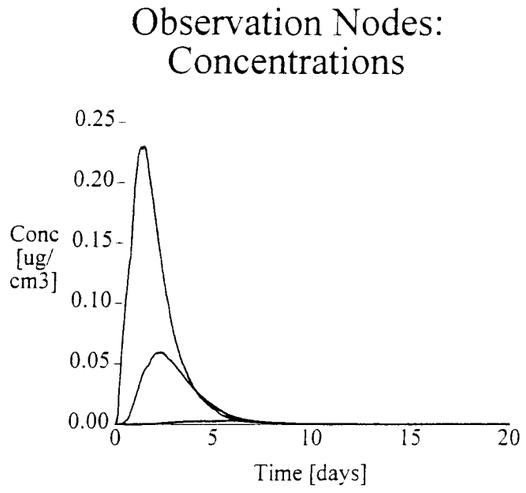
Observation Nodes:
Concentrations
0.25
0.20
0.15
0.10
0.05
0.00
Conc [ug/ cm3]
0
5
10
15
20
Time [days]

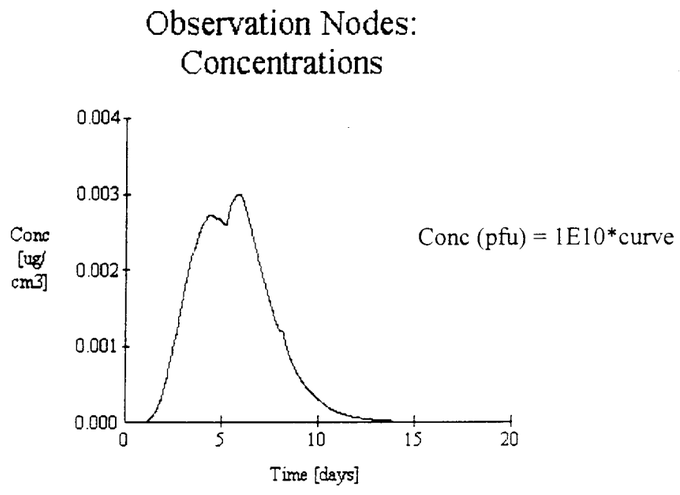
Observation Nodes:
Concentrations
0.004
0.003
0.002
0.001
0.000
Conc [ug/ cm3]
0
5
10
15
20
Time [days]
Conc (pfu) = 1E10*curve

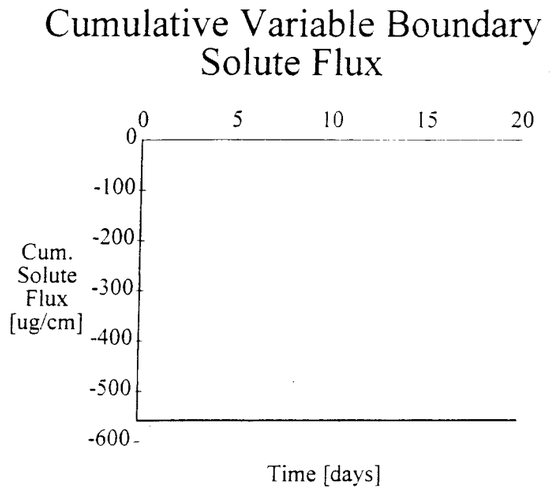
Cumulative Variable Boundary
Solute Flux
0
5
10
15
20
0
-100
-200
-300
-400
-500
-600
Cum.
Solute
Flux
[ug/cm]
Time [days]

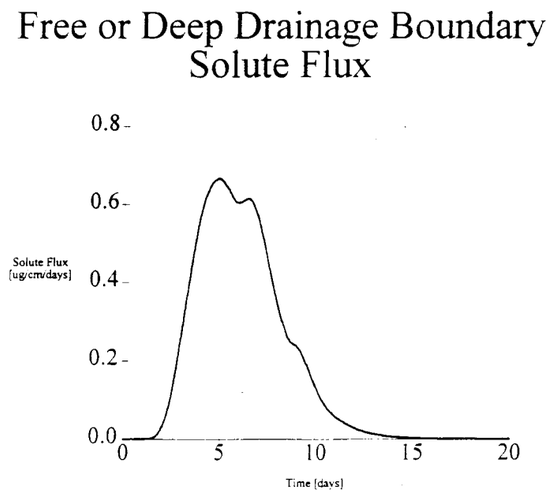
Free or Deep Drainage Boundary
Solute Flux
0.8
0.6
0.4
0.2
0.0
Solute Flux
[ug/cm/days]
0
5
10
15
20
Time [days]

# Constant Boundary Solute Flux

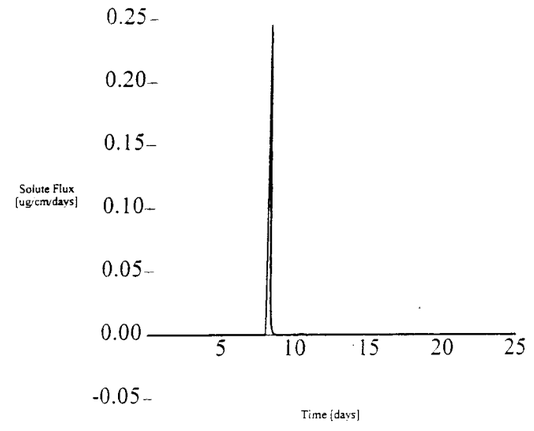


# Seepage Face Solute Flux

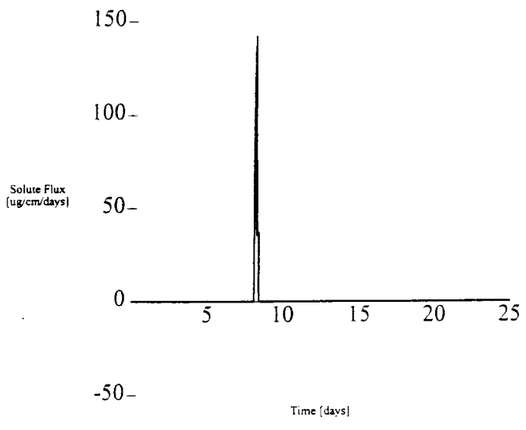

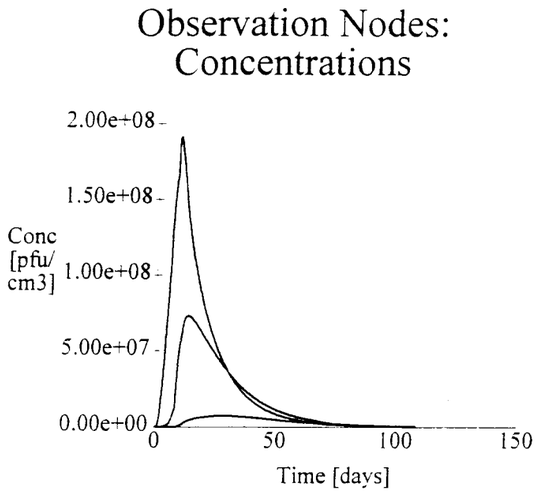
Observation Nodes:
Concentrations
2.00e+08
1.50e+08
1.00e+08
5.00e+07
0.00e+00
Conc
[pfu/
cm3]
0
50
100
150
Time [days]

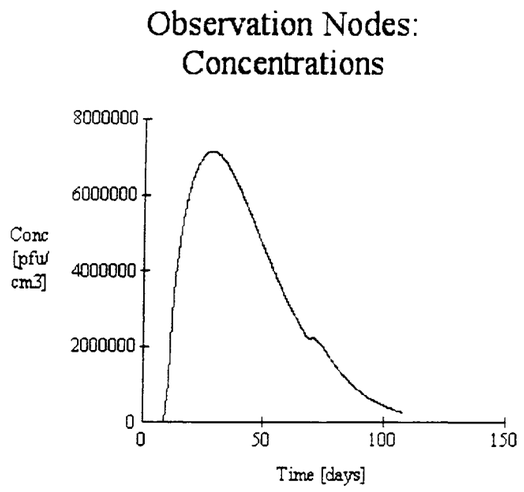
Observation Nodes:
Concentrations
8000000
6000000
4000000
2000000
0
Conc
[pfu/
cm3]
0
50
100
150
Time [days]

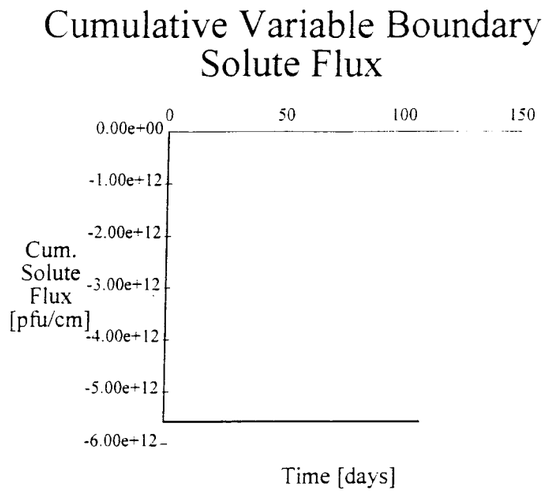
Cumulative Variable Boundary
Solute Flux
0
50
100
150
0.00e+00
-1.00e+12
-2.00e+12
-3.00e+12
-4.00e+12
-5.00e+12
-6.00e+12
Cum.
Solute
Flux
[pfu/cm]
Time [days]

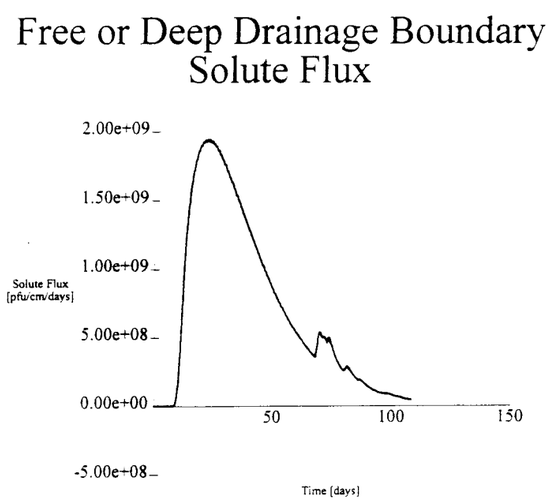
Free or Deep Drainage Boundary
Solute Flux
2.00e+09
1.50e+09
1.00e+09
5.00e+08
0.00e+00
-5.00e+08
Solute Flux
[pfu/cm/days]
50
100
150
Time [days]

## Constant Boundary Solute Flux

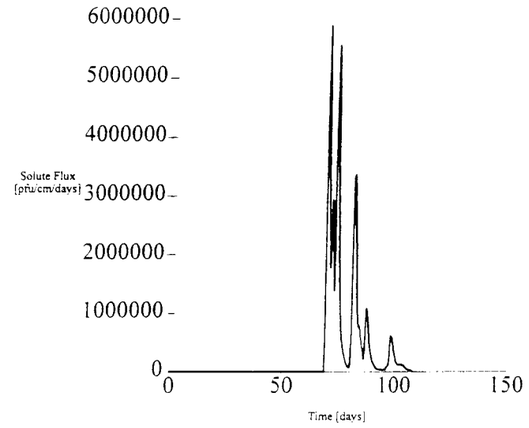


## Seepage Face Solute Flux

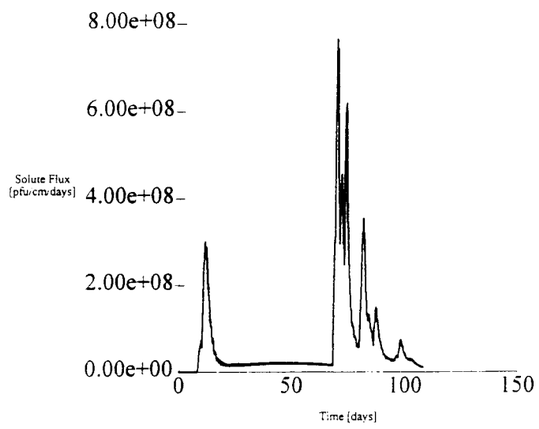

Observation Nodes: Pressure Heads

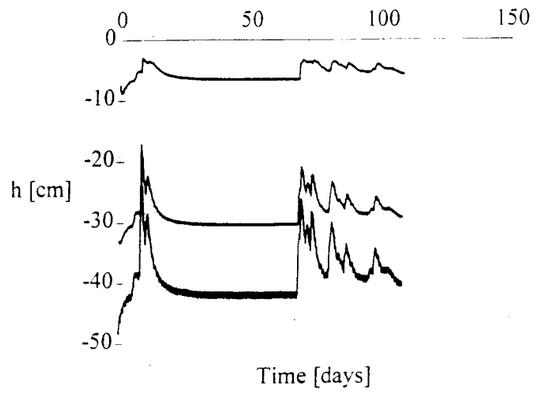


Observation Nodes: Water Contents

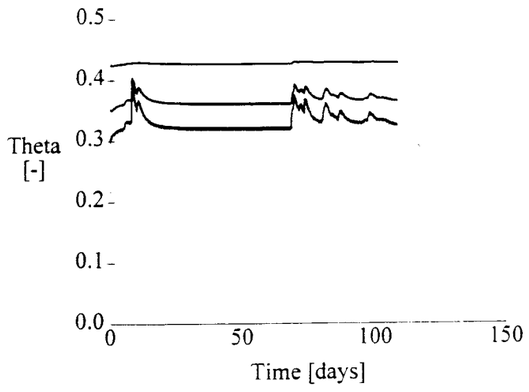

Observation Nodes:
Concentrations

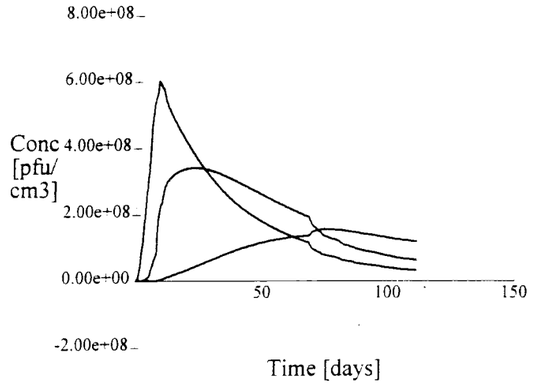


Observation Nodes:
Concentrations

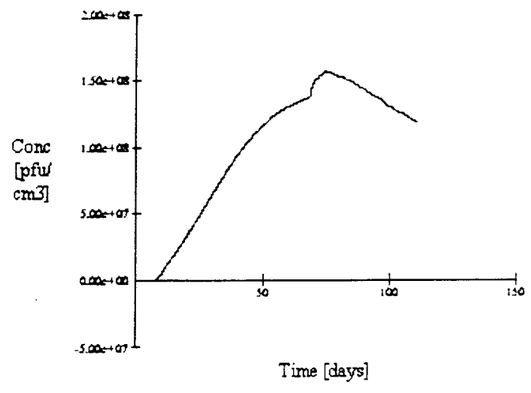

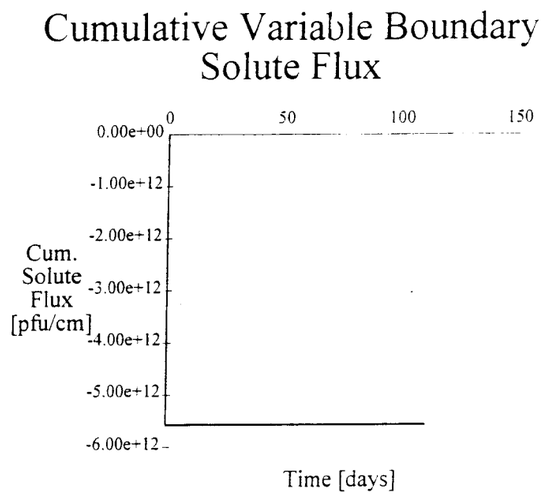
Cumulative Variable Boundary
Solute Flux
0
50
100
150
0.00e+00
-1.00e+12
-2.00e+12
-3.00e+12
-4.00e+12
-5.00e+12
-6.00e+12
Cum.
Solute
Flux
[pfu/cm]
Time [days]

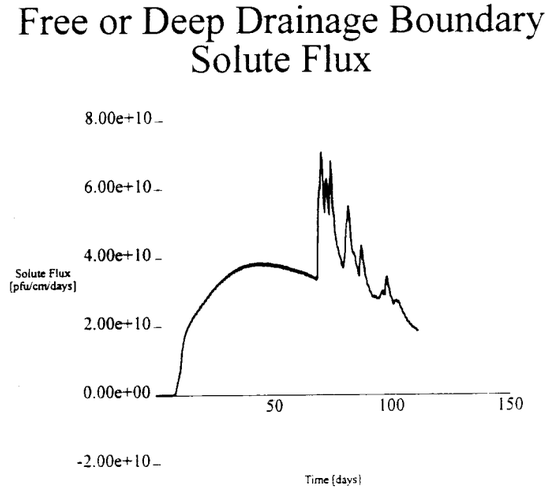
Free or Deep Drainage Boundary
Solute Flux
8.00e+10
6.00e+10
4.00e+10
2.00e+10
0.00e+00
-2.00e+10
Solute Flux
[pfu/cm/days]
50
100
150
Time [days]

# Constant Boundary Solute Flux

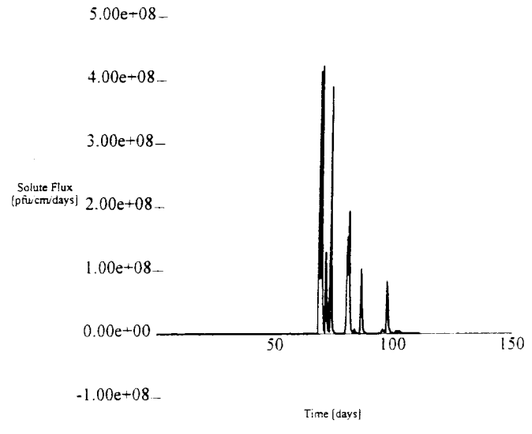


# Seepage Face Solute Flux

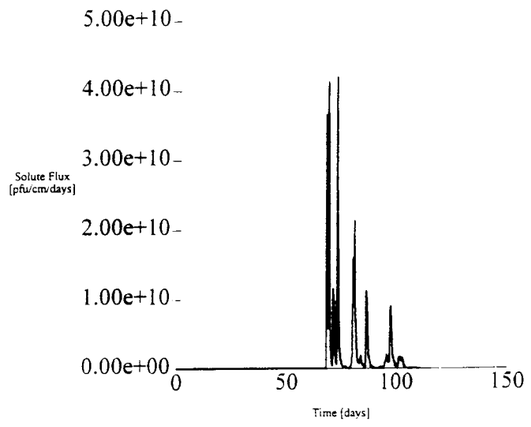

Observation Nodes: Pressure Heads

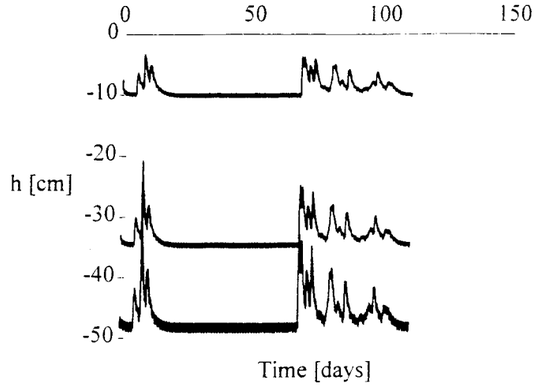


Observation Nodes: Water Contents

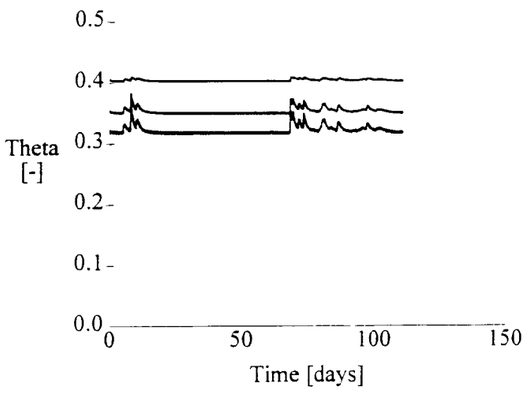

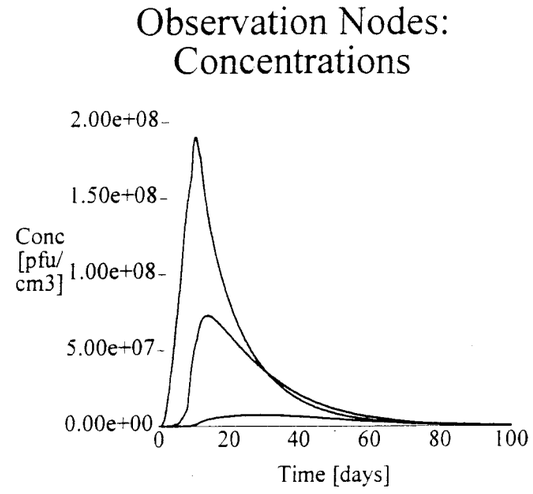
Observation Nodes:
Concentrations
2.00e+08
1.50e+08
Conc
[pfu/
cm3]
1.00e+08
5.00e+07
0.00e+00
0
20
40
60
80
100
Time [days]

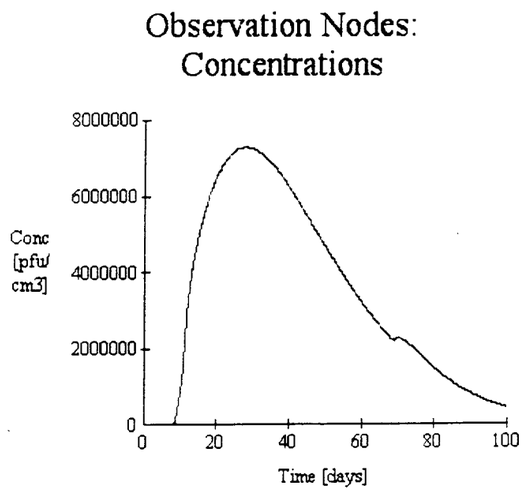
Observation Nodes:
Concentrations
8000000
6000000
Conc
[pfu/
cm3]
4000000
2000000
0
0
20
40
60
80
100
Time [days]

## Cumulative Variable Boundary Solute Flux

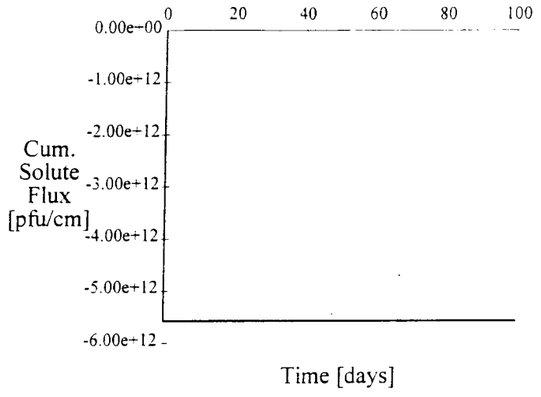


## Free or Deep Drainage Boundary Solute Flux

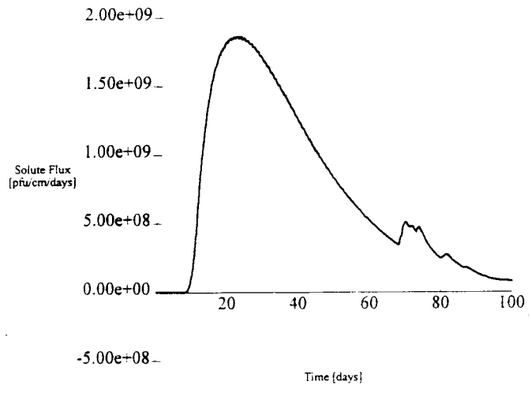

# Constant Boundary Solute Flux

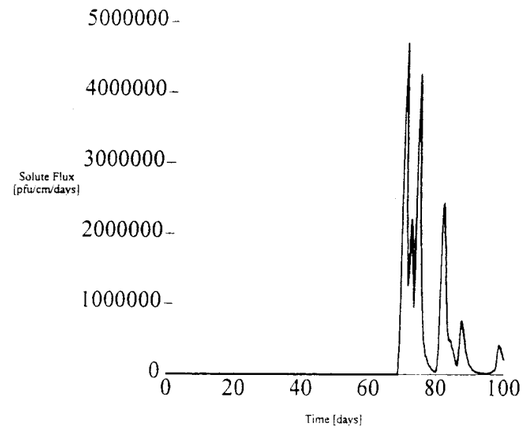


# Seepage Face Solute Flux

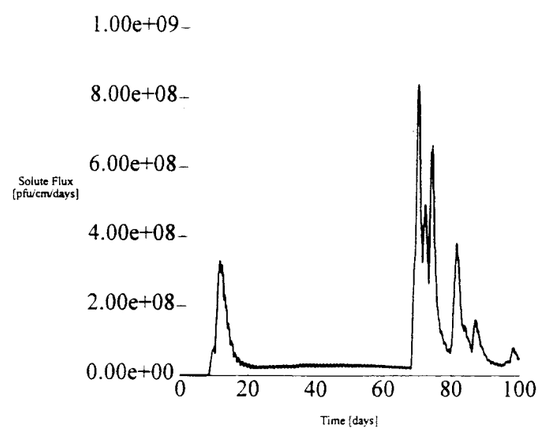

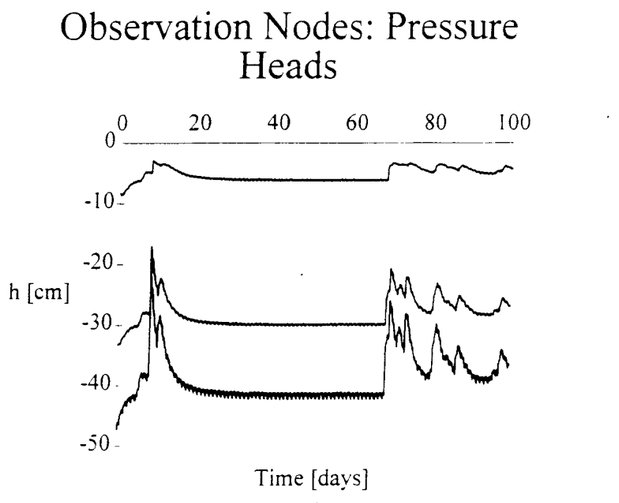
Observation Nodes: Pressure Heads
0
20
40
60
80
100
0
-10
-20
-30
-40
-50
h [cm]
Time [days]

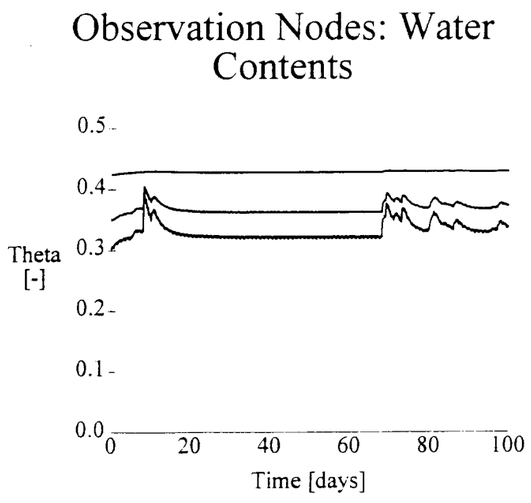
Observation Nodes: Water Contents
0.5
0.4
0.3
0.2
0.1
0.0
Theta [-]
0
20
40
60
80
100
Time [days]

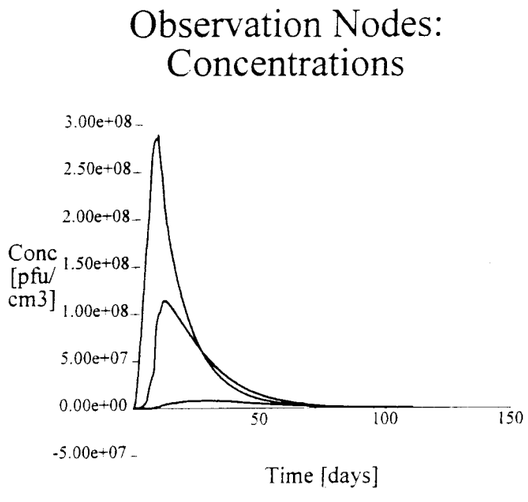
Observation Nodes:
Concentrations
3.00e+08
2.50e+08
2.00e+08
1.50e+08
1.00e+08
5.00e+07
0.00e+00
-5.00e+07
Conc
[pfu/
cm3]
50
100
150
Time [days]

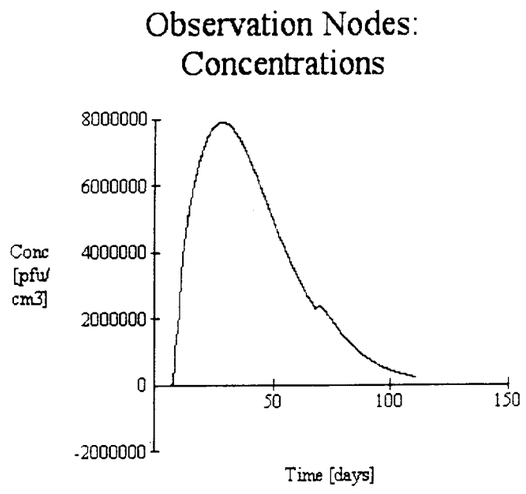
Observation Nodes:
Concentrations
8000000
6000000
4000000
2000000
0
-2000000
Conc
[pfu/
cm3]
50
100
150
Time [days]

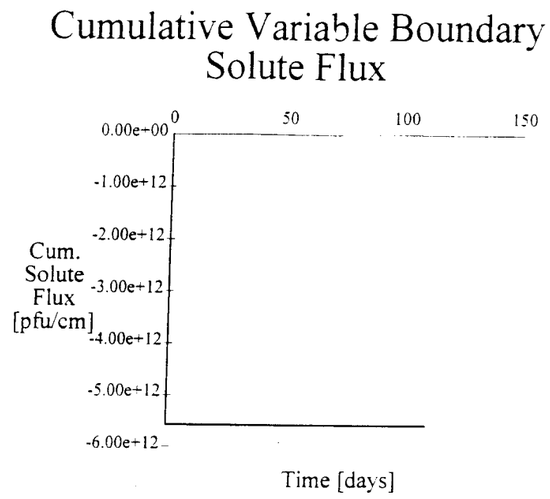
Cumulative Variable Boundary
Solute Flux
0
50
100
150
0.00e+00
-1.00e+12
-2.00e+12
-3.00e+12
-4.00e+12
-5.00e+12
-6.00e+12
Cum.
Solute
Flux
[pfu/cm]
Time [days]

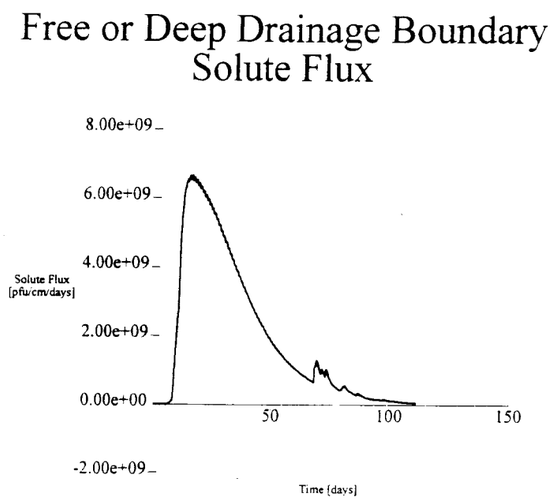
Free or Deep Drainage Boundary
Solute Flux
8.00e+09
6.00e+09
4.00e+09
2.00e+09
0.00e+00
-2.00e+09
Solute Flux
[pfu/cm/days]
50
100
150
Time [days]

# Constant Boundary Solute Flux

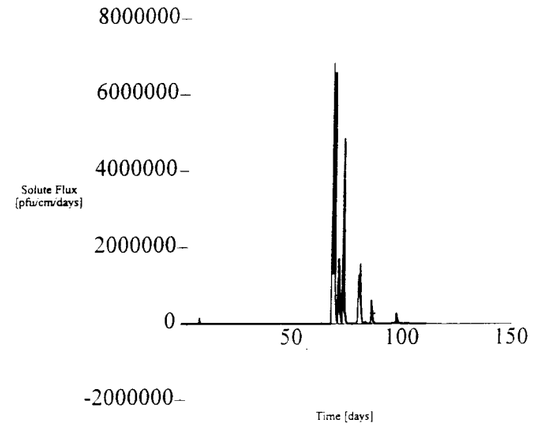


# Seepage Face Solute Flux

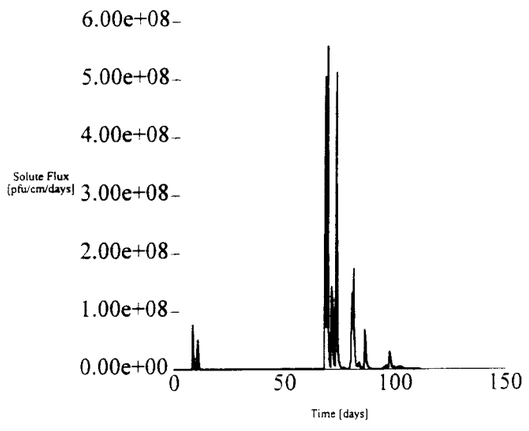

## Observation Nodes: Pressure Heads

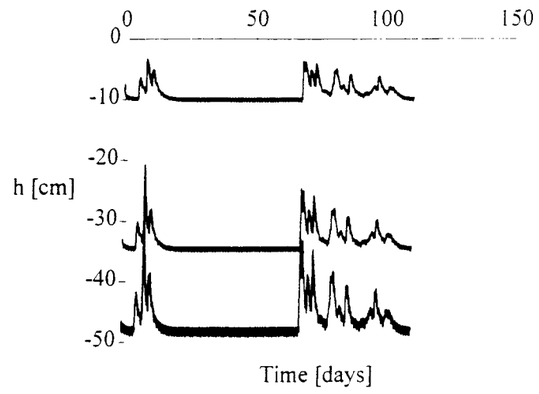


## Observation Nodes: Water Contents

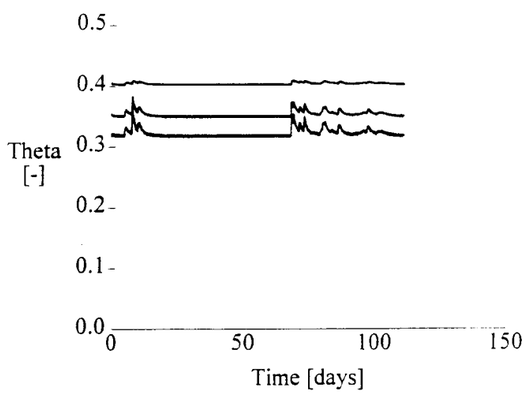

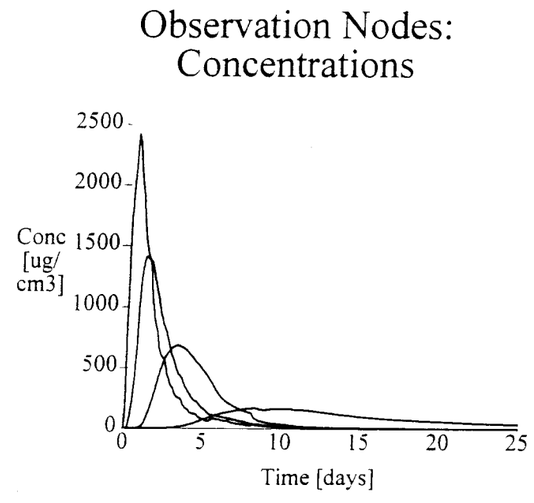
Observation Nodes:
Concentrations
2500
2000
1500
1000
500
0
Conc
[ug/
cm3]
0
5
10
15
20
25
Time [days]

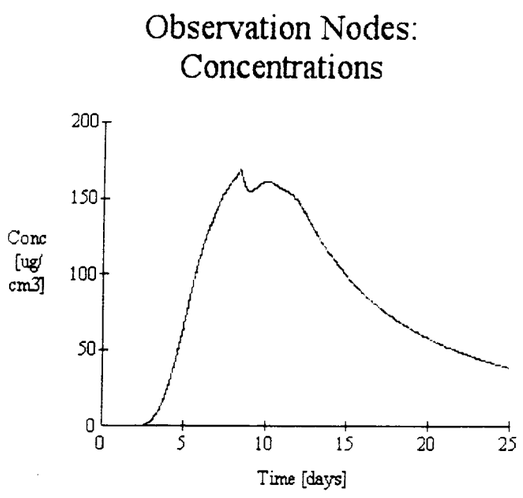
Observation Nodes:
Concentrations
200
150
100
50
0
Conc
[ug/
cm3]
0
5
10
15
20
25
Time [days]

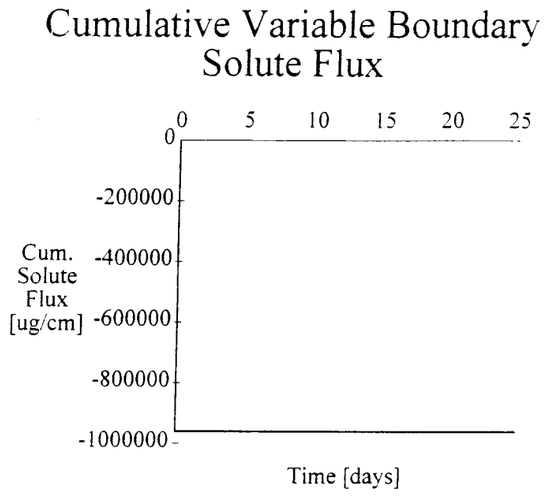
Cumulative Variable Boundary
Solute Flux
0
5
10
15
20
25
0
-200000
-400000
-600000
-800000
-1000000
Cum.
Solute
Flux
[ug/cm]
Time [days]

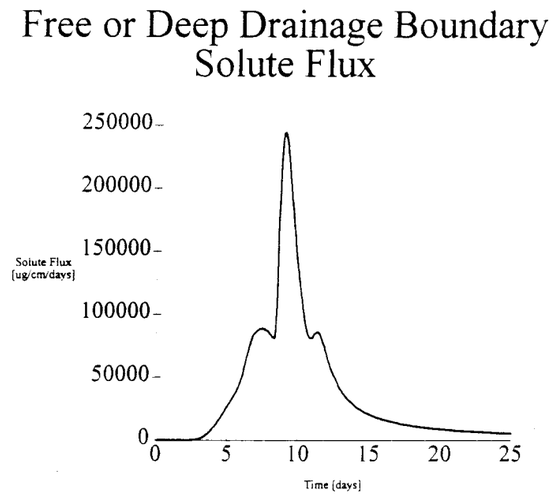
Free or Deep Drainage Boundary
Solute Flux
250000
200000
150000
100000
50000
0
Solute Flux
[ug/cm/days]
0
5
10
15
20
25
Time [days]

# Constant Boundary Solute Flux

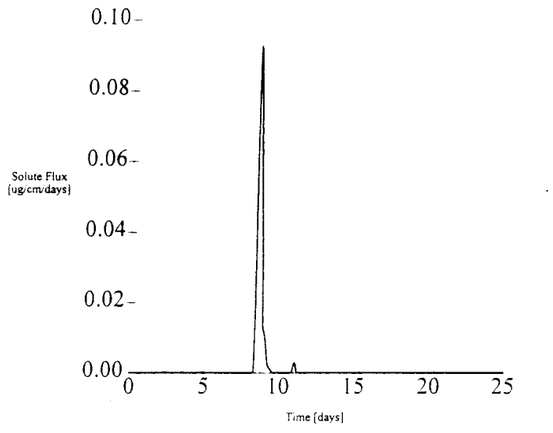


# Seepage Face Solute Flux

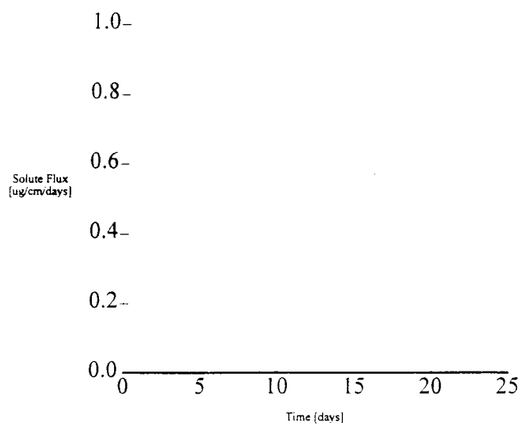

Observation Nodes: Pressure Heads

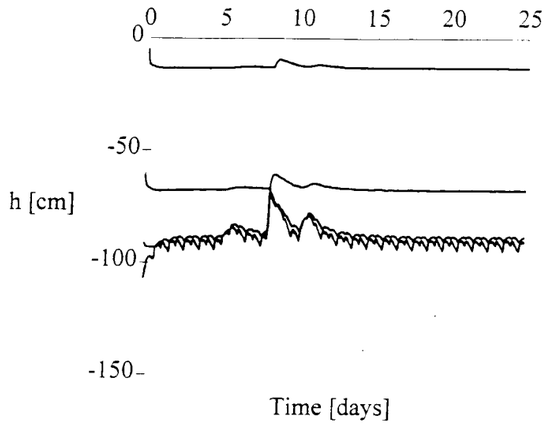


Observation Nodes: Water Contents

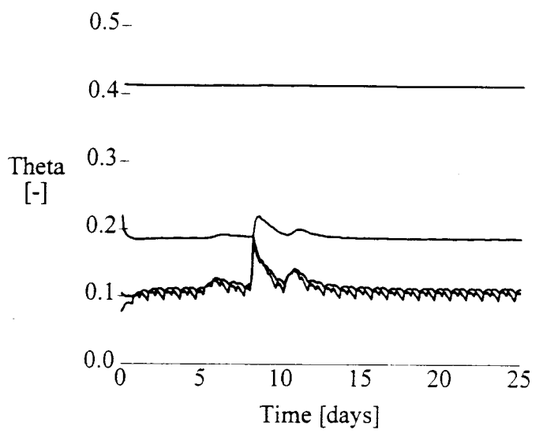

Observation Nodes: Concentrations

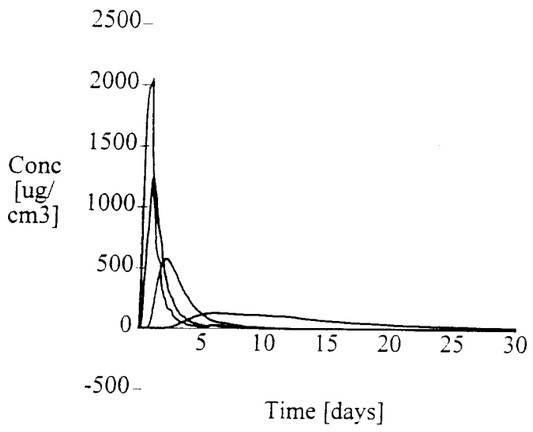


Observation Nodes: Concentrations

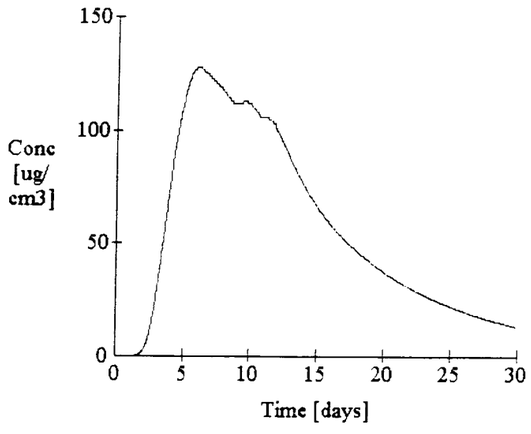

## Cumulative Variable Boundary Solute Flux

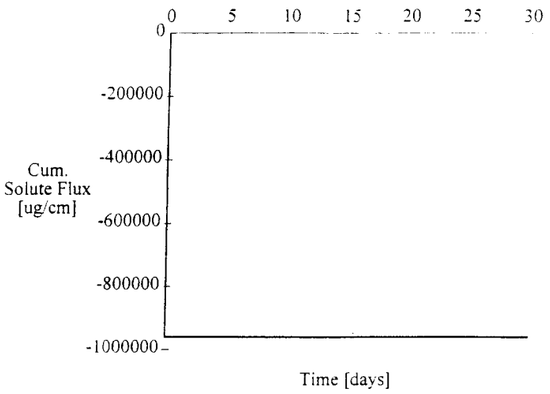


## Free or Deep Drainage Boundary Solute Flux

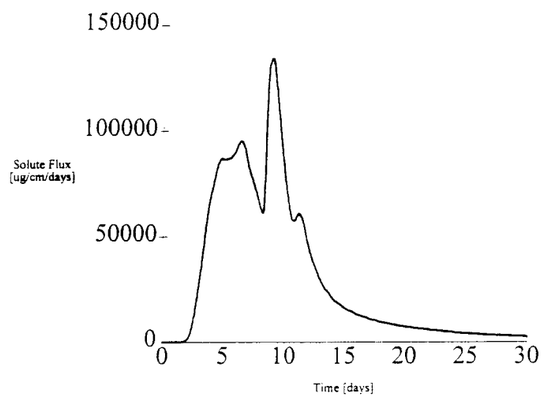

# Constant Boundary Solute Flux

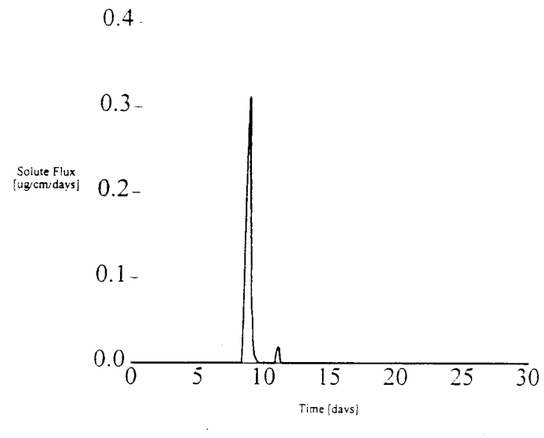


# Seepage Face Solute Flux

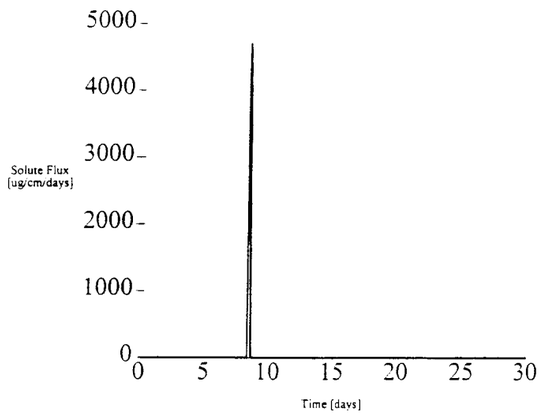

Observation Nodes: Pressure Heads

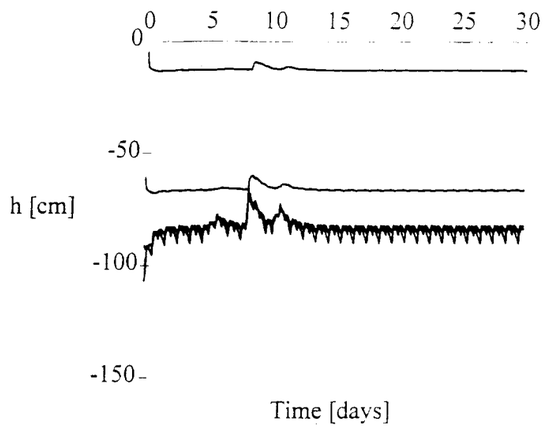


Observation Nodes: Water Contents

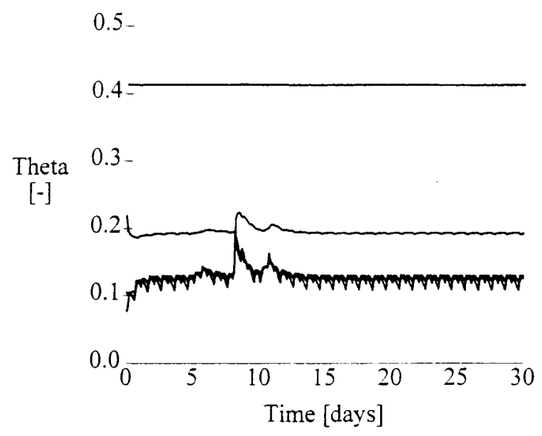

Observation Nodes: Concentrations

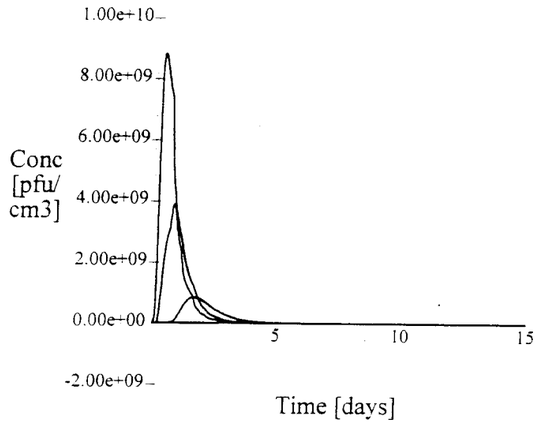


Observation Nodes: Concentrations

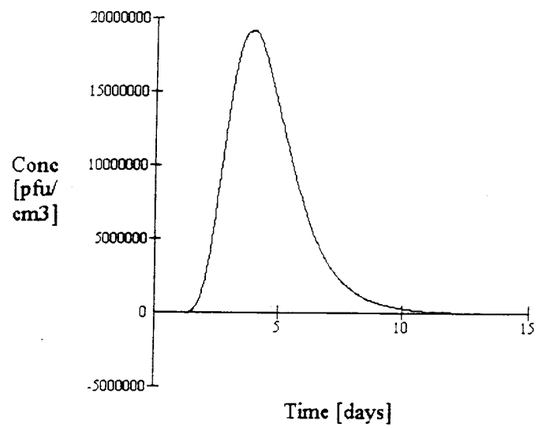

## Cumulative Variable Boundary Solute Flux

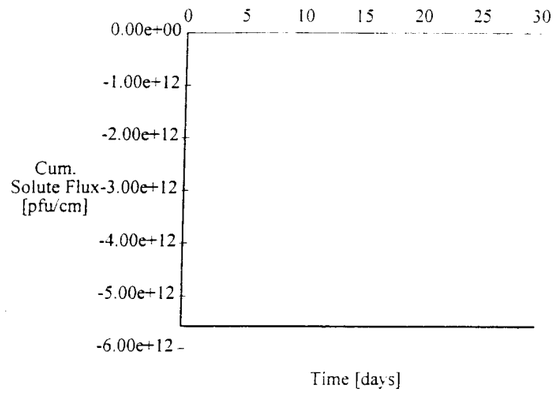


## Free or Deep Drainage Boundary Solute Flux

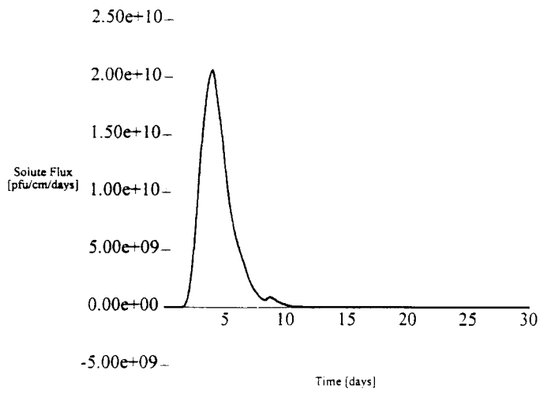

# Constant Boundary Solute Flux

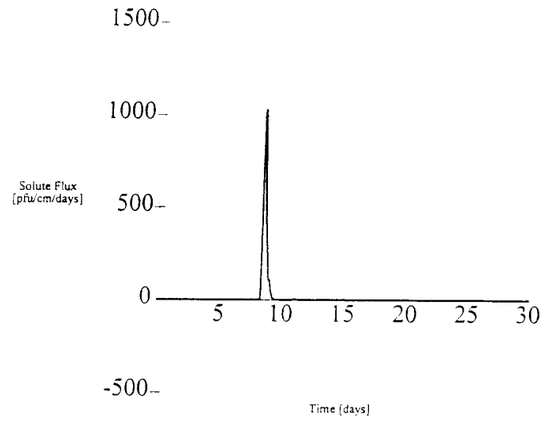


# Seepage Face Solute Flux

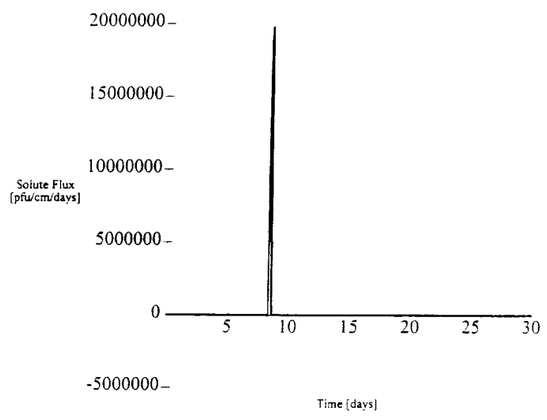

Observation Nodes: Pressure Heads

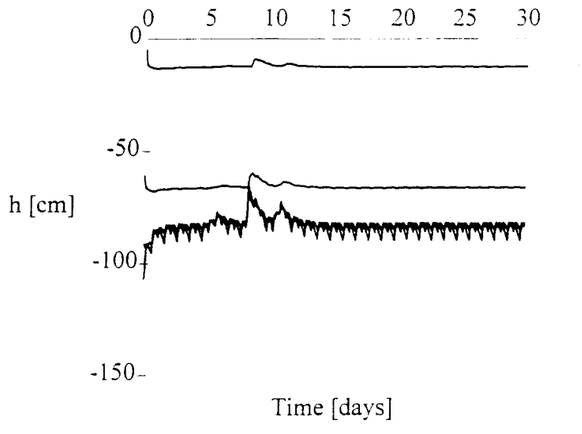


Observation Nodes: Water Contents

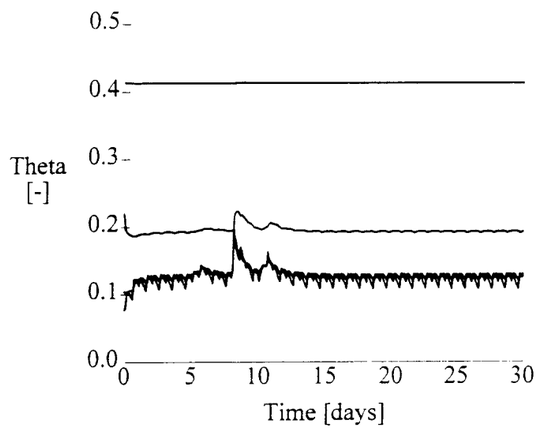

Observation Nodes:
Concentrations

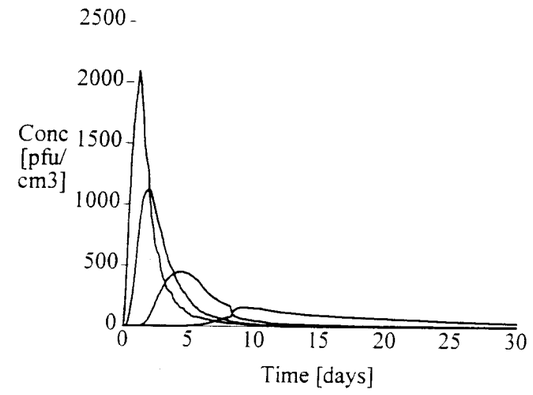


Observation Nodes:
Concentrations

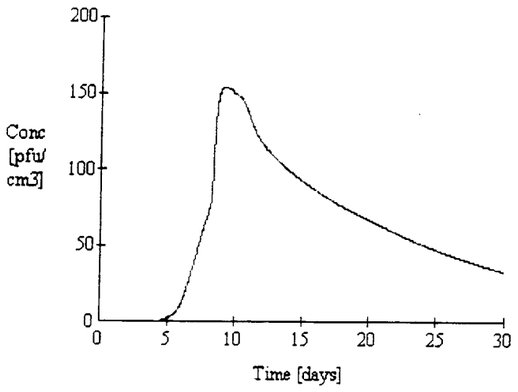

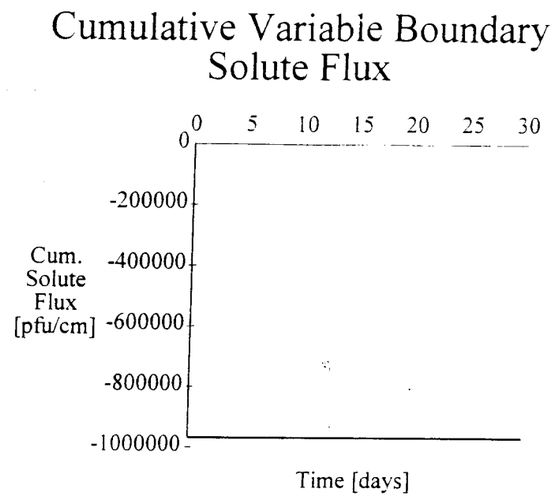
Cumulative Variable Boundary
Solute Flux
0
5
10
15
20
25
30
0
-200000
-400000
-600000
-800000
-1000000
Cum.
Solute
Flux
[pfu/cm]
Time [days]

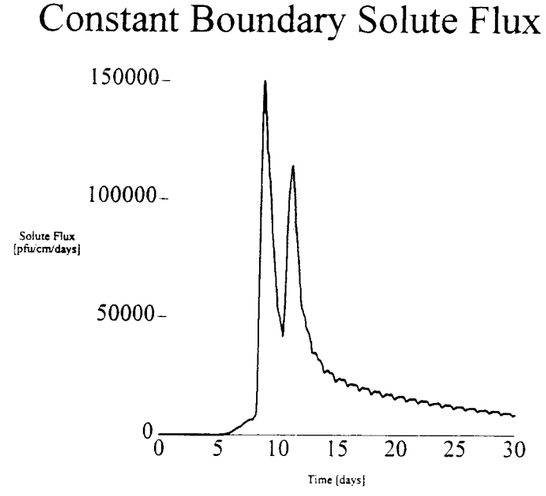
Constant Boundary Solute Flux
150000
100000
50000
0
Solute Flux
[pfu/cm/days]
0
5
10
15
20
25
30
Time [days]

## Observation Nodes: Pressure Heads

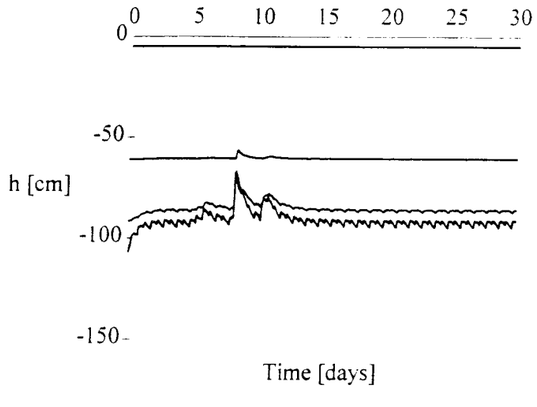


## Observation Nodes: Water Contents

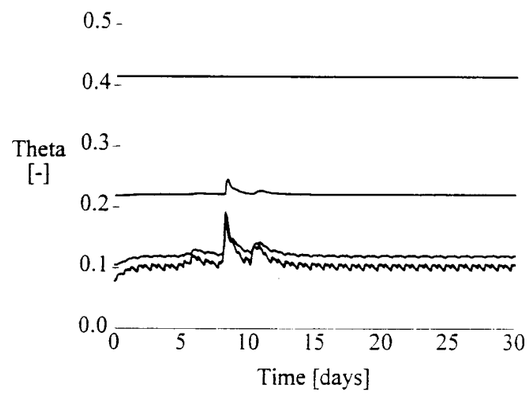

Observation Nodes: Concentrations

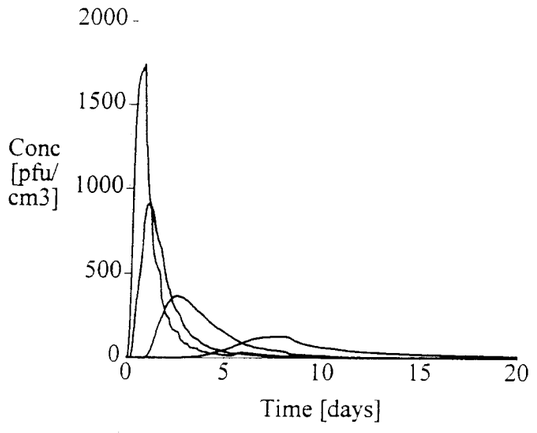


Observation Nodes: Concentrations

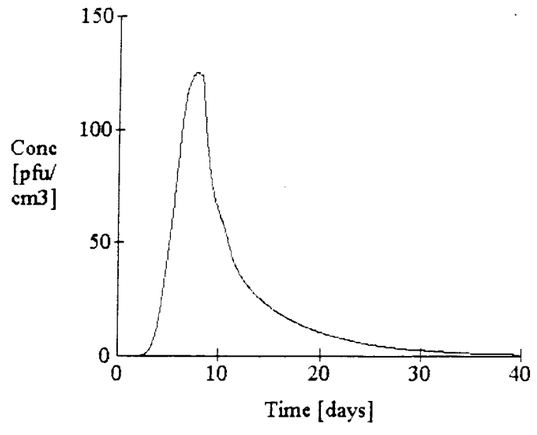

## Cumulative Variable Boundary Solute Flux

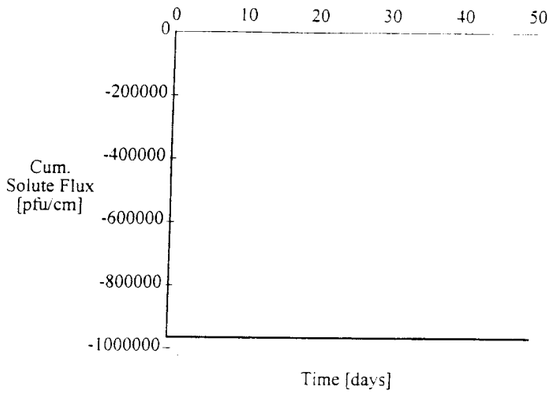


## Constant Boundary Solute Flux

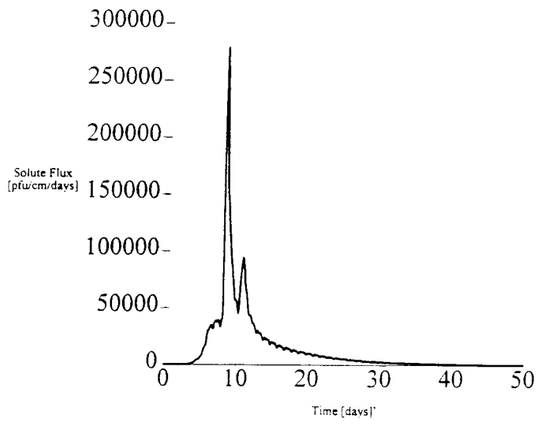

Observation Nodes: Pressure Heads

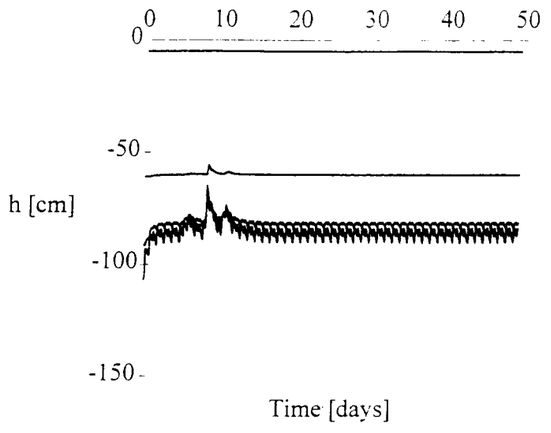


Observation Nodes: Water Contents

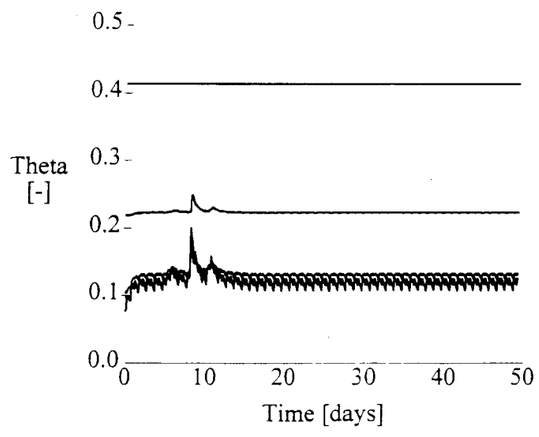

Observation Nodes: Concentrations

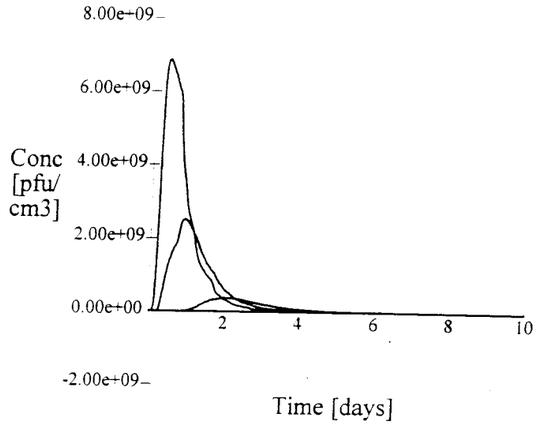


Observation Nodes: Concentrations

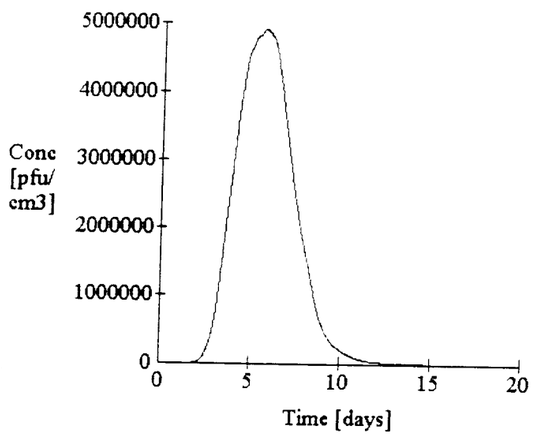

## Cumulative Variable Boundary Solute Flux

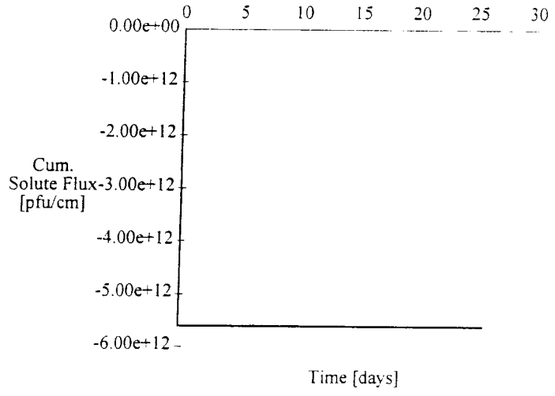


## Constant Boundary Solute Flux

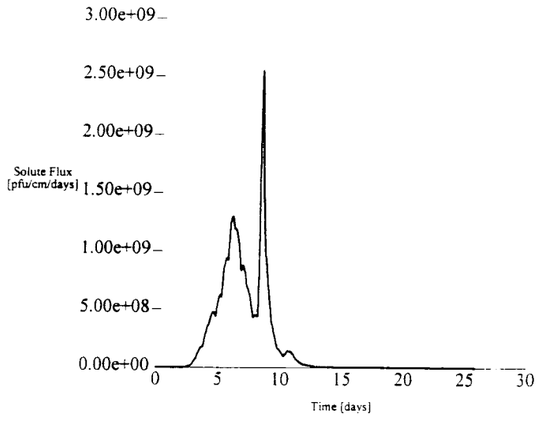

Observation Nodes: Pressure Heads

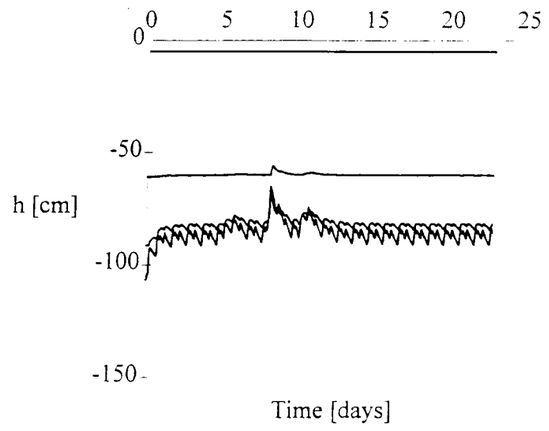


Observation Nodes: Water Contents

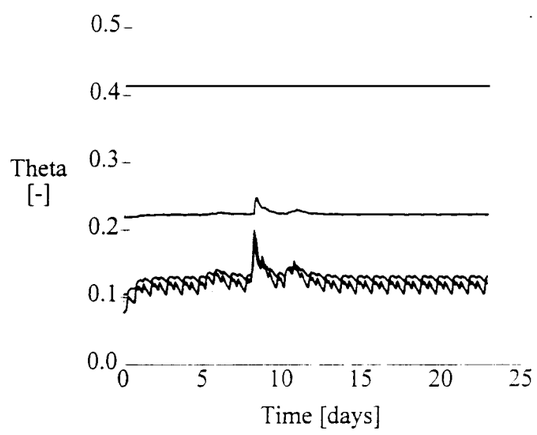

# Cumulative Variable Boundary Solute Flux

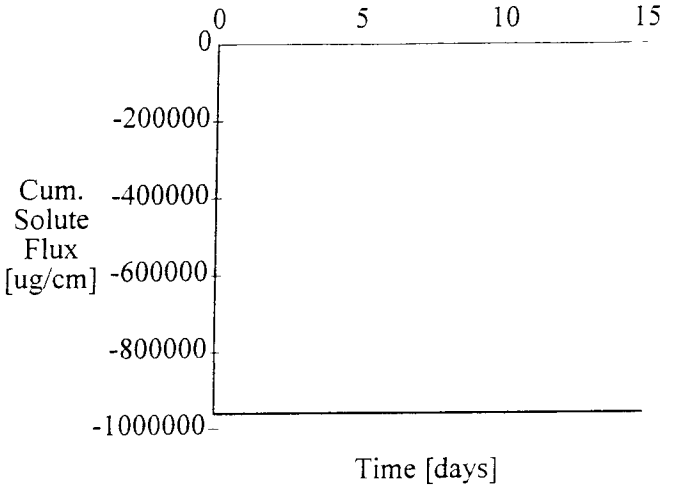


# Free or Deep Drainage Boundary Solute Flux

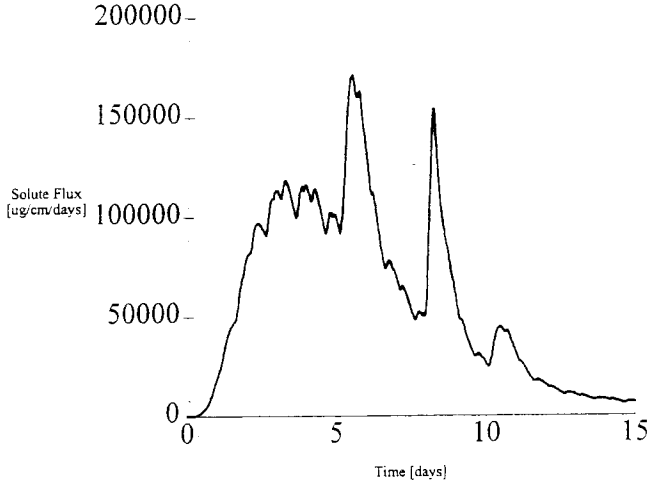

# Constant Boundary Solute Flux

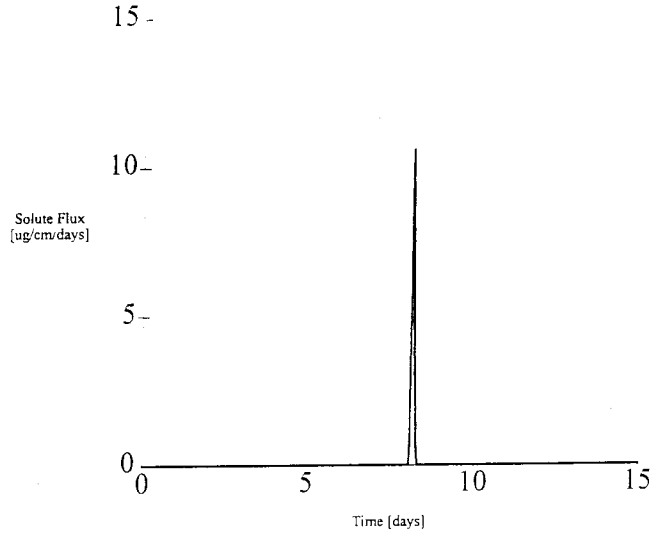


# Seepage Face Solute Flux

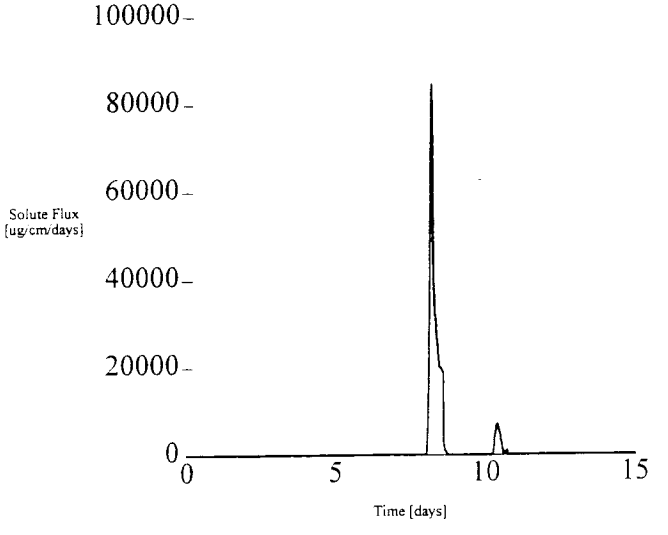

# Observation Nodes: Concentrations

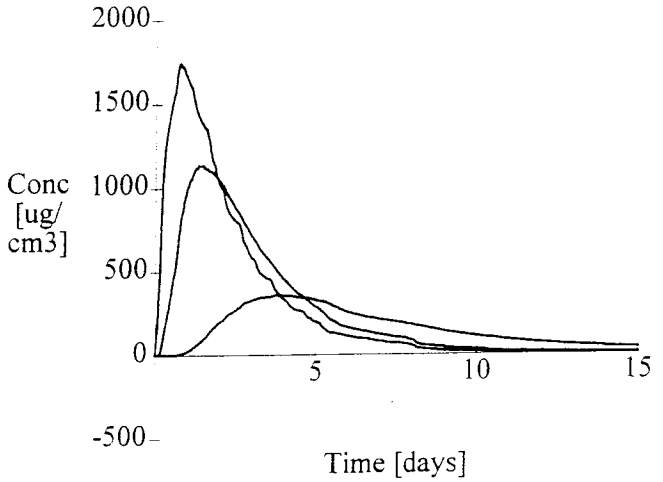


# Observation Nodes: Concentrations

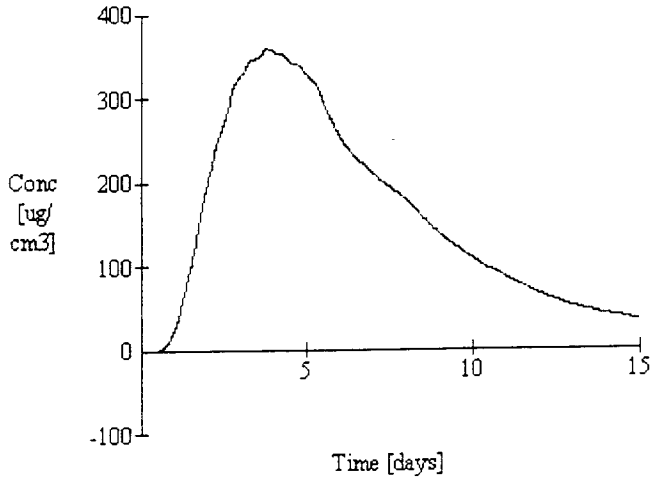

# Constant Boundary Solute Flux

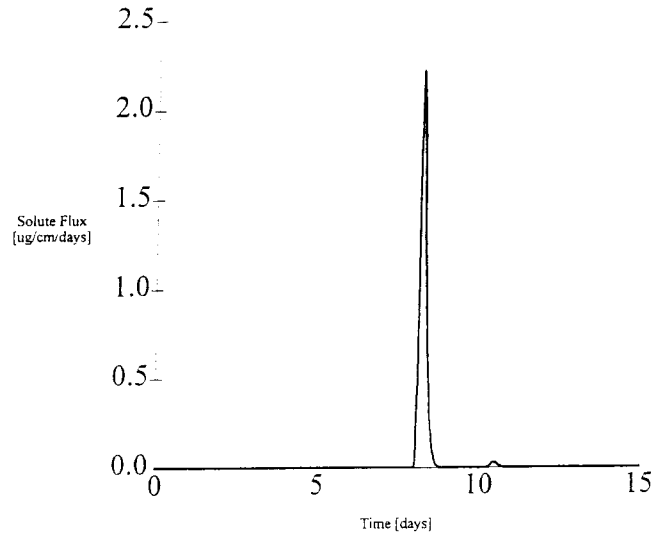


# Seepage Face Solute Flux

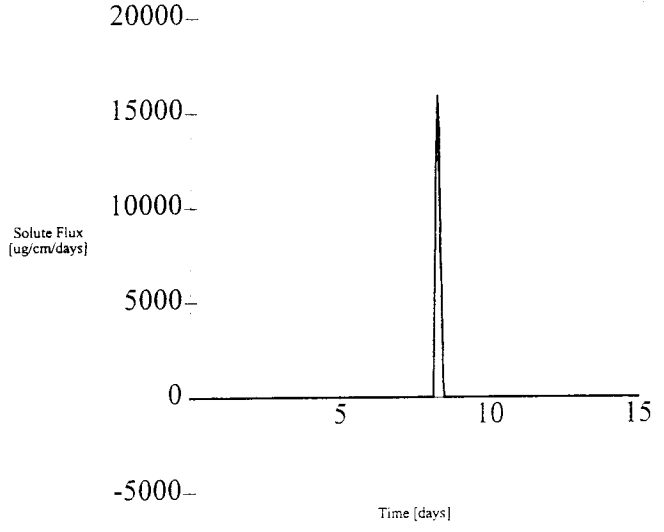

# Cumulative Variable Boundary Solute Flux

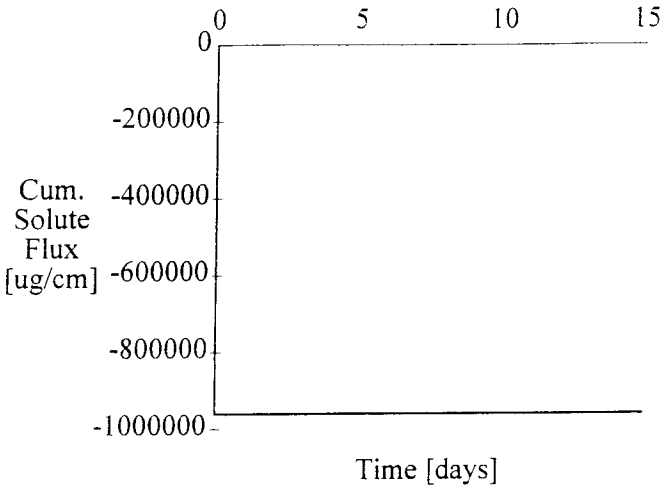


# Free or Deep Drainage Boundary Solute Flux

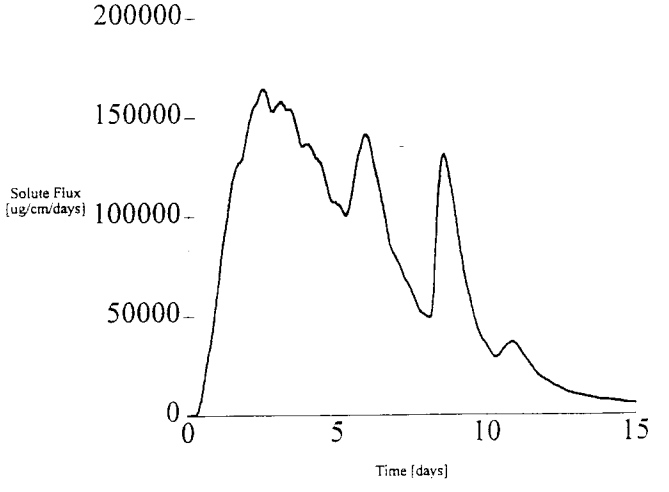

# Observation Nodes: Concentrations

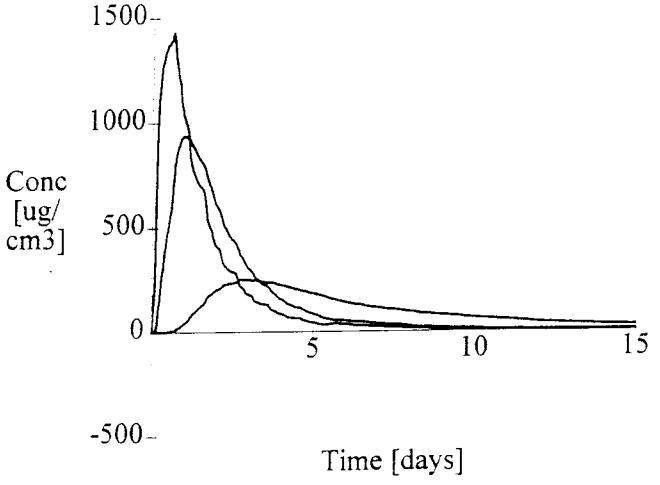


# Observation Nodes: Concentrations

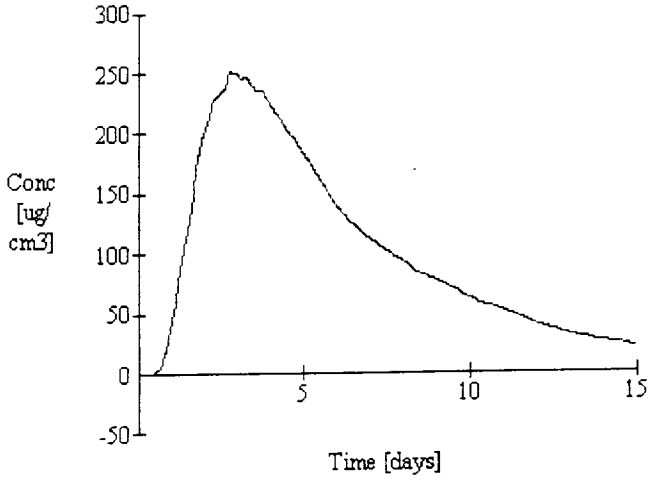

# Cumulative Variable Boundary Solute Flux

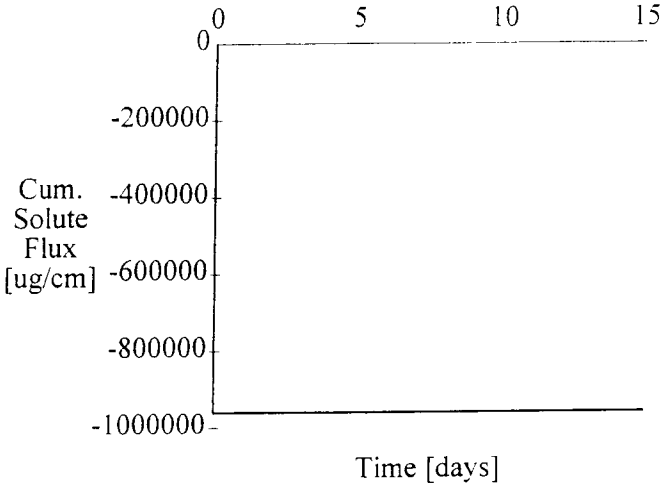


# Free or Deep Drainage Boundary Solute Flux

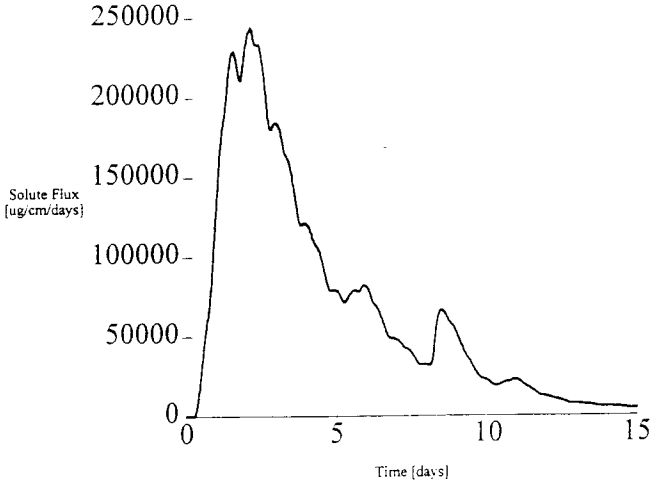

# Constant Boundary Solute Flux

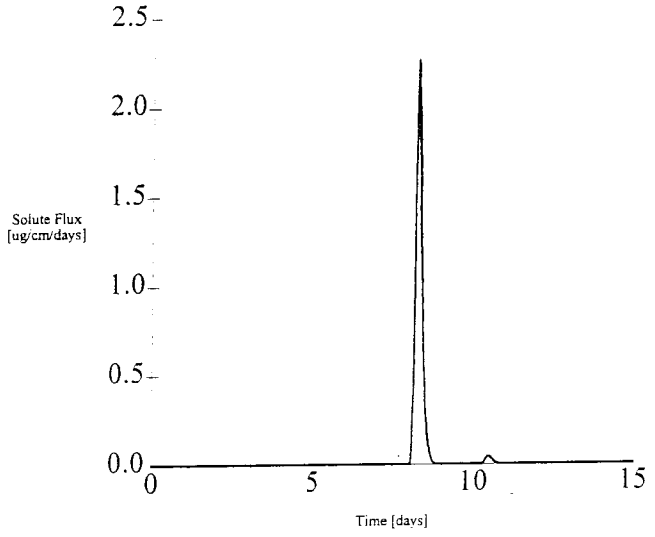


# Seepage Face Solute Flux

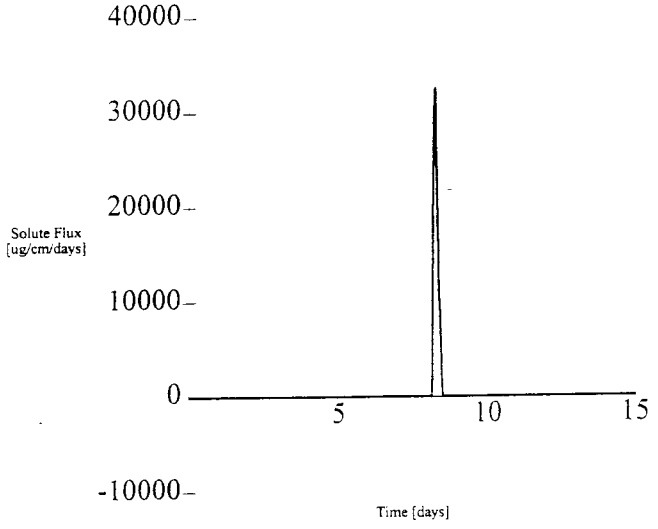

# Observation Nodes: Concentrations

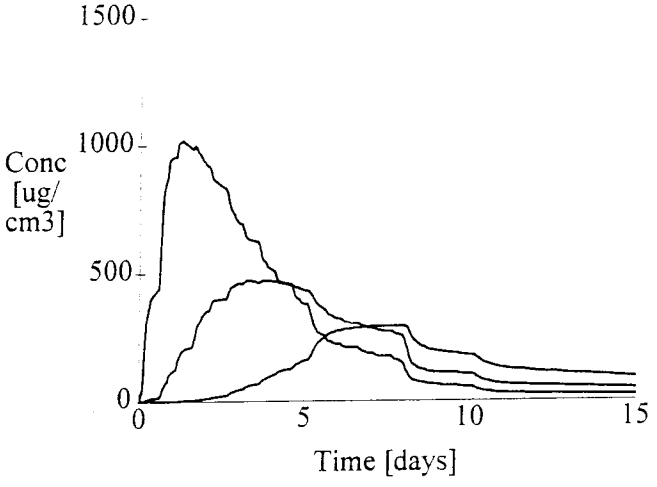


# Observation Nodes: Concentrations

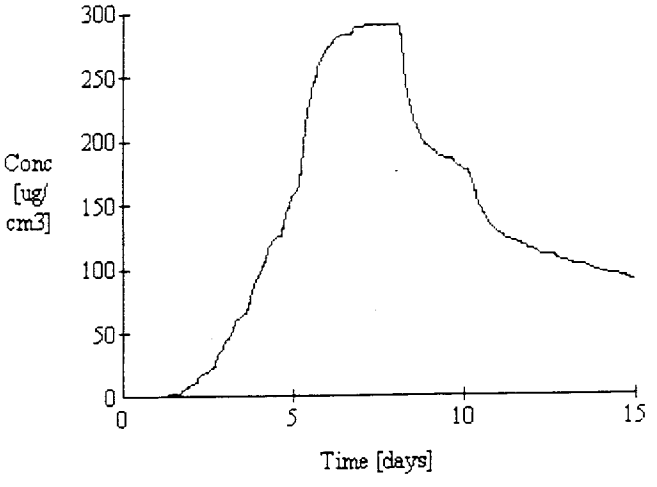

# Cumulative Variable Boundary Solute Flux

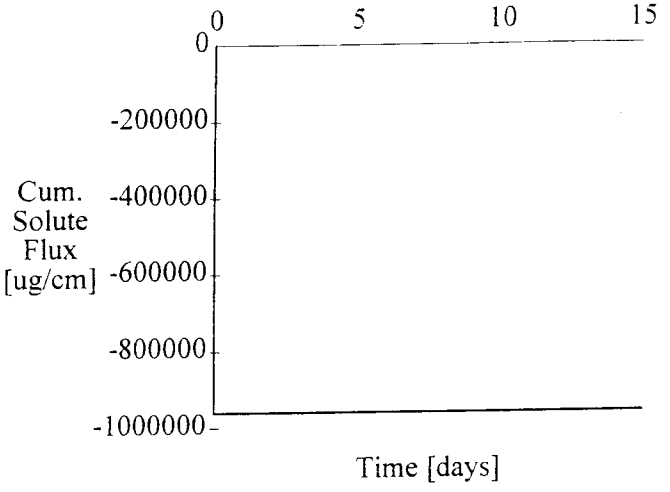


# Constant Boundary Solute Flux

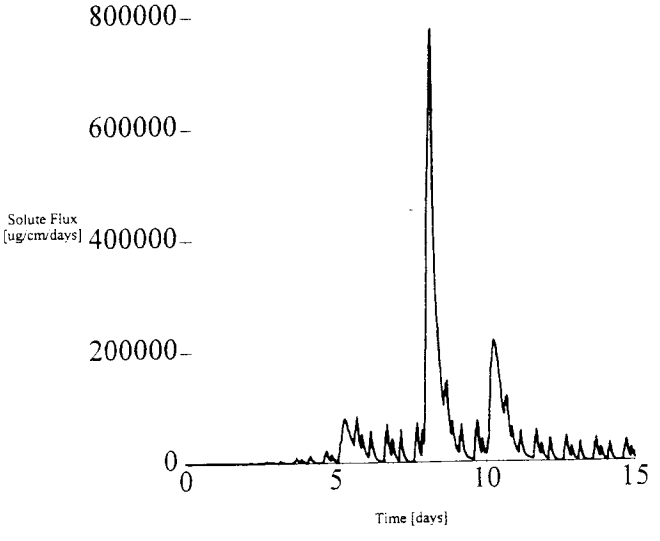

# Observation Nodes: Concentrations

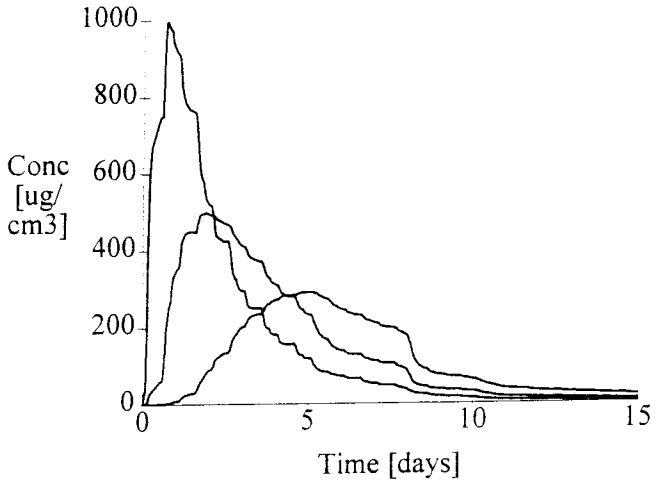


# Observation Nodes: Concentrations

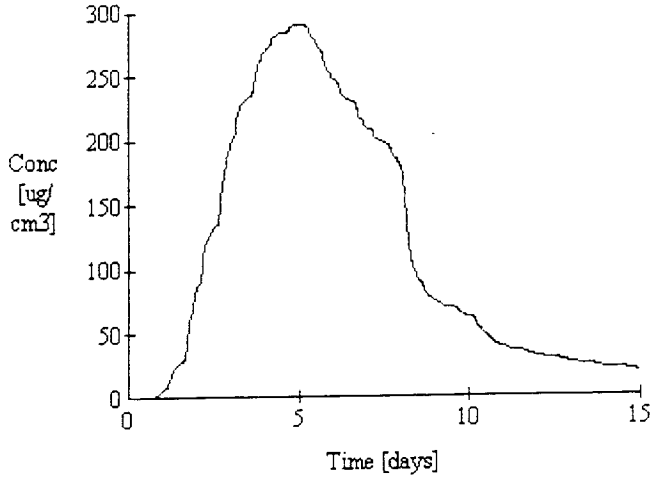

# Cumulative Variable Boundary Solute Flux

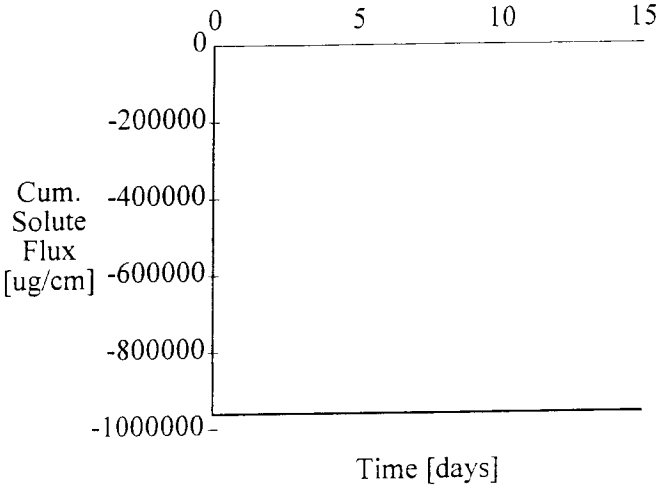


# Constant Boundary Solute Flux

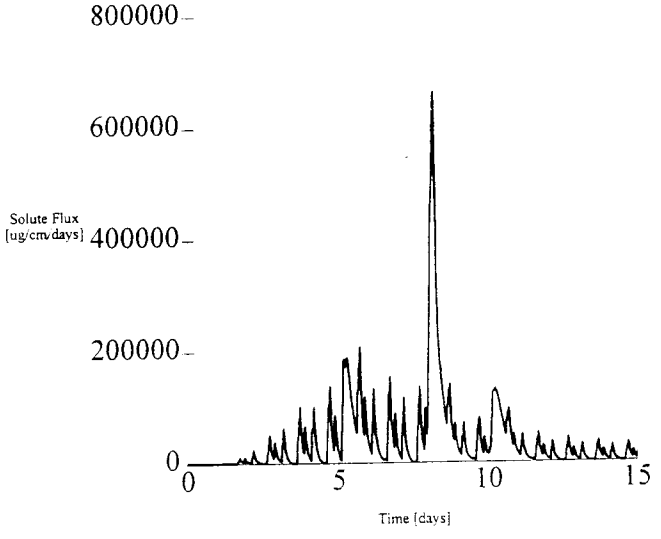

# Observation Nodes: Concentrations

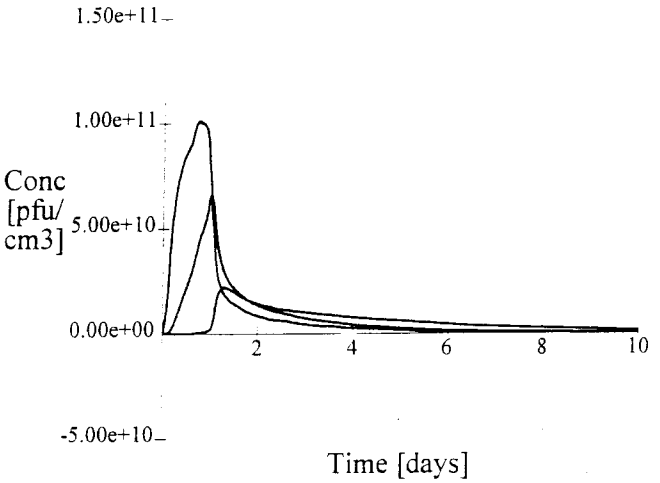


# Observation Nodes: Concentrations

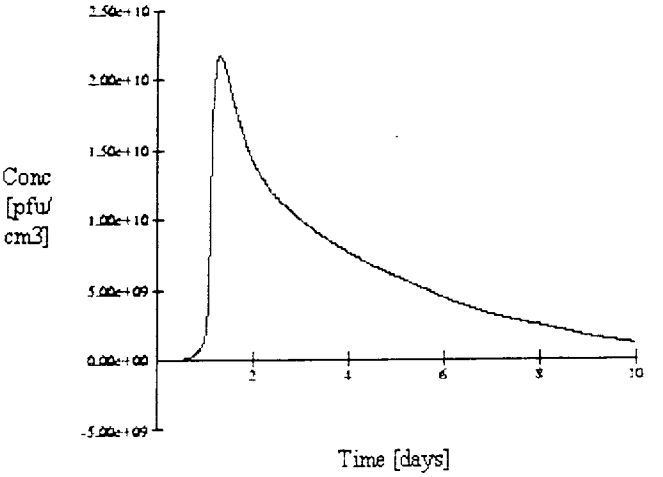

# Cumulative Variable Boundary Solute Flux

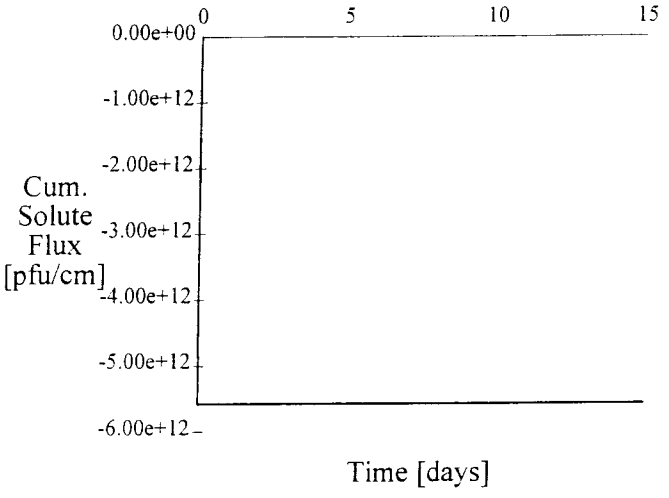


# Free or Deep Drainage Boundary Solute Flux

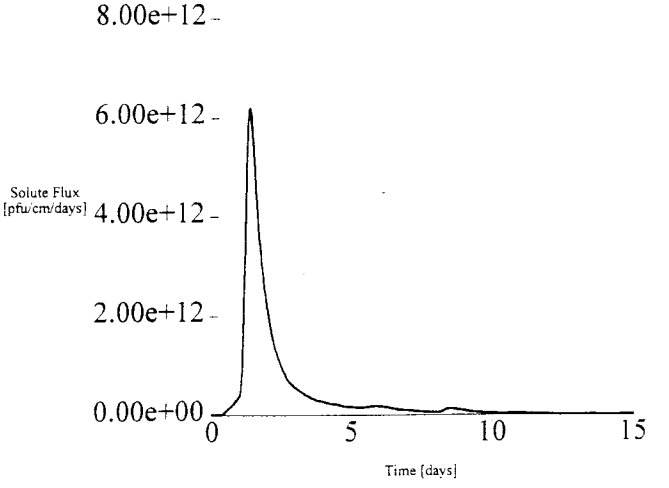

## Observation Nodes: Concentrations

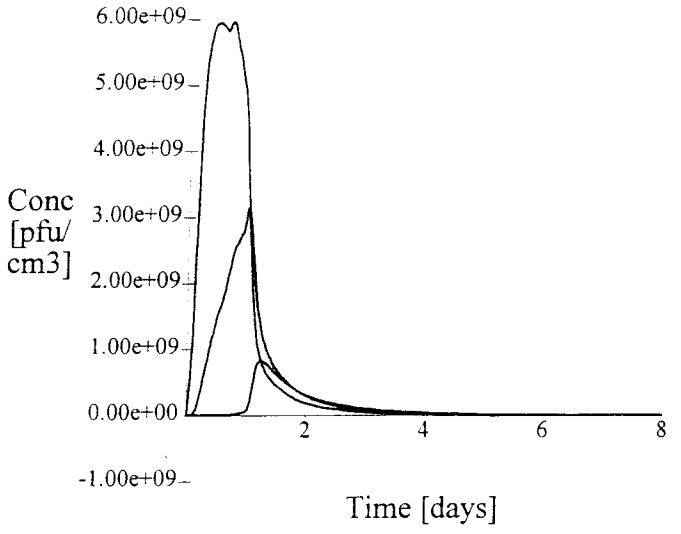


## Observation Nodes: Concentrations

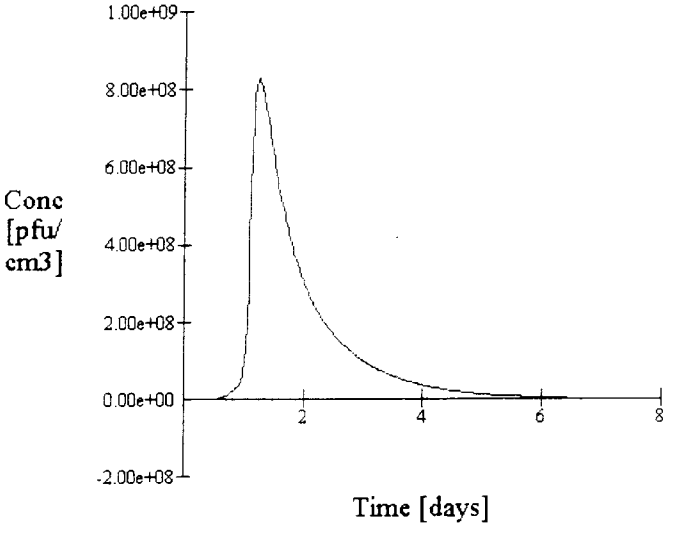

# Cumulative Variable Boundary Solute Flux

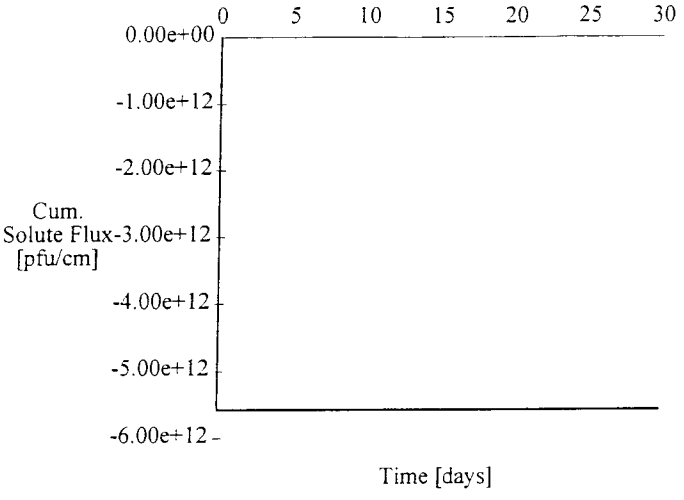


# Free or Deep Drainage Boundary Solute Flux

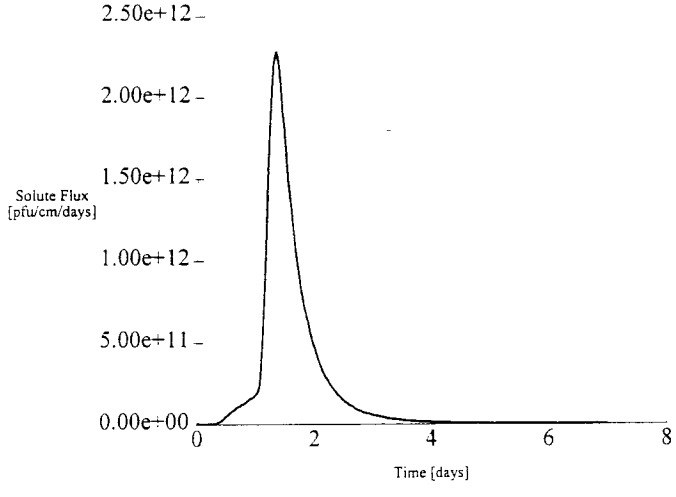

# Constant Boundary Solute Flux

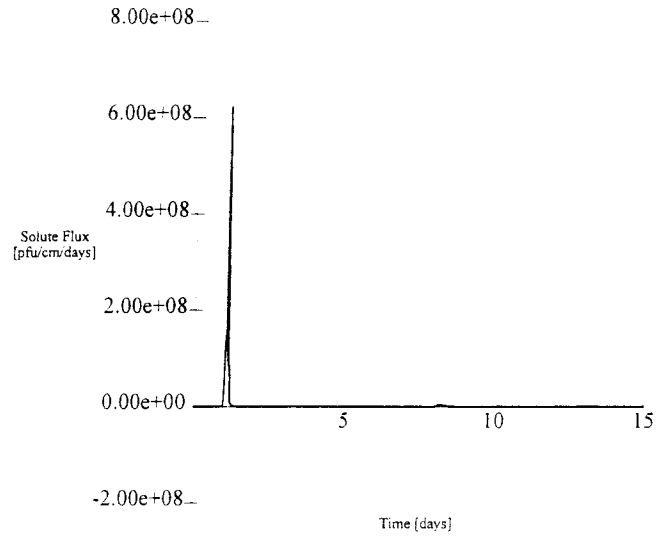


# Seepage Face Solute Flux

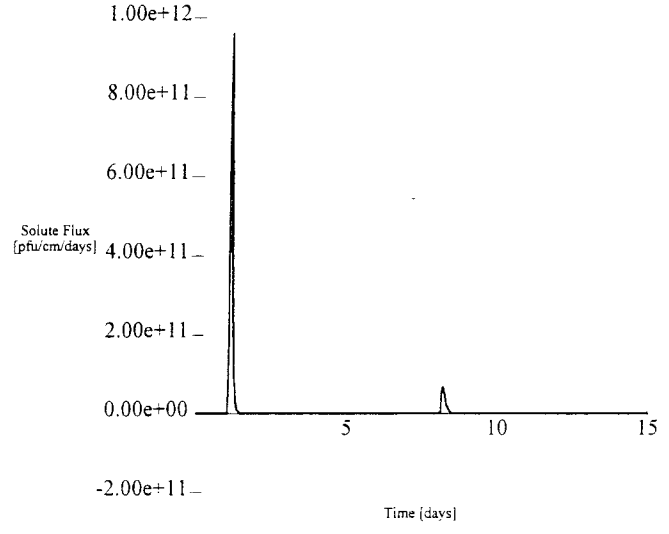

# Constant Boundary Solute Flux

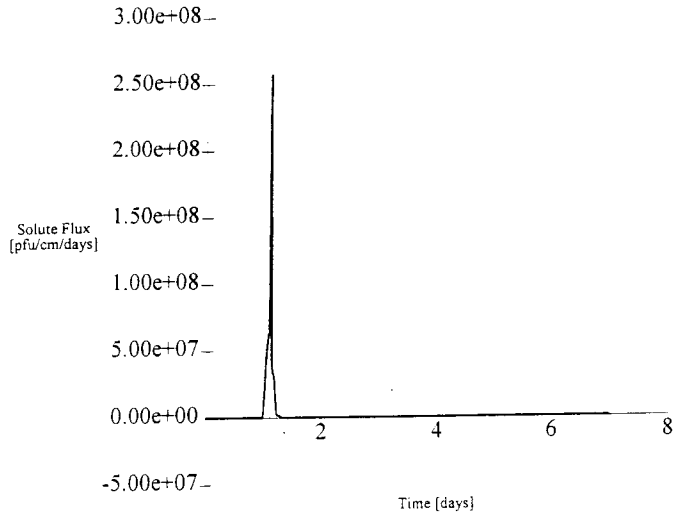


# Seepage Face Solute Flux

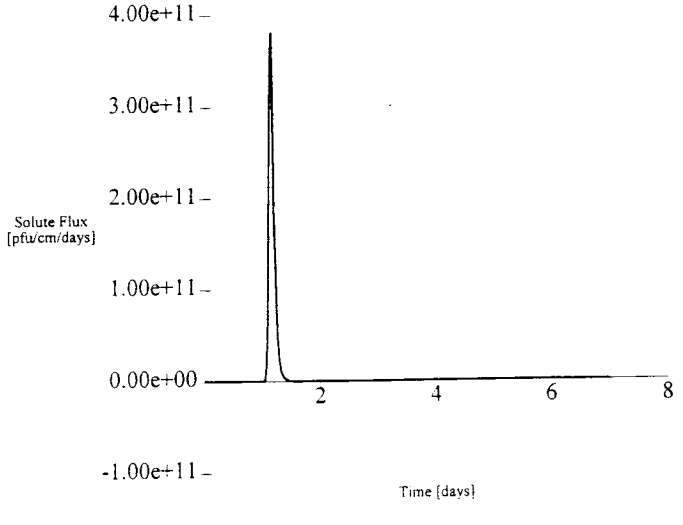

## Observation Nodes: Pressure Heads

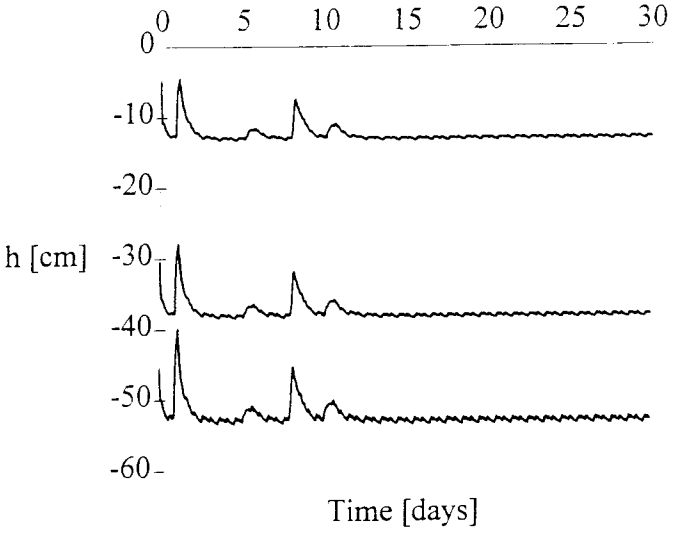


## Observation Nodes: Water Contents

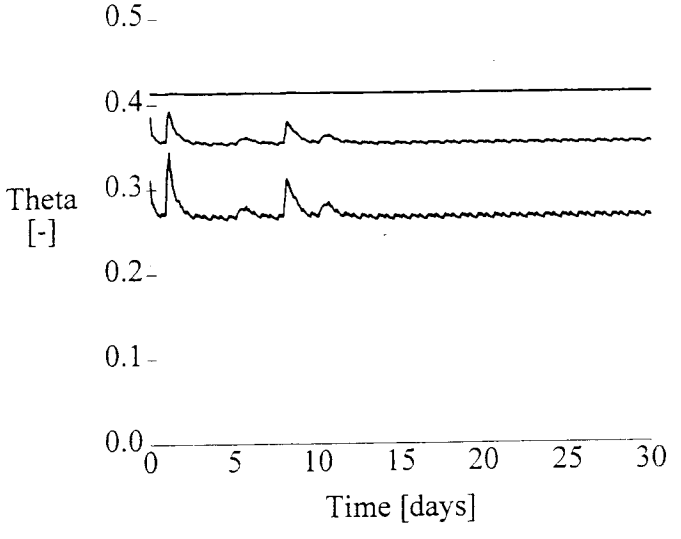

# Observation Nodes: Concentrations

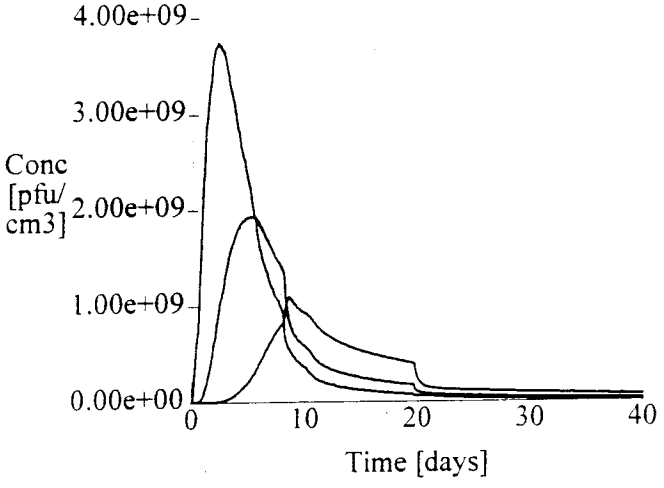


# Observation Nodes: Concentrations

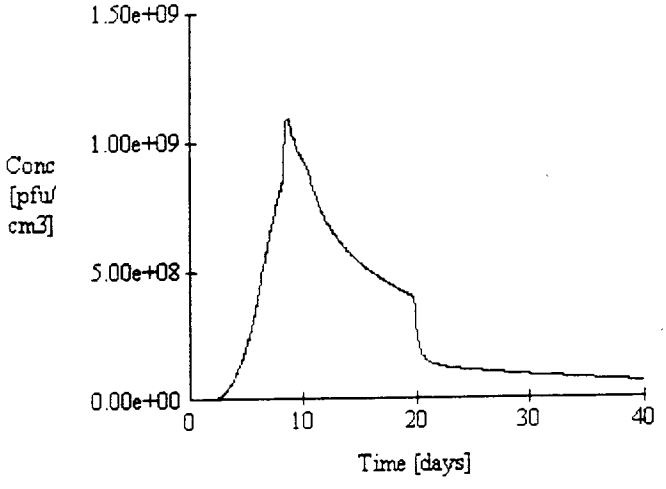

# Cumulative Variable Boundary Solute Flux

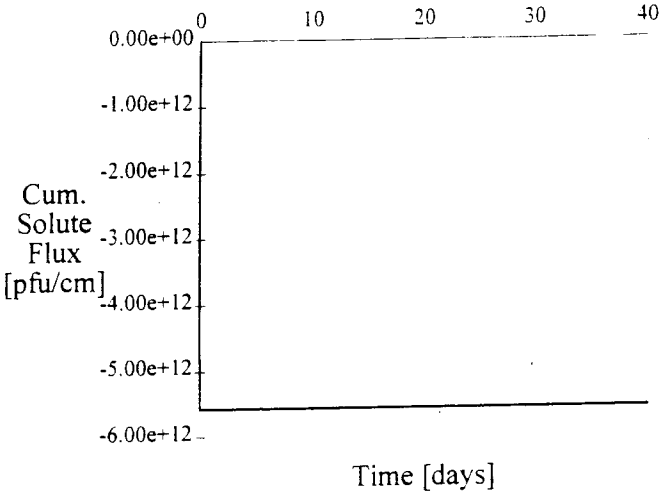


# Free or Deep Drainage Boundary Solute Flux

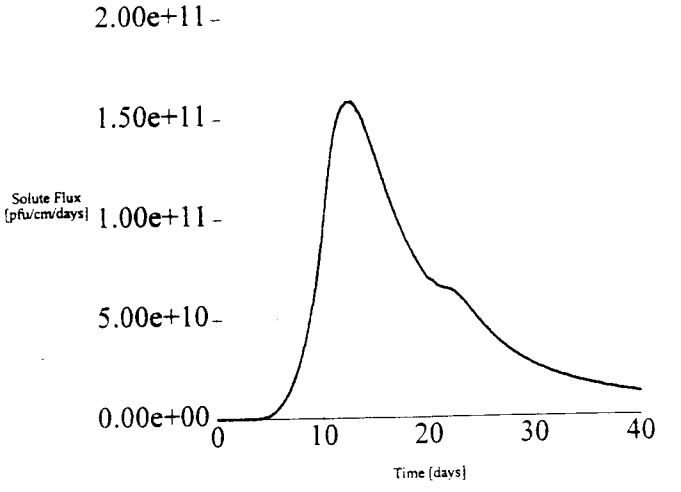

# Constant Boundary Solute Flux

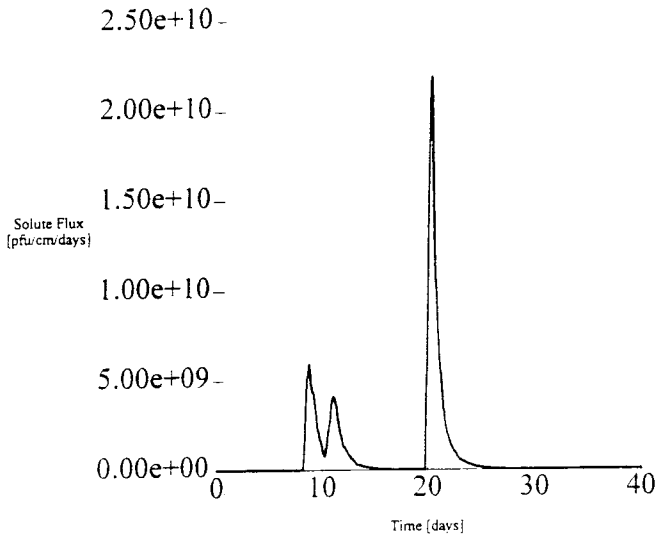


# Seepage Face Solute Flux

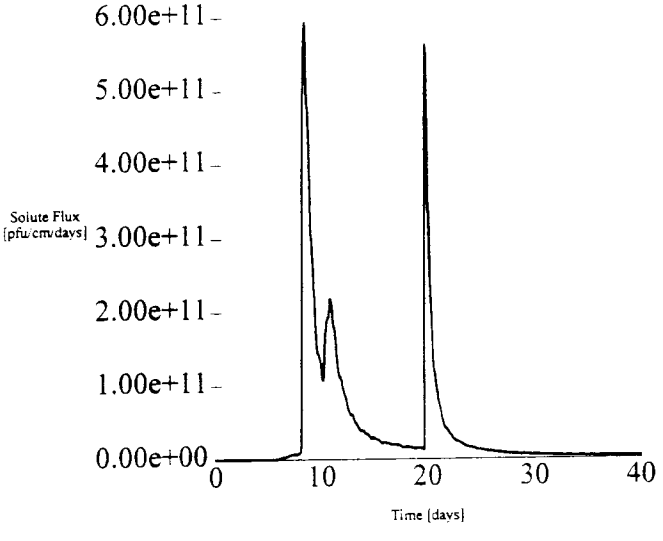

# Observation Nodes: Pressure Heads

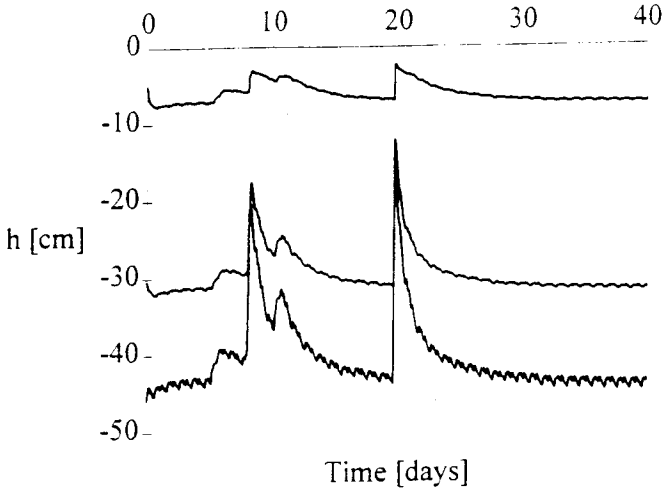


# Observation Nodes: Water Contents

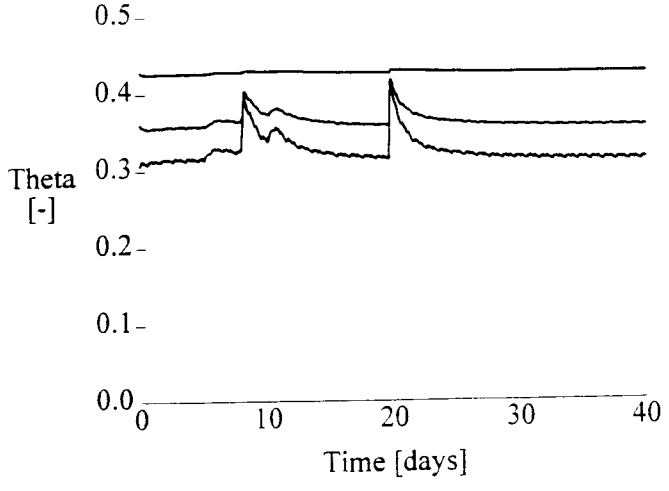

# Observation Nodes: Concentrations

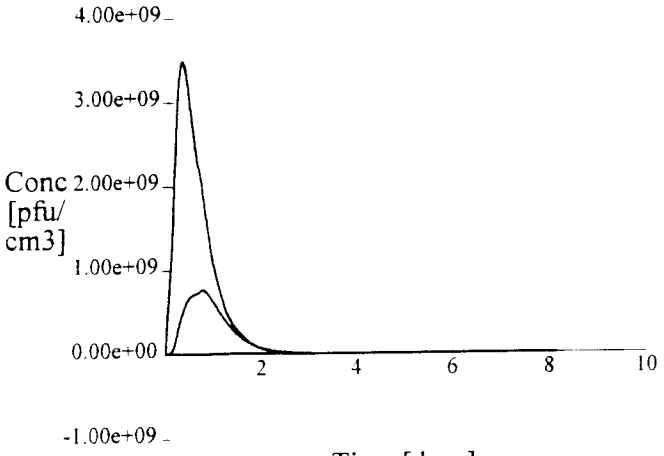


# Observation Nodes: Concentrations

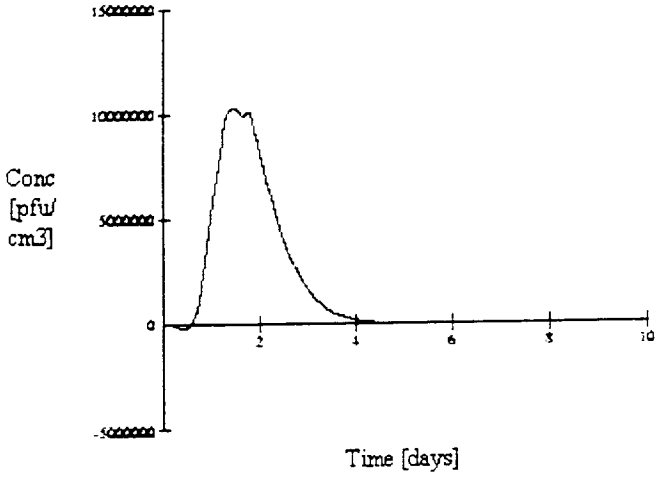

## Observation Nodes: Concentrations

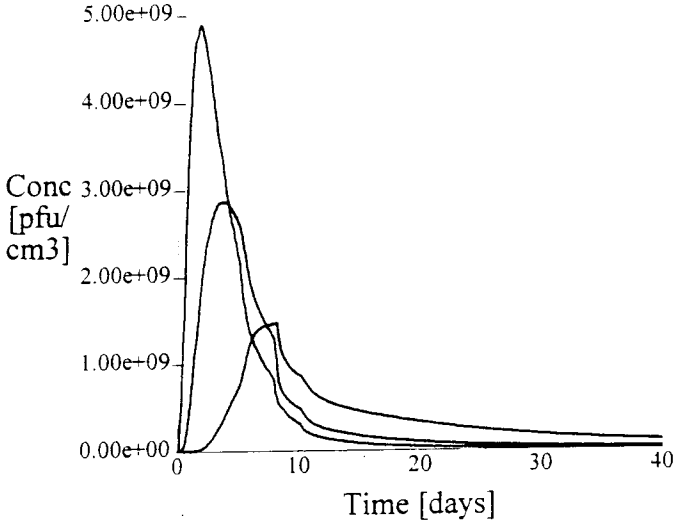


## Observation Nodes: Concentrations

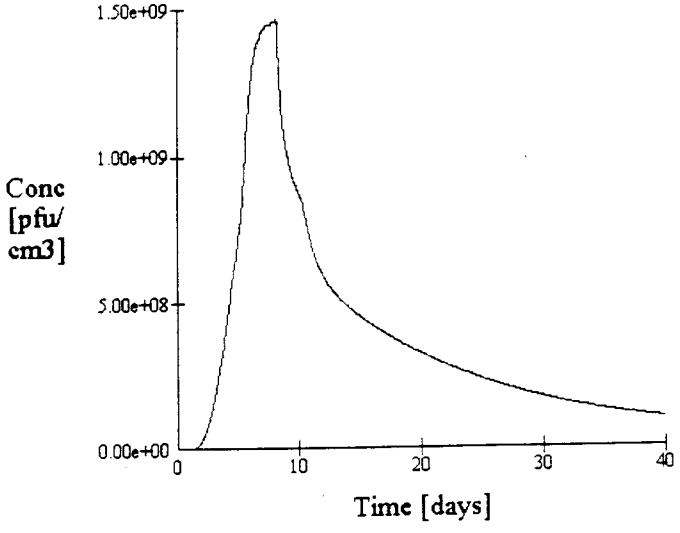

# Cumulative Variable Boundary Solute Flux

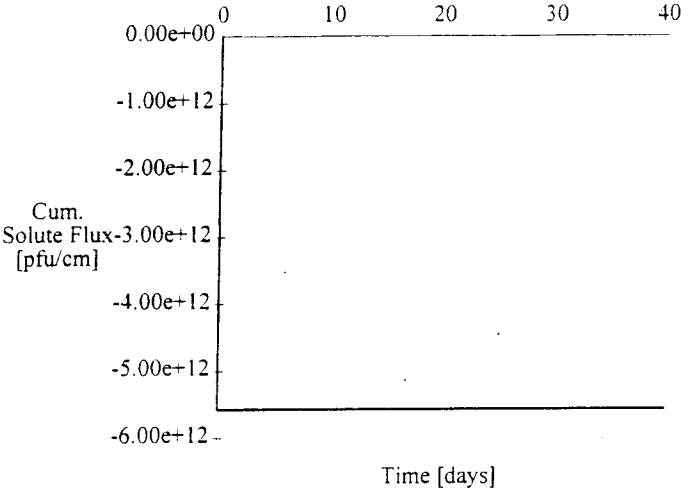


# Free or Deep Drainage Boundary Solute Flux

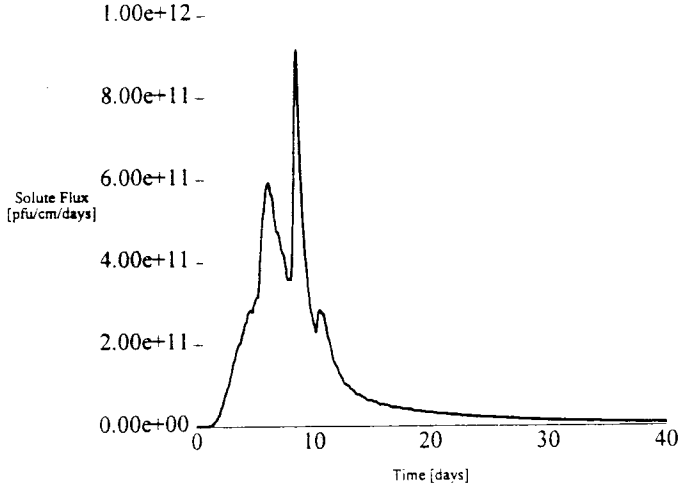

# Constant Boundary Solute Flux

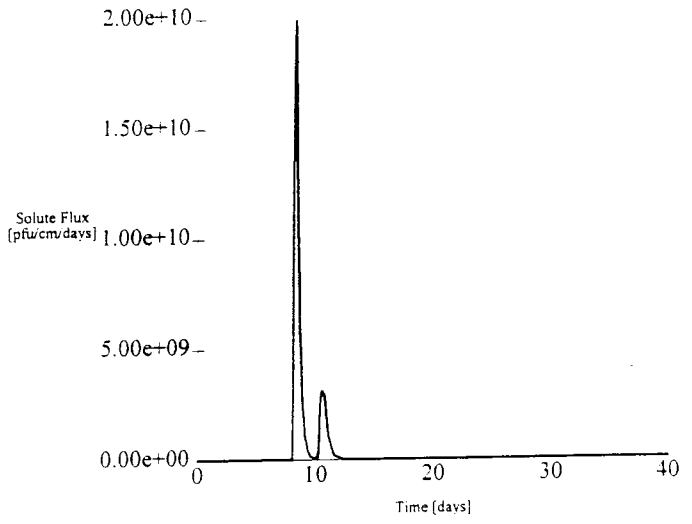


# Seepage Face Solute Flux

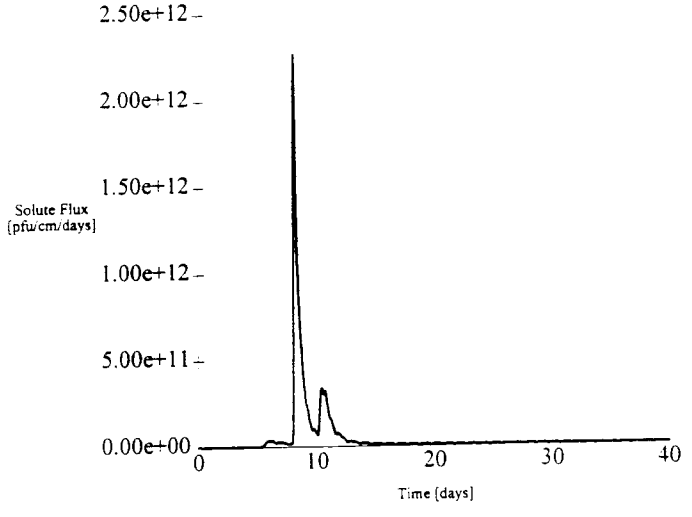

## Observation Nodes: Pressure Heads

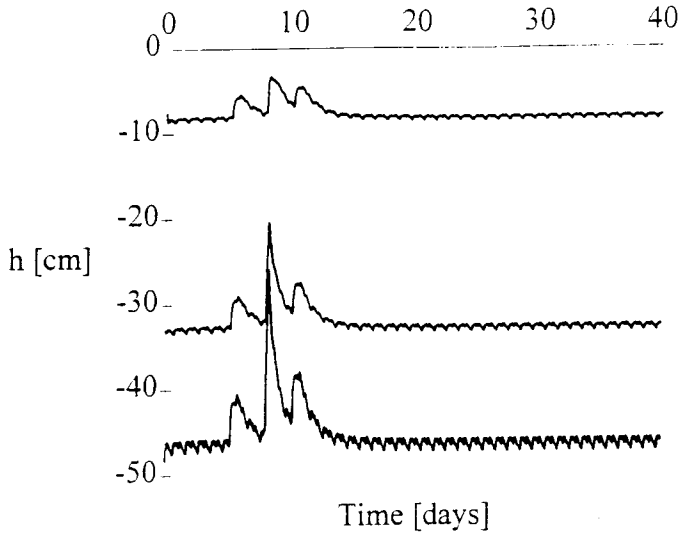


## Observation Nodes: Water Contents

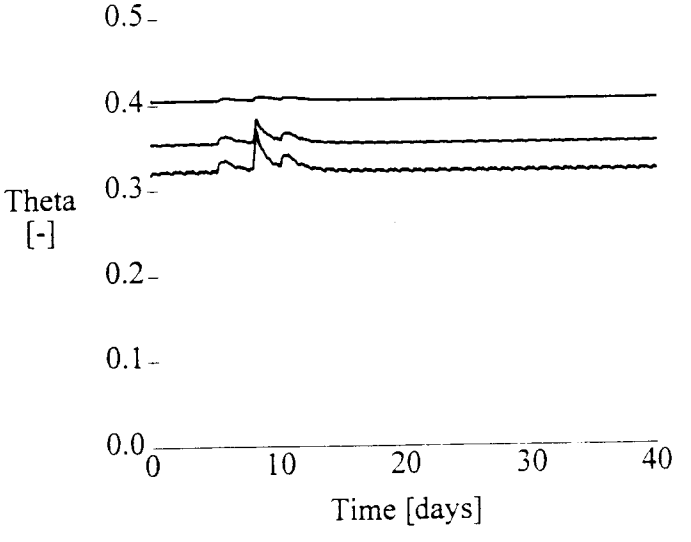

# Cumulative Variable Boundary Solute Flux

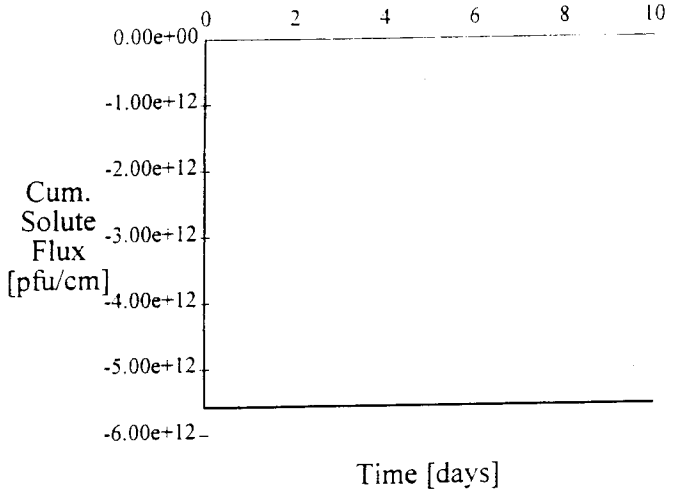


# Free or Deep Drainage Boundary Solute Flux

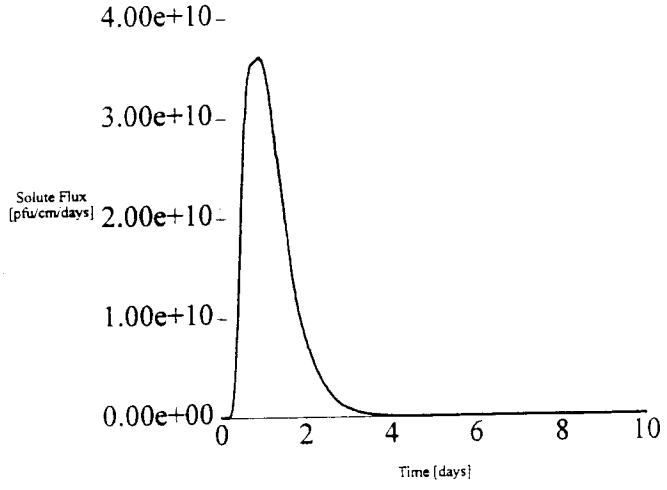

# Constant Boundary Solute Flux

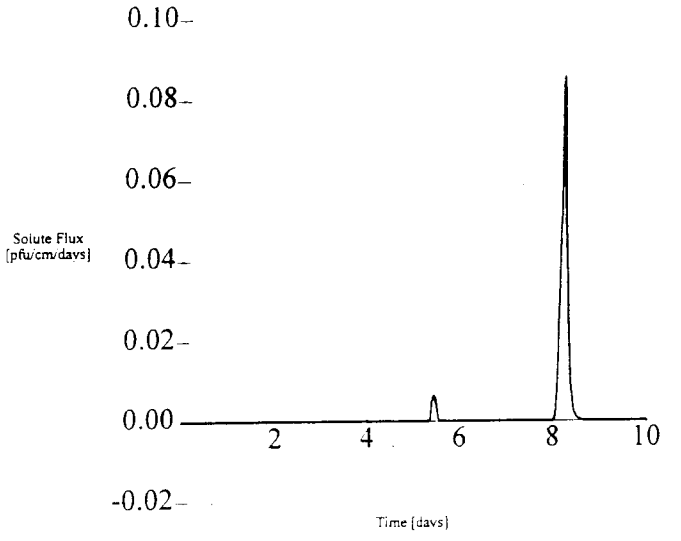


# Seepage Face Solute Flux

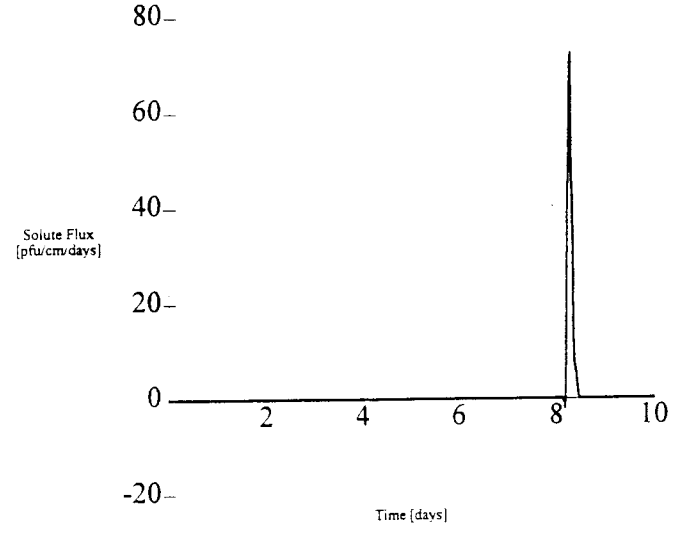

# Observation Nodes: Pressure Heads

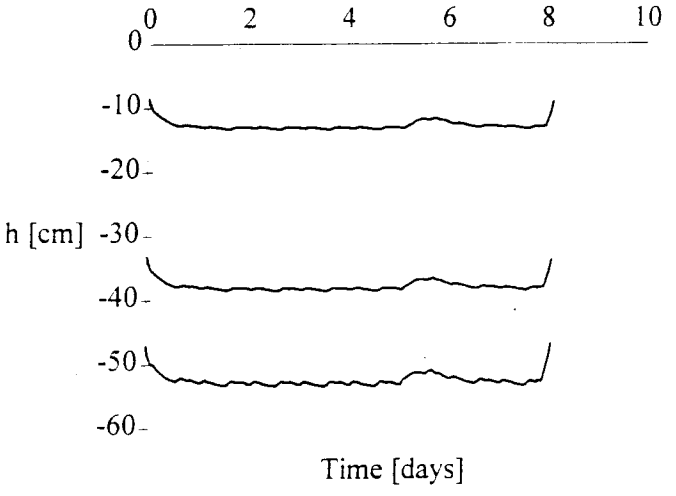


# Observation Nodes: Water Contents

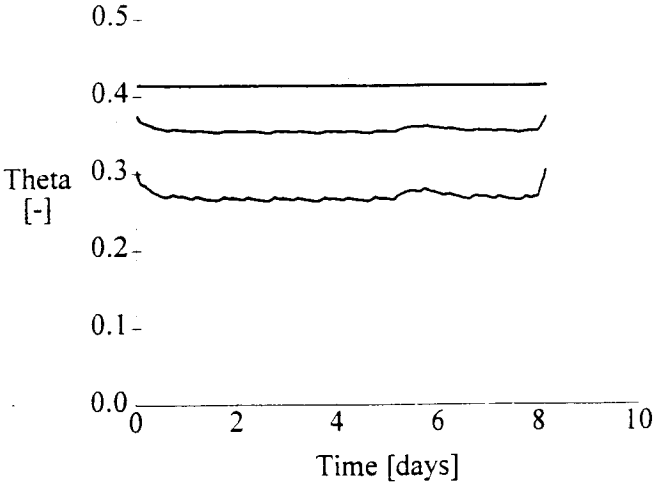

# Constant Boundary Solute Flux

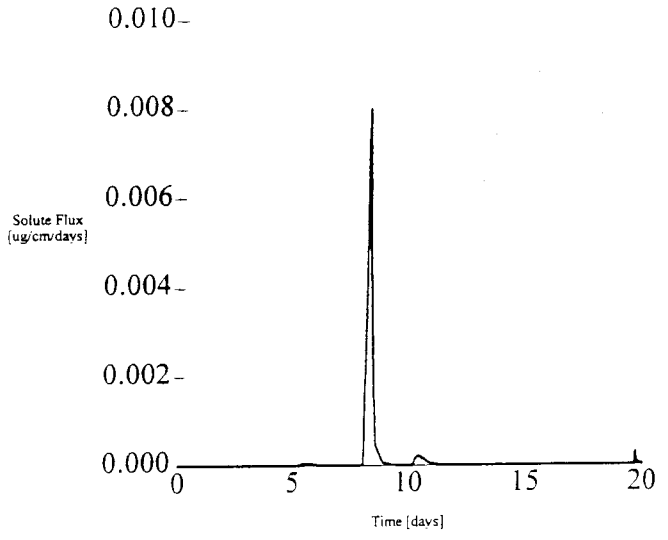


# Seepage Face Solute Flux

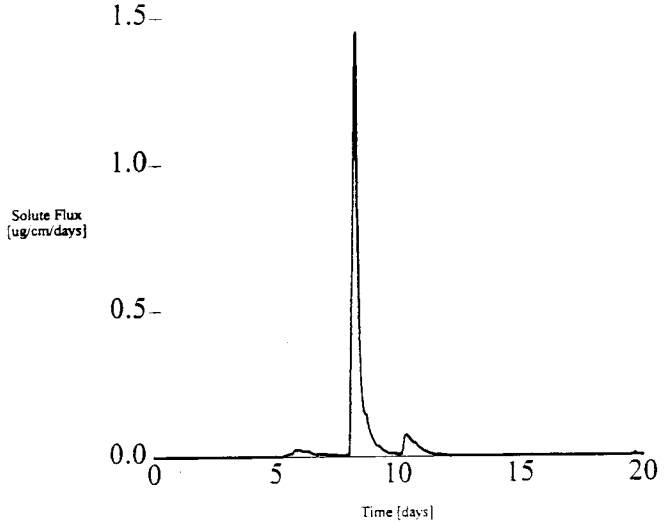

# Observation Nodes: Concentrations

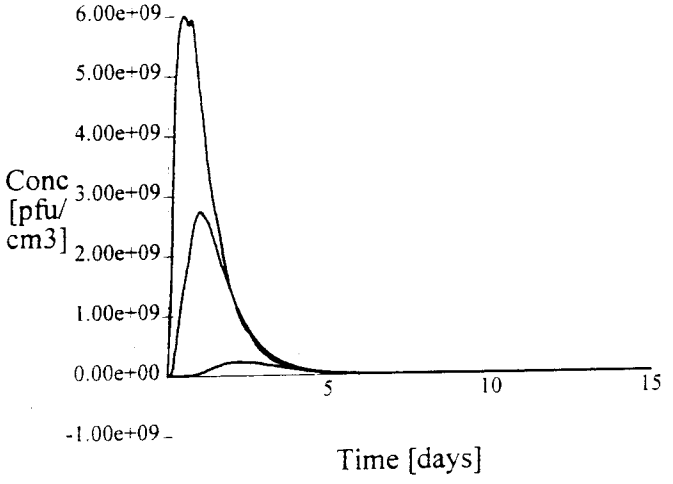


# Observation Nodes: Concentrations

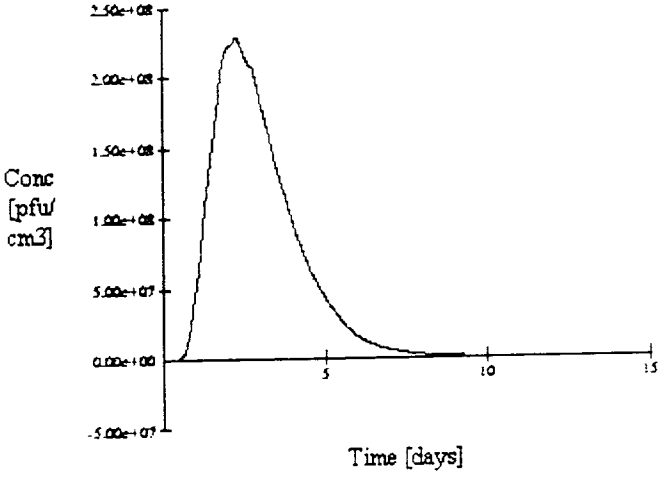

# Cumulative Variable Boundary Solute Flux

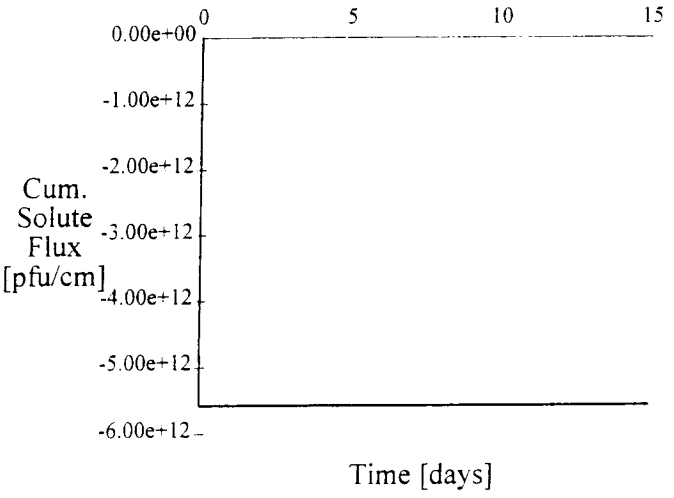


# Free or Deep Drainage Boundary Solute Flux

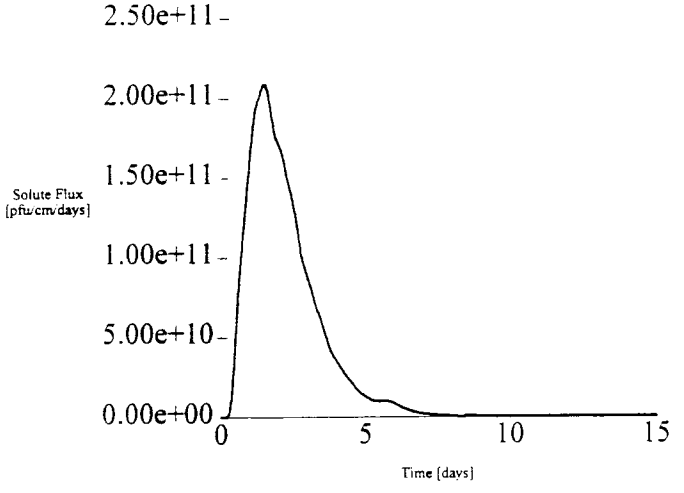

# Constant Boundary Solute Flux

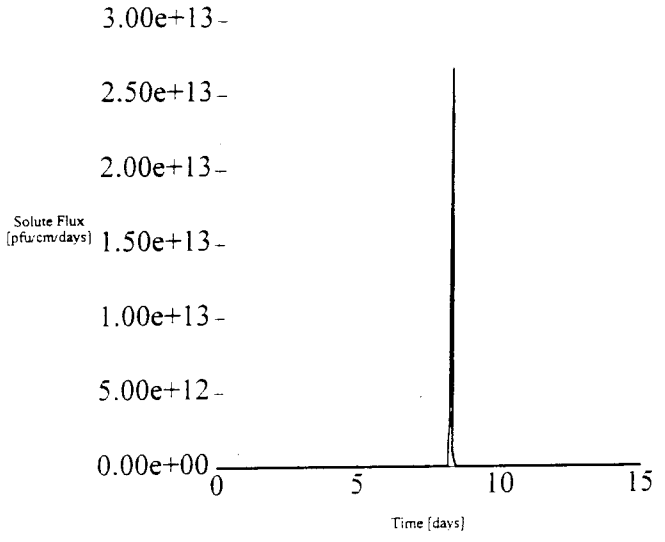


# Seepage Face Solute Flux

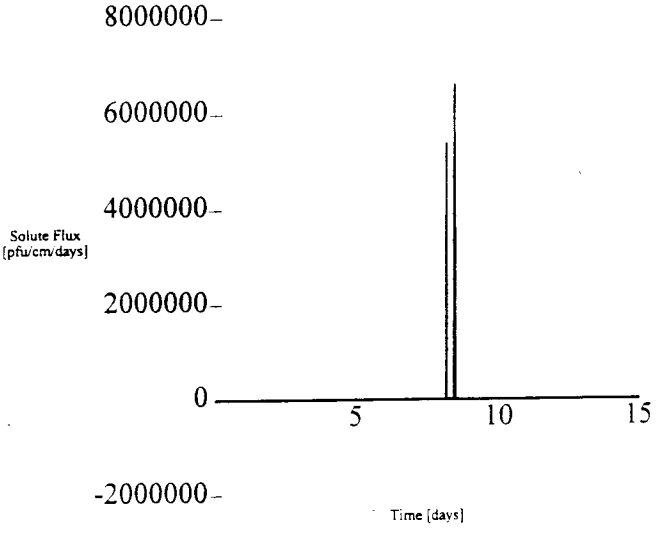

# Observation Nodes: Pressure Heads

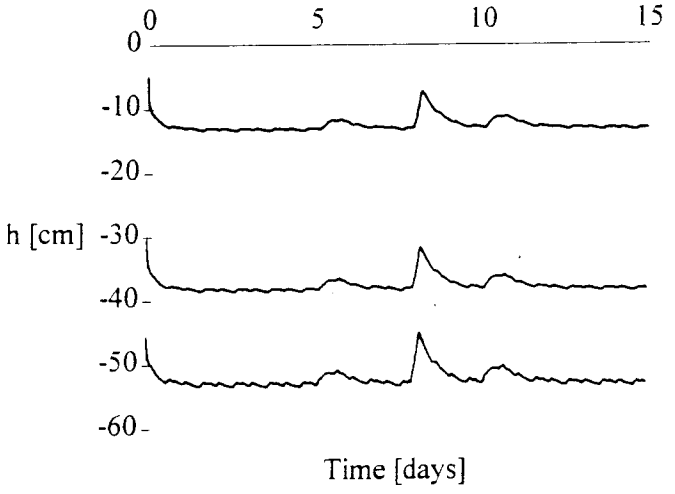


# Observation Nodes: Water Contents

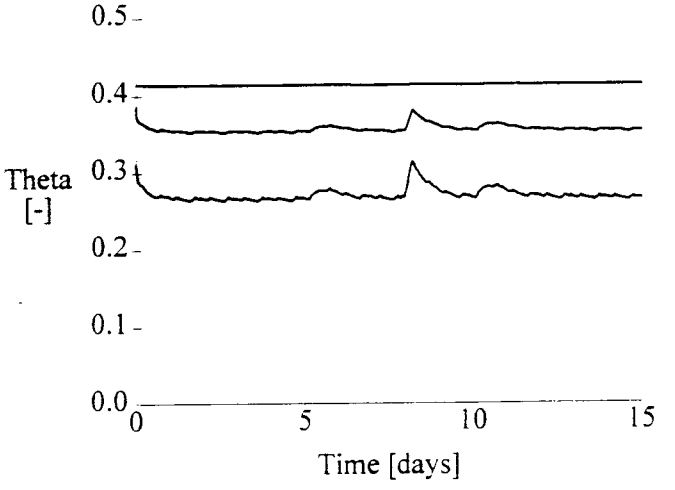

# Observation Nodes: Concentrations

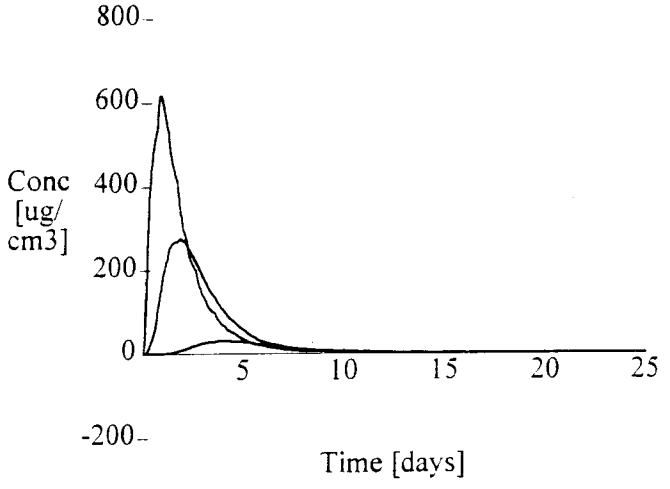


# Observation Nodes: Concentrations

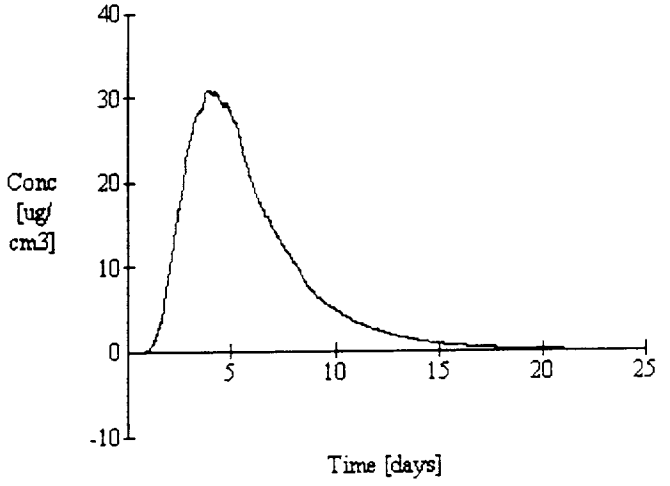

# Cumulative Variable Boundary Solute Flux

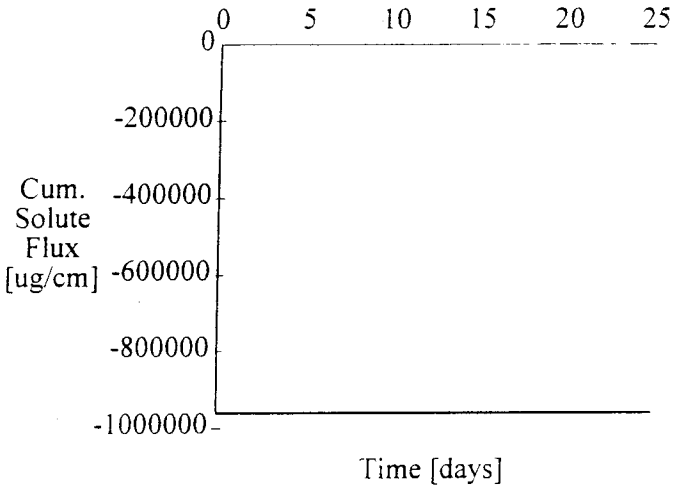


# Free or Deep Drainage Boundary Solute Flux

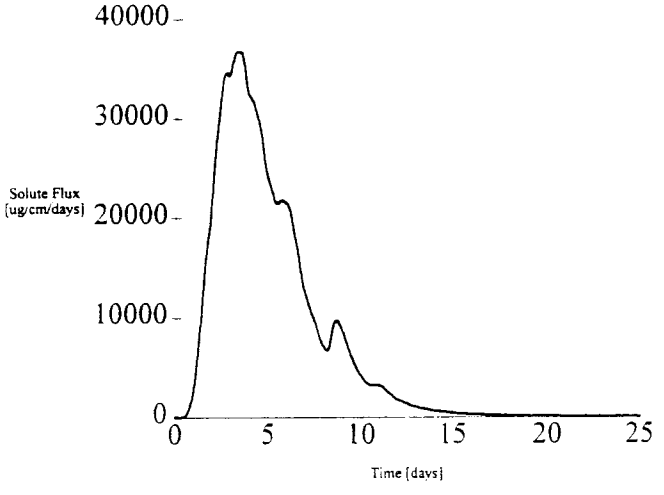

# Observation Nodes: Concentrations

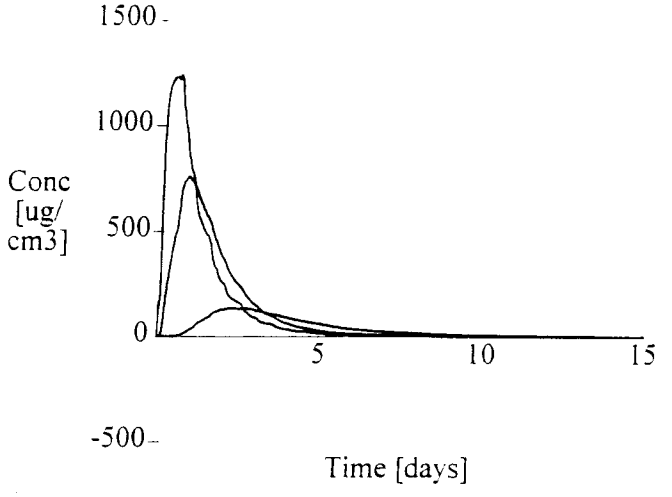


# Observation Nodes: Concentrations

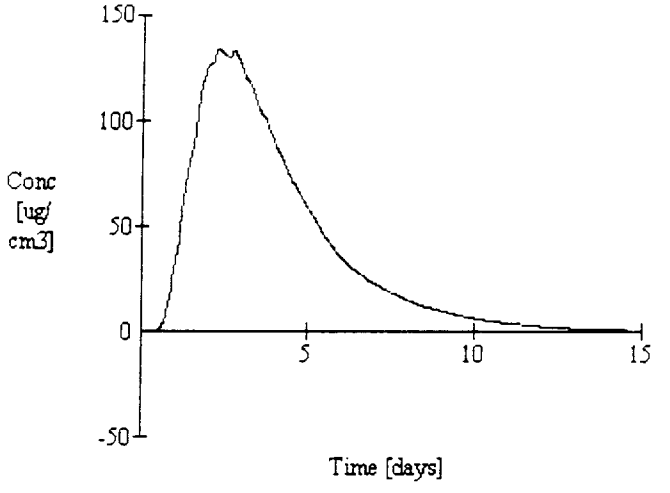

# Cumulative Variable Boundary Solute Flux

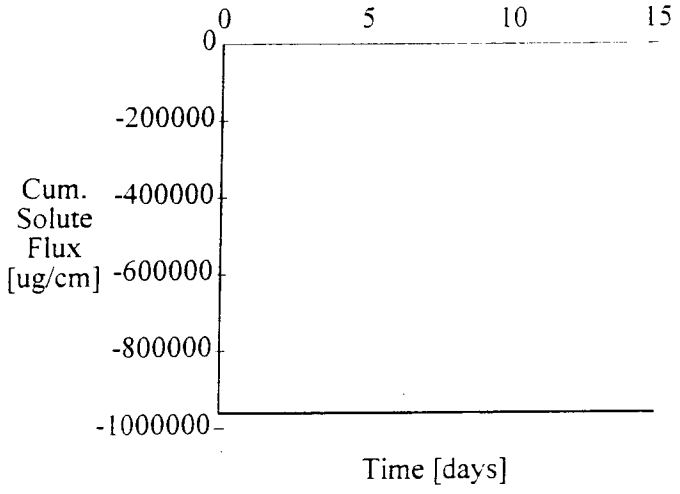


# Free or Deep Drainage Boundary Solute Flux

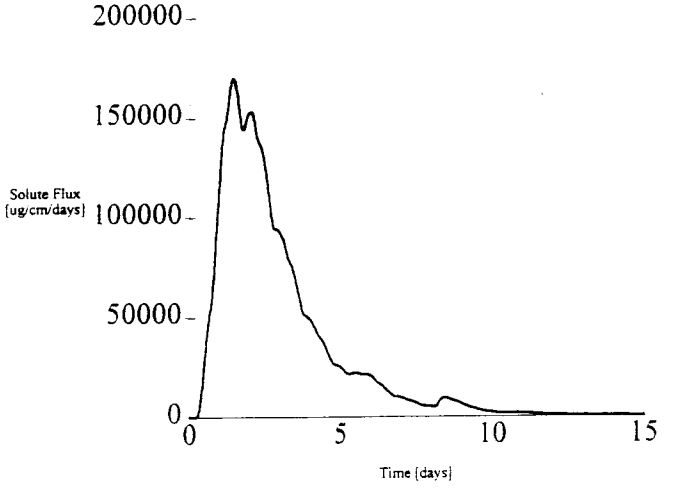

# Constant Boundary Solute Flux

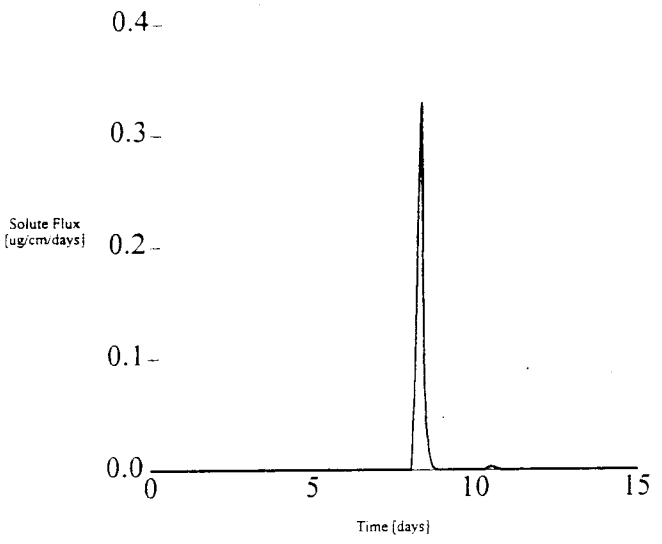


# Seepage Face Solute Flux

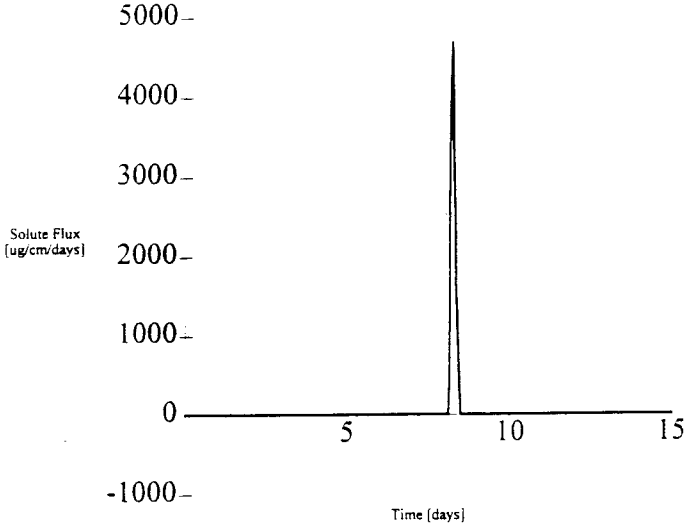

# Observation Nodes: Concentrations

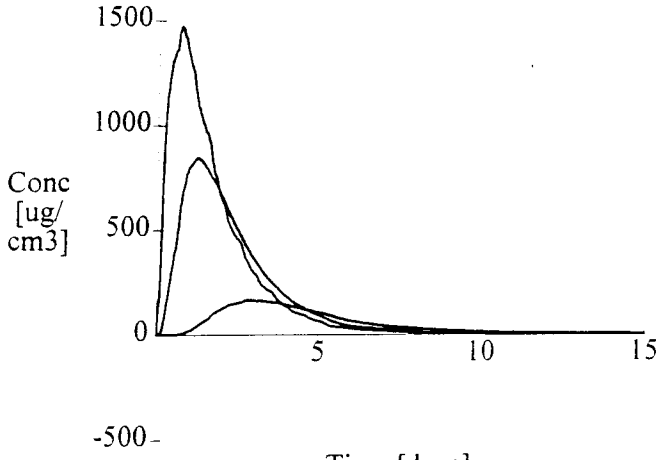


# Observation Nodes: Concentrations

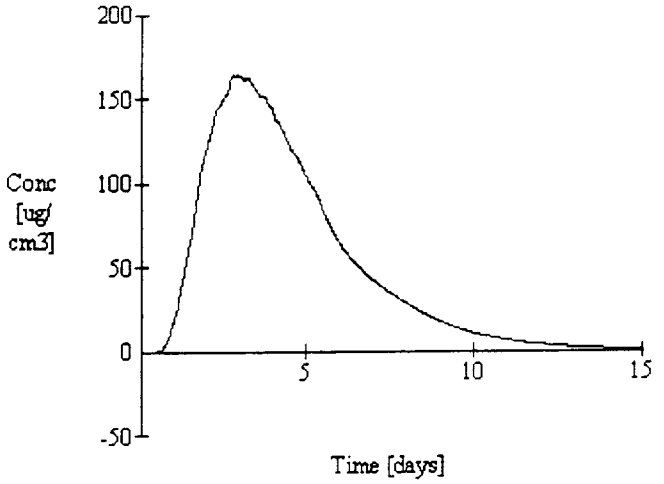

# Cumulative Variable Boundary Solute Flux

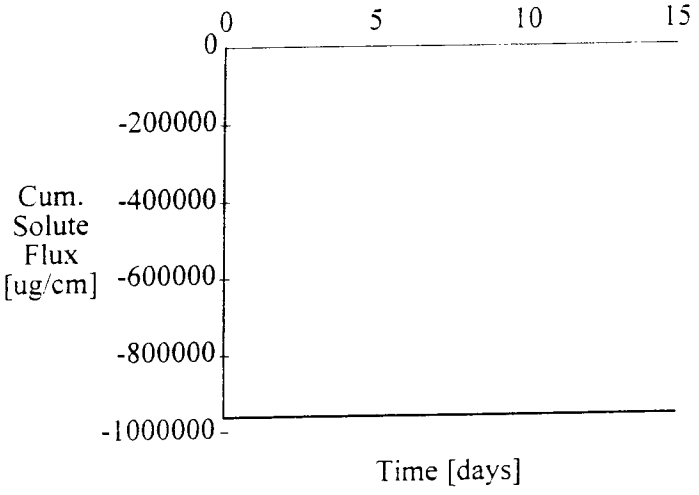


# Free or Deep Drainage Boundary Solute Flux

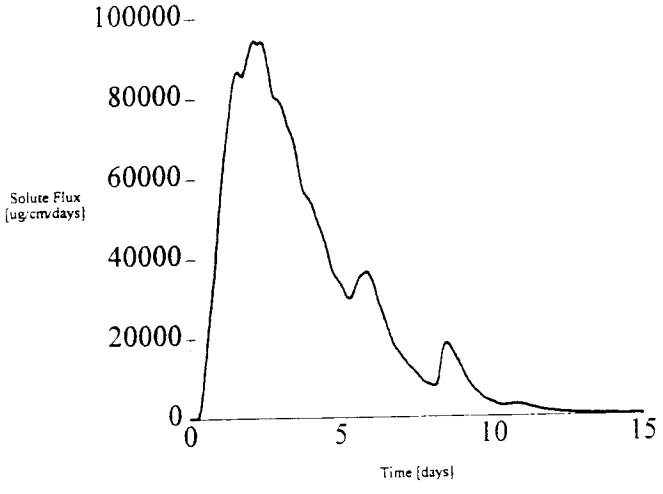

# Constant Boundary Solute Flux

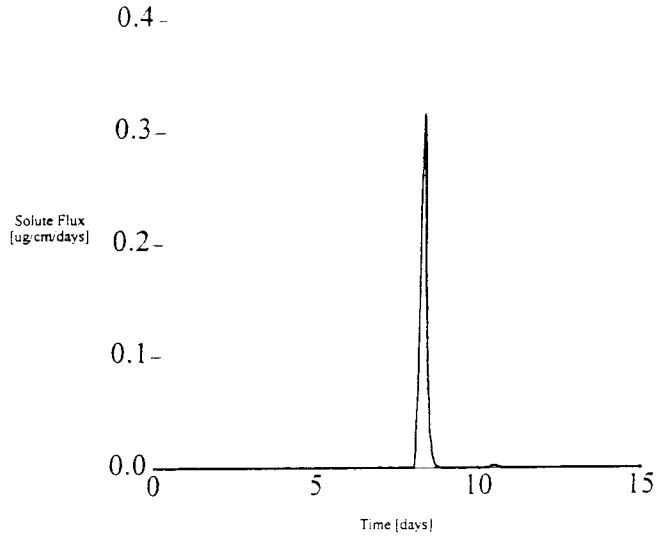


# Seepage Face Solute Flux

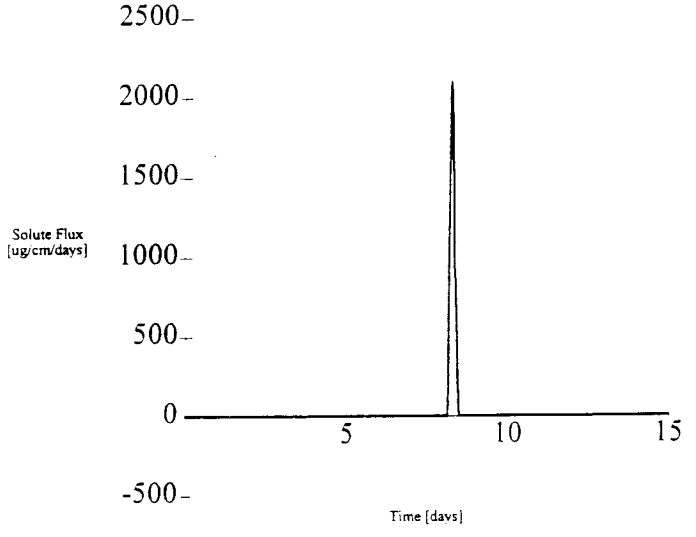

# Observation Nodes: Concentrations

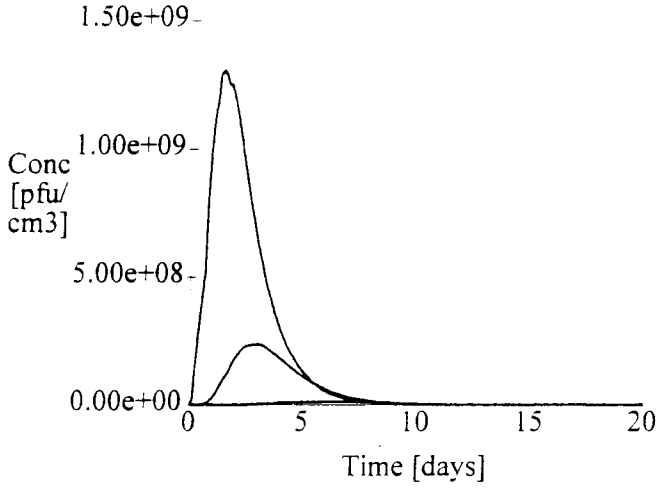


# Observation Nodes: Concentrations

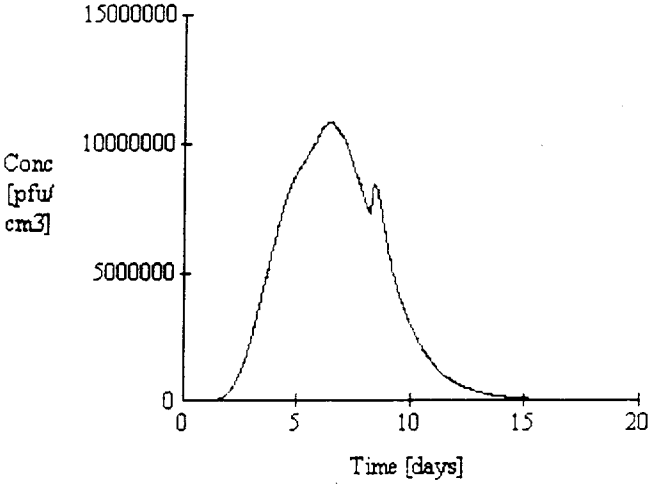


Loam

# Cumulative Variable Boundary Solute Flux

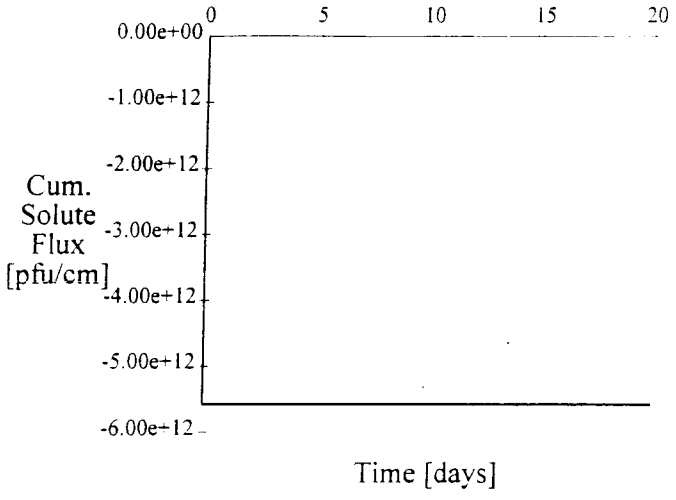


# Free or Deep Drainage Boundary Solute Flux

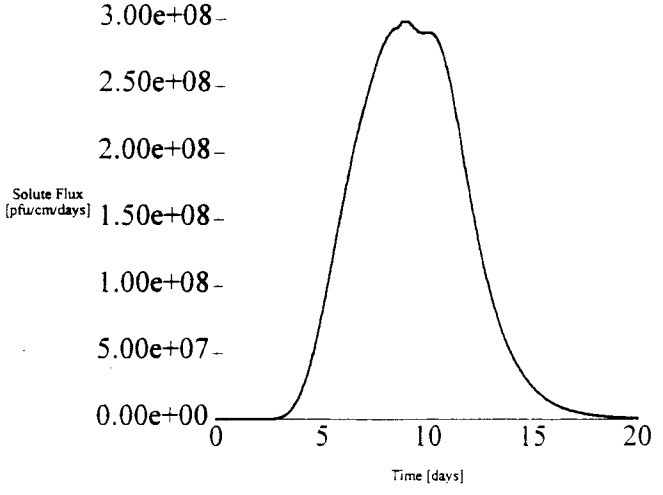

# Constant Boundary Solute Flux

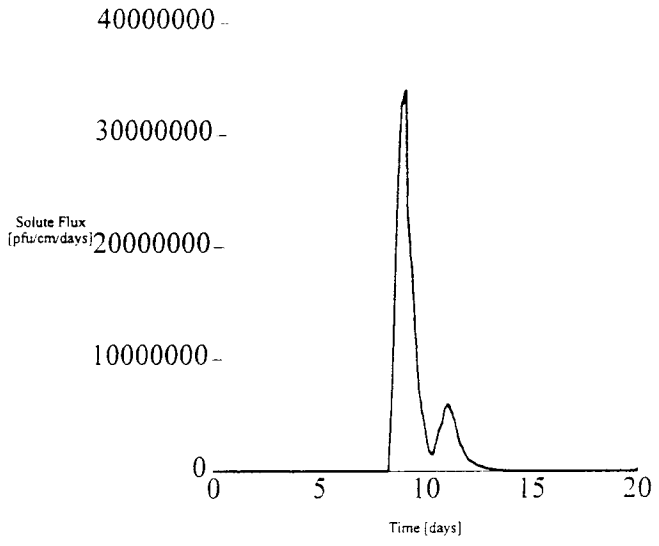


# Seepage Face Solute Flux

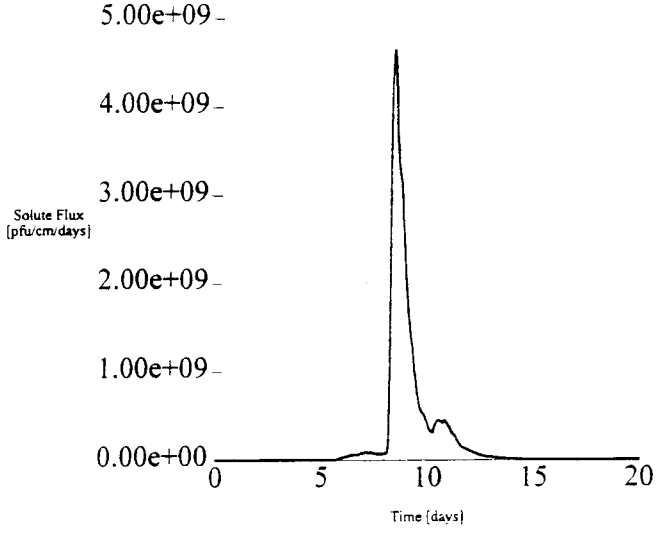

# Cumulative First-Order Reactions

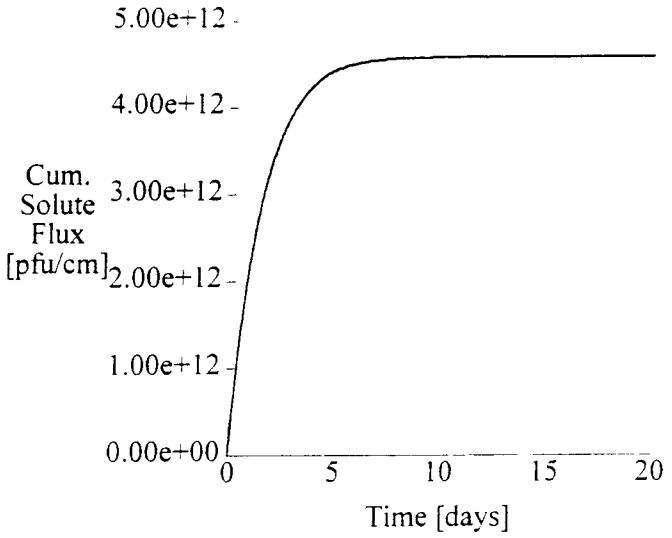

# Observation Nodes: Concentrations

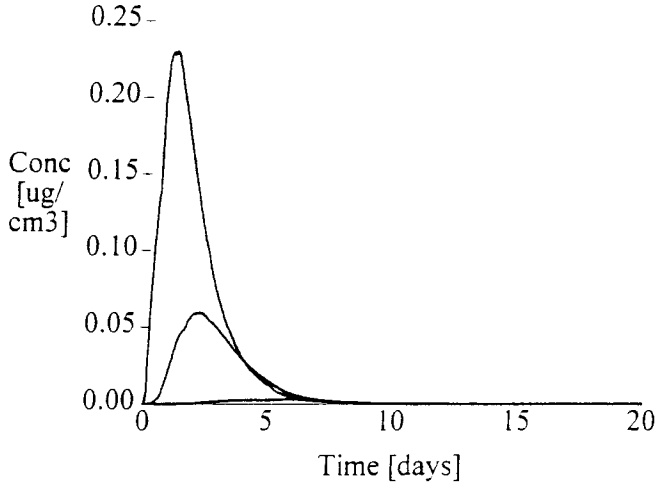


# Observation Nodes: Concentrations

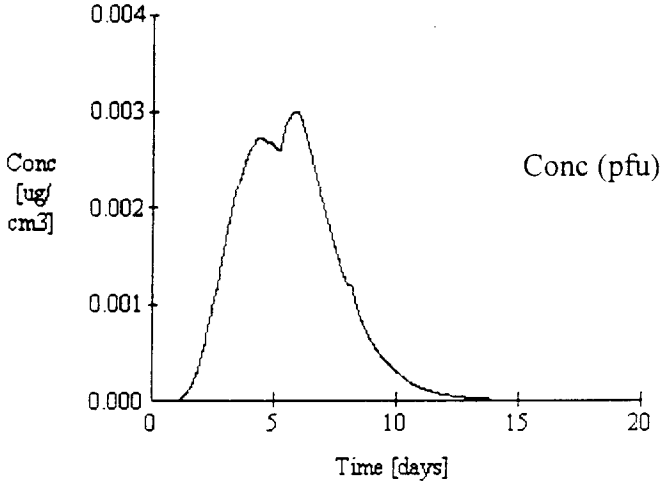


Conc (pfu) = 1E10*curve

# Cumulative Variable Boundary Solute Flux

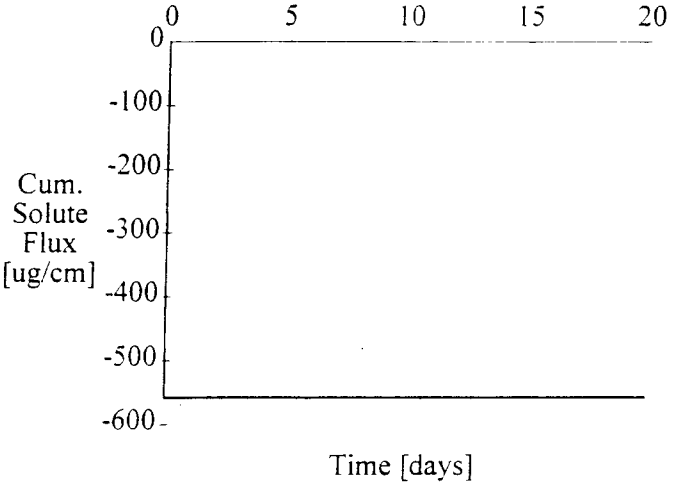


# Free or Deep Drainage Boundary Solute Flux

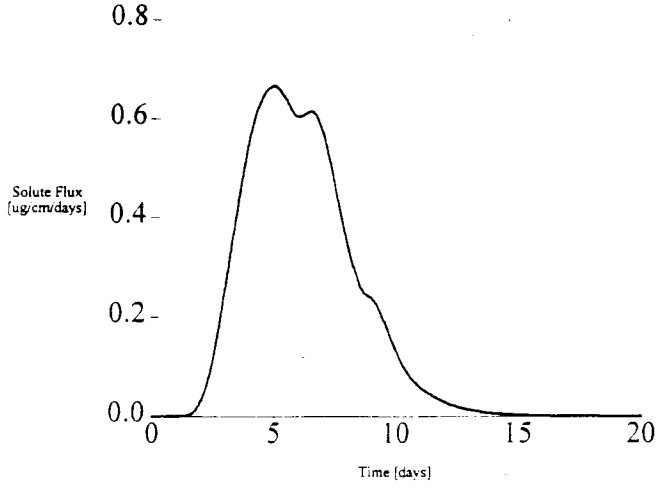

# Constant Boundary Solute Flux

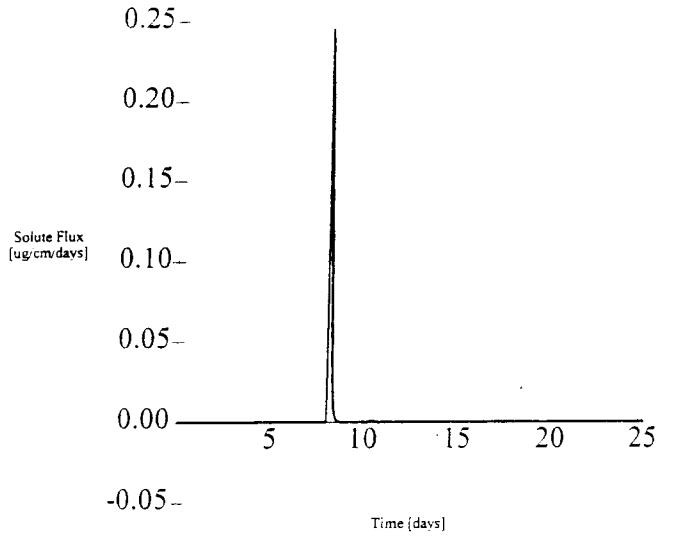


# Seepage Face Solute Flux

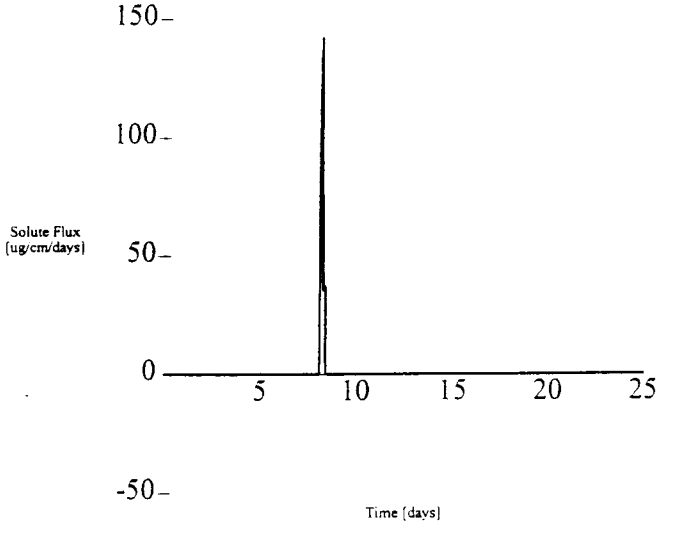

# Observation Nodes: Concentrations

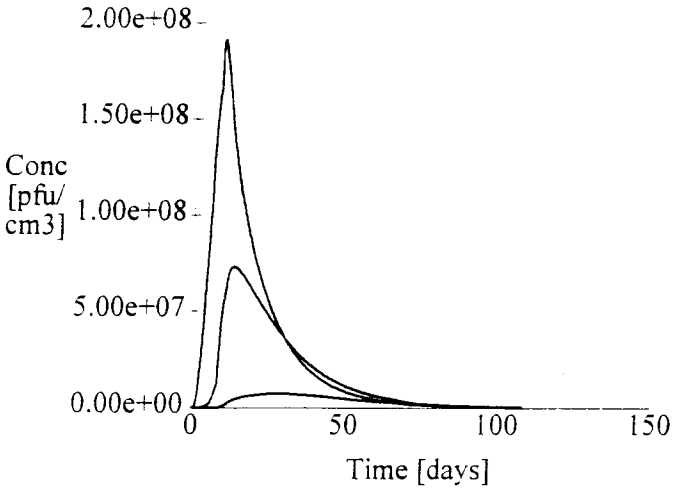


# Observation Nodes: Concentrations

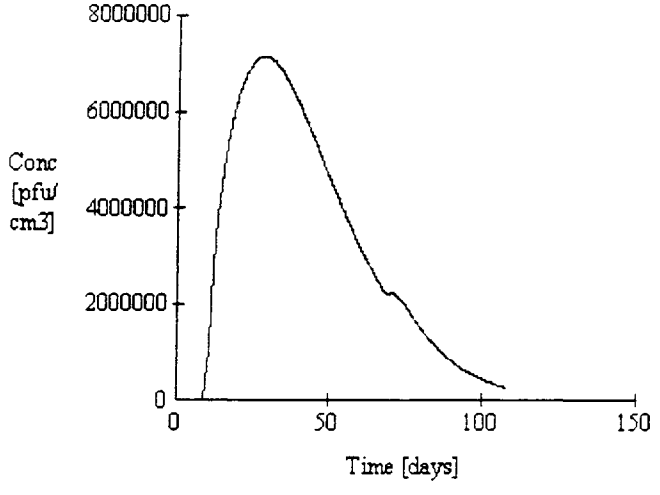

# Cumulative Variable Boundary Solute Flux

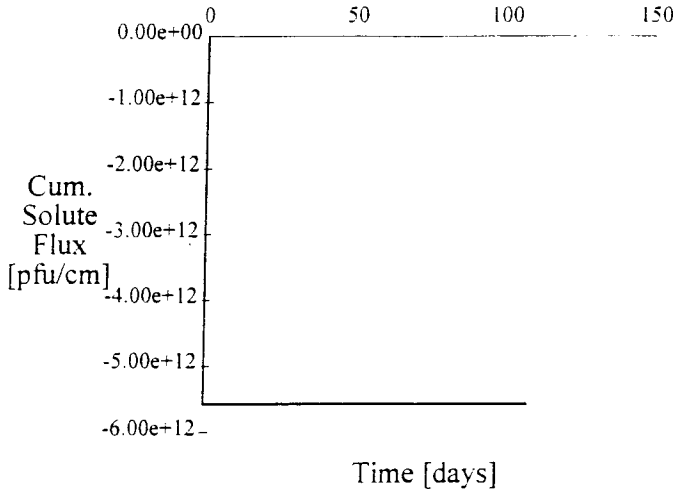


# Free or Deep Drainage Boundary Solute Flux

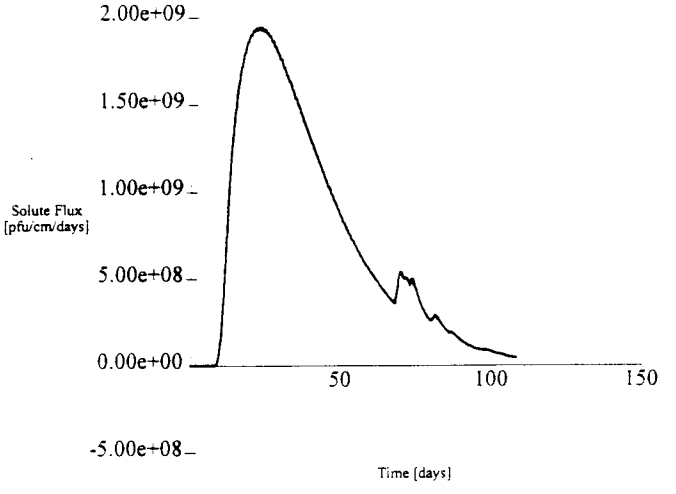

# Constant Boundary Solute Flux

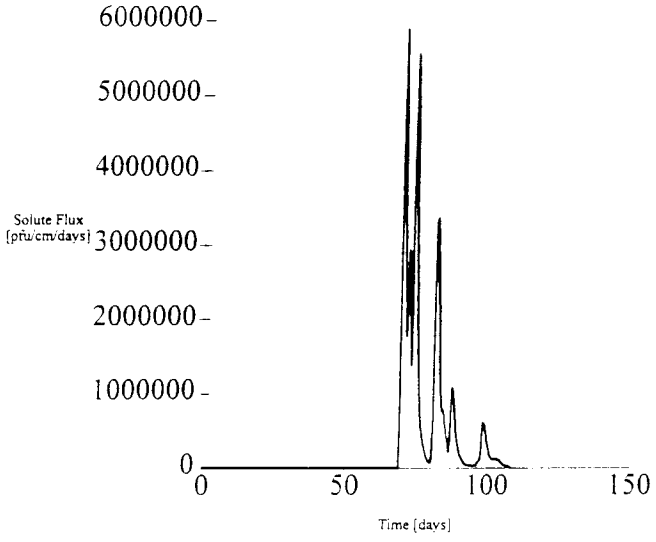


# Seepage Face Solute Flux

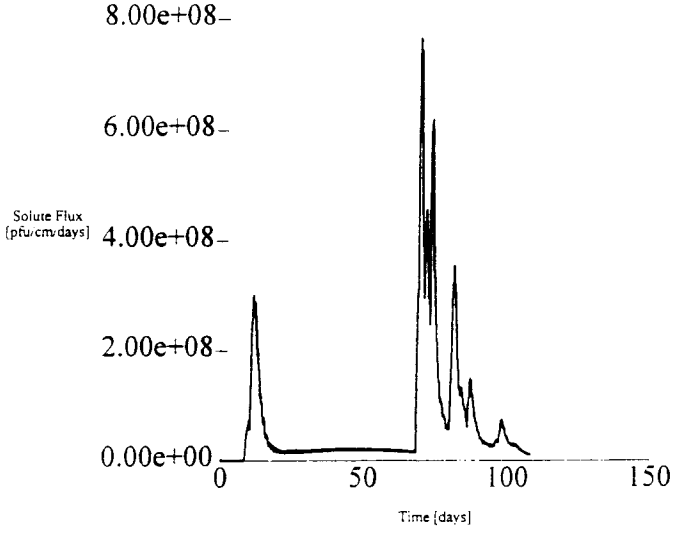

# Observation Nodes: Pressure Heads

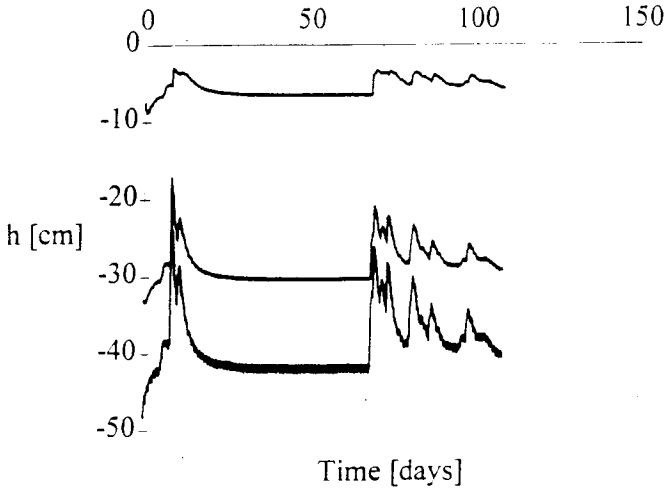


# Observation Nodes: Water Contents

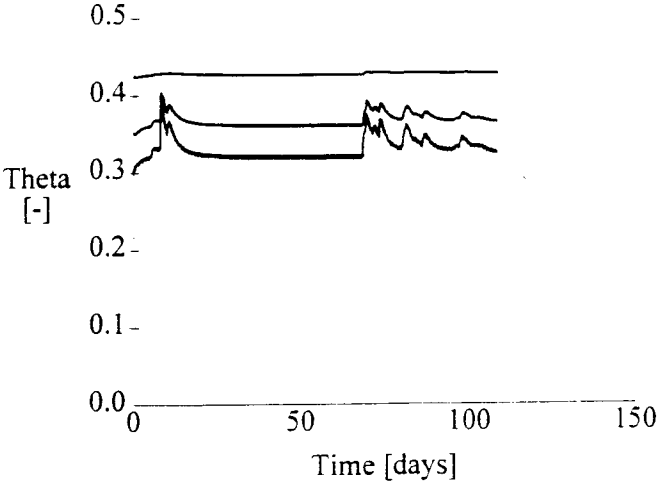

# Observation Nodes: Concentrations

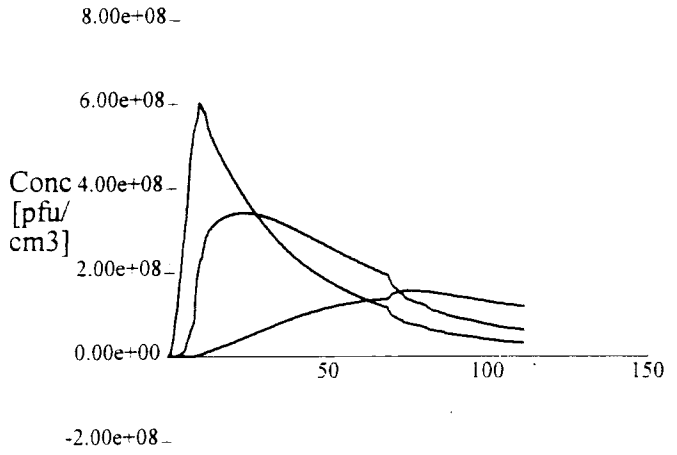


# Observation Nodes: Concentrations

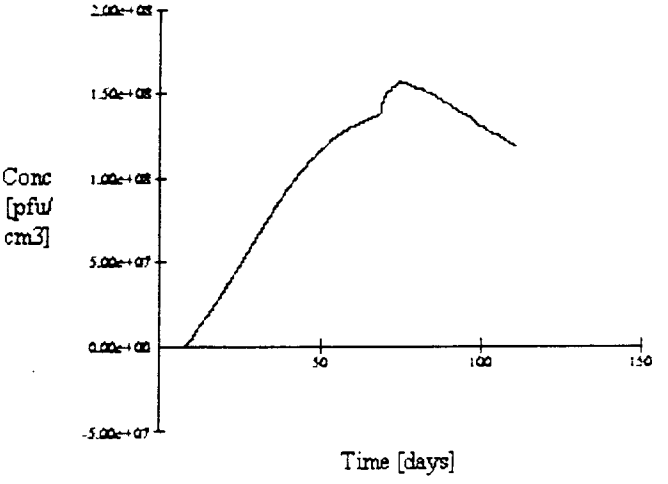

# Cumulative Variable Boundary Solute Flux

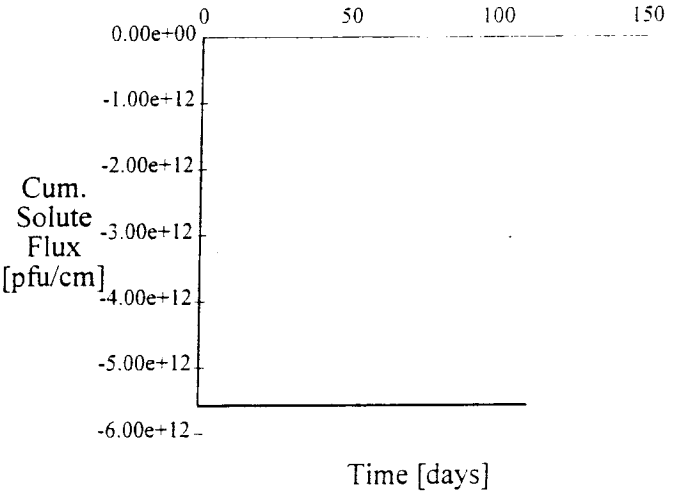


# Free or Deep Drainage Boundary Solute Flux

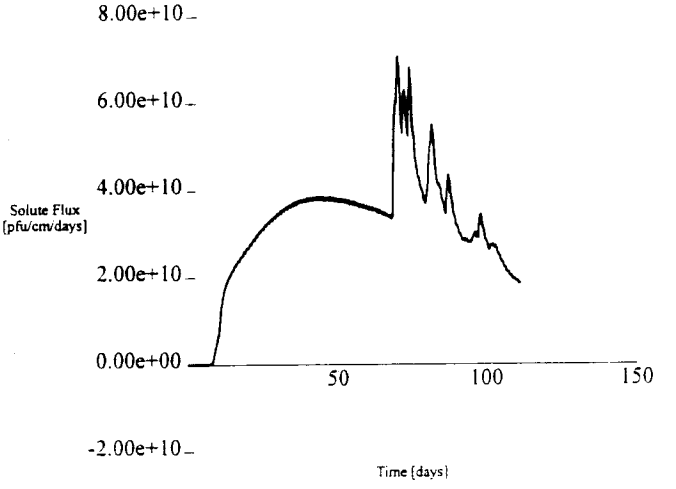

# Constant Boundary Solute Flux

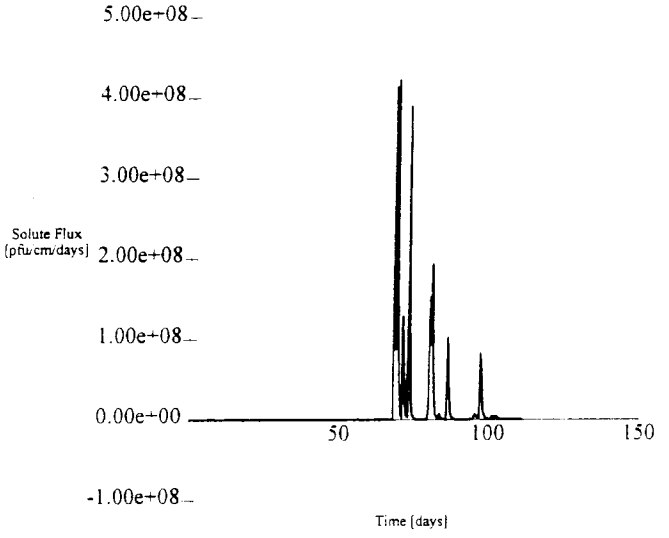


# Seepage Face Solute Flux

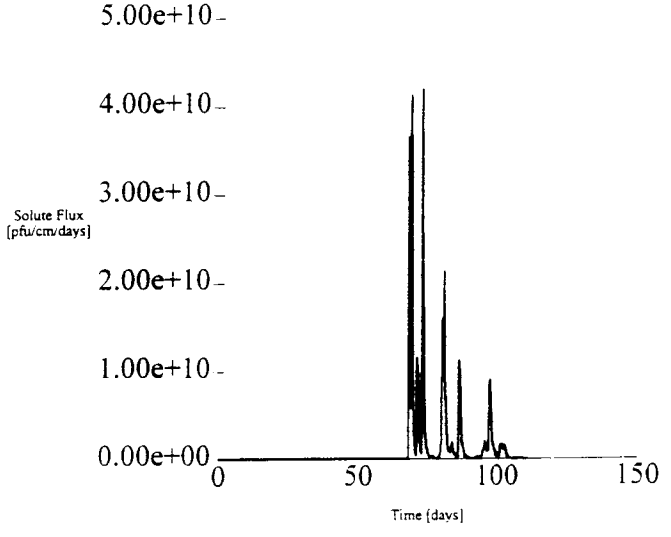

# Observation Nodes: Pressure Heads

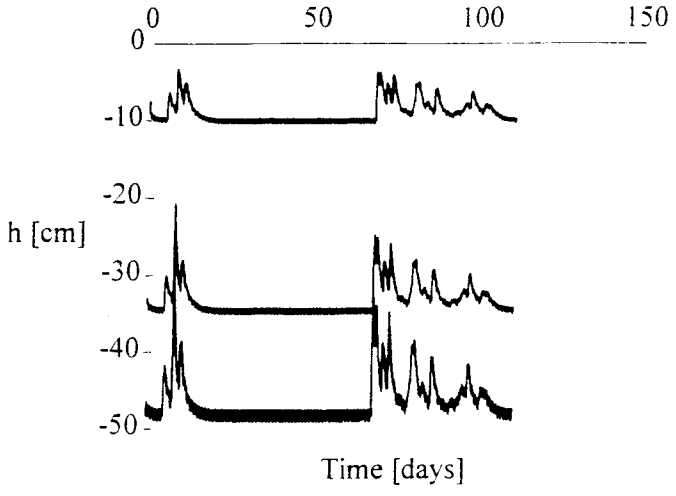


# Observation Nodes: Water Contents

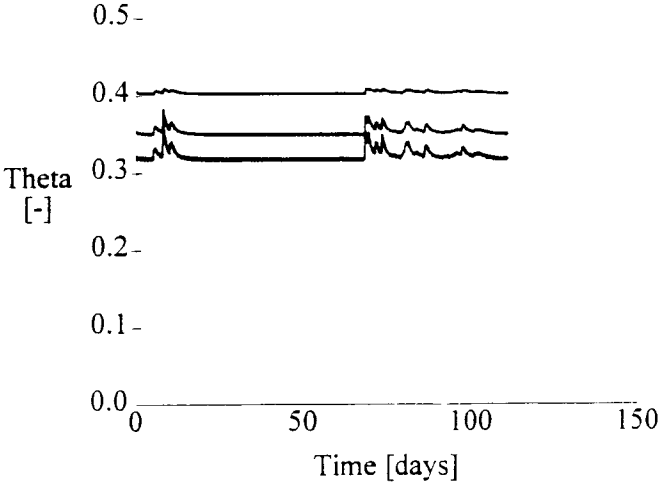

# Observation Nodes: Concentrations

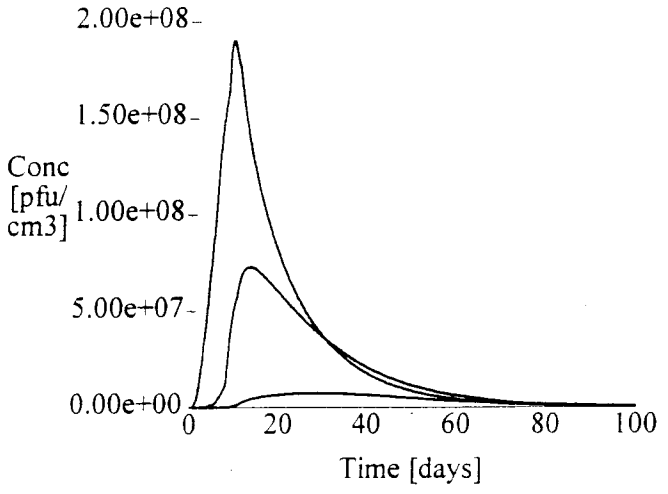


# Observation Nodes: Concentrations

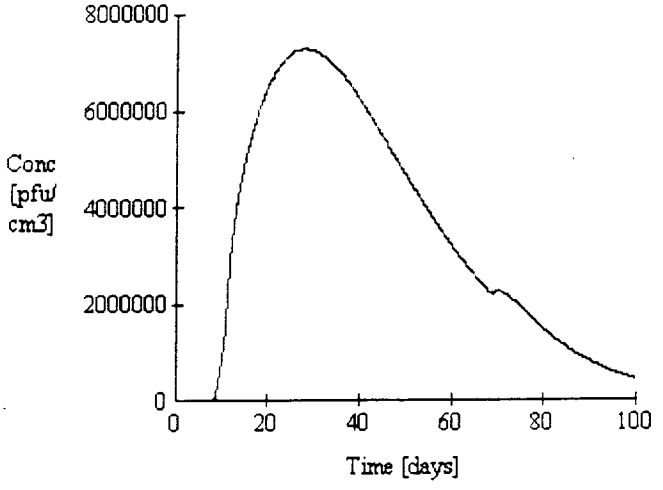

# Cumulative Variable Boundary Solute Flux

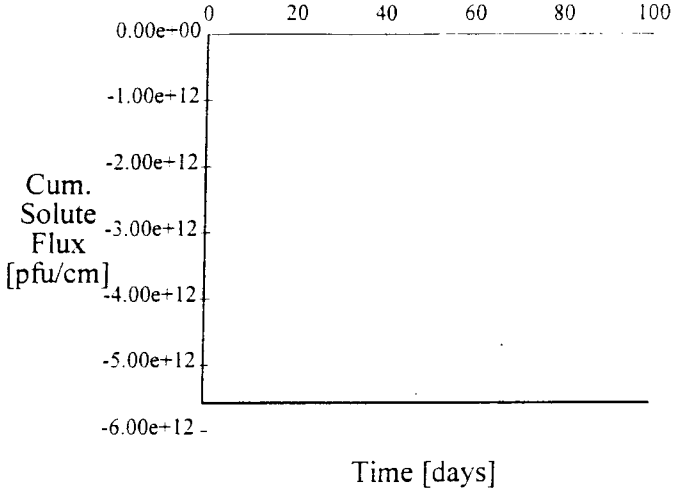


# Free or Deep Drainage Boundary Solute Flux

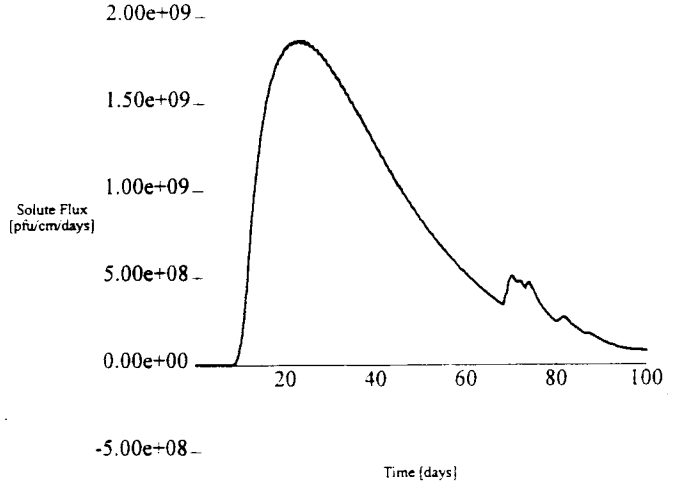

# Constant Boundary Solute Flux

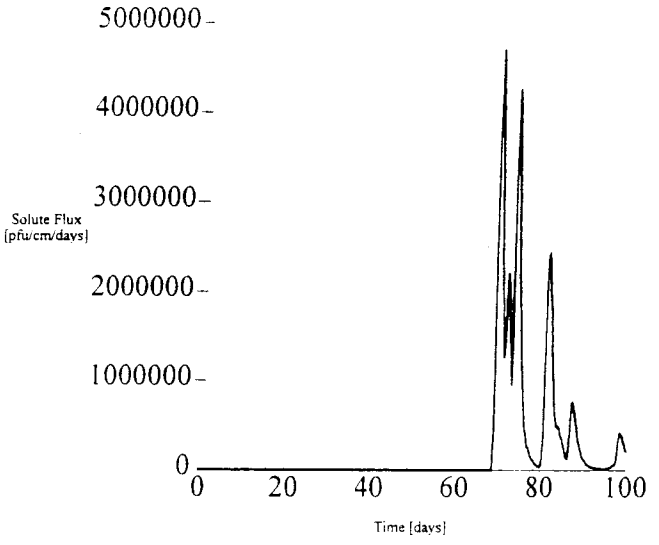


# Seepage Face Solute Flux

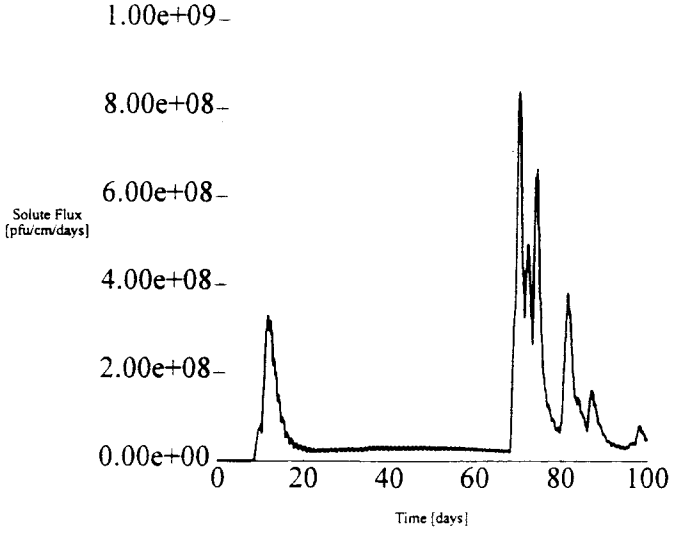

# Observation Nodes: Pressure Heads

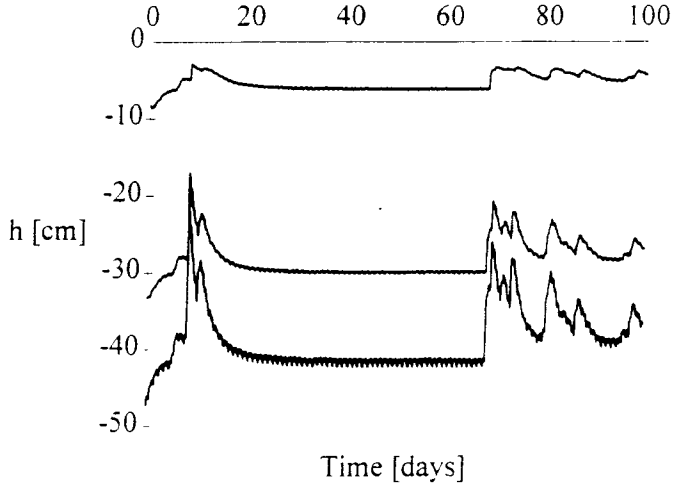


# Observation Nodes: Water Contents

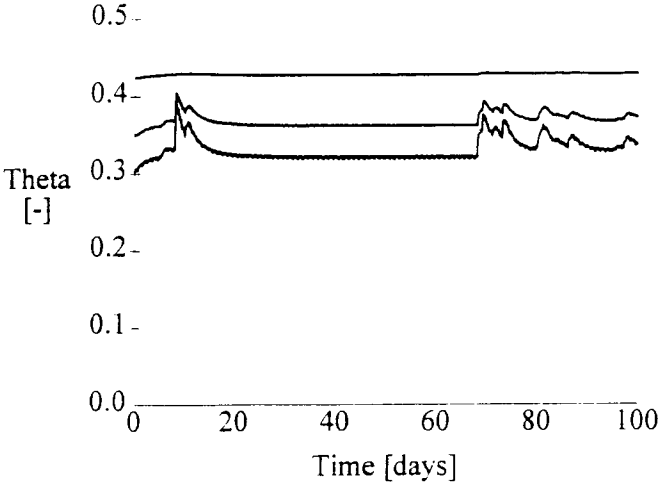

# Observation Nodes: Concentrations

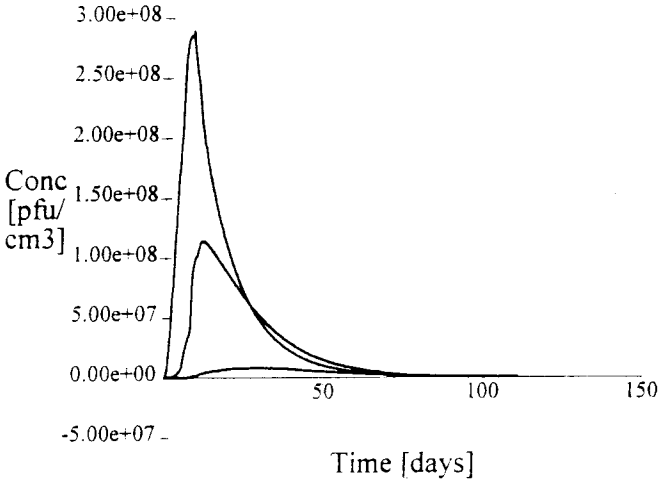


# Observation Nodes: Concentrations

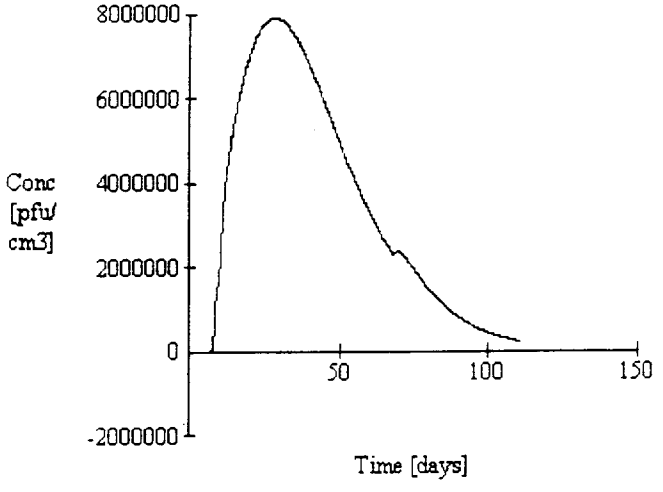

# Cumulative Variable Boundary Solute Flux

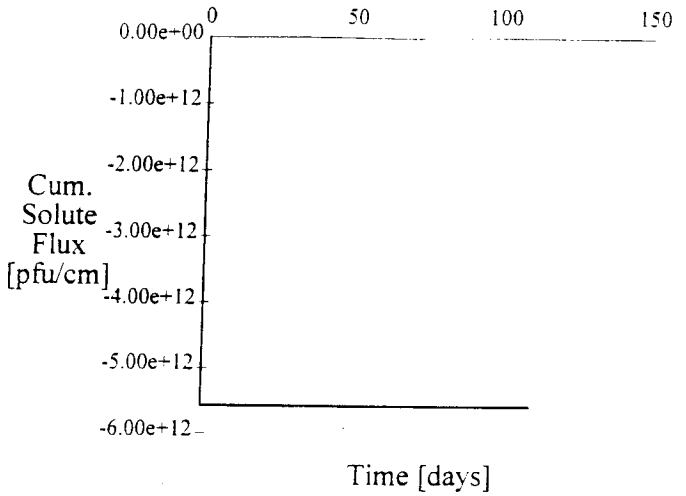


# Free or Deep Drainage Boundary Solute Flux

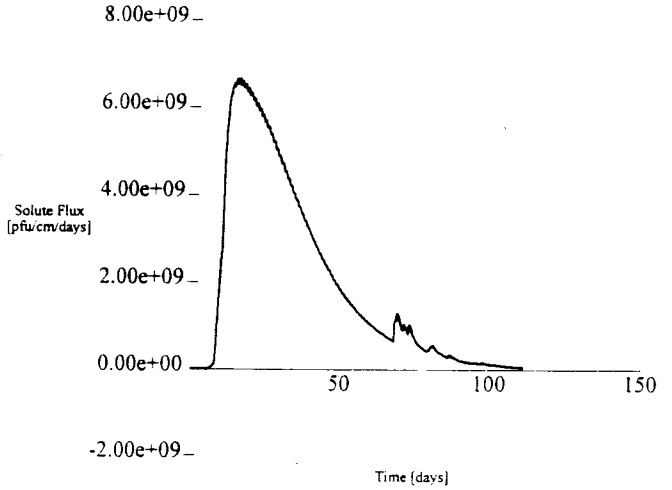

# Constant Boundary Solute Flux

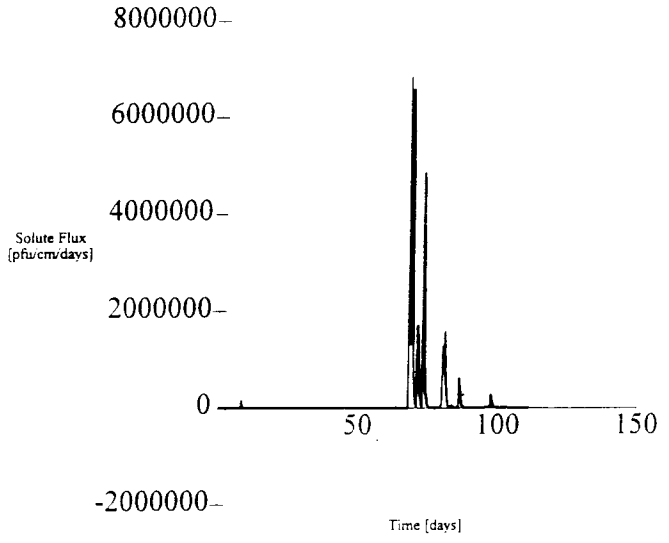


# Seepage Face Solute Flux

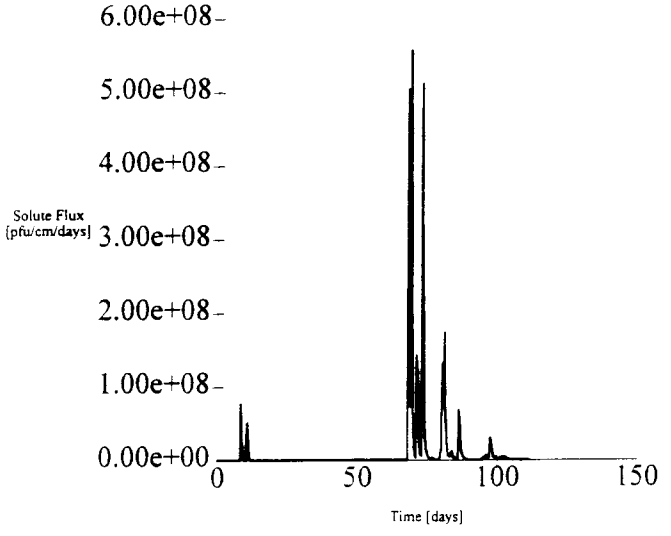

# Observation Nodes: Pressure Heads

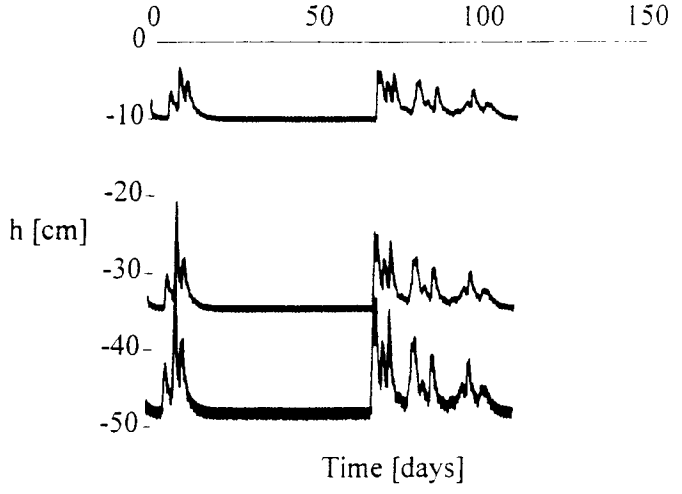


# Observation Nodes: Water Contents

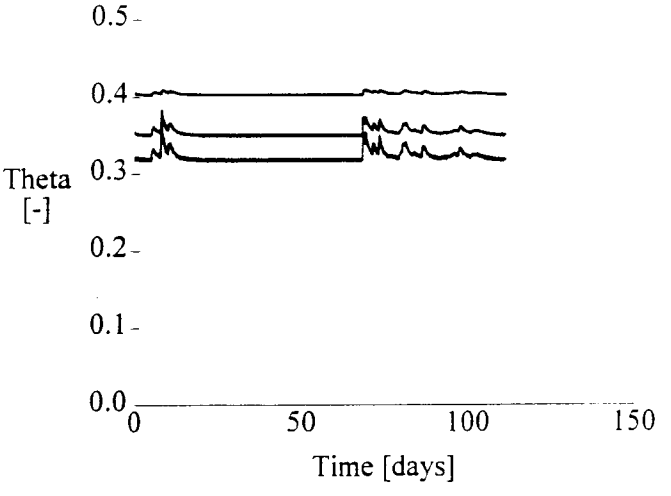

# Observation Nodes: Concentrations

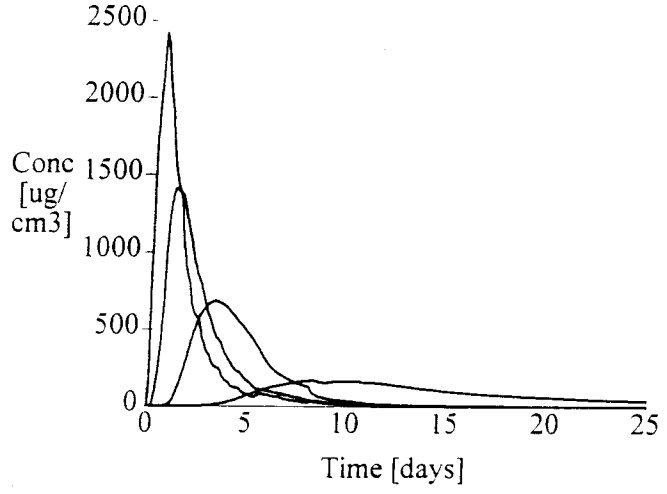


# Observation Nodes: Concentrations

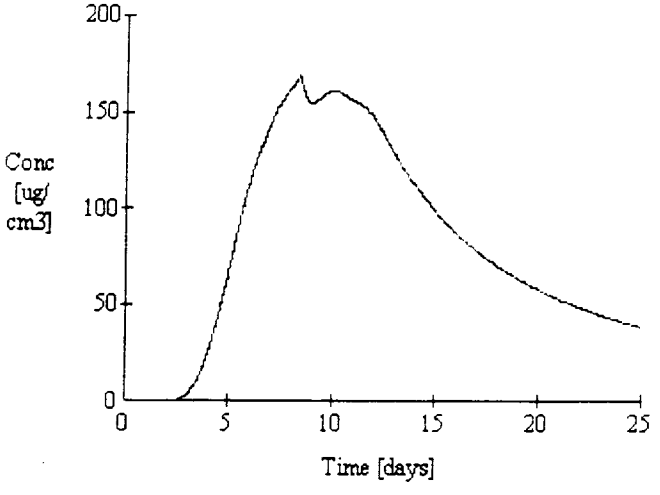

# Cumulative Variable Boundary Solute Flux

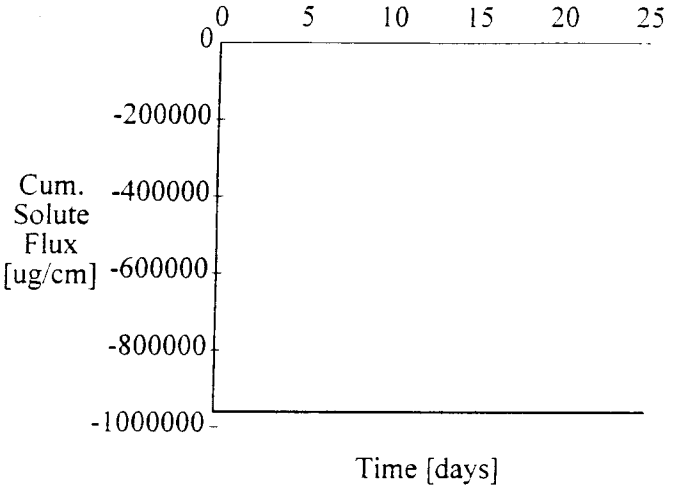


# Free or Deep Drainage Boundary Solute Flux

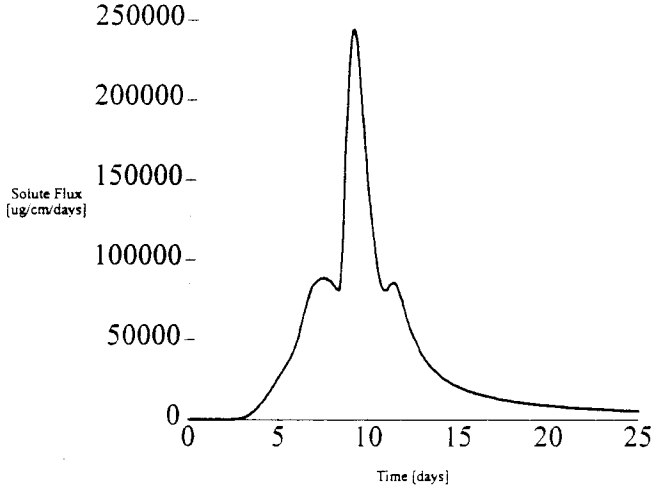

# Constant Boundary Solute Flux

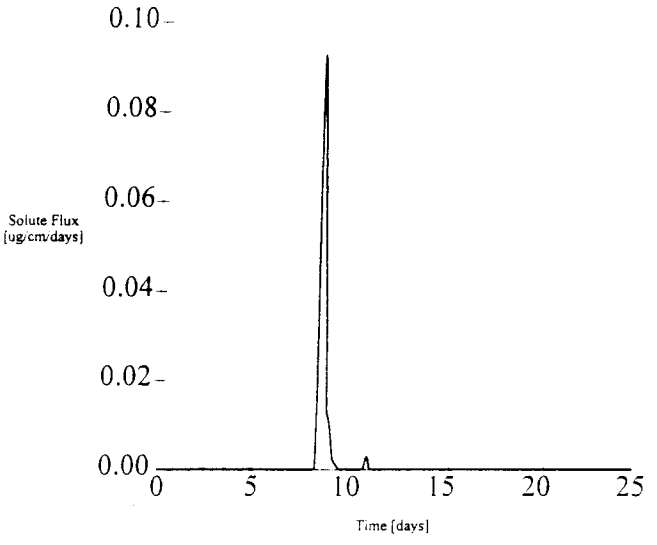


# Seepage Face Solute Flux

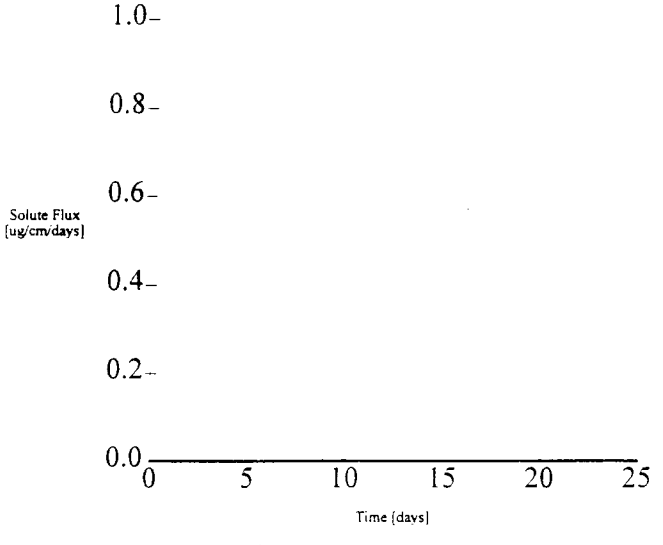

## Observation Nodes: Pressure Heads

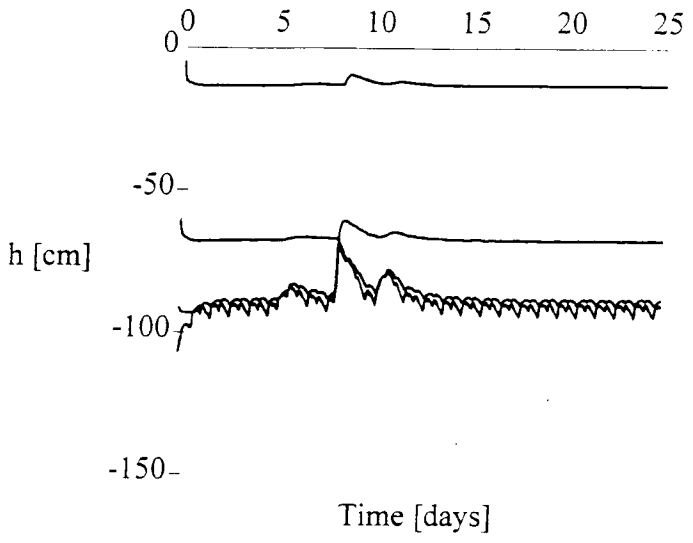


## Observation Nodes: Water Contents

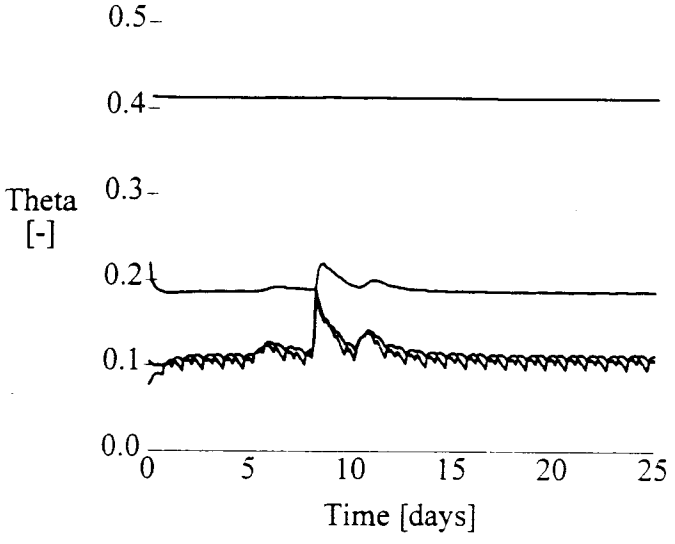

## Observation Nodes: Concentrations

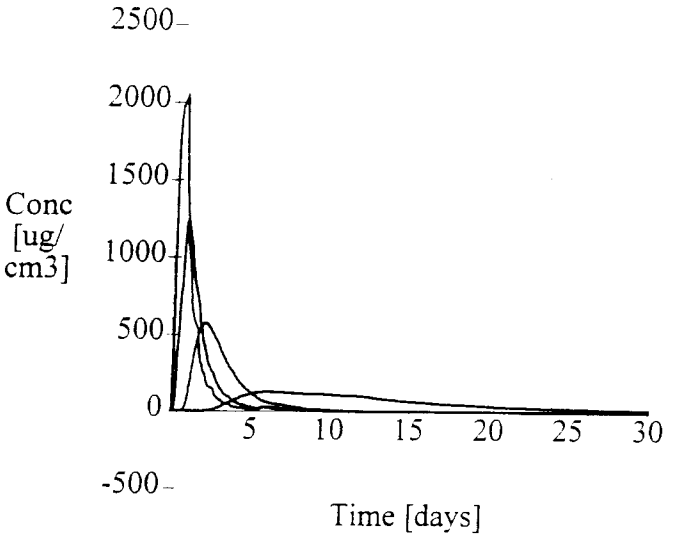


## Observation Nodes: Concentrations

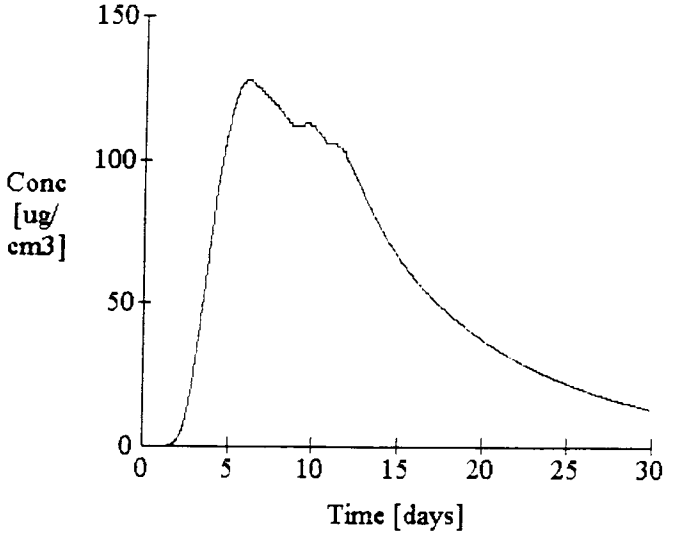

# Cumulative Variable Boundary Solute Flux

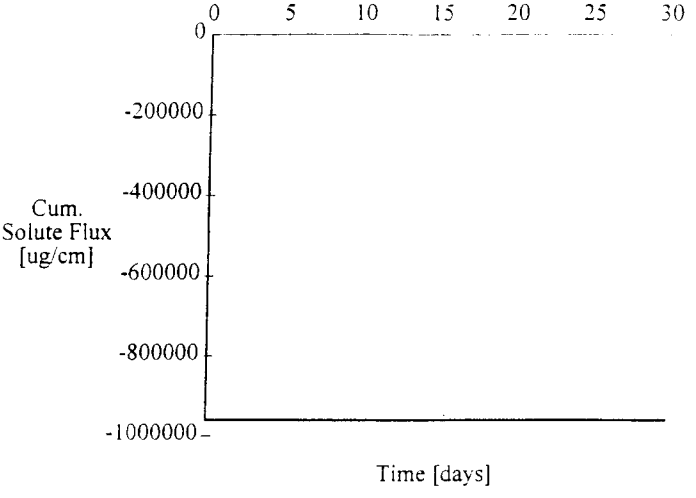


# Free or Deep Drainage Boundary Solute Flux

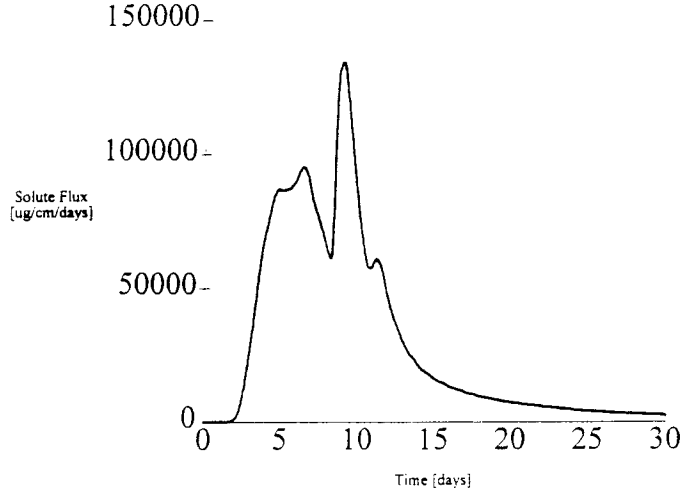

# Constant Boundary Solute Flux

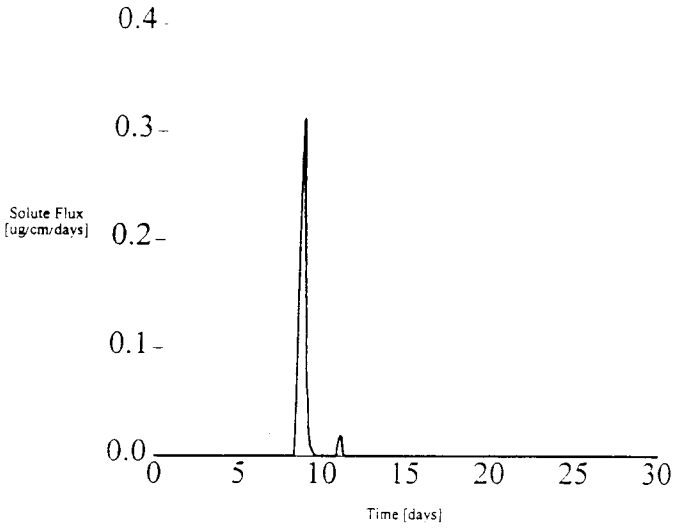


# Seepage Face Solute Flux

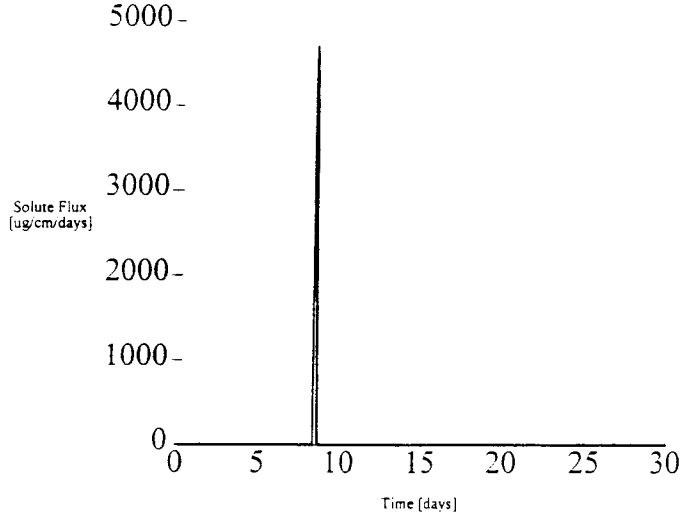

## Observation Nodes: Pressure Heads

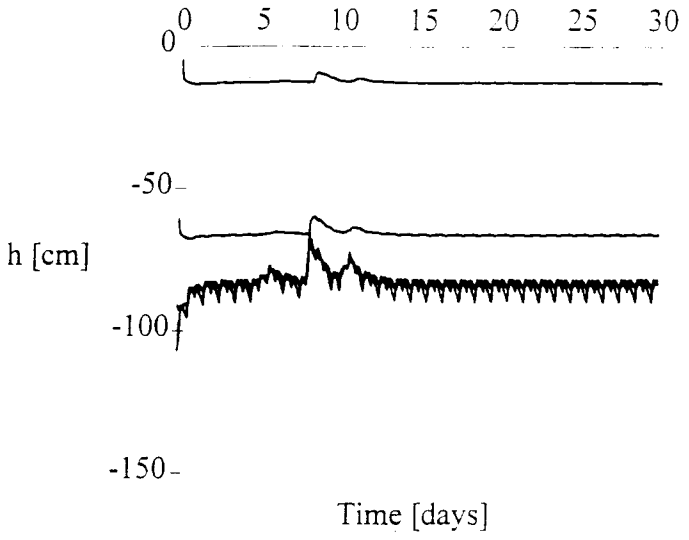


## Observation Nodes: Water Contents

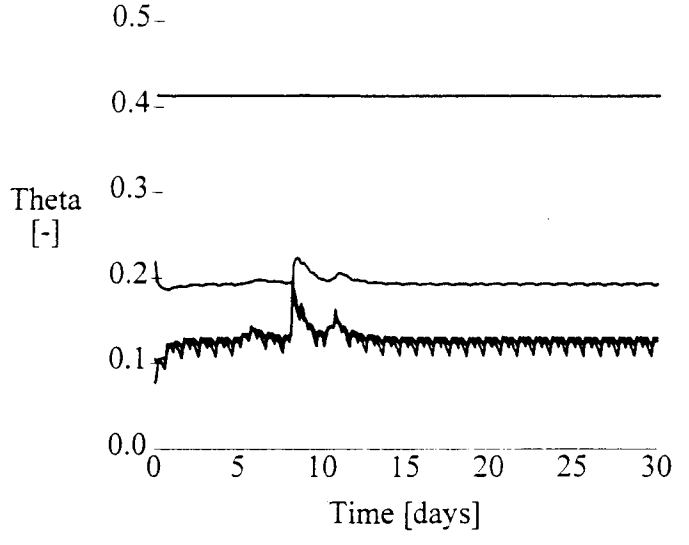

## Observation Nodes: Concentrations

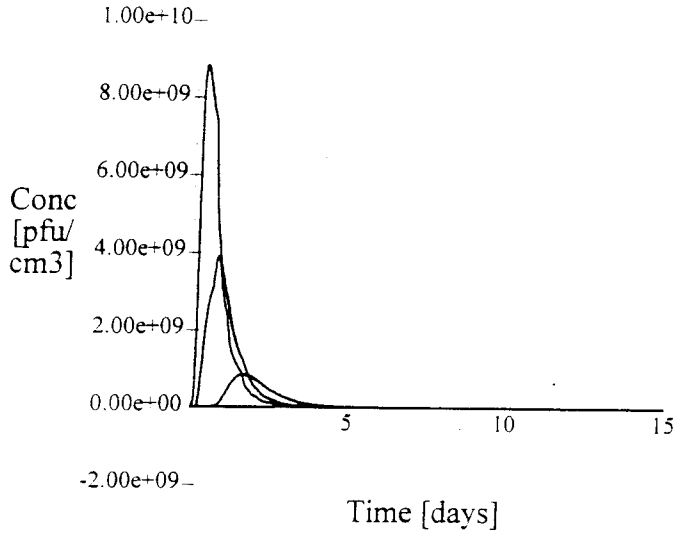


## Observation Nodes: Concentrations

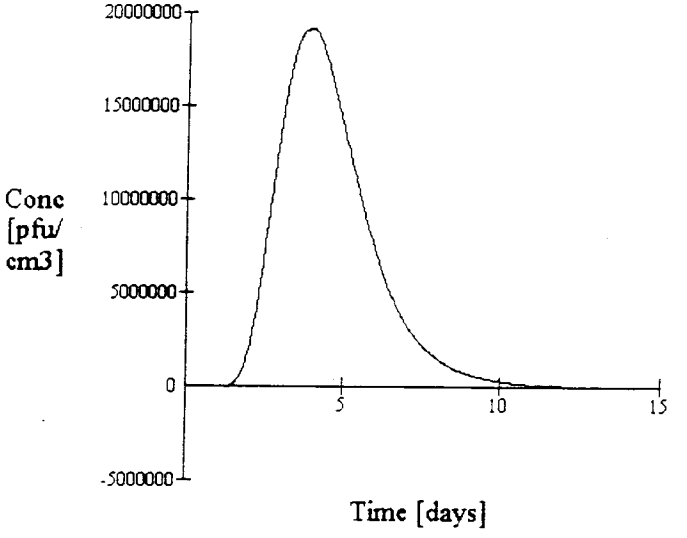

# Cumulative Variable Boundary Solute Flux

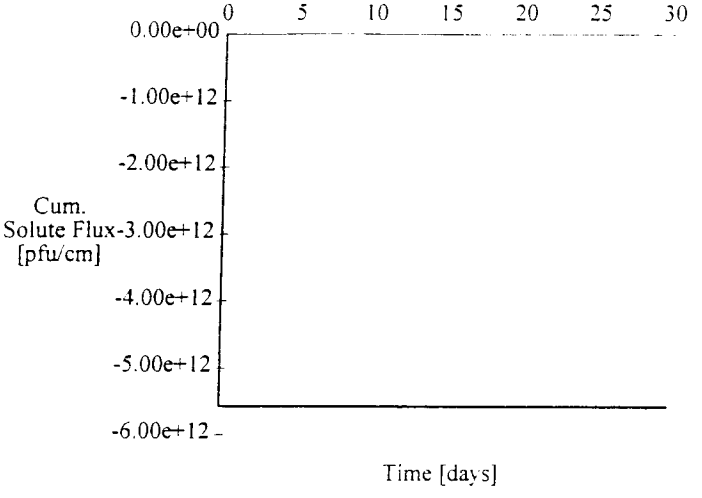


# Free or Deep Drainage Boundary Solute Flux

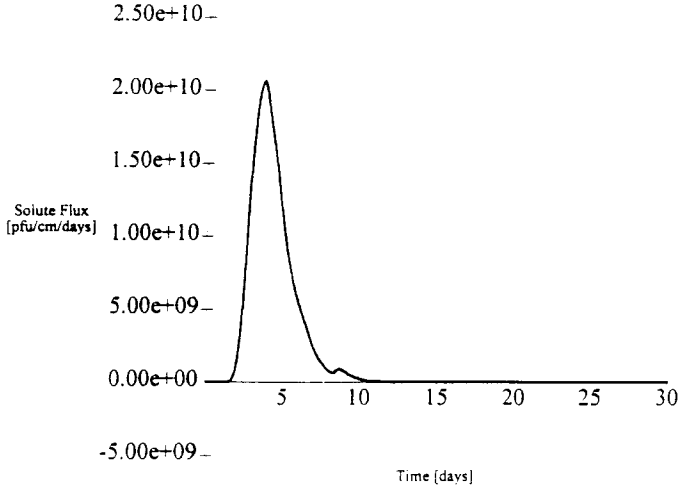

# Constant Boundary Solute Flux

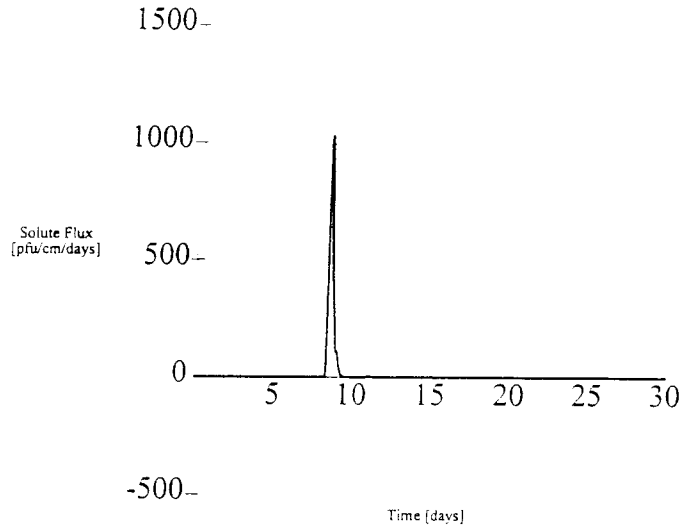


# Seepage Face Solute Flux

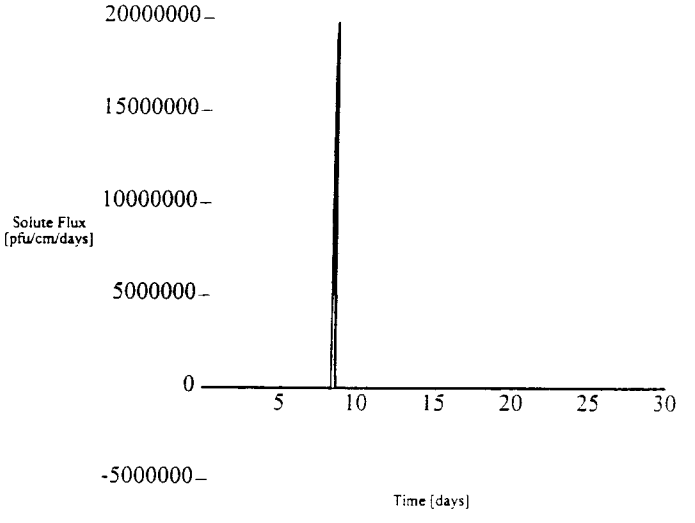

## Observation Nodes: Pressure Heads

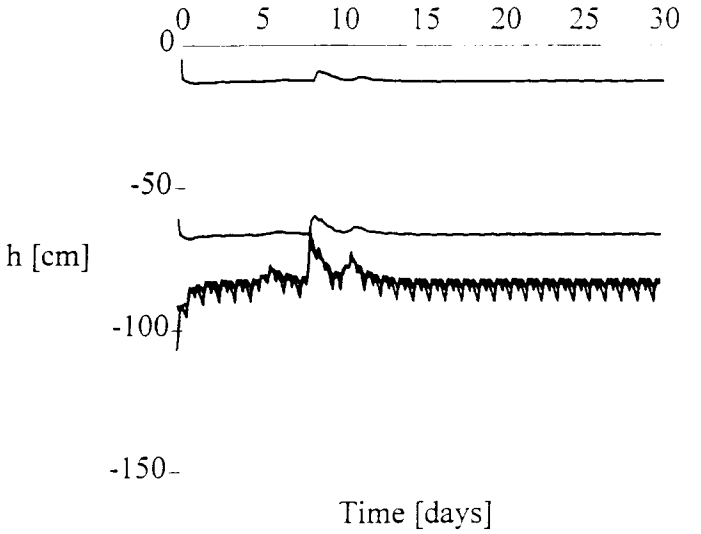


## Observation Nodes: Water Contents

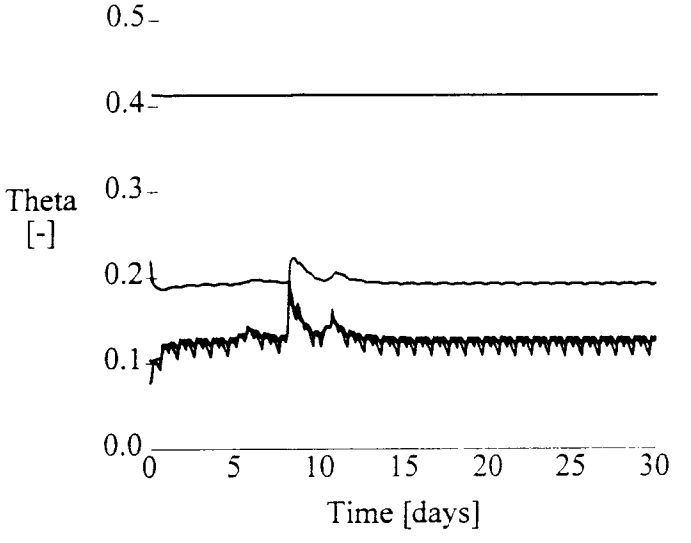

# Observation Nodes: Concentrations

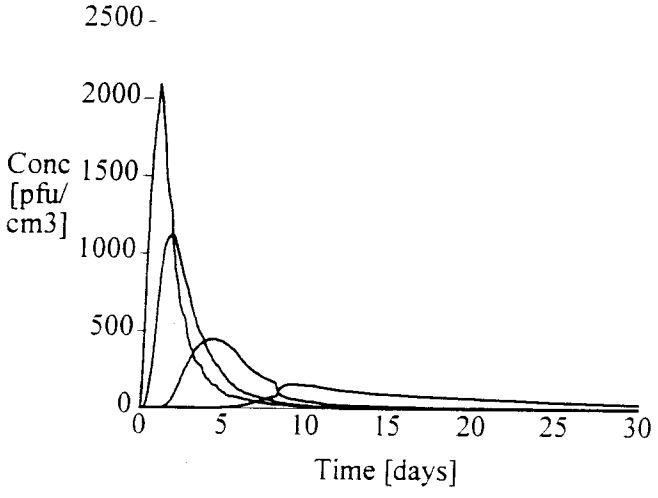


# Observation Nodes: Concentrations

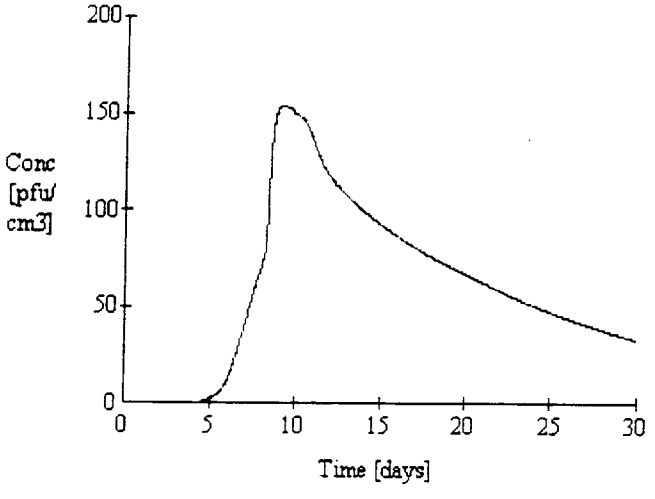

# Cumulative Variable Boundary Solute Flux

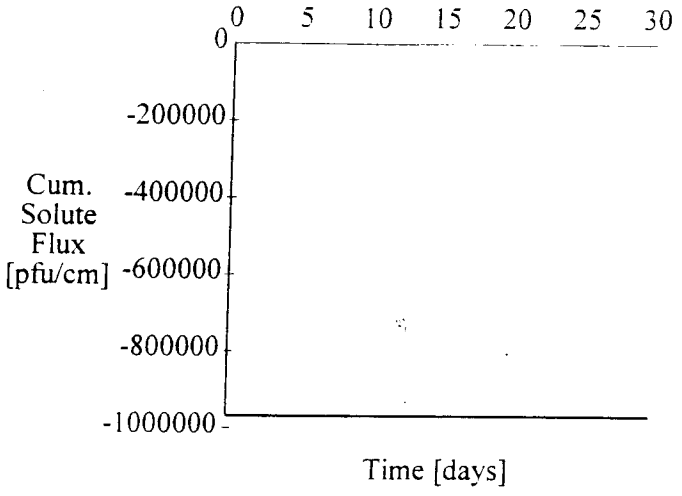


# Constant Boundary Solute Flux

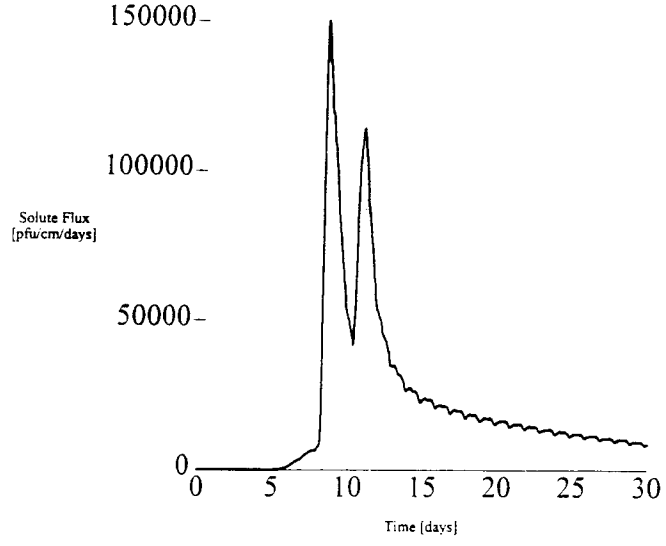

# Observation Nodes: Pressure Heads

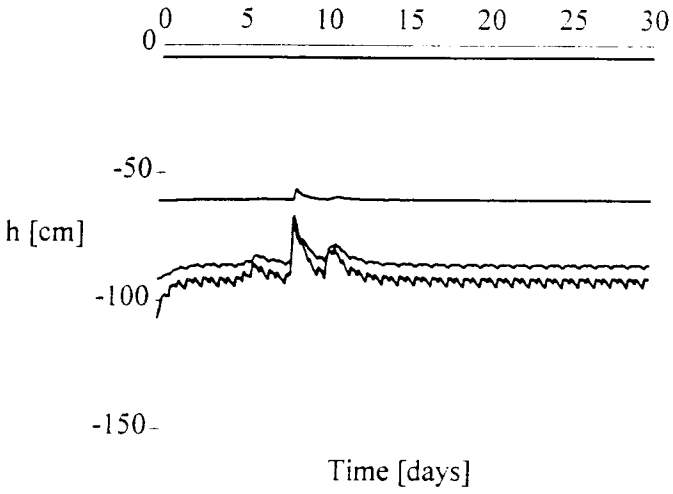


# Observation Nodes: Water Contents

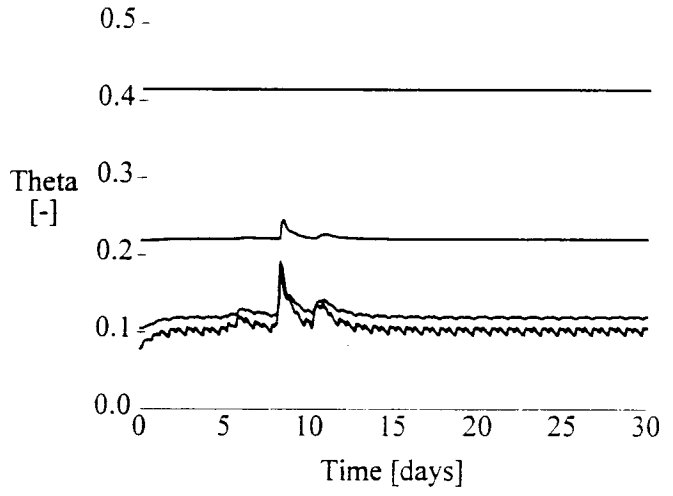

## Observation Nodes: Concentrations

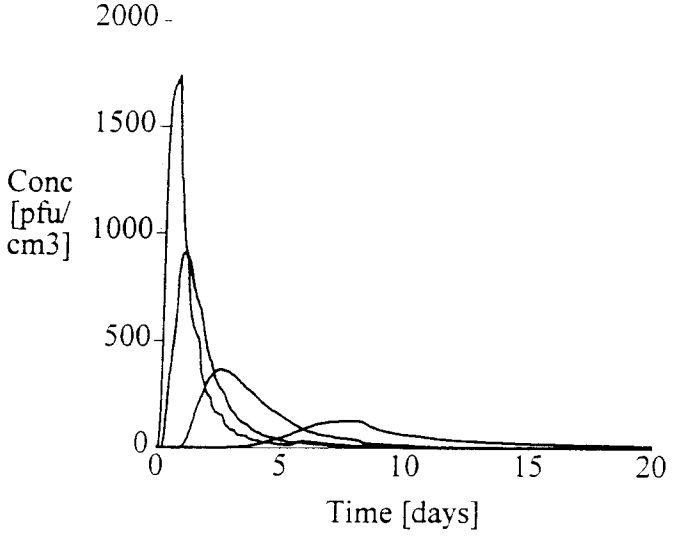


## Observation Nodes: Concentrations

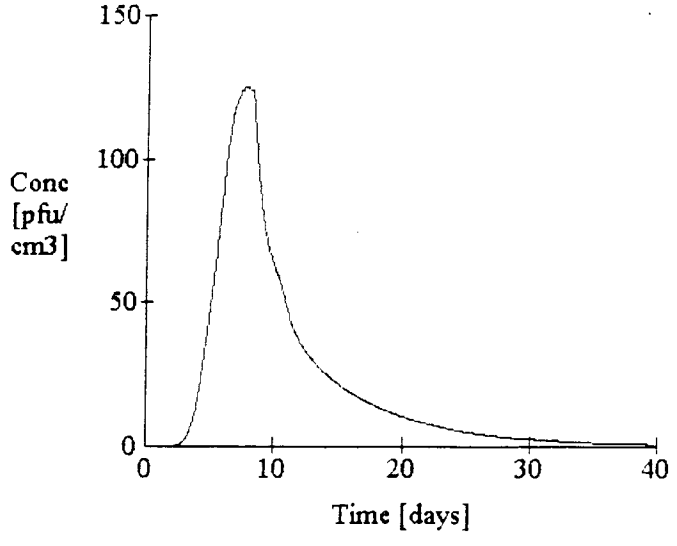

# Cumulative Variable Boundary Solute Flux

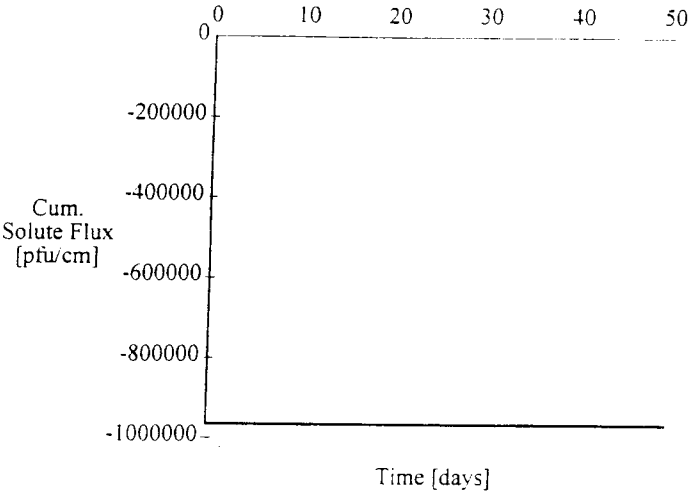


# Constant Boundary Solute Flux

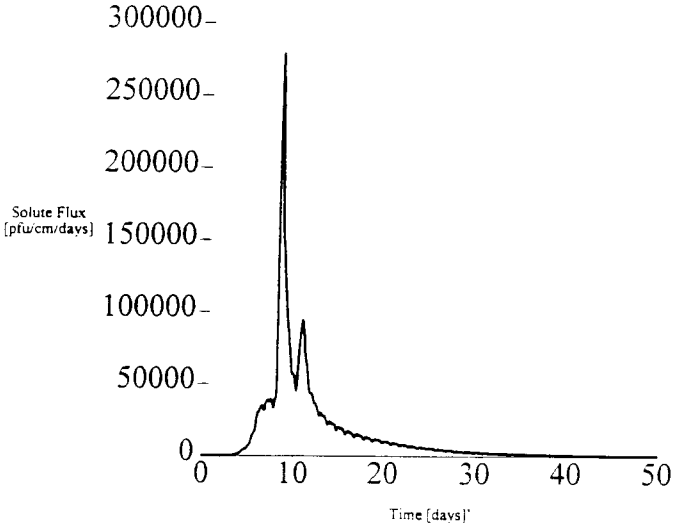

## Observation Nodes: Pressure Heads

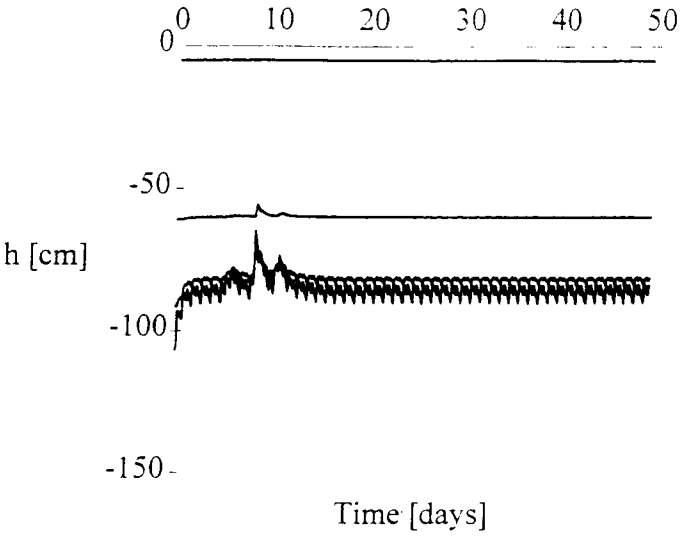


## Observation Nodes: Water Contents

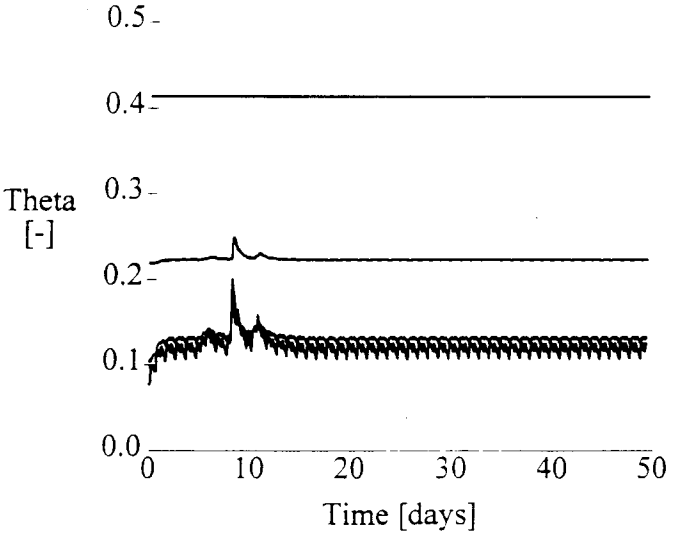

## Observation Nodes: Concentrations

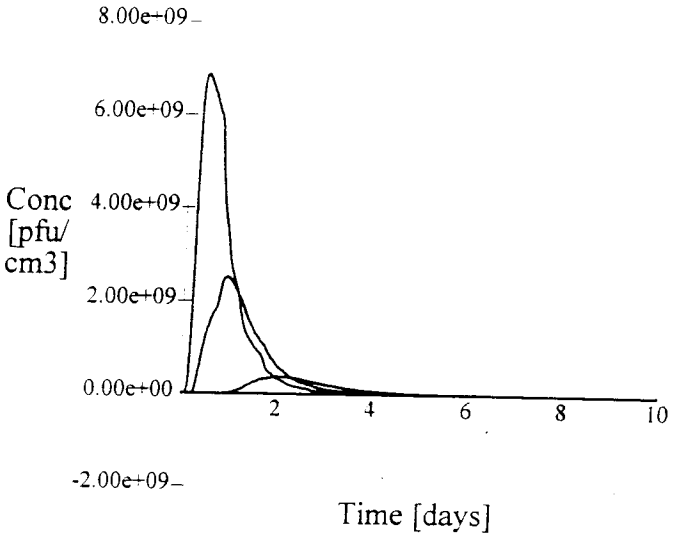


## Observation Nodes: Concentrations

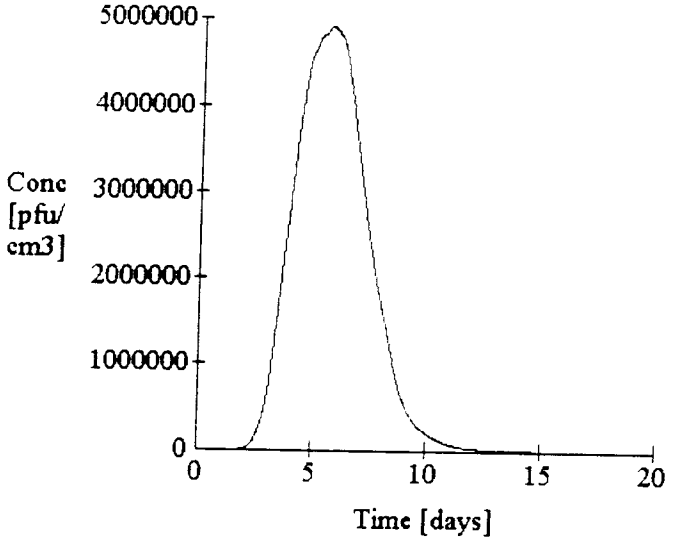

# Cumulative Variable Boundary Solute Flux

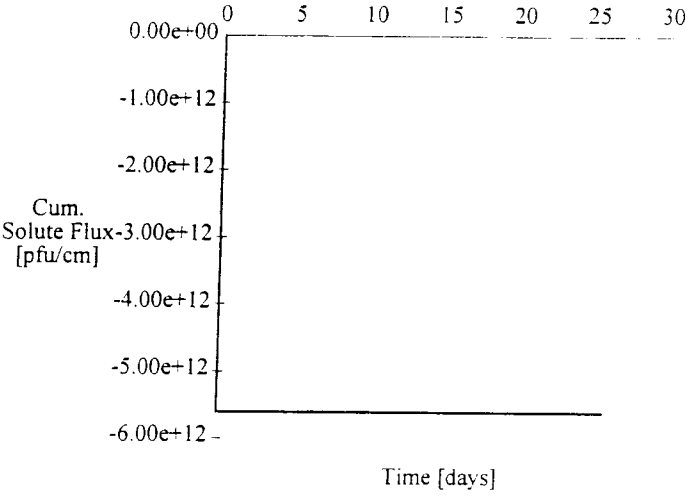


# Constant Boundary Solute Flux

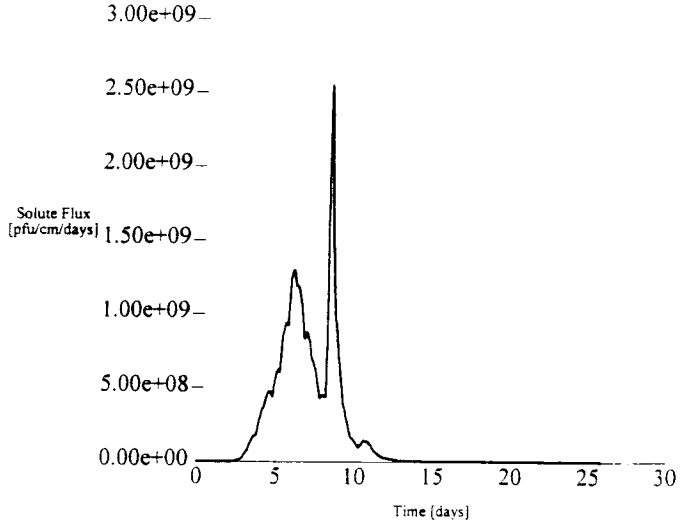

## Observation Nodes: Pressure Heads

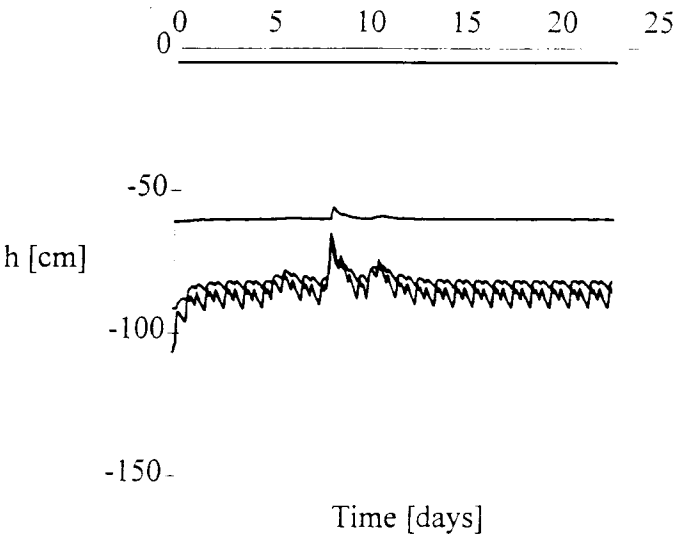

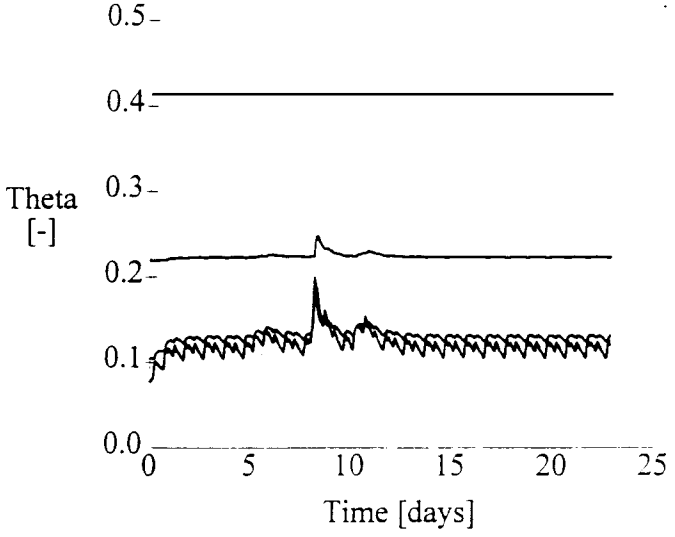
## Observation Nodes: Water Contents